



Cleared: January 30th, 1981
Clearing Authority: Air Force Wright Aeronautical Laboratories

AFFDL-TR-68-67

VUILLEUMIER CYCLE CRYOGENIC REFRIGERATOR DEVELOPMENT

F. N. Magee and R. D. Doering

Hughes Aircraft Company
Research and Development Division
Culver City, California

*** Export controls have been removed ***

TECHNICAL REPORT AFFDL-TR-68-67

AUGUST 1968

This document is subject to special export controls and each transmittal to foreign governments or foreign nationals may be made only with prior approval of Air Force Flight Dynamics Laboratory (FDFE), Wright-Patterson Air Force Base, Ohio 45433

Air Force Flight Dynamics Laboratory
Air Force Systems Command
Wright-Patterson Air Force Base, Ohio 45433

Contracts

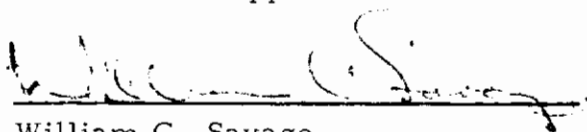
FOREWORD

This report covers the unclassified aspects of the Phase I effort of an exploratory development program to evaluate the Vuilleumier heat driven refrigeration cycle for aircraft and spacecraft cryogenic applications. It covers the period from 13 March 1967 through 13 April 1968. The work was done at Hughes Aircraft Company, Culver City, California, under Project 1470, "Cryogenic Cooling Technology," Task 147001, "Cryogenic Cooling Systems," contract F33615-67-C-1532 through sponsorship extended by the Air Force Flight Dynamics Laboratory. The project monitor was Ronald White (FDFE). Those responsible for various tasks are listed below:

| | |
|---------------------------|---------------|
| Technical Supervision | K. W. Cowans |
| Theoretical Cycle Studies | B. S. Leo |
| 30°/75°K Breadboard Unit | S. E. Spencer |
| 77°K Breadboard Unit | R. L. Berry |

This report was submitted by the authors in March 1968.

This technical report has been reviewed and is approved.



William C. Savage
Chief, Environmental Control Branch
Vehicle Equipment Division

Contrails

ABSTRACT

This report covers Phase I effort in an exploratory development program to evaluate the Vuilleumier heat driven refrigeration cycle for aircraft and spacecraft cryogenic applications. The effort includes a study of the theoretical aspects of the cycle and development of three miniature breadboard cryogenic refrigerators based on the cycle and operated by electric powered heating capsules. Two of the breadboard units are of identical design; these deliver 2 watts cooling capacity at 77°K. The remaining breadboard is a two-stage unit designed to deliver 0.5 watt at 30°K and 5 watts at 75°K. Performance data from these units were incorporated in the theoretical study. All units met their design requirements and confirmed the feasibility and inherent advantages of the Vuilleumier cycle for miniature long-life cryogenic refrigerators for both aircraft and spacecraft applications.

This abstract is subject to special export controls and each transmittal to foreign governments or foreign nationals may be made only with prior approval of the Air Force Flight Dynamics Laboratory (FDFE), Wright Patterson Air Force Base, Ohio, 45433.

Contrails

CONTENTS

I. INTRODUCTION 1

II. SUMMARY 3

 Task 1 Studies 3

 Task 2 30°/75°K Breadboard Refrigerator (X447550-100) 6

 Tasks 3 and 4 77°K Breadboard Refrigerator (X447525-100) 7

III. THERMODYNAMIC CYCLE AND HEAT TRANSFER ANALYSIS OF VUILLEUMIER CRYOGENIC REFRIGERATORS 13

 Introduction 13

 Basic Principles 13

 Basic Operation of the Vuilleumier Refrigeration 14

 The Idealized Vuilleumier Refrigerator 18

 Detailed Heat Transfer Losses 25

 Undesirable Heat Transfer Loads 30

 Discussion 37

IV. THEORETICAL COMPARISON OF VUILLEUMIER REFRIGERATOR WITH OTHER PRACTICAL CRYOGENIC REFRIGERATORS AND FUTURE APPLICATIONS ENVELOPE OF VUILLEUMIER REFRIGERATOR 39

 Introduction 39

 Comparison of Vuilleumier with Other Refrigeration Systems 39

 Vuilleumier Cycle and Refrigerator Limitation 45

 Development and Performance Summaries of Other Practical Closed Cycle Cryogenic Systems 46

 Maintenance Interval and the Coefficient of Performance of the Vuilleumier Refrigerator and the Other Practical Closed Cycle Cryogenic Systems 46

 Future Applications Envelope for Vuilleumier Refrigeration 51

 Discussion of Graphs 86

V. 30°/75°K BREADBOARD REFRIGERATOR (X447550-100) 123

 Introduction 123

 Design Requirements 123

 Unit Specifications 124

 Physical Configuration 129

 Thermodynamic Design 135

 Mechanical Design 138

 Performance 141

 Crankcase and Mechanism Development 144

 Hot Cylinder Assembly 147

| | |
|---|-----|
| Heater | 153 |
| Drive Motor and Inverter | 156 |
| Cold Cylinder Assembly | 158 |
| Test Station | 160 |
| Future Areas of Effort | 163 |
| VI. 77°K BREADBOARD REFRIGERATORS (X447525-100) | 167 |
| Introduction | 167 |
| Design Requirements | 167 |
| Unit Specifications | 168 |
| Physical Configuration | 172 |
| Thermodynamic Design | 175 |
| Mechanical Design | 181 |
| Unit Mounting | 184 |
| Design Features | 185 |
| Performance | 186 |
| Crankcase and Mechanism | 189 |
| Hot Cylinder Assembly | 192 |
| Input Heater | 194 |
| Drive Motor and Inverter | 196 |
| Cold Cylinder Assembly | 198 |
| Test Station | 203 |
| Future Areas of Effort | 206 |
| APPENDIX: OTHER PRACTICAL CRYOGENIC CYCLES AND REFRIGERATORS | 213 |
| Dynamic Refrigeration Systems | 213 |
| Solid-State Devices | 224 |

ILLUSTRATIONS

Figure

| | | |
|----|--|----|
| 1 | Milestone accomplishment chart for Vuilleumier cryogenic refrigerator development program | 4 |
| 2 | 30°/75°K Vuilleumier cryogenic refrigerator breadboard assembly | 8 |
| 3 | 30°/75°K Vuilleumier cryogenic refrigerator breadboard, detail parts | 8 |
| 4 | 77°K Vuilleumier cryogenic refrigerator, P/N 447525, final assembly | 11 |
| 5 | 77°K Vuilleumier cryogenic refrigerator, P/N 447525, detail parts | 11 |
| 6 | Schematic of basic Vuilleumier cryogenic refrigerator | 15 |
| 7 | Illustration of energy extraction by thermal effect | 16 |
| 8 | Indicator diagram of cold expansion volume | 19 |
| 9 | Indicator diagram of hot expansion volume | 19 |
| 10 | Indicator diagram of ambient temperature volume | 20 |
| 11 | Thermodynamic cycle of a volume of helium gas when Vuilleumier refrigerator completes a cycle | 21 |
| 12 | Values of 1/COP at a given temperature for Carnot and other cryogenic systems. The temperature at which heat is dissipated is 300°K | 49 |
| 13 | Maintenance interval as a function of refrigeration temperature range for various cryogenic systems | 50 |
| 14 | Gross refrigeration as a function of rpm when volume of cold cylinder is a parameter of VM refrigerating unit that produces no net power output when refrigerating temperature limit = 120°K heat rejection limit = 300°F power cylinder temperature = 1200°F | 52 |
| 15 | Required heat input to power cylinder as a function of refrigerator rpm with volume of cold cylinder as a parameter for VM machine of Figure 14 | 53 |

Contrails

Figure

| | | |
|----|--|----|
| 16 | Gross refrigeration as a function of rpm when volume of cold cylinder is a parameter of VM refrigerating unit that produces no net power output when refrigerating temperature limit = 120°K heat rejection limit = 160°F power cylinder temperature = 1200°F | 54 |
| 17 | Required heat input to power cylinder as a function of refrigerator rpm with volume of cold cylinder as a parameter for VM machine of Figure 16 | 55 |
| 18 | Gross refrigeration as a function of rpm when volume of cold cylinder is a parameter of VM refrigerating unit that produces no net power output when refrigerating temperature limit = 120°K heat rejection limit = 70°F power cylinder temperature = 1200°F | 56 |
| 19 | Required heat input to power cylinder as a function of refrigerator rpm with volume of cold cylinder as a parameter for VM machine of Figure 18 | 57 |
| 20 | Gross refrigeration as a function of rpm when volume of cold cylinder is a parameter of VM refrigerating unit that produces no net power output when refrigerating temperature limit = 120°K heat rejection limit = -65°F power cylinder temperature = 1200°F | 58 |
| 21 | Required heat input to power cylinder as a function of refrigerator rpm with volume of cold cylinder as a parameter for VM machine of Figure 20 | 59 |
| 22 | Gross refrigeration as a function of rpm when volume of cold cylinder is a parameter of VM refrigerating unit that produces no net power output when refrigerating temperature limit = 70°K heat rejection limit = 300°F power cylinder temperature = 1200°F | 60 |
| 23 | Required heat input to power cylinder as a function of refrigerator rpm with volume of cold cylinder as a parameter for VM machine of Figure 22 | 61 |

Contrails

Figure

| | | |
|----|---|----|
| 24 | Gross refrigeration as a function of rpm when volume of cold cylinder is a parameter of VM refrigerating unit that produces no net power output when refrigerating temperature limit = 70°K heat rejection limit = 160°F power cylinder temperature = 1200°F | 62 |
| 25 | Required heat input to power cylinder as a function of refrigerator rpm with volume of cold cylinder as a parameter for VM machine of Figure 24. | 63 |
| 26 | Gross refrigeration as a function of rpm when volume of cold cylinder is a parameter of VM refrigerating unit that produces no net power output when refrigerating temperature limit = 70°K heat rejection limit = 70°F power cylinder temperature = 1200°F | 64 |
| 27 | Required heat input to power cylinder as a function of refrigerator rpm with volume of cold cylinder as a parameter for VM machine of Figure 26 | 65 |
| 28 | Gross refrigeration as a function of rpm when volume of cold cylinder is a parameter of VM refrigerating unit that produces no net power output when refrigerating temperature limit = 70°K heat rejection limit = -65°F power cylinder temperature = 1200°F | 66 |
| 29 | Required heat input to power cylinder as a function of refrigerator rpm with volume of cold cylinder as a parameter for VM machine of Figure 28 | 67 |
| 30 | Gross refrigeration as a function of rpm when volume of cold cylinder is a parameter of VM refrigerating unit that produces no net power output when refrigerating temperature limit = 30°K heat rejection limit = 300°F power cylinder temperature = 1200°F | 68 |
| 31 | Required heat input to power cylinder as a function of refrigerator rpm with volume of cold cylinder as a parameter for VM machine of Figure 30 | 69 |

Contrails

Figure

| | | |
|----|---|----|
| 32 | Gross refrigeration as a function of rpm when volume of cold cylinder is a parameter of VM refrigerating unit that produces no net power output when refrigerating temperature limit = 30°K heat rejection limit = 160°F power cylinder temperature = 1200°F | 70 |
| 33 | Required heat input to power cylinder as a function of refrigerator rpm with volume of cold cylinder as a parameter for VM machine of Figure 32 | 71 |
| 34 | Gross refrigeration as a function of rpm when volume of cold cylinder is a parameter of VM refrigerating unit that produces no net power output when refrigerating temperature limit = 30°K heat rejection limit = 70°F power cylinder temperature = 1200°F | 72 |
| 35 | Required heat input to power cylinder as a function of refrigerator rpm with volume of cold cylinder as a parameter for VM machine of Figure 34 | 73 |
| 36 | Gross refrigeration as a function of rpm when volume of cold cylinder is a parameter of VM refrigerating unit that produces no net power output when refrigerating temperature limit = 30°K heat rejection limit = -65°F power cylinder temperature = 1200°F | 74 |
| 37 | Required heat input to power cylinder as a function of refrigerator rpm with volume of cold cylinder as a parameter for VM machine of Figure 36 | 75 |
| 38 | Cold loss as a function of volume and temperature. Ambient temperature = 300°F | 76 |
| 39 | Cold loss as a function of volume and temperature. Ambient temperature = 160°F | 77 |
| 40 | Cold loss as a function of volume and temperature. Ambient temperature = 70°F | 78 |
| 41 | Cold loss as a function of volume and temperature. Ambient temperature = -65°F | 79 |

Contrails

Figure

| | | |
|-----|--|-----|
| 42 | Hot volume as a function of cold volume for four temperatures. Cold temperature = 120°K | 80 |
| 43 | Hot volume as a function of cold volume for four temperatures. Cold temperature = 70°K | 81 |
| 44 | Hot volume as a function of cold volume for four temperatures. Cold temperature = 30°K | 82 |
| 45A | Hot losses as a function to volume and temperature Hot temperature = 1200°F Cold temperature = 70°K | 83A |
| 45B | Hot losses as a function of volume and temperature Hot temperature = 1200°F Cold temperature = 30°K | 83B |
| 45 | Hot losses as a function of volume and temperature. Hot temperature = 1200°F Cold temperature = 120°K | 83 |
| 46 | Optimum stroke of hot piston as a function of swept volume with thickness of piston wall as a parameter. | 84 |
| 47 | Optimum piston stroke as a function of rpm for five cold volumes. Cold temperature = 120°K Ambient temperature = 300°F | 85 |
| 48 | Optimum piston stroke as a function of rpm for five cold volumes. Cold temperature = 120°K Ambient temperature = 160°F | 87 |
| 49 | Optimum piston stroke as a function of rpm for five cold volumes. Cold temperature = 120°K Ambient temperature = 70°F | 88 |

Contrails

Figure

| | | |
|----|--|----|
| 50 | Optimum piston stroke as a function of rpm for five cold volumes. Cold temperature = 120°K Ambient temperature = -65°F | 89 |
| 51 | Optimum piston stroke as a function of rpm for five cold volumes. Cold temperature = 70°K Ambient temperature = 300°F | 90 |
| 52 | Optimum piston stroke as a function of rpm for five cold volumes. Cold temperature = 70°K Ambient temperature = 160°F | 91 |
| 53 | Optimum piston stroke as a function of rpm for five cold volumes. Cold temperature = 70°K Ambient temperature = -70°F | 92 |
| 54 | Optimum piston stroke as a function of rpm for five cold volumes. Cold temperature = 70°K Ambient temperature = -65°F | 93 |
| 55 | Optimum piston stroke as a function of rpm for five cold volumes Cold temperature = 30°K Ambient temperature = 300°F | 94 |
| 56 | Optimum piston stroke as a function of rpm for five cold volumes. Cold temperature = 30°K Ambient temperature = 160°F | 95 |
| 57 | Optimum piston stroke as a function of rpm for five cold volumes. Cold temperature = 30°K Ambient temperature = 70°F | 96 |
| 58 | Optimum piston stroke as a function of rpm for five cold volumes. Cold temperature = 30°K Ambient temperature = -65°F | 97 |
| 59 | Weight as a function of hot volume and piston stroke | 98 |

Contrails

Figure

| | | |
|----|--|-----|
| 60 | COP as a function of rpm for five cold volumes. Cold temperature = 120 ^o K Ambient temperature = 300 ^o F | 99 |
| 61 | COP as a function of rpm for five cold volumes. Cold temperature = 120 ^o K Ambient temperature = 160 ^o F | 100 |
| 62 | COP as a function of rpm for five cold volumes. Cold temperature = 120 ^o K Ambient temperature = 70 ^o F | 101 |
| 63 | COP as a function of rpm for five cold volumes. Cold temperature = 120 ^o K Ambient temperature = -65 ^o F | 102 |
| 64 | COP as a function of rpm for five cold volumes. Cold temperature = 70 ^o K Ambient temperature = 300 ^o F | 103 |
| 65 | COP as a function of rpm for five cold volumes. Cold temperature = 70 ^o K Ambient temperature = 160 ^o F | 104 |
| 66 | COP as a function of rpm for five cold volumes. Cold temperature = 70 ^o K Ambient temperature = 70 ^o F | 105 |
| 67 | COP as a function of rpm for five cold volumes. Cold temperature = 70 ^o K Ambient temperature = -65 ^o F | 106 |
| 68 | COP as a function of rpm for five cold volumes. Cold temperature = 30 ^o K Ambient temperature = 300 ^o F | 107 |
| 69 | COP as a function of rpm for five cold volumes. Cold temperature = 30 ^o K Ambient temperature = 160 ^o F | 108 |
| 70 | COP as a function of rpm for five cold volumes. Cold temperature = 30 ^o K Ambient temperature = 70 ^o F | 109 |

Contents

Figure

| | | |
|----|---|-----|
| 71 | COP as a function of rpm for five cold volumes. Cold temperature = 30°K Ambient temperature = -65°F | 110 |
| 72 | Technical areas in which Vuilleumier refrigerator can be applied | 121 |
| 73 | Outline and mounting drawing of 30°/75°K VM refrigerator . . . | 130 |
| 74 | 30°/75°K breadboard unit 447550-100 assembled for test | 131 |
| 75 | Schematic diagram of 30°/75°K VM refrigerator P/N 447550 | 132 |
| 76 | Layout of 30°/75°K VM refrigerator breadboard | 133 |
| 77 | Schematic of a VM cryogenic refrigerator | 135 |
| 78 | Crankcase and drive mechanism of unit 447550-100 | 145 |
| 79 | Fixture for testing bearing life of unit 447550-100 | 148 |
| 80 | Setup for bearing life test of unit 447550-100 | 149 |
| 81 | Hot cylinder assembly parts of unit 447550-100 | 149 |
| 82 | Hydroformed hot displacer shell of unit 447550-100 | 151 |
| 83 | Side view of failed hot displacer unit of 447550-100 | 152 |
| 84 | End view of failed hot displacer unit of 447550-100 | 152 |
| 85 | Heater life test fixture for unit 447550-100 | 155 |
| 86 | Heater life test setup for unit 447550-100 | 155 |
| 87 | Drive motor and inverter unit of 447550-100 | 157 |
| 88 | Cold cylinder assembly parts of unit 447550-100 | 159 |
| 89 | View of 30°/75°K VM test area | 160 |
| 90 | Test equipment flow chart for 30°/75°K VM breadboard refrigerator | 161 |
| 91 | Load capacity curves for 30°/75°K VM refrigerator unit X447550-100 | 165 |
| 92 | Cooldown time for 30°/75°K VM refrigerator | 165 |

Contents

Figure

| | | |
|-----|--|-----|
| 93 | Outline and mounting drawing of VM refrigerator X447525-100 | 173 |
| 94 | Electrical schematic of 77°K VM refrigerator P/N 447525 . . . | 175 |
| 95 | Cutaway of 77°K VM refrigerator | 177 |
| 96 | Refrigeration capacity as a function of crankcase temperature for unit X447525-100 | 180 |
| 97 | Input power and cooling capacity as a function of crankcase temperature for unit X447525-100 | 181 |
| 98 | Cooling fan and sheet metal trim of unit 447525-100 | 185 |
| 99 | Crankcase of unit 447525-100 | 189 |
| 100 | Crankshaft assembly parts of unit X447525-100 | 190 |
| 101 | Hot displacer mechanism parts in unit X447525-100 | 192 |
| 102 | Hot displacer parts in unit X447525-100 | 193 |
| 103 | Input heater brazed to hot cylinder of unit 447525-100 | 195 |
| 104 | 77°K Vuilleumier Refrigerator Breadboard with Instrumentation | 199 |
| 105 | Cold displacer - cold cylinder assemblies | 203 |
| 106 | Flow diagram of test equipment for 77°K VM refrigerator | 205 |
| 107 | Loaded capacity curve (VM refrigerator unit X447525-100) | 208 |
| 108 | Cool down time (VM refrigerator unit X447525-100) | 208 |
| 109 | Joule-Thomson refrigeration system and thermodynamic cycle . | 214 |
| 110 | Claude liquid cycle | 216 |
| 111 | Claude gas cycle | 218 |
| 112 | Stirling-cycle refrigeration systems with ideal pressure-volume and temperature-entropy diagrams | 219 |
| 113 | Modified Ericsson system | 220 |
| 114 | Solvay cryogenic refrigerator | 222 |

Contrails

Figure

| | | |
|-----|---|-----|
| 115 | Pulse tube system | 223 |
| 116 | Thermoelectric refrigeration system | 224 |
| 117 | Schematic of Etingshausen cooler | 227 |
| 118 | Thermomagnetic and thermoelectric refrigerators | 228 |

TABLES

Table

| | | |
|----|---|-----|
| 1 | Performance summary for X447550-100 cryogenic refrigerator | 9 |
| 2 | Performance summary for X447525-100 cryogenic refrigerator | 12 |
| 3 | Development and performance summary of other practical closed cycle cryogenic systems | 47 |
| 4 | Design losses and load capacity of 30°K stage | 136 |
| 5 | Design losses and load capacity of 75°K stage | 136 |
| 6 | Design power requirements of the 920°K stage (1200°F) | 138 |
| 7 | Weight summary, 30°/75°K Vuilleumier cryogenic refrigerator (X447550-100) | 142 |
| 8 | Performance summary for X447550-100 cryogenic system | 143 |
| 9 | Summary of heat losses for unit X447525-100 | 176 |
| 10 | Weight summary for 77°K VM cryogenic refrigerator P/N 447525-100 | 186 |
| 11 | Performance summary for VM cryogenic refrigerator P/N X447525-100 | 187 |

Contrails

LIST OF SYMBOLS

| | | |
|-----------|---|---|
| a | = | height of thermomagnetic refrigerator |
| a' | = | parameter that reflects the charge of gas in the refrigerator |
| A_p | = | cross-sectional area for heat transfer through piston |
| A_{reg} | = | cross-sectional area for fluid flow in regenerator |
| A_w | = | cross-sectional area for heat transfer through cylinder wall |
| b | = | length of thermomagnetic refrigerator |
| b' | = | parameter that reflects the effect of the movement of the warm end displacer on the total pressure. |
| C | = | circumferential length of cylinder - wetted perimeter |
| C' | = | specific heat |
| c | = | width of thermomagnetic refrigerator |
| c' | = | parameter that reflects the effect of the movement of the cold end displacer on the pressure |
| C_p | = | specific heat of gas at constant pressure |
| C_{pi} | = | specific heat of gas under constant pressure when flowing from hot end of regenerator to cold end |
| C_{po} | = | specific heat of gas under constant pressure when flowing from cold end of regenerator to hot end |
| COP | = | coefficient of performance |
| D_c | = | diameter of cylinder |
| D_e | = | equivalent or hydraulic diameter |
| D_{op} | = | outer diameter of hollow piston |
| D_{ip} | = | inner diameter of hollow piston |
| E_y | = | applied voltage in y direction |
| f | = | friction factor |

Contrails

| | | |
|-----------|---|---|
| F_f | = | friction force in direction of travel |
| G_i | = | mass velocity (\dot{m}/S') when gas flows from hot end of regenerator to cold end |
| G_o | = | mass velocity when gas flows from cold end of regenerator to hot end |
| g_c | = | gravitational conversion factor |
| h | = | heat transfer coefficient |
| h' | = | heat transfer coefficient when gas flows from hot end of regenerator to cold end |
| h'' | = | heat transfer coefficient when gas flows from cold end of regenerator to hot end |
| I_{app} | = | applied current |
| J | = | factor for converting ft-lbs force to Btu/hr |
| k_{cy} | = | thermal conductivity of cylinder |
| k_g | = | thermal conductivity of gas |
| k_{ij} | = | conductance |
| k_n | = | thermal conductivity of negative leg |
| k_p | = | thermal conductivity of positive leg |
| k_{xx} | = | thermal conductivity in x-direction |
| L_{cy} | = | length of cylinder between T_c and T_A or T_h and T_A |
| L_{ij} | = | distance between thermodynamic systems (i) and (j) |
| L_p | = | length of piston between T_c and T_A or T_h and T_A |
| L_r | = | length of regenerator |
| M | = | mass |
| dM | = | mass increment |
| \dot{m} | = | mass flow rate |

Contrails

| | |
|------------------------------------|---|
| \bar{m} | = average mass flow rate |
| \dot{m}_i | = mass flow rate from hot end of regenerator to cold end |
| \dot{m}_{ij} | = mass flow rate between thermodynamic systems (i) and (j) |
| $\dot{m}_{in},$ \dot{m}_{out} | = mass flow rate in and out of a thermodynamic system, respectively |
| \dot{m}_o | = mass flow rate from cold end of regenerator to hot end |
| N | = rpm of refrigerator |
| n | = number of moles |
| P | = pressure |
| P' | = power input to thermoelectric refrigerator |
| P _A | = pressure in the volume at the ambient or heat rejecting temperature level |
| P _C | = pressure in the volume at the cold or refrigerating end |
| dP | = pressure increment |
| P _H | = pressure in swept volume at the hot end |
| P _{in} | = power input to thermomagnetic refrigerator |
| P _{max} | = maximum pressure of gas in refrigerator |
| P _{min} | = minimum pressure of gas in refrigerator |
| Q | = heat transfer into working fluid |
| Q' | = actual heat exchanged in regenerator |
| Q _C | = heat transfer into cold volume |
| dQ | = heat increment |
| Q _f | = heat generated due to friction |
| Q _{gross} | = gross refrigeration |
| Q _H | = heat transfer into hot volume |
| Q _{id} | = ideal heat exchanged in regenerator |

Contrails

| | | |
|---------------|---|---|
| Q_{in} | = | heat absorbed by thermomagnetic refrigerator |
| Q_{max} | = | maximum coefficient of performance of a thermoelectric refrigerator |
| $Q_{max COP}$ | = | heat absorbed for a maximum value of the coefficient of performance |
| Q_p | = | heat transferred through piston |
| Q_{pu} | = | pumping heat transfer |
| Q_{rh} | = | heat load to cold cylinder due to regenerator inefficiency |
| Q_{rf} | = | heat generated due to friction in the regenerator |
| Q_{sh} | = | shuttle heat transfer |
| Q_{ut} | = | total undesirable heat transfer load |
| Q_w | = | heat transfer along cylinder wall |
| R | = | gas constant |
| r_{avg} | = | average radius of cylinder |
| r_h | = | hydraulic radius = S'/C |
| S | = | radial clearance between piston and ID of cylinder |
| S' | = | area for fluid flow |
| s | = | specific entropy |
| T | = | temperature |
| \bar{T} | = | average temperature |
| T' | = | cryogenic temperature of interest |
| t | = | cylinder wall thickness |
| T_A | = | (temperature of compression space) - ambient temperature |
| T_c | = | temperature at the colder end of the hot or cold cylinder |
| T_{cj} | = | absolute temperature of cold junction |

Contrails

| | | |
|-----------|---|--|
| dT | = | temperature increment |
| T_h | = | temperature at the warmer end of the hot or cold cylinder |
| T_{hj} | = | absolute temperature of hot junction |
| T_{ht} | = | high temperature of regenerator |
| T_{lt} | = | low temperature of regenerator |
| T_N | = | actual temperature of gas |
| T_v | = | temperature of void volume |
| U | = | velocity of working fluid |
| V | = | volume |
| V_A | = | volume at ambient or heat rejecting level |
| V_a | = | volume of annulus |
| V_{app} | = | applied voltage |
| V_C | = | swept volume at the cold or refrigerating end |
| V_{C_o} | = | full swept volume at the cold end |
| dV | = | volume increment |
| V_{H_o} | = | full swept volume at the hot end |
| V_H | = | swept volume at the hot end |
| V_N | = | actual volume |
| V_{n-s} | = | voltage between negative thermoelectric material and standard material |
| V_{p-s} | = | voltage between positive thermoelectric material and standard material |
| V_v | = | void volume |
| W | = | work |
| Y_p | = | piston stroke |
| Z | = | figure of merit |
| Z_{yx} | = | thermomagnetic figure of merit |

Contrails

| | |
|--------------------------------|--|
| α_p | = Seebeck coefficient for positive leg |
| α_n | = Seebeck coefficient for negative leg |
| α_{yx} | = applied magnetic field in two-direction lines |
| $\delta T', \delta T''$ | = temperature increments |
| $\delta \rho$ | = density increment |
| $\delta \tau$ | = time increment |
| ΔP_{ij} | = pressure drop between thermodynamic systems (i) and (j) |
| ΔP_{reg} | = pressure drop in regenerator |
| ΔT | = temperature difference across thermoelectric material |
| ΔT_{max} | = maximum temperature difference between the hot and cold ends of a thermodynamic refrigerator |
| η_r | = regenerator efficiency |
| $\lambda, \lambda', \lambda''$ | = dimensionless regenerator parameters |
| ρ | = density of fluid |
| ρ_p | = electrical sensitivity of positive leg |
| ρ_n | = electrical sensitivity in negative leg |
| ρ_{yy} | = electrical sensitivity in y direction |
| σ | = allowable stress |
| τ', τ'' | = time |
| Φ_{max} | = maximum coefficient of performance of thermoelectric refrigerator |
| \oint | = integration around a thermodynamic cycle |

SECTION I

INTRODUCTION

The Vuilleumier refrigeration cycle is not new, having been initially patented in 1918. Few practical applications have been made in the intervening years, however, due apparently to the fact that its efficiency is less than other known cryogenic refrigeration cycles at commercial load size applications.

Recent requirements for miniature flightweight cryogenic refrigerators to cool the low heat loads associated with infrared detectors and similar cryoelectronic devices coupled with some potentially inherent advantages of the cycle have precipitated renewed interest in its evaluation. The cycle can produce cryogenic refrigeration with a source of heat as the only input required. This concept of utilizing heat energy in lieu of more conventional mechanical energy for producing refrigeration may seem somewhat paradoxical; however, it is inherent in the Vuilleumier cycle and offers a number of advantages. For example, in space applications, the required heat source might be obtained via solar collector or through use of isotope capsule, thus obviating the requirement for large amounts of electrical power.

The cycle operates through the use of displacers requiring minimal seals, since the pressures throughout the system are nearly equal at any moment. The displacers simply move the gas from one section to another without the requirement to compress the gas within a closed volume. This results in minimal loading on bearings and seals with inherent long life potential for the machine.

There are obviously other advantages and disadvantages associated with the miniature Vuilleumier refrigerator. These are explored in detail in the main body of this report.

Contrails

SECTION II

SUMMARY

This report documents the Phase I effort on the Vuilleumier Cycle Cryogenic Refrigerator Development Program. The objective of this phase was to advance Vuilleumier heat cycle cryogenic refrigerator technology and to utilize this knowledge to develop three lightweight, long life breadboard cryogenic refrigerators with electric powered heat capsules. Although breadboard units, all refrigerators were to be delivered in a form suitable for application and test evaluation aboard military aircraft.

Phase I effort consisted of four major task areas:

- Task 1 - Conduct an intensive study of the Vuilleumier cycle to provide a description and discussion of the theoretical aspects and a prediction of future applications envelope of Vuilleumier cycle refrigerators.
- Task 2 - Design, fabricate and test one breadboard cryogenic refrigerator based on the Vuilleumier cycle with cooling capacity 1/2 watt at $<30^{\circ}\text{K}$ and 5 watts at 75°K .
- Task 3 - Design, fabricate and test one breadboard cryogenic refrigerator based on the Vuilleumier cycle with cooling capacity of 2 watts at 77°K .
- Task 4 - Fabricate one additional breadboard cryogenic refrigerator of same design as unit in Task 3.

Figure 1 milestone accomplishment chart for Phase I of the program shows the detailed schedule performance of these tasks.

TASK 1 STUDIES

The study of the Vuilleumier refrigeration cycle resulted in two individual reports, the first defines and describes the theoretical aspects of the cycle and the second compares the Vuilleumier refrigerator with other known cryogenic refrigerators, predicting its applications area through use of a number of graphs and charts.

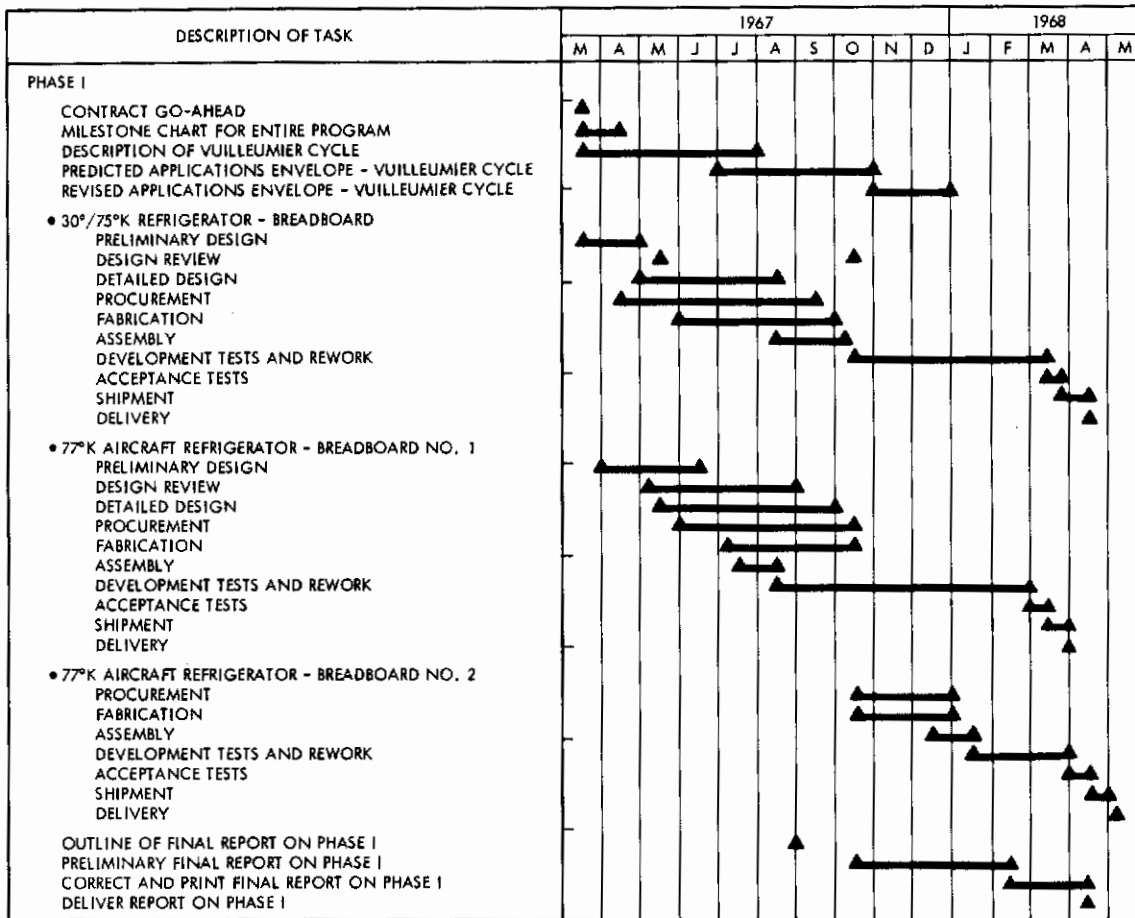


Figure 1. Milestone accomplishment chart for Vuilleumier cryogenic refrigerator development program.

The "Thermodynamic Cycle and Heat Transfer Analysis of Vuilleumier Cryogenic Refrigerator," Section III, describes the basic principles of the refrigerator operation together with equations needed for design. The equations were divided into two groups; one describes the thermodynamic principles on which the refrigerator is based and the other expresses the various modes of heat transfer involved in the system. The thermodynamic expressions are further subdivided into those describing the ideal Vuilleumier refrigeration cycle and those modified to explain the working principles of an actual Vuilleumier refrigerator. The equations assume isothermal operation in refrigerator expansion and compression volumes since such an assumption makes it possible to derive a set of thermodynamic equations that are relatively simple and that are fairly representative of the thermodynamics of the Vuilleumier refrigerator. The isothermal operation is not achieved in an actual refrigerator, but it can be approached by careful design. The heat transfer equations cover the various thermal processes involved in the operation of the refrigerator. It is shown that undesirable heat transfer can be minimized if the values of certain parameters of the refrigerator are maintained constant.

Another method of describing the thermodynamics and heat transfer process that are peculiar to the Vuilleumier refrigerator is also outlined. It is applicable to an actual refrigerator in which the operation of the expansion and compression volumes is somewhere between isothermal and adiabatic. This method, which is based on subdividing the refrigerator into several thermodynamic systems and then determining their thermal state as the refrigerator completes a thermodynamic cycle, usually provides a large number of thermodynamic, pressure, and heat transfer equations that must be solved simultaneously by means of an extensive computer program. However, it does give a complete history of the thermodynamic processes that occur in all portions of the refrigerator and therefore shows to what extent isothermal conditions are approached in the expansion and compression volumes. This method of analysis also yields a clear description of the thermal conditions in the regenerators and heat exchangers during any instant of refrigerator operation.

Section IV is entitled "Theoretical Comparison of Vuilleumier Refrigerator with Respect to Other Practical Cryogenic Refrigerators and the Future Applications Envelope of the Vuilleumier Refrigerator." It presents a theoretical comparison between the thermodynamic cycle of the Vuilleumier refrigerator and the thermodynamic cycles that are applied in other practical cryogenic refrigeration systems. Thermoelectric and thermomagnetic refrigerators are also briefly discussed because of their simple design and because there is a continuing effort toward improving the material properties of these devices. The solid cryogen cooling devices are not discussed since they are not closed-cycle refrigerating systems.

A discussion is presented of the advantages and the limitations of the Vuilleumier refrigerator, and the future applications envelope for the theoretical cryogenic Vuilleumier refrigerator is indicated by means of a number of graphs. These graphs were constructed by applying the equations that were derived in the first report and show the functional relationship between the various design parameters of a single-stage Vuilleumier refrigerator relative to the requirements that might be encountered in the technical areas where the refrigerator could be applied for cooling at cryogenic temperatures. These graphs describe the performance of the refrigerator only and do not include the effects of radiator or heat source since these parameters depend on boundary conditions and on mission requirements. By applying the graphs, it is possible to obtain the size and weight of a single-stage cryogenic Vuilleumier refrigerator that can provide refrigeration for several technical applications.

The graphs and charts in this report were amended to include actual performance data available from the development testing of the breadboard refrigerators. This data comprises what is termed a revised applications envelope for the Vuilleumier cryogenic refrigerator.

TASK 2 30°/75°K BREADBOARD REFRIGERATOR (X447550-100)

The X447550-100 refrigerator is an end item in Phase I of the development program to demonstrate the feasibility and applicability of the Vuilleumier two-stage refrigeration cycle. It was designed as a breadboard

model for cooling a typical space based infrared receiver to investigate and define various interface problems associated with this type application. However, although designed as a space breadboard, it was delivered with capability of operating an application aboard a military aircraft. Figure 2 shows the unit assembled with vacuum dewar in place but without hot cylinder insulation. Figure 3 is of the same unit disassembled in an exploded view to show the internal parts.

Initial testing of the unit was plagued with interference problems and premature heater failures. Despite these problems which required the initial tests be run at approximately half design charge pressure and speed, the unit attained cold temperature of 117°K and 86°K at first and second stages respectively. Subsequent development work resulted in a unit capable of 0.50 watt at 27°K and 6.0 watts at 75°K which was somewhat better than design goal of 1/2 watt at <30°K and 5 watts at 75°K. The unit, however, requires more input power than the original design estimate.

Table 1 presents a comparative summary of specific performance data for the X447550-100 refrigerator.

The developmental testing confirmed that the unit was straight-forward relative to thermodynamic design. It was possible to predict unit performance when thermodynamic conditions had been established from the data.

Development problems were primarily concerned with mechanical aspects of the unit. Major area of design revision resulted from modifications to reduce excessive internal friction and prevent hot displacer distortion.

TASKS 3 AND 4 77°K BREADBOARD REFRIGERATOR (X447525-100)

The X447525-100 refrigerator is an end item in Phase I of the development program to demonstrate the feasibility and applicability of the Vuilleumier refrigeration cycle. It was designed as a breadboard model capable of direct mount cooling of infrared detector package for typical aircraft application. Although designed as a breadboard the unit was delivered capable of operating aboard a military aircraft. After initial development on the first X447525-100 unit proved the design, a second breadboard was fabricated, tested and



Figure 2. 30°/75°K Vuilleumier cryogenic refrigerator breadboard, assembly (HAC photo 5R00588)

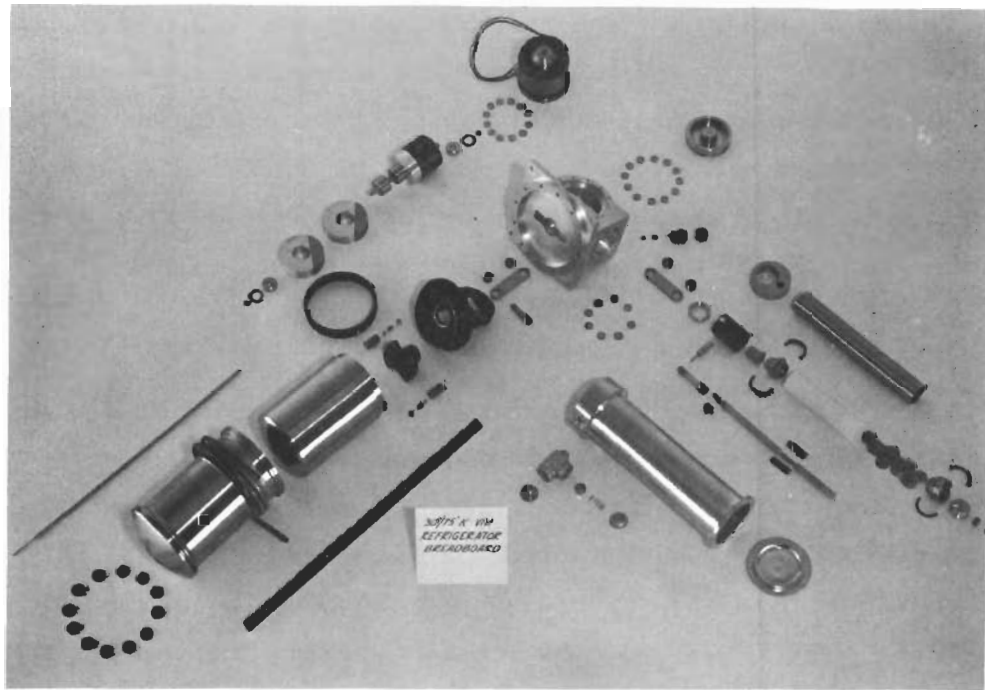


Figure 3. 30°/75°K Vuilleumier cryogenic refrigerator breadboard, detail parts (HAC photo 5R00587)

Table 1. Performance summary for X447550-100 cryogenic refrigerator

| | Breadboard, A/C* | | Flight Weight, Space** | |
|------------------------------|--------------------|-----------------------------|------------------------|----------|
| | Contract Spec. | Achieved | Contract Spec. | Achieved |
| A. Refrigerator | | | | |
| 1. Weight | - | 18 lb | - | |
| 2. Power input | | | | |
| Heater | - | 450 | - | |
| Motor | - | 30 | - | |
| Total | - | 480 (approx) | 200 W | |
| 3. Temperature/capacity | | | | |
| 75°K stage | 5.0 W | 75°K/6.0W | 5.0 W | |
| 30°K stage | 0.5 W | 30°K/0.5W | 0.5 W | |
| 4. Cooldown | - | 75°K/22 min 30°K/23 min | - | |
| 5. Engine speed | - | 240 RPM | - | |
| 6. Charge pressure | - | 400 psi | - | |
| 7. Life (hours) | 10 ⁴ hr | 200 hr to date | - | |
| B. Inverter | | | | |
| 1. Size | - | 3-1/4 x 2-3/8 x 1-3/4 in | - | |
| 2. Weight | - | 1.1 lb | - | |
| * Liquid cooled | | | | |
| ** Will not be liquid cooled | | | | |

Contrails

delivered. Figure 4 shows the unit assembled and equipped with glass double wall dewar. Figure 5 is the same unit configuration disassembled in an exploded view of the internal parts. The cooling fan and electrical power inverter are not shown.

Performance of the unit matured from initial test run results of 215°K at no load to 1.6 watts at 77°K. During developmental testing one major design revision was effected. This involved primary rework of the internal mechanism parts to minimize interference and dead volume in the machine.

Table 2 presents a comparative summary of specific performance data for the X447525-100 refrigerator.

The test data proved also that the unit was relatively simple and straightforward to design. This was especially true in the thermodynamic area. In all cases it was possible to predict unit performance thermodynamically once conditions had been identified through use of PV diagrams, dead volume, temperatures, etc. Primarily, development problems were associated with mechanical and mechanism features of the unit.

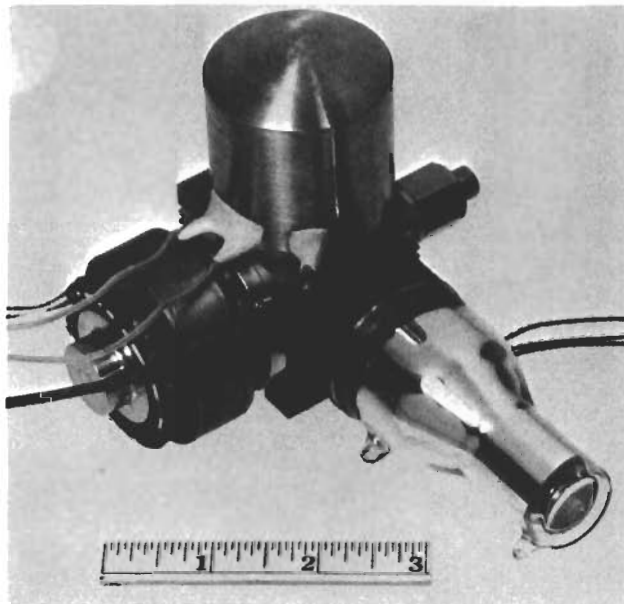


Figure 4. 77°K Vuilleumier cryogenic refrigerator, P/N 447525, final assembly (HAC photo 4R00173)

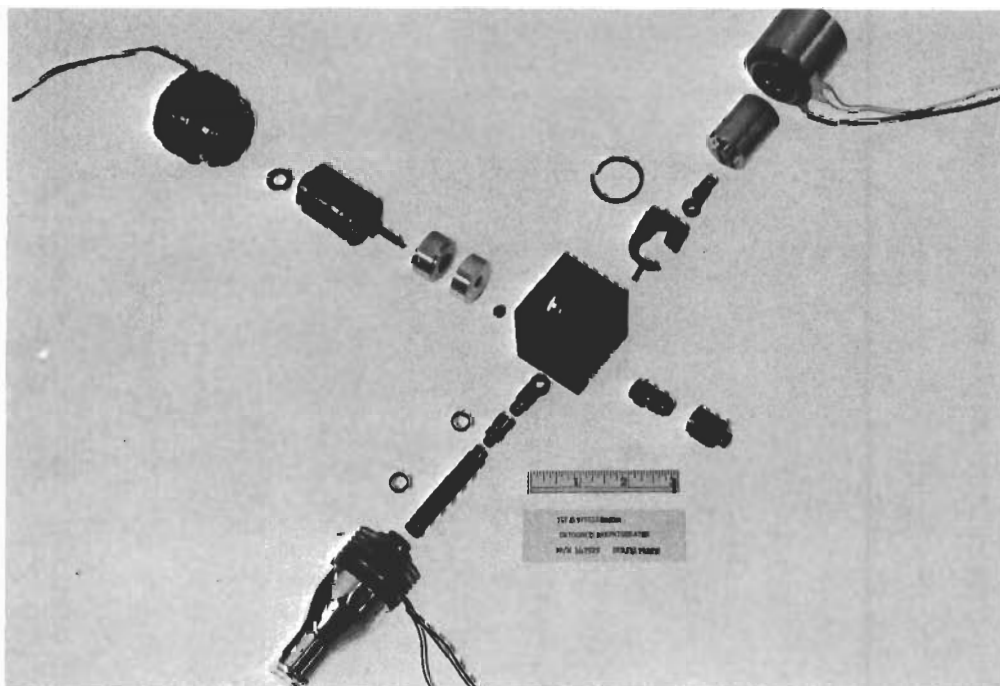


Figure 5. 77°K Vuilleumier cryogenic refrigerator, P/N 447525, detail parts (HAC photo 5R00175)

Table 2. Performance summary for X447525-100 cryogenic refrigerator

| | Performance Achieved | | Contract Performance Goals |
|--|--|--|--|
| <p>A. Refrigerator</p> <p>1. Weight</p> <p>2. Power input</p> <p style="padding-left: 20px;">Heater</p> <p style="padding-left: 20px;">Motor</p> <p style="padding-left: 20px;">Fan</p> <p style="padding-left: 20px;">Total (without fan)</p> <p>3. Temperature/capacity</p> <p style="padding-left: 20px;">77°K</p> <p>4. Cooldown</p> <p>5. Engine speed</p> <p>6. Maintenance free life</p> <p>7. Charge pressure</p> <p>B. Inverter</p> <p style="padding-left: 20px;">1. Size</p> <p style="padding-left: 20px;">2. Weight</p> | <p>3.1 lb (without fan)</p> <p>150</p> <p>30</p> <p>17</p> <p>180</p> <p>1.6 watts at 77°K</p> <p>7 min*</p> <p>600 RPM</p> <p>744 hours - to date</p> <p>600 psi</p> <p>3-1/4 x 2-3/8 x 1-3/4 in.</p> <p>1.1 lb</p> | | <p>Not specified</p> <p>-</p> <p>-</p> <p>-</p> <p>-</p> <p>-</p> <p>2 watts at 77°K</p> <p>10 minutes</p> <p>Not specified</p> <p>3000 hours</p> <p>Not specified</p> <p>Not specified</p> <p>-</p> |
| <p>*To 100°K</p> | | | |

SECTION III

THERMODYNAMIC CYCLE AND HEAT TRANSFER ANALYSIS OF VUILLEUMIER CRYOGENIC REFRIGERATORS

INTRODUCTION

The Vuilleumier Refrigerator, patented by R. Vuilleumier in 1918, is very suitable for closed-cycle cryogenic refrigeration in the small sizes needed by most ultra-sensitive electronic equipment for military systems. The report here describes the basic principles and those technical relationships which enter into the design and performance of the Vuilleumier Refrigerator.

BASIC PRINCIPLES

All cryogenic refrigerators employ three basic processes to obtain cooling. In general, all of these refrigerators (Stirling, Claude, Ericsson, Reversed-Brayton, etc.) compress a more or less ideal gas at ambient temperature and then expand this gas at a low temperature in a quasireversible manner; this method of expanding subtracts an amount of energy from the gas that can be then absorbed from the heat energy of a device thereby cooling or refrigerating it. The three aforementioned processes, then, are:

1. Compression at ambient temperature.
2. Expansion at low (cryogenic) temperature.
3. The heat-transfer process wherein the gas is heated and cooled between the limits of ambient temperature and the low cryogenic temperature.

Processes 1 and 2 are basically simple in concept: A change of pressure is effected either by an addition of work (compression) or a subtraction of work (expansion). Process 3 is somewhat more complicated conceptually. To accomplish this in an efficient manner the heat that is removed from the gas in cooling it to the low temperature must be added to the gas in heating it to ambient temperature. The process is accomplished either by the

countercurrent heat exchanger (in the Claude and reversed-Brayton refrigerators) or the thermal regenerators (in the Stirling, Ericsson and the Vuilleumier refrigerators). The description of the Vuilleumier refrigerator will consider these three basic processes separately and combined as required for a complete presentation.

BASIC OPERATION OF THE VUILLEUMIER REFRIGERATOR

A schematic representation of a Vuilleumier refrigerator is shown in Figure 6. It may be seen that the unit consists of 2 cylinders, each containing a displacer. These displacers are moved by a mechanism (shown as a crankshaft in Figure 6) so that their motions are separated by about 90 degrees of mechanism rotation. The end of one displacer/cylinder is maintained at a high temperature (1000°F) by means of an external heat source, and the common ends of the 2 cylinders are maintained at ambient temperature by means of some form of cooling (air fan or liquid circulation). The remaining cylinder end will cool to some low temperature when the mechanism is rotated as shown by the process described below. Assuming that this low temperature has been obtained, and steady-state conditions are obtained, the basic operation is as follows:

It can be seen from Figure 6, that the Vuilleumier refrigerator is a constant-volume device. That is, it is not possible for the geometrical working volume to vary because of any motion of either of the two displacers. However, the pressure can and does vary as the displacer moves. This occurs because of changes in the average temperature of the gas that fills the working volume of the refrigerator. Motion of the power displacer toward the center of the crankshaft forces gas to move from the crankcase, which is at ambient temperature, to the hot end of the power cylinder. This movement naturally increases the average temperature of the gas in the working volume, and hence the pressure in this fixed volume increases. Likewise, motion of the cooling displacer forces some gas to pass from the ambient-temperature crankcase to the cold end of the cooling cylinder. In this way, the working gas is cooled and its pressure therefore decreases. Reversing either of the motions just described would, of course, produce an opposite effect, i. e.,

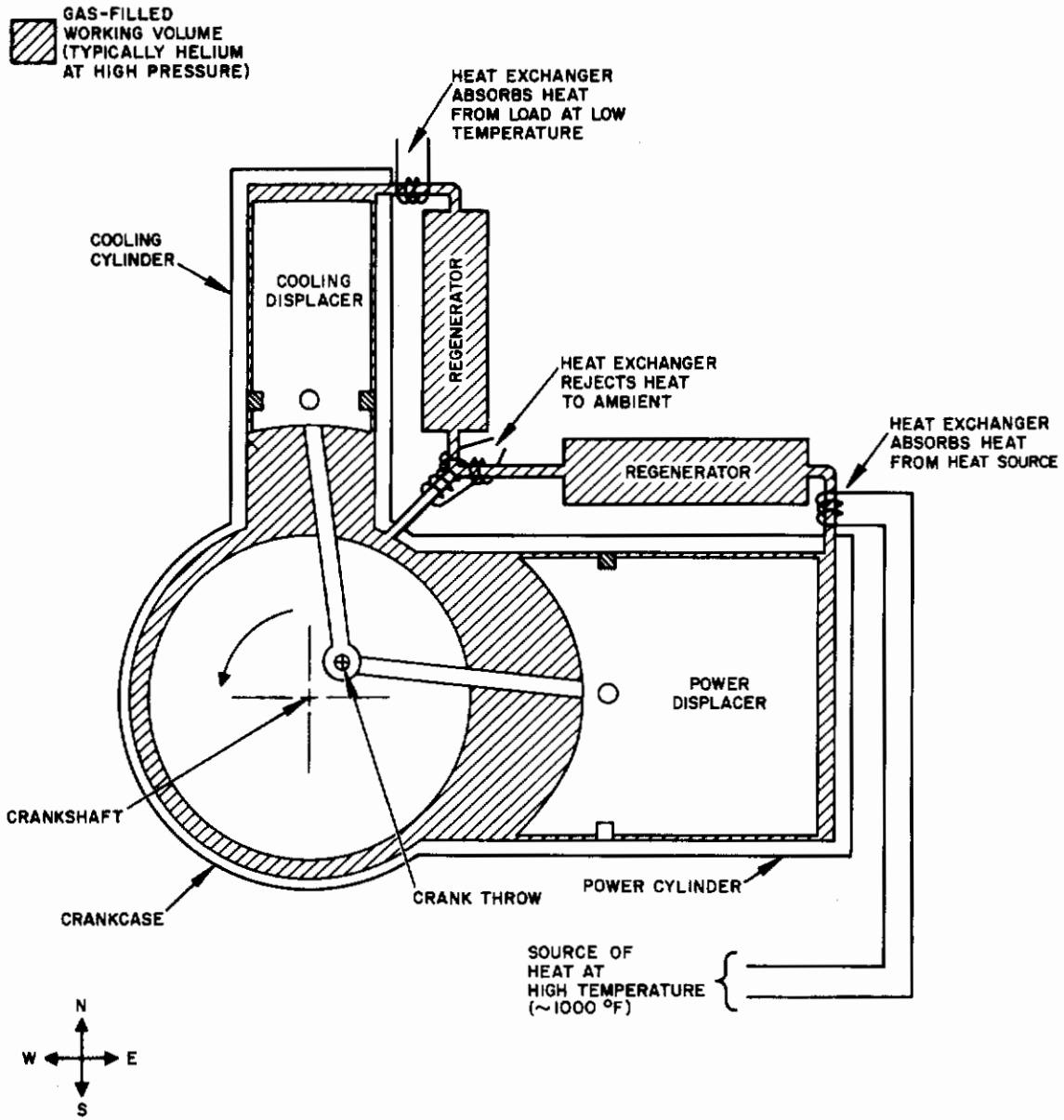


Figure 6. Schematic of basic Vuilleumier cryogenic refrigerator.

expansion in the former case and compression in the latter. It is therefore correct to state that motion of the power displacer toward the center compresses the gas, and that motion of the cooling displacer towards the center expands the gas; each motion being reversible.

Before proceeding it would be advantageous to discuss the processes of a simpler device as shown in Figure 7, which illustrates the principle used in extracting energy by the thermal effects only. This diagram shows a simple cylinder with a displacer and a connecting rod of zero area; therefore, the area on the top and bottom of this displacer are equal. Further, because the pressure is equal throughout the system there is no force acting to move the piston or displacer in one direction or the other. Let the displacer move from the top position down to the bottom position. The gas then moves along

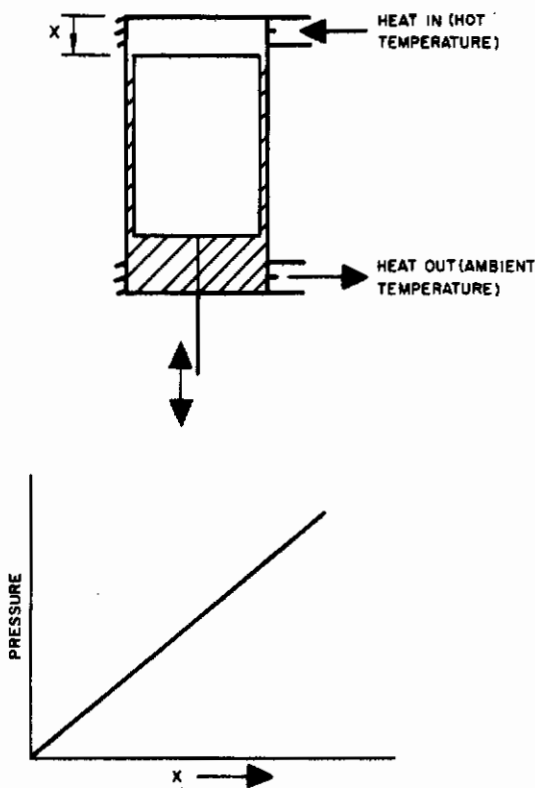


Figure 7. Illustration of energy extraction by thermal effect

Contrails

the walls into the opening volume. Assume that the top of the cylinder is held at the hot temperature by means of a heat exchanger which conducts heat into the cylinder as required, and also assume that the bottom of the piston is held at the ambient temperature with a heat exchanger which will extract heat as required. The operation is then as follows:

As the piston is brought from the top toward the bottom the ambient gas flows into the passages along the piston to the warm end where it picks up energy from the hot heat exchanger; the gas temperature increases from ambient to the hot temperature. Because the volume is closed and there is a fixed amount of gas in the cylinder, the pressure in the cylinder will rise as the gas is brought from the ambient temperature to the hot temperature. This is depicted on the graph showing that as the piston is pulled down the pressure will go up. When the piston is pushed back to the top, the gas flows back from the hot volume to the ambient volume where the ambient heat exchanger extracts any excess heat from the gas. This causes the pressure to return to its initial low point at the beginning of the graph.

With these facts in mind, and referring to Figure 6 the operation of a Vuilleumier refrigerator can be explained.

When the crankshaft is in the North position, the pressure in the working volume assumes some high value, P_h . As the crankshaft moves in the direction indicated as West, the power displacer is compressing and the cooling displacer is expanding. In a well designed Vuilleumier refrigerator these actions are essentially balanced, and there is little pressure change. The net effect is that a certain amount of the working gas is transferred to the cold end of the cooling cylinder with little change in pressure. As the crankshaft moves from West to South, both displacers expand and the pressure falls to a low value P_l . With further motion to East, the cooling displacer compresses and the power displacer expands with little change in pressure. Motion to the North causes both displacers to compress, and the pressure returns to the value P_h . An indicator diagram of the cold volume, in the cooling cylinder, is shown in Figure 8. It can be seen that the net amount of work that has been done by the gas in this volume exactly matches the amount of work that has been supplied to the gas at the other end of the cylinder in the ideal case with

no irreversible pressure drops. However, the work done at the cold end produces refrigeration.

At the hot end of the hot cylinder an indicator diagram similar to that shown in Figure 9 is obtained. The area within this diagram is equal to the energy that must be supplied to the hot cylinder during each cycle to provide the prime energy to drive the system. Figure 10 shows the indicator diagram of the ambient temperature volume.

In the elementary discussion given above only the basic qualitative aspects of the Vuilleumier refrigerator are discussed. For a more complete understanding of the operation a slightly more detailed, but still idealized model will be discussed. Subsequently, the difference between the idealized model and the real machine will be discussed to indicate the methods of design that must be used. Finally the expressions that quantitatively describe the heat transfer relationships within a Vuilleumier refrigerator will be discussed.

THE IDEALIZED VUILLEUMIER REFRIGERATOR

The following description is after Chellis and Hogan (Reference 1). The model employed is idealized with the following assumptions.

Basically, this engine is assumed to consist of two cylinders fitted with two displacers which separate the cylinder into three volumes, V_H , V_A and V_C . The subscripts H, A, and C refer to the temperature levels hot, ambient and cold, respectively. V_A actually consists of the summation of two volumes at the ambient ends of the two cylinders (refer to Figure 6). There are no pressure drops assumed within the refrigerator in the idealized model. The thermal regenerators are assumed to be perfect (i. e., no temperature difference is required between gas flows in each direction in order to transfer heat and therefore no heat flows through the regenerators over a complete cycle); moreover, the regenerators are assumed to have an infinite heat capacity and therefore the temperature of a regenerator is invariant with time.

An idealized Temperature-Entropy diagram is shown in Figure 11 to represent the path of the two gas flows. It may be seen here (the compass directions refer to the same given in Figure 6) that the gas is compressed at ambient temperature (T_A) polytropically to a slightly higher temperature T_A'

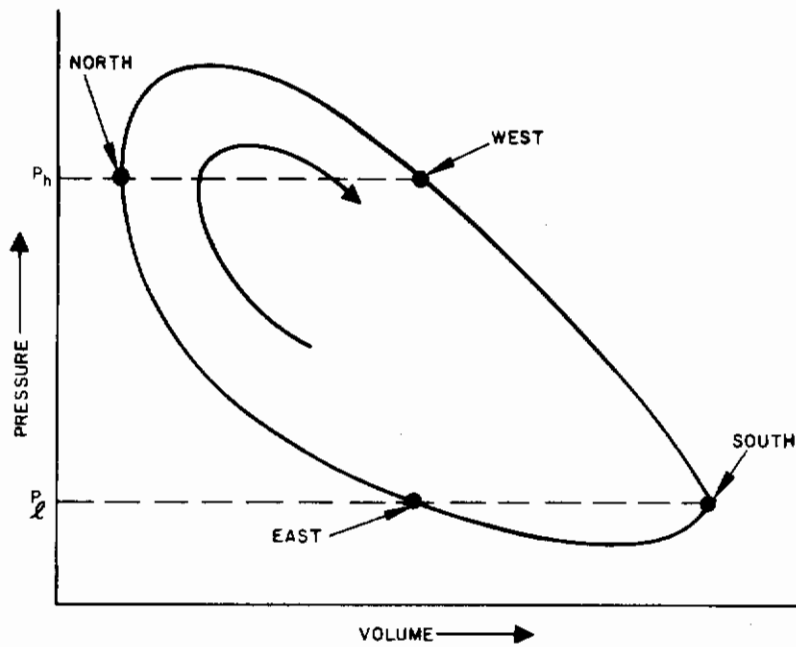


Figure 8. Indicator diagram of cold expansion volume

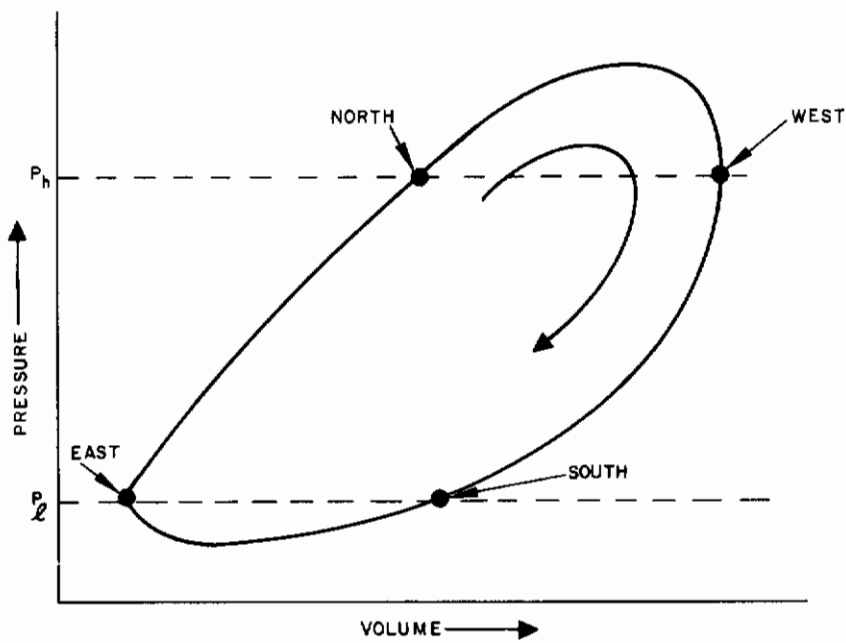


Figure 9. Indicator diagram of hot expansion volume

cooled back to T_A in the ambient temperature heat exchangers (East to North). Hence the gas is separately passed through the two regenerators to cool or heat to T_C (cold temperature) or T_H (hot temperature) respectively, (North to West). The polytropic expansion to low pressure produces a drop in temperature to T_C' and T_H' and a reheating in the two cold and hot heat exchangers to the original temperature (West to South). A retracing of the gas through the regenerators returns the gas to ambient temperature T_A (South to East) whence the cycle is repeated. The Temperature-Entropy plot given is idealized and artificial in that a great many simultaneous operations occur at the same time. For example a portion of gas is compressed in the hot portion of the hot cylinder at the same time that the bulk of the gas is being compressed at ambient temperature. In actuality the Pressure-Volume diagram for each volume (Figures 8 through 10) provides a clearer and more

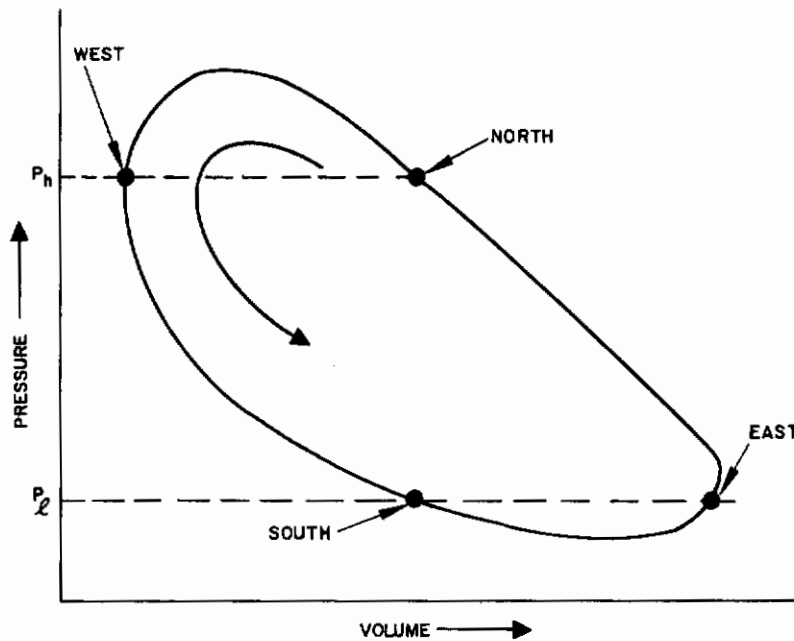


Figure 10. Indicator diagram of ambient temperature volume.

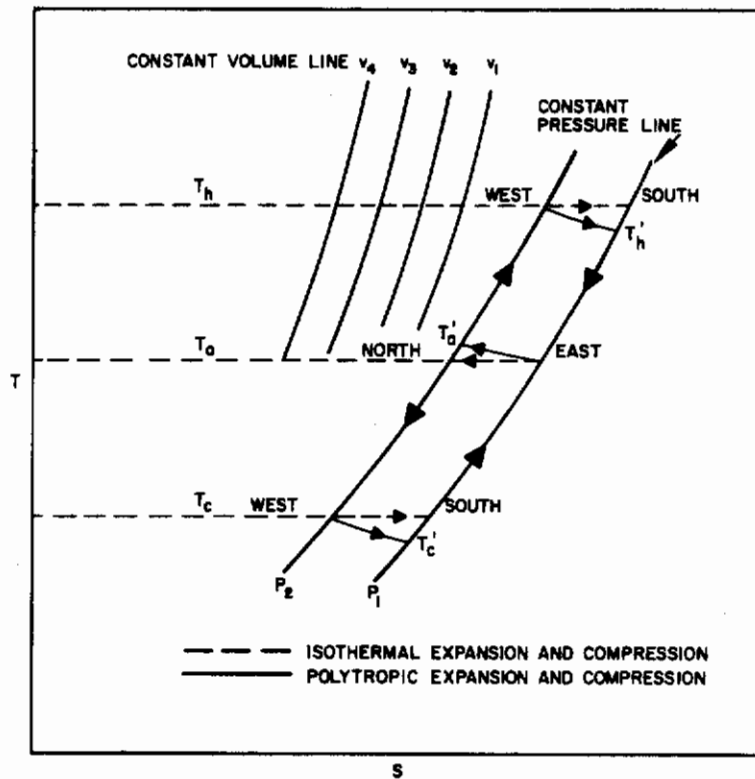


Figure 11. Thermodynamic cycle of a volume of helium gas when Vuilleumier refrigerator completes a cycle

accurate picture of operation than does the Temperature-Entropy plane. At each volume the heat flows for the idealized model are such that

$$Q = \oint PdV = W \tag{1}$$

or the heat flow is equal to the work at that volume. There is, of course, no net work resulting in the idealized refrigerator because no pressure differences exist within the machine at any given time. Since the pressure at each

Contrails

end of the displacer is equal and by elementary geometry a change of volume at one end of a cylinder is exactly equal to the negative of the volume change at the other end:

$$\oint P_A dV_A = \oint P_H dV_H + \oint P_C dV_C \quad (2)$$

If the displacer motions are assumed to be harmonic and at a phase separation of exactly 90 degrees some useful relations can be derived as shown by Chellis and Hogan, if the pressure changes are assumed to occur isothermally,

The volumes are:

$$V_H = 1/2 V_{H_o} (1 - \cos \theta)$$

$$V_C = 1/2 V_{C_o} (1 - \sin \theta)$$

$$V_A = 1/2 V_{H_o} (1 + \cos \theta) + 1/2 V_{C_o} (1 + \sin \theta) \quad (3)$$

where the subscript o refers to the full swept volume of the cylinder. If the gas is assumed to be ideal,

$$n = \frac{P}{R} \left[\frac{V_{H_o} (1 - \cos \theta)}{2 T_H} + \frac{V_{H_o} (1 + \cos \theta)}{2 T_A} + \frac{V_{C_o} (1 - \sin \theta)}{2 T_C} + \frac{V_{C_o} (1 + \sin \theta)}{2 T_A} + \frac{V_v}{T_v} \right] \quad (4)$$

with the additional simplification of considering the void volumes (V_v) of the regenerators, heat exchangers, etc., as existing at some artificial temperature

$$T_v = \frac{\int T_v dV_v}{\int dV_v}$$

Then Equation (4) can be simplified using symbols a' , b' , and c' defined by

$$\begin{aligned} a' &= \left[V_{H_o} \left(1 + \frac{T_A}{T_h} \right) + V_{C_o} \left(1 + \frac{T_A}{T_c} \right) + 2V_v \left(\frac{T_A}{T_v} \right) \right] \\ b' &= V_{H_o} \left[1 - \frac{T_A}{T_h} \right] \\ c' &= V_{C_o} \left[1 - \frac{T_A}{T_c} \right] \end{aligned} \tag{5}$$

where a' reflects the charge of gas in the refrigerator, b' reflects the effect of the movement of the warm end displacer on the total pressure, and c' reflects the effect of the cold-end displacer on the pressure. Then, the pressure P may be expressed as:

$$P = \frac{2 n R T_A}{a' + b' \cos \theta + c' \sin \theta} \tag{6}$$

This relation gives the indicator areas Q_C and Q_H as

$$Q_C = \oint PdV = -nR V_C T_A \int_0^{2\pi} \frac{\cos \theta}{a' + b' \cos \theta + c' \sin \theta} d\theta \tag{7}$$

Contrails

$$Q_H = \oint PdV = nRV_H T_A \int_0^{2\pi} \frac{\sin \theta}{a' + b' \cos \theta + c' \sin \theta} d\theta \quad (8)$$

After integration the following expressions are obtained (after White, Reference 2).

$$Q_C = - \frac{2\pi nRT_A V_{C_o} b'}{b'^2 + c'^2} \quad (9)$$

$$Q_H = \frac{2\pi nRT_A V_{H_o} c'}{b'^2 + c'^2} \quad (10)$$

As necessary:

$$\begin{aligned} Q_C/Q_H &= \left(- V_{C_o}/V_{H_o} \right) (b'/c') \\ &= \frac{[T_H - T_A]}{T_H} \frac{T_C}{[T_A - T_C]}, \end{aligned} \quad (11)$$

which is the Carnot relationship for the COP of a heat engine (operating between T_H and T_A) driving a refrigerator from T_A to T_C . The maximum pressure ratio may be obtained by differentiating Equation (6).

$$\frac{P_{\max}}{P_{\min}} = \frac{a' + (b'^2 + c'^2)^{1/2}}{a' - (b'^2 + c'^2)^{1/2}} \quad (12)$$

In actuality the assumptions given above are not realized exactly. The gas in going through the regenerators and heat exchangers undergoes an irreversible pressure drop which requires that work be applied to the

displacers to maintain motion and this modifies the work relation of Equation (2). Also, as indicated on Figure 11 the temperatures T_A , T_H and T_C actually vary with time in a complicated manner due to quasi-adiabatic conditions existing in the expansion volumes. Also, due to the finite specific heat of the thermal regenerators the temperature T_v will vary with time. A concept that is useful in detailed computation is that of "reduced volume," defined by the basic relationship

$$P \text{ system} = \frac{MRT'}{\Sigma V \text{ reduced}} \quad (13)$$

where T' is some conveniently chosen temperature, usually the cryogenic temperature of interest. Therefore:

$$V_{N(\text{reduced})} = V_{N(\text{actual})} \times \frac{T'}{T_N} \quad (14)$$

where

V_N = actual volume of gas

T_N = actual temperature of gas

This concept allows the variation of temperature to be manipulated easily during design computation. However, the concept is only useful to the designer and will not be used in any other manner. Generally the result is such that harmonic motion is not obtained and a detailed study is necessary to obtain mass flow rates and pressure changes. The approximations given above are only adequate for illustration.

DETAILED HEAT TRANSFER LOSSES

The regenerators of the Vuilleumier refrigerator must be very efficient if the refrigerator is to be a practical device for producing refrigeration at temperatures below 100°K . In fact, the performance of the machine as a whole depends directly on the efficiency of the regenerators.

Contrails

The efficiency η_r of the regenerators is defined as

$$\eta_r = \frac{\tau' \dot{m}_i C_{pi} (T_{ht} - T_{lt})}{\tau' \dot{m}_i C_{pi} (T_{ht} + \delta T') - \tau'' \dot{m}_o C_{po} (T_{lt} - \delta T'')} = \frac{Q'}{Q_{id}}, \quad (15)$$

Where Q' is the heat that is actually exchanged and Q_{id} is an ideal amount of heat, which would be exchanged if the entrance temperature of (hot) gas could be decreased to the entrance temperature of the (cold) gas (as the gas flows from the hot end of the regenerator to the cold end during the time, τ' , and in the reverse direction during the time, τ''). If the conditions are such that $\dot{m}_i C_{pi} \tau' = \dot{m}_o C_{po} \tau''$, then the heat transfer efficiency of the regenerators becomes

$$\eta_r = \frac{T_{ht} - T_{lt}}{T_{ht} - T_{lt} + (\delta T' + \delta T'')}. \quad (16)$$

At the beginning of a cycle, the temperature of the gas that flows through the regenerator from the hot end to the cold end is $T_{ht} + \delta T'$. When the gas flows in the reverse direction, its temperature is $T_{lt} - \delta T''$. The expression for the heat transfer balance for these two conditions is

$$\dot{m}_i \cdot C_{pi} (T_{ht} - T_{lt}) = h' C L_r \delta T' \quad (17)$$

and where C is the "wetted perimeter."

$$\dot{m}_o \cdot C_{po} \cdot (T_{ht} - T_{lt}) = h'' C L_r \delta T''. \quad (18)$$

Contrails

Solving for the values of $\delta T'$ and $\delta T''$ in Equations (17) and (18) and substituting these values in Equation (16) give

$$\eta_r = \frac{1}{\left[1 + \frac{\dot{m}_i C_{pi}}{h' CL_r} + \frac{\dot{m}_o C_{po}}{h'' CL_r} \right]} \quad (19)$$

By defining $\dot{m}_i C_{pi}/h' CL_r$ to be equal to $1/\lambda'$ and $\dot{m}_o C_{po}/h'' CL_r$ to be equal to $1/\lambda''$ and then letting $1/\lambda' + 1/\lambda''$ equal $1/\lambda$, Equation (19) becomes

$$\eta_r = \frac{\lambda}{\lambda + 1} = \frac{1}{1 + \frac{1}{\lambda}} \quad (20)$$

From the above expression for λ' and λ'' , it is seen that

$$\lambda' = \frac{h' L_r}{C_{pi} G_i r h} \quad (21)$$

and

$$\lambda'' = \frac{h'' L_r}{C_{po} G_o r h} \quad (22)$$

It can also be seen from Equation (20) that the thermal efficiency η_r of the regenerator approaches 1 when λ approaches ∞ or when $(1/\lambda' + 1/\lambda'')$ approaches 0. Thus, it is clearly shown in Equations (21) and (22) that the values of h' and h'' should be large in order to obtain a high value of thermal efficiency for the regenerator and hence high performance for the refrigerator. These heat transfer coefficients h' and h'' can be computed from the graphed data in Reference 3, which also presents a more detailed discussion of regenerators; see also References 4 through 8.

The pressure drop in the regenerator is expressed in terms of a friction factor (See page 27 of Reference 9)

By

$$\Delta P_{\text{reg}} = \frac{\rho U_f^2 L_r}{2 g_c D_e} = \frac{\dot{m}^2 f L_r}{2 \cdot g_c \cdot A_{\text{reg}}^2 \rho \cdot D_e} \quad (23)$$

and the heat added to the working fluid because of friction in the regenerator by

$$Q_{\text{rf}} = \frac{\Delta P_{\text{reg}} \dot{m}}{\rho J} = \frac{\Delta P_{\text{reg}} (P_{\text{max}} + P_{\text{min}}) V_c N}{\rho J R T_c} \quad (24)$$

The limiting value of the film coefficient in the regenerator gives insufficient cooling of the working fluid as it flows from the hot to the cold end of the regenerator. The energy that is left in the working fluid because of the limiting value of film coefficient is computed from

$$Q_{\text{rh}} = (1 - \eta_r) \bar{m} C_p (T_h - T_c) = (1 - \eta_r) C_p (T_h - T_c) \frac{(P_{\text{max}} + P_{\text{min}}) V_c N}{2 R T_c} \quad (25)$$

The pressure of the working fluid as function of crank angle in an actual Vuilleumier refrigerator, which operates with negligible pressure drops (Δp in heat exchangers and regenerators), is computed by Equation (6). The pressure-volume diagrams for the power- and refrigeration-producing sections of the refrigerator are then constructed. The performance of the

refrigerator is determined from these diagrams by integrating them graphically since

$$\oint dQ = \oint PdV. \quad (26)$$

Thus, the basic amount of heat that must enter the power-producing section and the net amount of heat absorbed by the refrigerating section of the Vuilleumier refrigerator are determined in this manner.

Generally, the flow passages are such that aerodynamic friction cannot be neglected and the associated pressure drop has to be accounted for in constructing the pressure-volume diagrams. The mass flow rates in and out of the compression and expansion volumes can be computed since the rates of change of volume and pressure with respect to time can be calculated from within a knowledge of the exact motion of the machine. The mass flow rates in the heat exchangers are computed by taking the average values of the mass flow rates of the gas entering and leaving the heat exchangers. The mass flow velocities in the various flow passages are computed from the mass flow rates since the dimensions of these passages are fixed. The pressure drops in the flow passages are computed from the equation

$$\Delta P_{ij} = \frac{\rho U_f^2 L_{ij}}{8g_c r_h} \quad (27)$$

and the fluid pressure in the regenerator is taken to be the average pressure between the two ends of the regenerator.

The first set of computed pressure drops is then applied in calculating a second value of the mass flow rates since new pressures of the working fluid in the various sections of the refrigerator are computed from the pressure drops and since new values of the rate of change of pressure with respect to time are computed by applying the new values of pressure. The second set of values of mass flow rate is then applied to calculate a second set of values of pressure drops. These values are then applied to calculate

a third set of values of mass flow rates and so on until the difference between the last and previous sets of calculated values of pressure and mass flow rate is negligible from the viewpoint of Vuilleumier refrigerator design. The final Pressure-Volume diagrams are constructed from the last computed values of the pressure, and the performance of the refrigerator is determined from these diagrams by applying Equation (26).

UNDESIRABLE HEAT TRANSFER LOADS

The discussion in the preceding sections did not consider the various undesirable heat transfer loads that are associated with the power- and refrigeration-producing sections of the Vuilleumier refrigerator.

Heat transfer takes place between the ends of the two cylinders of the Vuilleumier refrigerator shown in Figure 6. Hence, heat flows or is transported by the pistons from cylinder volumes V_H to V_A and from cylinder volumes V_A to V_C because of the differences in the temperatures of the respective cylinders. Thus, the refrigeration producing section of the refrigerator has to be designed so that it can handle the required cooling load plus the heat that is transferred from V_A to V_C . The power-producing section of the refrigerator must be so designed that it can absorb from the applied heat source the amount of heat needed to produce the necessary work output, i. e., the amount of heat necessary to supply power plus the heat that is transferred from V_H to V_A . Clearly, it is desirable to try to minimize the sum of the heat transfer modes between the respective volumes. This sum consists of the shuttle heat transfer, the pumping heat transfer, the heat conducted through the piston, the heat conducted along the cylinder wall, and the heat generated by friction between the piston and the cylinder wall.

Shuttle Heat Transfer

Shuttle heat transfer is a transfer of heat that is caused by the oscillation of the piston within its cylinder if the thermal gradients of the piston and the cylinder are nearly identical at the midpoint of the stroke. The heat

transfer occurs when the piston absorbs heat at the hotter half of its travel because at this position there is a difference between the temperature of the cylinder (cold end) wall and that of the piston and heat flows from the cylinder wall to the piston. During the other portion of the stroke, the difference between the temperature of the piston and that of the cylinder causes this heat to be deposited in the vicinity of the load. If the piston motion is approximately harmonic and the thermal time lag of the cylinder and piston materials is small compared with the reciprocating time the shuttle heat transfer can be computed as:

$$Q_{sh} = \frac{Y_p^2 C k_g (T_h - T_c)}{8 S L_{cy}} \int_0^{2\pi} (1 + \sin \theta)^2 d\theta \quad (28)$$

Integrating the shuttle heat transfer over one cycle gives the shuttle power loss

$$Q_{sh} = 0.186 Y_p^2 C \frac{k_g}{S} \frac{(T_h - T_c)}{L_{cy}} \quad (29)$$

Pumping Heat Transfer

Pumping heat transfer occurs as the expansion chamber undergoes pressure changes and the annular space around the expansion piston therefore alternately becomes pressurized and depressurized. This variation in pressure follows the system pressure, and the gas that enters and leaves the annular space transports heat to or from the gas in the expansion volume V_C or V_H .

The mass of gas in the annular space is

$$M = V_a \rho; \quad (30)$$

Contrails

hence, the rate at which this mass flows out of the annular space is

$$\dot{m} = \frac{dM}{d\tau} = V_a \frac{d\rho}{d\tau} = V_a \frac{d\rho}{dP} \frac{dP}{d\tau}. \quad (31)$$

By applying the perfect gas law and using the average temperature between the hot and cold ends of the expansion cylinder, Equation (31) becomes

$$\bar{m} = \frac{V_a (P_{\max} - P_{\min}) N}{R \bar{T}} = \frac{D_c \pi L_{cy} S (P_{\max} - P_{\min}) N}{R \frac{T_h + T_c}{2}} \quad (32)$$

The annulus wall acts as a regenerator, and pumping heat transfer is therefore expressed as

$$Q_{pu} = \bar{m} C_p (T_h - T_c) (1 - \eta_r) \quad (33)$$

or, if the value of λ is large and the annulus walls are the same material, by

$$Q_{pu} = \frac{\bar{m} C_p (T_h - T_c)}{\lambda} = \frac{\bar{m} C_p (T_h - T_c)}{\frac{h \pi D_c L_{cy}}{\bar{m} C_p}} \quad (34)$$

In order to apply Equation (34) the heat transfer coefficient h has to be known or it must be expressed in terms of some known variables. For laminar flow, Reference 3 presents the relationship

$$\frac{h D_e}{k_g} = 1.5 \left(\frac{\bar{m} C_p}{k_g L_{cy}} \right)^{0.4} \quad (35)$$

If the equivalent diameter D_e is replaced with the hydraulic diameter of an annulus, the heat transfer coefficient is expressed as

$$h = \frac{1.5k_g}{2S} \left(\frac{\bar{m}C_p}{k_g L_{cy}} \right)^{0.4} \quad (36)$$

Substituting Equation (36) into Equation (34) gives

$$Q_{pu} = \frac{2\bar{m}C_p(T_h - T_c)S}{1.5\pi D_c \left(\frac{\bar{m}C_p}{k_g L_{cy}} \right)^{-0.6}} \quad (37)$$

and applying Equation (32) gives

$$Q_{pu} = \frac{2(\pi D_c)^{0.6} L_{cy}^{1.0} (P_{max} - P_{min})^{1.6} N^{1.6} C_p^{1.6} (T_h - T_c) k_g^{-0.6}}{1.5R^{1.6} \left(\frac{T_h + T_c}{2} \right)^{1.6}} S^{2.6} \quad (38)$$

Heat Transfer Through Piston

The heat transfer through the piston is due to the difference in the temperatures of the ends of the piston; it is expressed as

$$Q_p = \frac{k_p A_p}{L_p} (T_h - T_c). \quad (39)$$

Note: Since S is the radial clearance of an annulus, $D_e = 2S$.

The outer diameter of the hollow piston is computed from

$$D_{op} = D_c - 2S; \quad (40)$$

hence, the cross-sectional area of the piston is

$$A_p = \frac{\pi(D_c - 2S)^2}{4} - \frac{\pi D_{ip}^2}{4} = \frac{\pi}{4} \left[(D_c - 2S)^2 - D_{ip}^2 \right]. \quad (41)$$

Thus, by substituting Equation (41) into Equation (39) the heat transfer through the piston becomes

$$Q_p = \frac{k_p \pi \left[(D_c - 2S)^2 - D_{ip}^2 \right] (T_h - T_c)}{4L_p}. \quad (42)$$

Heat Transfer Through Cylinder Wall

The heat transfer along the cylinder wall is computed from

$$Q_w = \frac{k_{cy} A_w}{L_{cy}} (T_h - T_c). \quad (43)$$

The thickness of the cylinder wall is calculated with respect to stress and is

$$t = \frac{P_{\max} r_{\text{avg}}}{\sigma}, \quad (44)$$

where the average radius r_{avg} is expressed by

$$r_{avg} = \frac{D_c}{2 \left(1 - \frac{P_{max}}{2\sigma} \right)}. \quad (45)$$

Thus, the cross-sectional area of the cylinder wall is

$$A_w = \frac{\pi P_{max} D_c r_{avg}}{\sigma \left(1 - \frac{P_{max}}{2\sigma} \right)}, \text{ or } \frac{\pi P_{max} D_c^2}{2\sigma \left(1 - \frac{P_{max}}{2\sigma} \right)^2} \quad (46)$$

and the heat transfer through the cylinder wall becomes

$$Q_w = \frac{\pi k_{cy} P_{max} D_c^2}{2L_{cy} \sigma \left(1 - \frac{P_{max}}{2\sigma} \right)} (T_h - T_c). \quad (47)$$

Heat Generated by Friction Between Piston and Cylinder Wall

From simple mechanics, the heat generated by this friction is computed to be

$$Q_f = \oint F_f dL \quad (48)$$

where

F_f = friction force in the direction of travel

Contrails

The summation of the undesirable heat transfer loads is

$$Q_{ut} = Q_{sh} + Q_{pu} + Q_p + Q_w + Q_f + Q_{rf} + Q_{rh} \quad (49)$$

which in general is the amount of "lead loss" that must be cooled at V_C or supplied to V_H in the reflective cases.

Another method of studying the thermodynamics and heat transfer of the Vuilleumier refrigerator consists of dividing the refrigerator into several volumes, each volume representing a thermodynamic system, and then deriving an energy balance on each system (References 10 through 14). The result of applying this method is a number of unsteady-state energy equations of the form

$$\begin{aligned} \Sigma \text{ energy} &= MC' \frac{dT}{d\tau} & (50) \\ \dots & \\ \dots & \end{aligned}$$

a number of mass flow rate equations of the form

$$\begin{aligned} \dot{m}_{in} - \dot{m}_{out} &= \frac{d(\dot{m})}{d\tau} & (51) \\ \dots & \\ \dots & \end{aligned}$$

and a number of pressure drop equations of the form

$$\begin{aligned} \Delta P_{ij} &= \frac{\dot{m}_{ij}}{k_{ij}} & (52) \\ \dots & \\ \dots & \end{aligned}$$

Contrails

By solving these equations simultaneously and by applying the perfect gas law, it is possible to determine the temperature, the mass of working fluid and the pressure in any one of the thermodynamic systems at any instant that the refrigerator is operating. Thus, a history of the unsteady- and steady-state thermodynamic behavior of the refrigerator is obtained for each particular design. The design and hence the inputs to the equations can be varied so that the last solutions of the equations give an optimum design for the refrigerator. This method is complicated and requires computer solutions since the number of energy equations is generally large and they have to be solved by means of the finite difference technique. However, if accurate values of the coefficients of heat transfer within the cylinders are available or can be computed, this method presents a means of determining the thermodynamic and heat transfer characteristics of the Vuilleumier refrigerator when the refrigerator cannot be considered to operate isothermally in the power- and refrigeration- producing volumes and when the aerodynamic friction in the refrigerator cannot be neglected.

DISCUSSION

In developing the equations that control the thermodynamic behavior of the Vuilleumier refrigerator, it was assumed that the temperature of the working fluid in the expansion and compression volumes remained constant during a cycle. This assumption resulted in relatively simple computations; however, the isothermal condition is not achieved in practice since the refrigerator would have to run at almost zero speed or the heat transfer film coefficient of the working fluid in the expansion and compression volumes would have to be infinitely large for a fixed heat transfer area. The thermodynamic state of the working fluid in the expansion and compression volumes of an actual Vuilleumier refrigerator therefore lies somewhere between adiabatic and isothermal conditions and generally closer to the adiabatic conditions. Isothermal conditions in the expansion and compression volumes make the refrigerator produce more power and refrigeration than it would if the conditions in these volumes were adiabatic. Hence, it is

Contrails

very desirable to construct the refrigerator so that the working fluid in the expansion and compression volumes comes as close as possible to the isothermal condition. This usually requires operation at low speed (rpm), a large area for heat transfer to the working fluid, and a high degree of turbulence in the working fluid in the expansion and compression volumes, but it can be achieved if special techniques are applied in designing the refrigerator.

A refrigerator employing a regular cylinder and piston operates almost adiabatically in its expansion and compression volumes. It is shown in Reference 13 that a Stirling refrigerator which operated adiabatically in the expansion and compression cylinders and which operates at an expansion-compression cylinder volume ratio of unity, a phase angle of 90 degrees and an absolute temperature ratio of 2 has a coefficient of performance that is only about 50 percent of the coefficient of performance when the thermal conditions in the expansion and compression cylinders are isothermal. The thermal efficiency of a Stirling heat engine, with the same volume ratio, phase angle, and absolute temperature ratio as above, is also only about 50 percent of the value of thermal efficiency when the thermal conditions in the expansion and compression cylinders are isothermal; see Reference 14.

The dead volumes which are associated with the power- and refrigeration-producing sections of the Vuilleumier refrigerator should be as small as possible since the performance of the refrigerator per unit weight of working fluid decreases when the dead volume increased. However, the design of a Vuilleumier refrigerator generally involves many compromises because of the particular conditions under which the refrigerator is to be used. For instance, the optimum phase angle design is in many cases replaced with one based on the maximum allowable pressure in order that the weight of the refrigerator may become acceptable.

SECTION IV

THEORETICAL COMPARISON OF VUILLEUMIER REFRIGERATOR WITH OTHER PRACTICAL CRYOGENIC REFRIGERATORS AND FUTURE APPLICATIONS ENVELOPE OF VUILLEUMIER REFRIGERATOR

INTRODUCTION

The basic version of the Vuilleumier refrigerator and its thermodynamic cycles are discussed in Section III. The purpose of this section is to present a study of the advantages and disadvantages of the theoretical Vuilleumier thermodynamic cycle with respect to the thermodynamic cycles that are applied in other practical cryogenic refrigerators. The study also includes a discussion of the advantages and limitations of the Vuilleumier thermodynamic cycle together with graphs that relate the refrigerator cooling power, temperature, size, and weight to the future applications envelope of the Vuilleumier refrigerator.

COMPARISON OF VUILLEUMIER WITH OTHER REFRIGERATION SYSTEMS

This section presents the various features of the Vuilleumier refrigerator. It discusses the advantages and disadvantages of this refrigerator and points out the design factors which are important in constructing a high-performance refrigerator. It also compares this refrigerator with other cryogenic refrigerating systems.

Vuilleumier Refrigerator

The thermodynamic cycles of a Vuilleumier refrigerator that operates in a step-wise and discrete manner are either of the Stirling or the Ericsson type. These cycles consist of two isothermal processes – two constant-volume processes, and two isothermal processes – two constant-pressure processes, respectively. The motion of the pistons in a practical Vuilleumier refrigerator is not step-wise and discrete but sinusoidal and the constant-volume or the constant-pressure processes are therefore not strictly followed. The result is that the processes in the regenerators are

polytropic. However, the cycles in a practical Vuilleumier refrigerator are still thermodynamically reversible if the expansion and compression volumes operate isothermally and if the regenerators have a thermal efficiency of 100 percent. Since, with careful design, it is possible to reach nearly isothermal conditions in the expansion and compression volumes and since the regenerators can be designed so that they have a thermal efficiency that is close to 100 percent, a practical Vuilleumier refrigerator can be constructed that operates on cycles which are almost thermodynamically reversible. The thermodynamic cycles of a real Vuilleumier refrigerator are shown on pressure-volume diagrams in Section III.

From the above discussion, it is clear that a practical and well designed Vuilleumier refrigerator has a thermal efficiency and a coefficient of performance which approaches the thermal efficiency and the coefficient of performance of a Carnot heat engine and a Carnot refrigerator that operate between the same temperature limits as the Vuilleumier refrigerator.

The Vuilleumier refrigerator can also be designed so that it has a net power output which can be used, for instance, to generate electrical power for infrared electronics by means of an alternator. This unique feature is accomplished by sealing off the working volumes with respect to the crankcase and holding a gas pressure in the crankcase that is less than the pressure in the working volumes. The wear on the seals is small since the required pressure difference for a net power output is relatively small.

The noise level of the Vuilleumier refrigerator is low because of the nonexistent or very small gas pressure difference between the faces of the double-acting pistons. This also results in low bearing loadings and less wear.

In summary, the Vuilleumier refrigerator is a very compact and high-performance refrigerator that can produce refrigeration at cryogenic temperatures for long periods of time without maintenance. It can be powered by direct solar energy, electrical heating, exothermic chemical reactions, a gas burner and nuclear energy or isotopes. The refrigerator can be designed for ground, space and airborne operation. Its size and weight,

however, may render it impractical with respect to other cryogenic cooling systems when the required refrigeration power is above 100 watts. The advantages and disadvantages of the Vuilleumier cycle refrigerator, to supply cryogenic temperature cooling, can be summarized as follows:

1. The thermal efficiency and the coefficient of performance of the Vuilleumier cryogenic refrigerator are high because of the applied thermodynamic cycle and low mechanical friction. These are important features in any application.
2. The refrigerator can be designed so that it produces a net power output which can be converted to electrical power for operating electronic equipment together with the refrigerator in a specific mission or task. Thus, this design gives a compact power-and refrigeration producing unit.
3. The Vuilleumier refrigerator has a low wear rate on seals since the pressure difference across a dynamic seal in the machine is small or negligible. This is particularly true of a slow running unit that is designed so that no net power output is produced. This type of unit is driven with a small electrical motor in order to overcome the internal friction, and the low wear rate gives long maintenance-free operation.
4. The refrigerator can be powered by any practical heat source that can supply the desired temperature limit at the power cylinder. Thus, onboard fuel or electrical power can be used to power the machine.
5. The size and weight of the Vuilleumier refrigerator depends on the required refrigeration temperature and power. Other closed cryogenic cooling systems should therefore be investigated with respect to size, weight and performance when the required cooling power is around 100 watts since some of these systems may have a smaller size and weight at this refrigeration power level than the Vuilleumier refrigerator.

6. The refrigerator is an excellent spot cooler at relatively low refrigeration power levels because it is possible to obtain good performance even in very small size units. However, cooling can also be supplied to remove points by using an external cooling loop which contacts the cold cylinder of the refrigerator and the object to be cooled by means of a coolant circulated in a closed loop.
7. The practical Vuilleumier refrigerator is capable of producing refrigeration down to about 10°K . At lower temperatures the size of the high thermal efficiency regenerators becomes impractically large, since the value of the specific heat for all materials approaches zero when the absolute temperature approaches 0°K . This is a disadvantage to all refrigerators using regenerators. The regenerators must have a high thermal efficiency or the performance of the refrigerator will be poor.
8. The performance of the Vuilleumier cycle is strongly influenced by the total dead volume in the refrigerator since it causes the thermodynamic expansion-and compression paths of the gas in the refrigerating cylinder to come closer to each other. Thus, the result is a thin pressure-volume diagram and a smaller cooling power when the dead volume is increased. The effect of an increase in the dead volume is very pronounced in smaller refrigerators and every effort should, therefore, be made to keep the dead volume as low as possible in the smaller Vuilleumier refrigerators. The effect of increasing the dead volume is readily seen in a pressure-volume diagram by applying Equations 3 and 6 in Section III and plotting the gas pressure versus the swept volume of the piston in the refrigerating cylinder.
9. The performance of the refrigerator is also affected by the thermodynamic processes in the expansion and compression spaces. Ideally, these processes should be isothermal and, hence, the expansion-and compression spaces should be designed so that a

large heat transfer coefficient or a large heat transfer area is obtained for transferring heat across the boundaries of these spaces.

The Vuilleumier refrigerator is still in its development stage, but data from the first operating units indicates they are performing well. It can, therefore, be expected that the future Vuilleumier type refrigerators will show better performance as the design is improved. The latter sections of this report will incorporate actual data from several developmental machines.

A comparison between the Vuilleumier refrigerator and other cryogenic refrigerating systems points out several important features of the Vuilleumier refrigerator. These are:

1. The thermodynamic cycle of the ideal refrigerator is thermodynamically reversible, but this can never be accomplished practically since it would require the speed of the refrigerator to approach zero. However, the refrigerator is quite insensitive to irreversibilities because of the shape of its pressure-volume diagrams since the enclosed area of these diagrams is large, and not of the thin shape like the Carnot pressure-volume diagram. Therefore, the ideal cycle has become a practical cycle which can be applied in designing and constructing a real piece of machinery that provides cooling at cryogenic temperatures. The Stirling, the Gifford-McMahon, the Solvay, and the Pulse Tube cycles are also relatively insensitive to irreversibilities. The Vuilleumier refrigerators that have been built to date show a performance that is comparable to that of the Stirling refrigerator.
2. The refrigerator is very compact since refrigeration and power can be obtained from a unit that has only two cylinders.
3. The refrigerator can be powered by any practical heat source and the wear on seals is very low because of the small pressure differential between parts of the refrigerator. This small pressure differential also gives a low noise level to the refrigerator.

The Joule-Thomson, Claude, Stirling, Gifford-McMahon, Solvay and the Pulse Tube systems operate with greater pressure differences and have therefore a higher wear rate on seals and valves and have a higher noise level. The thermoelectric and thermomagnetic refrigerators operate silently, but show poor performance efficiency at cryogenic temperatures.

4. The refrigerator can be fitted into very small spaces because of its compact design; thus, no high pressure lines are necessary in order to supply refrigeration to remotely located objects. The Stirling refrigerator also has this feature. The Vuilleumier and the Stirling refrigerator are both excellent spot coolers since the object to be cooled can be connected to the refrigerators directly by means of the cold cylinder.
5. The design of the refrigerator is quite simple since its main parts are a crank, two cylinders with pistons, and two regenerators. No valves and no valve timing are involved as in the Gifford-McMahon and the Pulse Tube refrigerators.

The Joule-Thomson cycle refrigerator is also a very simple device to apply for obtaining cryogenic temperatures, but it has a low performance since the expansion in the throttling process is completely irreversible. A compressor with inlet and outlet valves is also needed when this technique is used.

The Claude cycle refrigerator is the only one that applies thermodynamic reversibility in producing refrigeration down to liquid helium temperatures. It is not possible to do this by using the Vuilleumier cycle only. However, a Vuilleumier refrigerator that is equipped with a compressor and a Joule-Thomson valve in a special loop is also capable of producing refrigeration at liquid helium temperatures.

The thermoelectric and the thermomagnetic refrigerators are both very simple in design since there are no moving parts. However, their refrigeration capacity and lower temperature level is limited by material properties and these refrigerators are, therefore, limited to cryogenic applications

where very low cooling power is required. Thus, the material for the thermoelectric and thermomagnetic cryogenic refrigerators has to be improved considerably if these refrigerators are to compete with the dynamic type cryogenic refrigerators.

VUILLEUMIER CYCLE AND REFRIGERATOR LIMITATIONS

The limitation on the Vuilleumier cycle, for low temperature refrigeration, is determined by the regenerators since these become impractically large when refrigeration is required below 10°K . As previously explained, this is due to the fact that the specific heat of any material approaches zero when the temperature approaches 0°K .

The limitation on the Vuilleumier cycle for power production at elevated temperatures is set by the metallurgical limit of the power producing cylinder of the refrigerator. Here again, it is a material problem since the strength of the hot cylinder material decreases as the temperature at which heat is added increases.

With respect to other practical cryogenic refrigerators, the Vuilleumier refrigerator is limited to a cooling power of about 100 watts because the size and weight of the refrigerator becomes relatively large at higher cooling power levels. Cryogenic turbo-expanders that are applied in a Claude cycle are probably the best devices when cooling powers of over 100 watts are required and when weight and size of the cryogenic refrigerator are important parameters in the application.

It is seen from the preceding discussion that the Vuilleumier refrigerator is a very good competitor in the cryogenic refrigerator field. Its thermodynamic cycle is sound and it is based on well defined thermodynamic principles that have been known for a long time, but which have not been practical until good material properties and machining techniques were developed. However, the fields of heat transfer, material properties, machining and manufacturing techniques are improving continuously. It is, therefore, expected that the overall performance of the Vuilleumier cryogenic refrigerator will also be improved in future designs.

DEVELOPMENT AND PERFORMANCE SUMMARIES OF OTHER PRACTICAL CLOSED CYCLE CRYOGENIC SYSTEMS

These development and performance summaries are shown in tabular form in Table 3. The table discusses other practical closed cycle refrigerating systems that produce refrigeration at cryogenic temperatures. Solid cryogen refrigerating devices are not discussed since they are open systems. The thermodynamic cycles of the dynamic systems and the controlling equations for the solid state refrigerating devices are presented in the appendix.

MAINTENANCE INTERVAL AND THE COEFFICIENT OF PERFORMANCE OF THE VUILLEUMIER REFRIGERATOR AND THE OTHER PRACTICAL CLOSED CYCLE CRYOGENIC SYSTEMS

These important factors are shown graphically in Figures 12 and 13. The various cryogenic refrigerators are compared with the Carnot refrigerator in Figure 12 which shows the ratio of power input to heat absorbed as a function of the temperature at which the heat is absorbed. The maintenance intervals and the ranges or operating temperatures for the refrigerators are shown in Figure 13.

Refrigerant Transfer Cycle

The cycle that results from combinations of an external refrigerant transfer loop and the previously described systems possesses no development problems that are not encountered with these systems. This cycle generally operates at the 1 atmosphere boiling temperature of suitable fluids, such as nitrogen, air, and neon, and one such system can produce 4 watts of cooling power at 80°K. The fluid in the external loop is circulated by means of a small pump and it is liquefied and vaporized at the cold cylinder and at the cooled object respectively. The fluid is transferred from the cold cylinder to the cooled object as small droplets that are surrounded by an insulating vapor envelope. Thus, the Leidenfrost phenomenon is applied in the transfer process. The refrigerant transfer cycle is very useful when cooling is required in small areas that are difficult to reach by other means.

Table 3. Development and performance summary of other practical closed cycle cryogenic systems

| System | Development | Performance | Application |
|--|--|--|---|
| I. Dynamic Systems | | | |
| 1. The Joule-Thomson System | The closed Joule-Thomson cycle has been well developed but has not been widely used because of its high power consumption and the possibility that the restricting orifice or J-T valve may become clogged when operating at small cooling loads. For cooling electronic devices, this system generally produces about 0.5 to 2.0 watts of refrigeration at a temperature of 88 or 77°K, depending on whether argon or nitrogen is used as the refrigerant. | The closed Joule-Thomson system has not been extensively used because of the low value of its coefficient of performance (COP). A typical value of COP is 1/250 at a temperature of 80°K; see Figure 12. Also, this system is not too reliable since the refrigerant may clog the valves or orifices when it is necessary to use small tubing at low refrigeration power levels. | All of the Dynamic systems can provide cooling down to 4.2°K. The J-T cycle uses three stages with N ₂ , H ₂ , He in the first, second, third stages, respectively. The other cycles apply a one stage He J-T cycle for the final expansion to 4.2°K. The Dynamic systems can be applied for cooling infrared devices, masers, parametric amplifiers, superconducting circuitry, superconducting computers and lasers. They can also be applied for extra-terrestrial hydrogen propellant reliquefaction. |
| 2. The Claude System | The Claude cycle is well developed and can provide about 2 watts of refrigeration at 2.5°K. By applying both the Claude liquid and gas cycles, temperatures ranging from 300 to 2.5°K can be theoretically achieved. Reciprocating engines or turbines are generally used for expanding the gas; however, the use of turbines in cooling loads of less than 2 watts has not as yet been successfully achieved. Helium is usually the refrigerant used in this system. | The reliability of the Claude system is good at the higher refrigeration powers (in the kilowatt range) but decreases as the refrigeration power decreases. The seals also pose a problem at these lower powers. Its COP is about 1/50 at 40°K, 1/100 at 20°K, and 1/200 at 4.2°K; see Figure 12. | |
| 3. The Stirling System | The Stirling cycle reached its greatest development after 1947, and its performance agrees fairly well with that predicted from theory. Systems of this kind can produce refrigeration power from milliwatts to kilowatts usually over a temperature range from 300 to 30°K. Helium is generally the working fluid and a temperature drop of 230°K from 300°K has been obtained and maintained by using a Stirling refrigerator with a one-stage expansion cylinder. Units weighing approximately 15 to 20 pounds have been operated for 400 hours before the working fluid had to be changed due to contamination from wear products. The performance of the units decreases sharply when the regenerator becomes contaminated from foreign material in the working fluid. These units provide about 10 to 15 watts of refrigeration at 77°K. | Although the Stirling system is quite reliable, difficulties with the seals may be encountered in multiple staging. The COP of an actual Stirling system is appreciably less than that of an ideal Stirling system, but it is still good in comparison with that of the other closed systems; see Figure 12. It usually ranges from 1/20 to 1/30 for systems cooling to 80°K and is about 1/350 at 30°K. | |
| 4. The Gifford-McMahon or Modified Ericsson System | This cycle is fairly well developed. ¹⁵ Systems with two stages have been built in which the first has 4 watts refrigeration capacity at 16°K, the second 18 watts at 50°K. One system has served as the base for a 4.2°K refrigerator. In these systems, too, helium is used as the working fluid. | The larger units of this type of system have good reliability, and one such unit has been in satisfactory operation for 2000 hours. This system has a COP of 1/500 at 14°K. A unit cooling a parametric amplifier was reported to have operated for 7000 hours before maintenance was necessary although scheduled interval was 2500 hours. | |

Table 3. Development and performance summary of other practical closed cycle cryogenic systems (continued)

| System | Development | Performance | Application |
|------------------------------|---|--|--|
| 5. The Solvay System | <p>The Solvay system has reached a fair stage of development. One model is a cascaded, two-stage machine that can provide 1 watt of refrigeration at 16°K. Another model is a three-stage Solvay system in which a Joule-Thomson system is used for the last expansion. The refrigeration power at the first, second, and third stages is 15, 9, and 1.5 watts, respectively. The corresponding temperature limits are 150, 50, and 15°K. The Joule-Thomson system, cooled by the Solvay system, expands helium down to about 1 atm and 4°K. The refrigeration power at this temperature level is 1 to 2 watts. In both models, helium is the refrigerant used.</p> | <p>The reliability of the Solvay system is about the same as that of the Stirling system. The valves in this system operate at approximately room temperature and do not pose any problems. Since the COP of the system is about 1/300 at 30°K and about 1/450 at 12°K, it is thermodynamically better than the Gifford-McMahon system; see Figure 12.</p> | |
| II. Solid-State Systems | | | |
| 1. The Thermoelectric System | <p>This type of system is well developed and is manufactured by several companies. Such systems have been built that can cool to 200°K. The basic thermoelectric material used is a negative- and positive-type (n- and p-type) bismuth-tellurium (Bi₂Te₃) alloy, which is doped with various impurities to increase the refrigeration potential.</p> <p>A negative-type (n-type) crystal of a semiconducting alloy consisting of bismuth and antimony with about 12-percent antimony has a figure of merit of 6×10^{-3} per degree at 77°K and this value can be increased to about 9×10^{-3} per degree if a magnetic field of about 700 gauss is applied perpendicular to the flow of current in the crystal.¹⁶</p> | <p>This system has good reliability; its COP is about 1/500 at 200°K (see Figure 12) but decreases rapidly as the refrigeration temperature level falls below 200°K. The low value of COP that is characteristic of thermoelectric systems is due to the materials of which they are made. The best semiconducting compound at present is Bi₂Te₃ and compounds composed of elements in Groups IV, V, and VI in the periodic table. These compounds have a figure of merit of 2.5 to 3.0×10^{-3} per degree at room temperature.</p> | <p>The thermoelectric system can provide cooling down to 200°K when it is cascaded and is thus applicable for cooling electronic devices above 200°K.</p> |
| 2. Thermomagnetic System | <p>The thermomagnetic system is still in the research stage; no practical commercial version has yet been built. However, this system is simpler than a thermoelectric system since it consists of only one material and can be staged¹⁷ simply by shaping the conductor. The best material at present for the conductor of a thermomagnetic system is a single crystal of bismuth that contains 0 to 5 percent antimony.¹⁸ A thermomagnetic system is most effective when it is combined with a thermoelectric system.</p> | <p>When it has been completely developed, a thermomagnetic system should be as reliable as a thermoelectric system. It will probably perform best when it is combined with a thermoelectric system to produce refrigeration at about 70°K. However, the COP of such a combined system is very low if materials now available are used. For instance, to absorb 1 milliwatt of heat at 70°K would require a power input of 10,000 watts if the system operates between 300 and 70°K. This optimized system consists of an optimized five-stage thermoelectric device and two shaped Ettingshausen devices. Such a system would occupy a volume of about 1700 to 3400 cubic inches and would weigh about 55 to 100 pounds.</p> | <p>The thermomagnetic system can provide cooling down to 230°K from an ambient temperature of 300°K. Theoretically, a combination of thermoelectric and a thermomagnetic system can provide a small cooling power at 70°K, but such a system is not practical because of its size and weight with respect to the dynamic systems. The thermoelectric-thermomagnetic system may be practical for cooling electronic devices between 150 and 400°K when the boundary conditions make it desirable to apply a solid-state refrigerator.</p> |

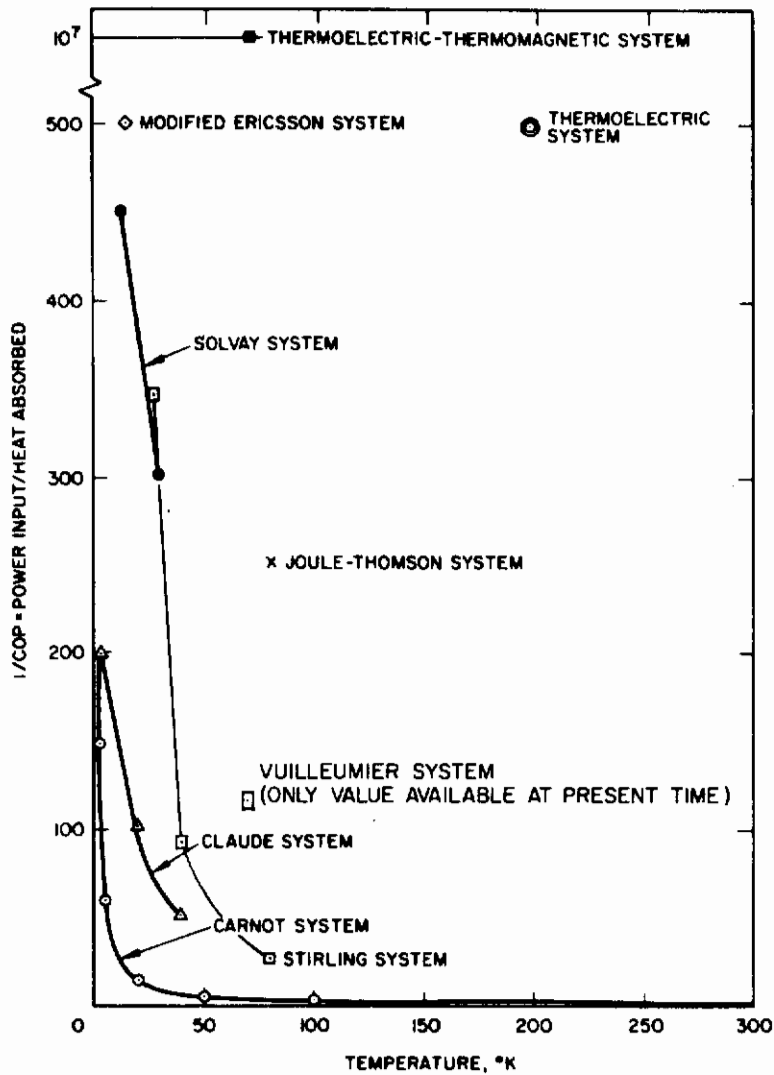


Figure 12. Values of 1/COP at a given temperature for Carnot and other cryogenic systems. The temperature at which heat is dissipated is 300°K.

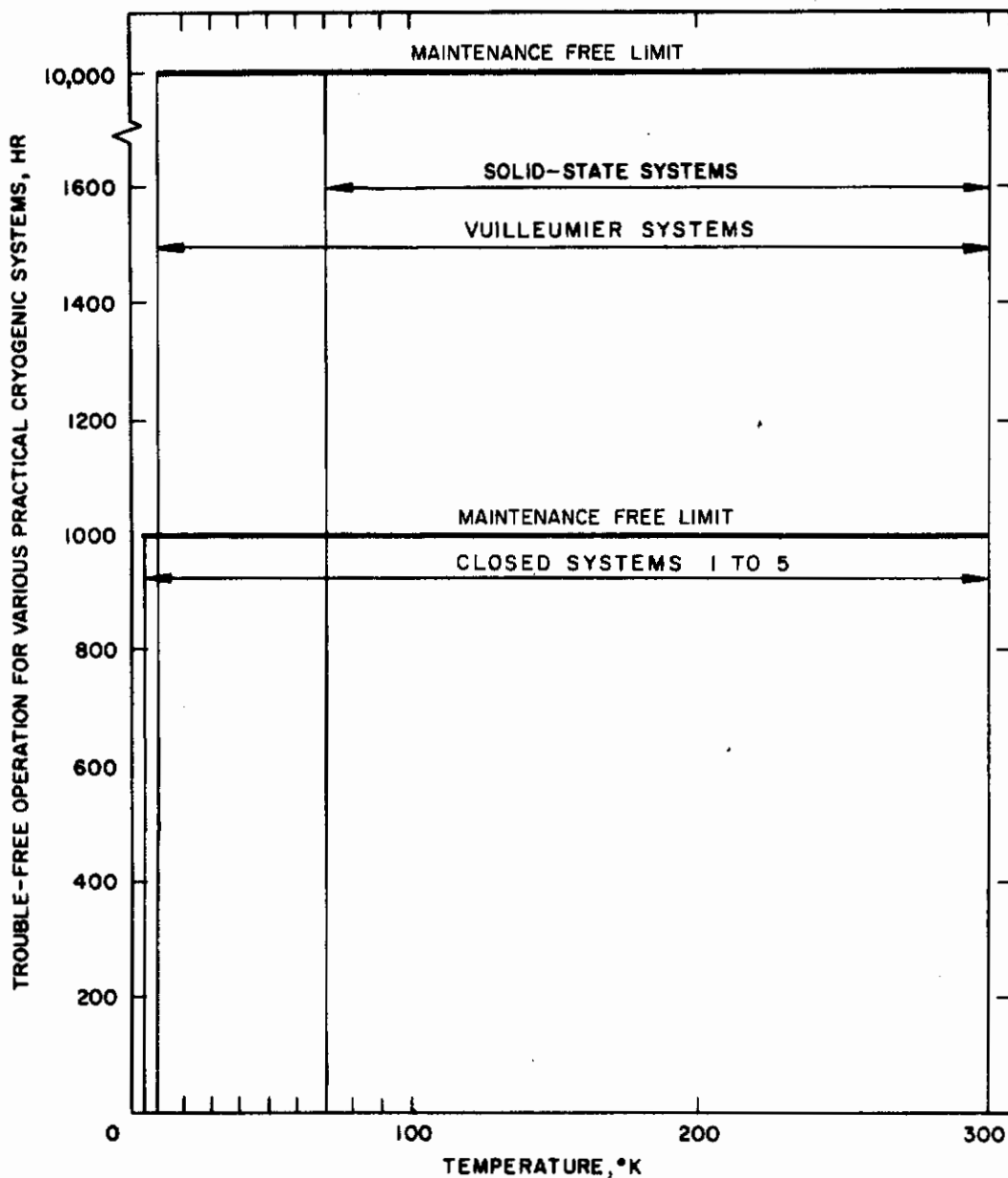


Figure 13. Maintenance interval as a function of refrigeration temperature range for various cryogenic systems.

FUTURE APPLICATIONS ENVELOPE FOR VUILLEUMIER REFRIGERATION

This section presents the future applications envelope for the Vuilleumier refrigerator by means of a number of graphs to determine descriptive refrigerator parameters, given the desired performance parameters. These graphs have been constructed by applying the thermodynamic and heat transfer equations that were derived in Section III.

Specifically, the graphs supply the designer of a Vuilleumier refrigerator that is to be used in an application in which the refrigeration load and the refrigeration and ambient temperatures are known with the following information:

1. The gross available refrigeration power at a chosen speed and swept cold cylinder volume of the unit is found from Figures 14, 16, 18, 20, 22, 24, 26, 28, 30, 32, 34, and 36.
2. The minimum required power to the hot cylinder at the chosen speed and swept cold cylinder volume is found from Figures 15, 17, 19, 21, 23, 25, 27, 29, 31, 33, 35, and 37.
3. The refrigeration losses at this speed and at the swept cold cylinder volume for a chosen length of the cold cylinder are found from Figures 38 through 41.
4. The net refrigeration power available from the unit is found by subtracting the losses from the gross available refrigeration power.
5. The required swept volume in the hot cylinder with respect to that in the cold cylinder at the given refrigeration and ambient temperatures is found from Figures 42 through 44.
6. The heat transfer losses for a chosen length of the hot cylinder at the required swept hot cylinder volume and at ambient temperature is found from Figure 45, 45A, and 45B.

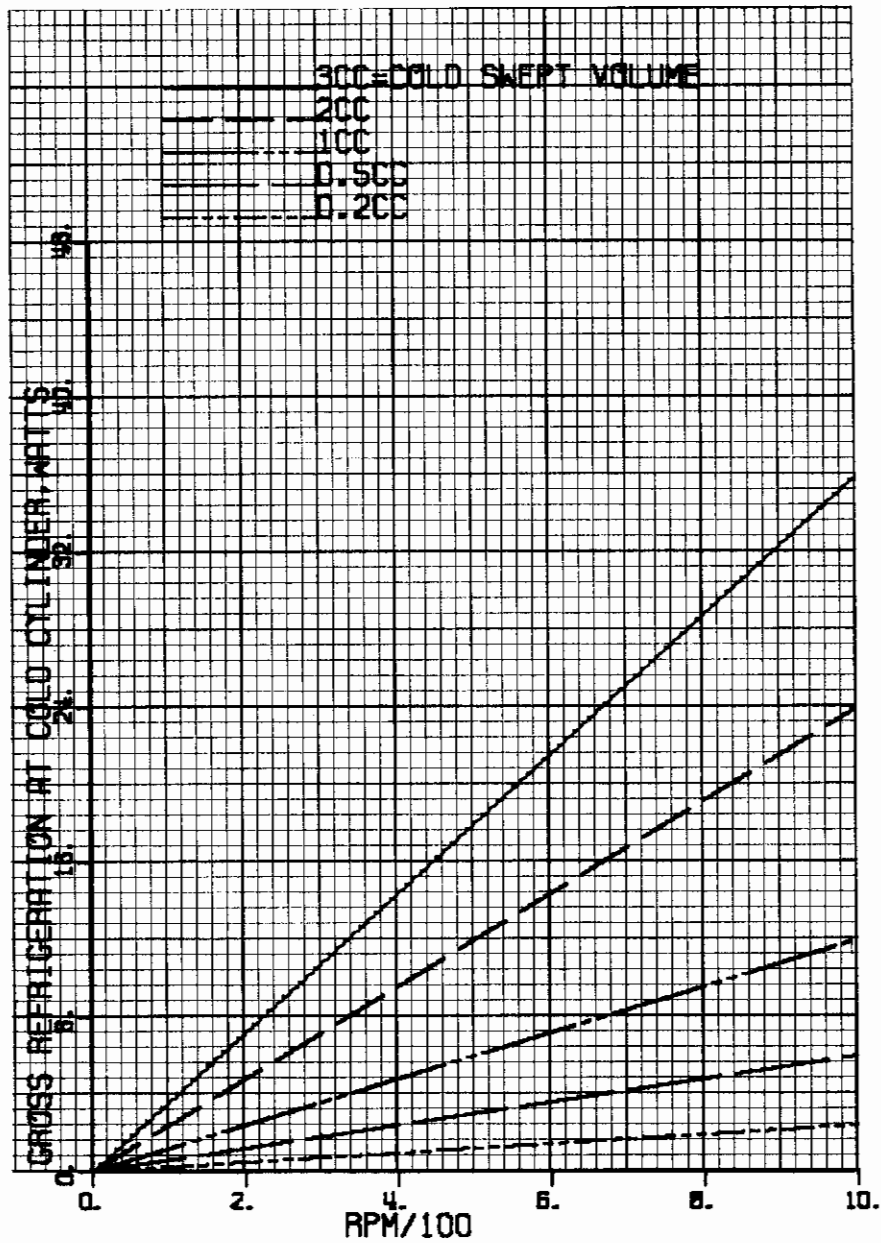


Figure 14. Gross refrigeration as a function of rpm when volume of cold cylinder is a parameter of VM refrigerating unit that produces no net power output when

refrigerating temperature limit = 120°K
 heat rejection limit = 300°F
 power cylinder temperature = 1200°F

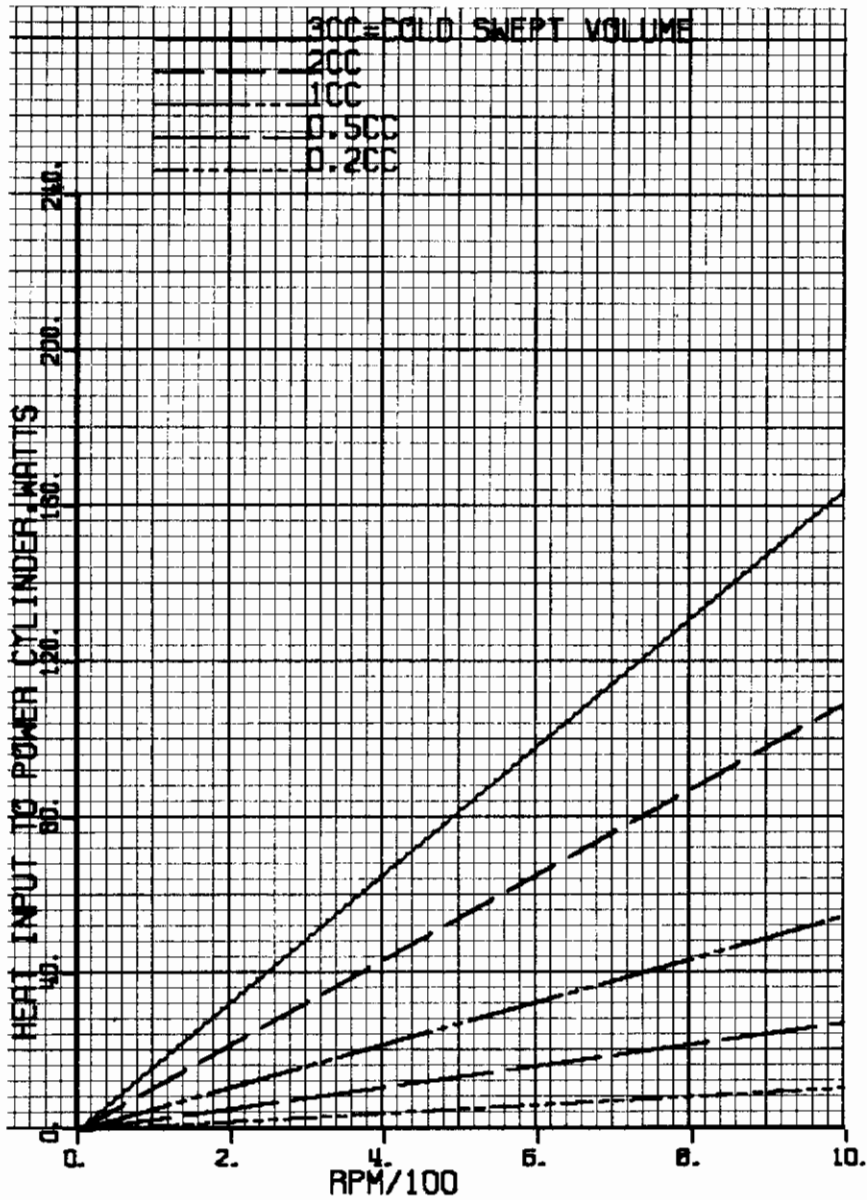


Figure 15. Required heat input to power cylinder as a function of refrigerator rpm with volume of cold cylinder as a parameter for VM machine of Figure 14.

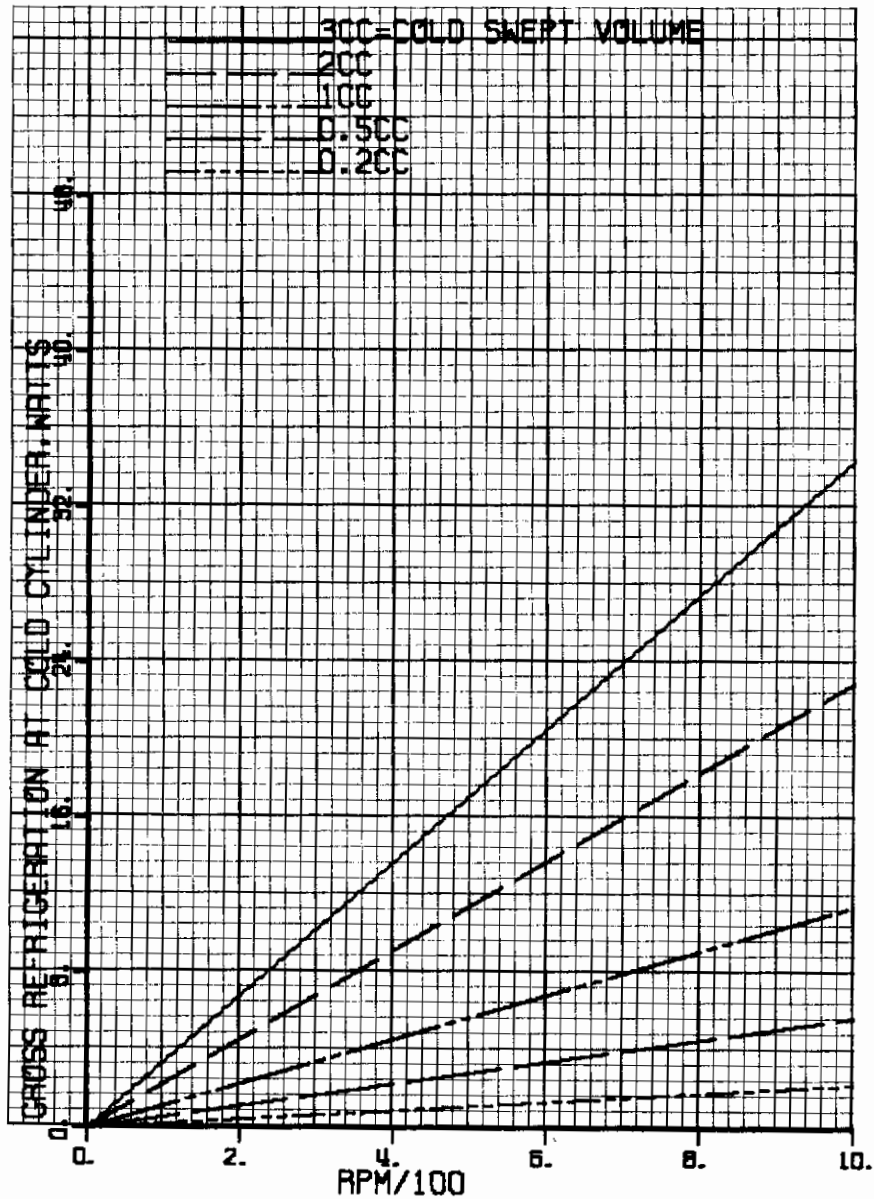


Figure 16. Gross refrigeration as a function of rpm when volume of cold cylinder is a parameter of VM refrigerating unit that produces no net power output when

refrigerating temperature limit = 120°K
 heat rejection limit = 160°F
 power cylinder temperature = 1200°F

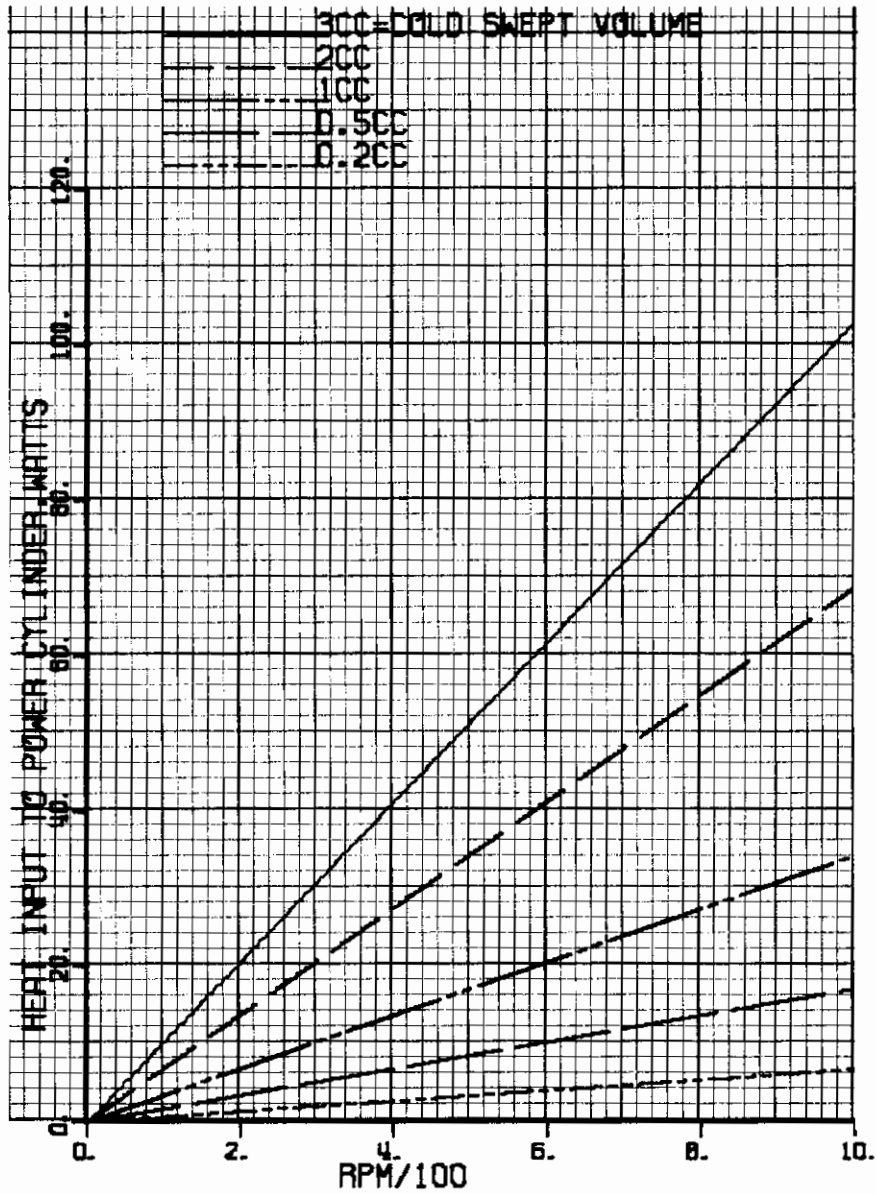


Figure 17. Required heat input to power cylinder as a function of refrigerator rpm with volume of cold cylinder as a parameter for VM machine of Figure 16.

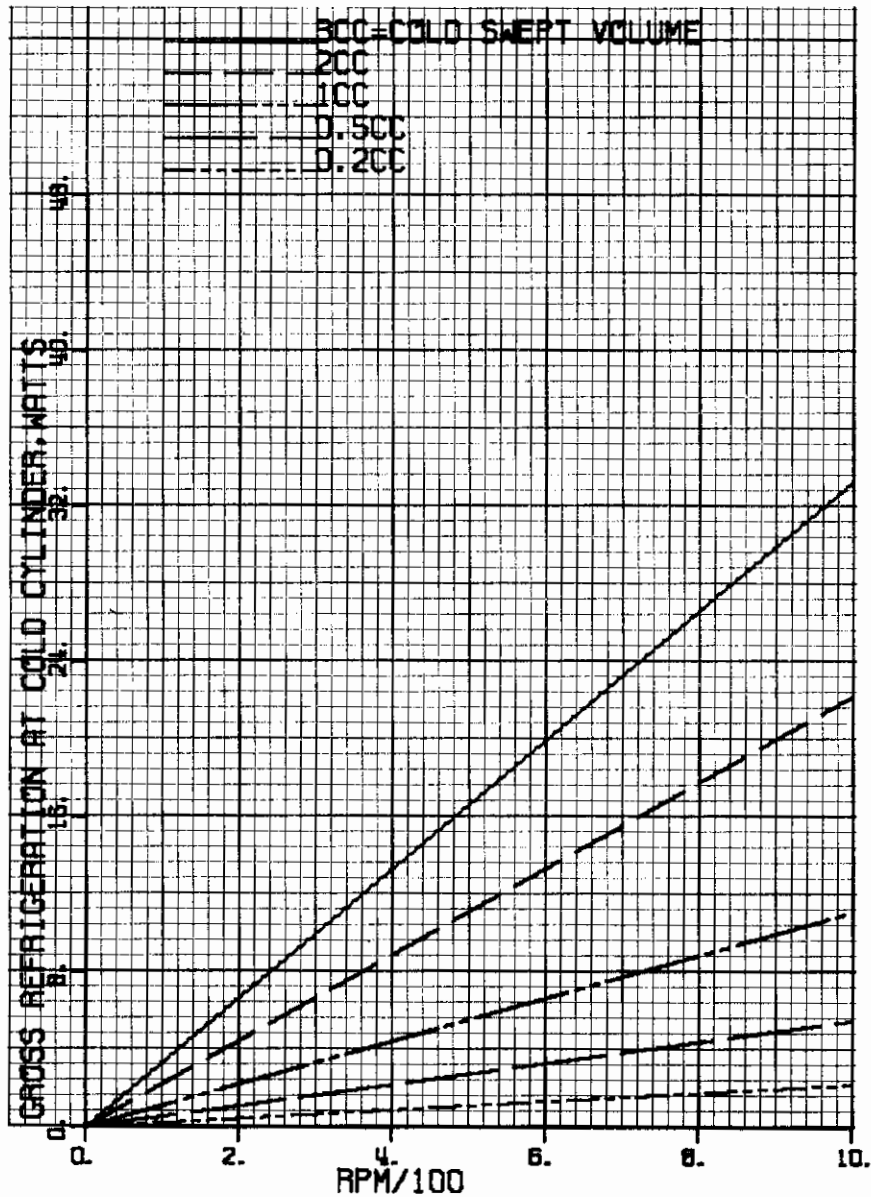


Figure 18. Gross refrigeration as a function of rpm when volume of cold cylinder is a parameter of VM refrigerating unit that produces no net power output when

refrigerating temperature limit = 120°K
 heat rejection limit = 70°F
 power cylinder temperature = 1200°F

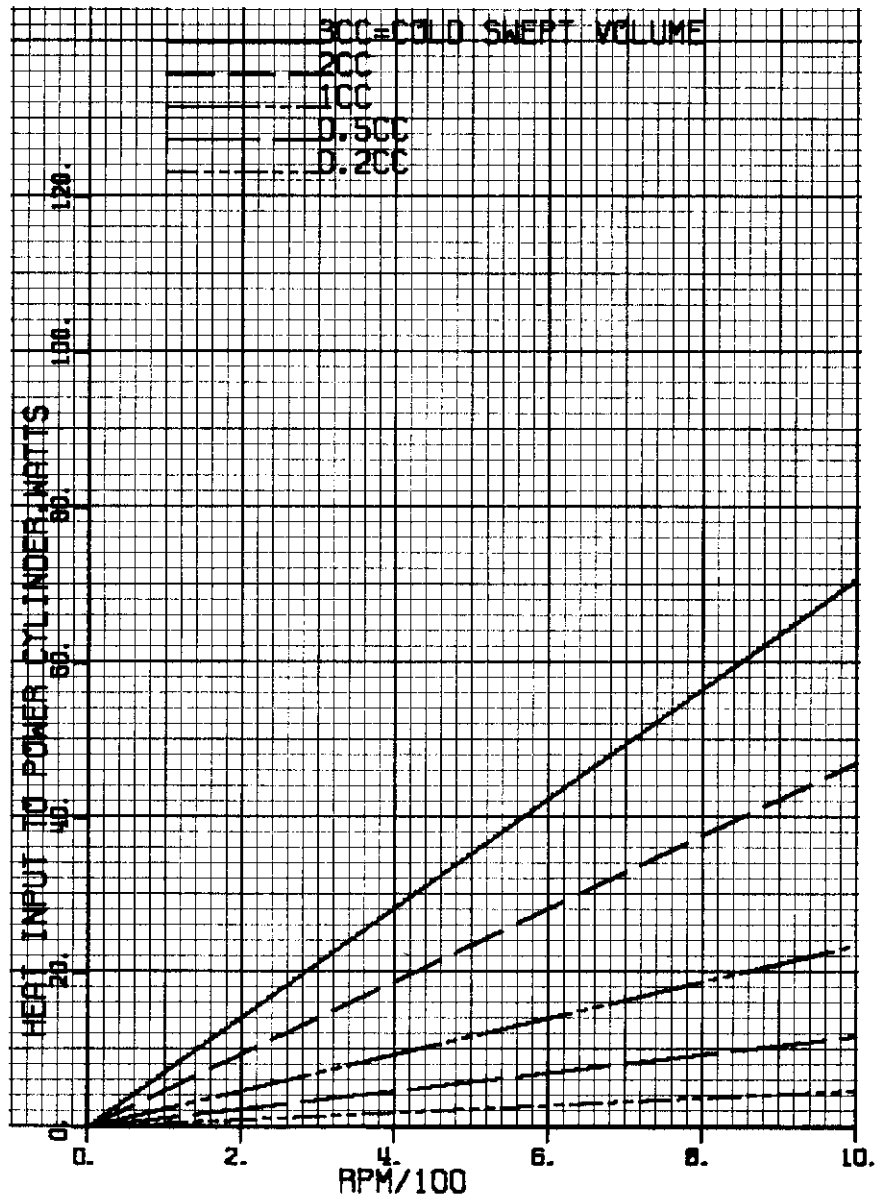


Figure 19. Required heat input to power cylinder as a function of refrigerator rpm with volume of cold cylinder as a parameter for VM machine of Figure 18.

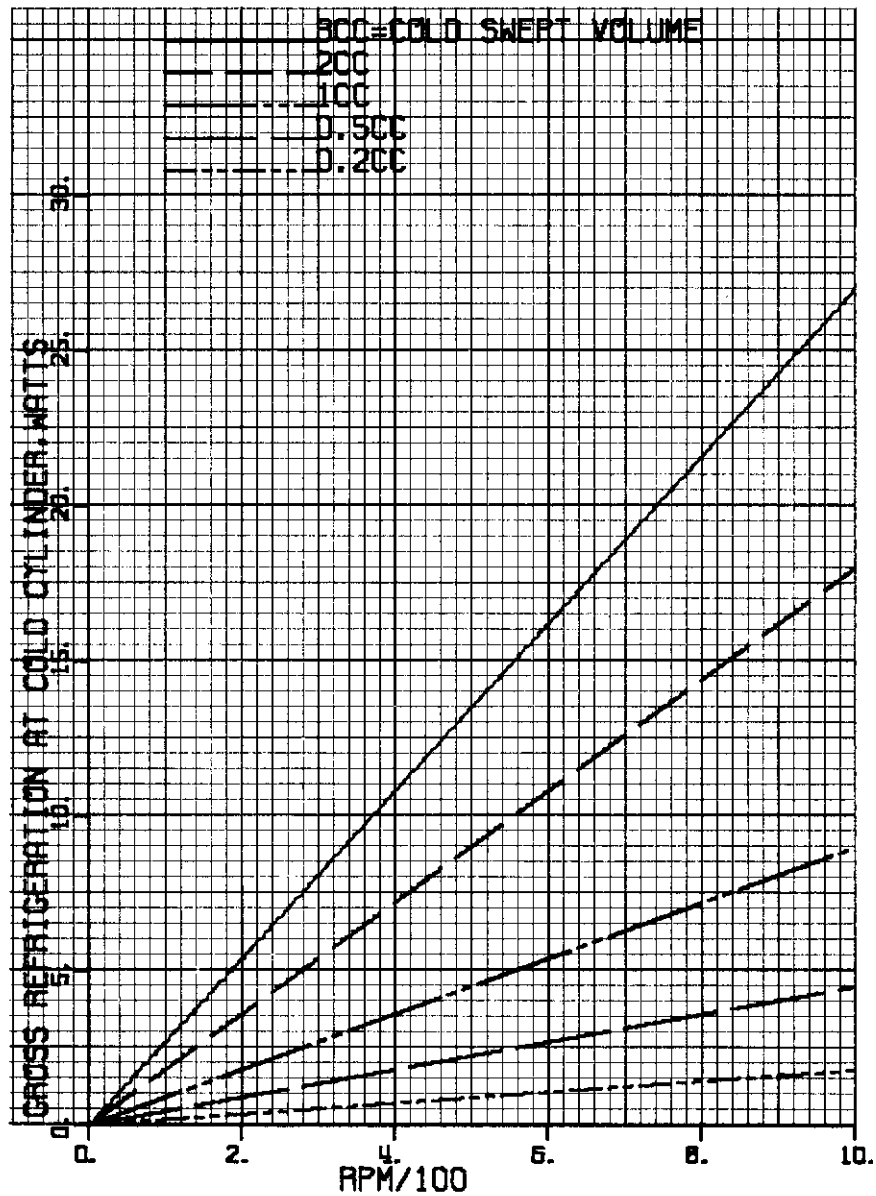


Figure 20. Gross refrigeration as a function of rpm when volume of cold cylinder is a parameter of VM refrigerating unit that produces no net power output when

refrigerating temperature limit = 120°K
 heat rejection limit = -65°F
 power cylinder temperature = 1200°F

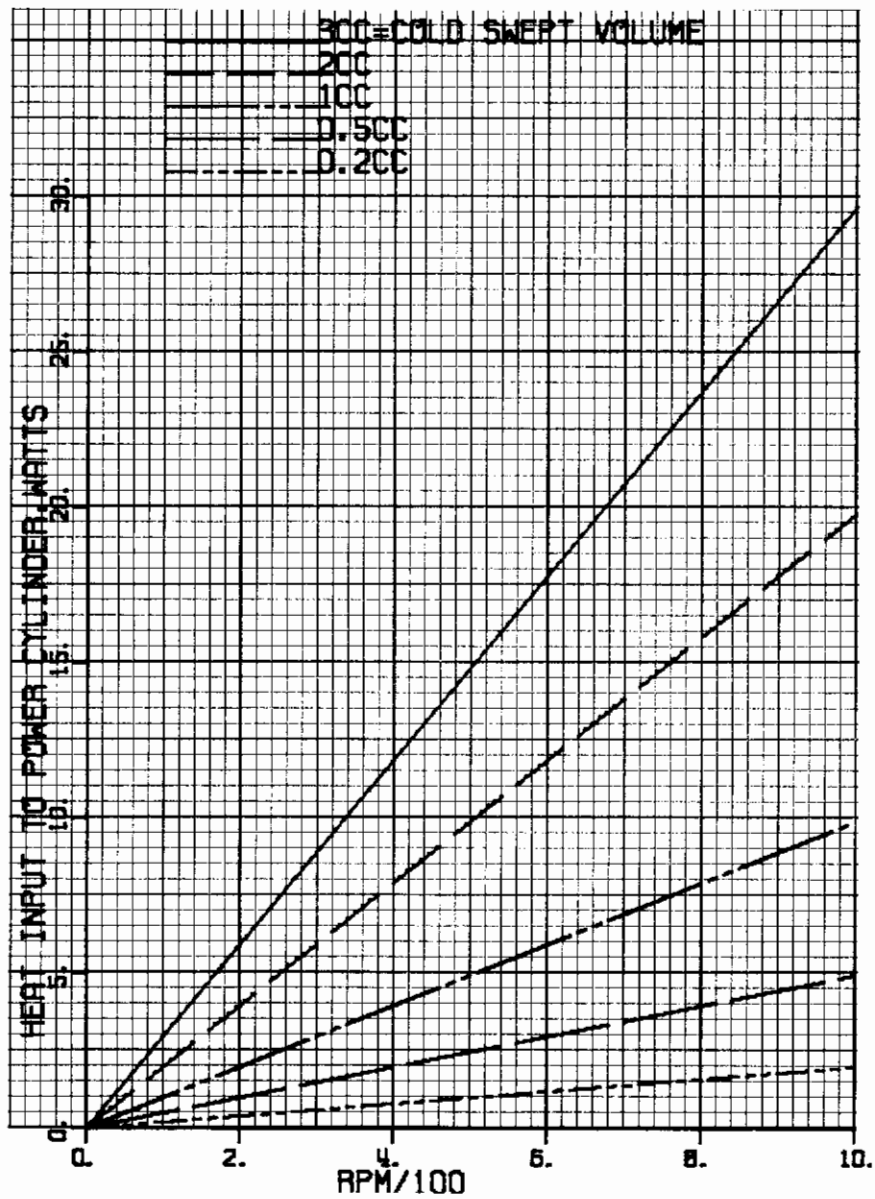


Figure 21. Required heat input to power cylinder as a function of refrigerator rpm with volume of cold cylinder as a parameter for VM machine of Figure 20.

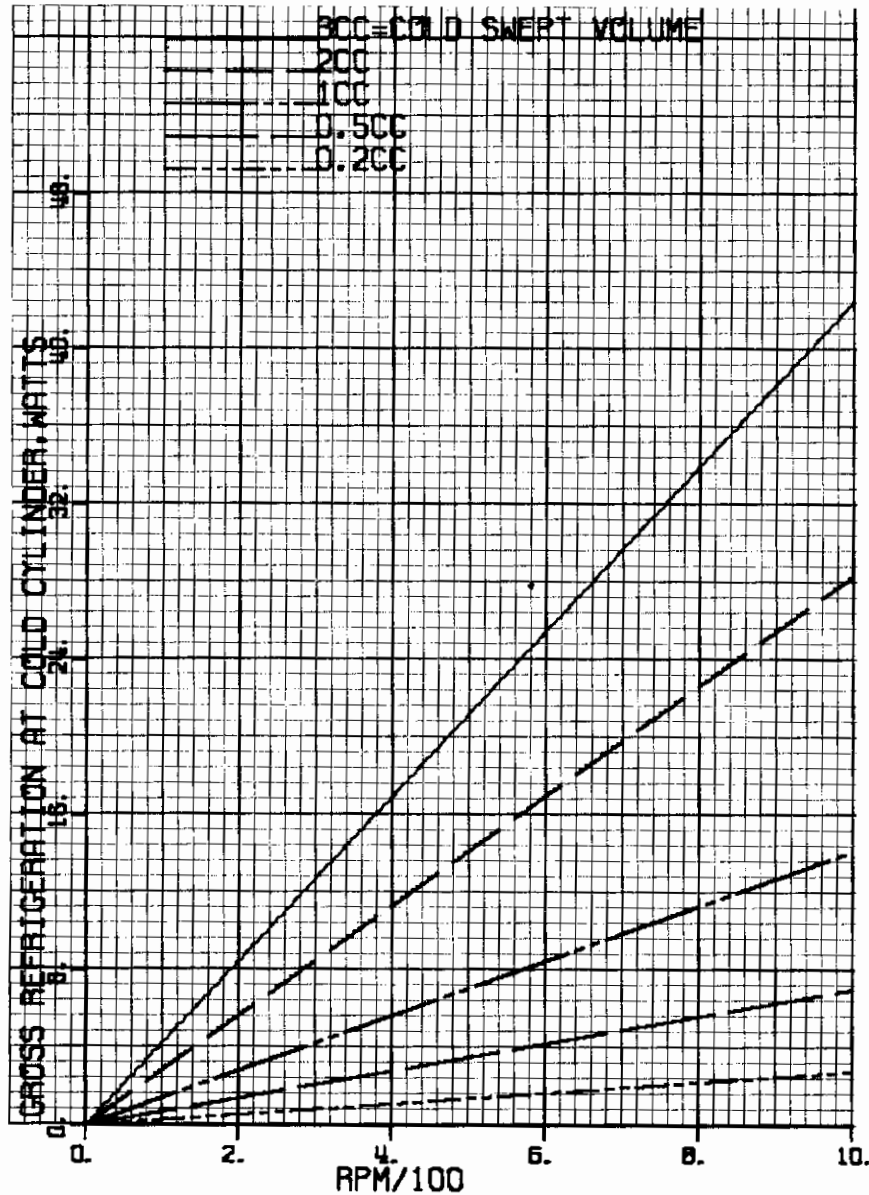


Figure 22. Gross refrigeration as a function of rpm when volume of cold cylinder is a parameter of VM refrigerating unit that produces no net power output when

| | |
|---------------------------------|----------|
| refrigerating temperature limit | = 70°K |
| heat rejection limit | = 300°F |
| power cylinder temperature | = 1200°F |

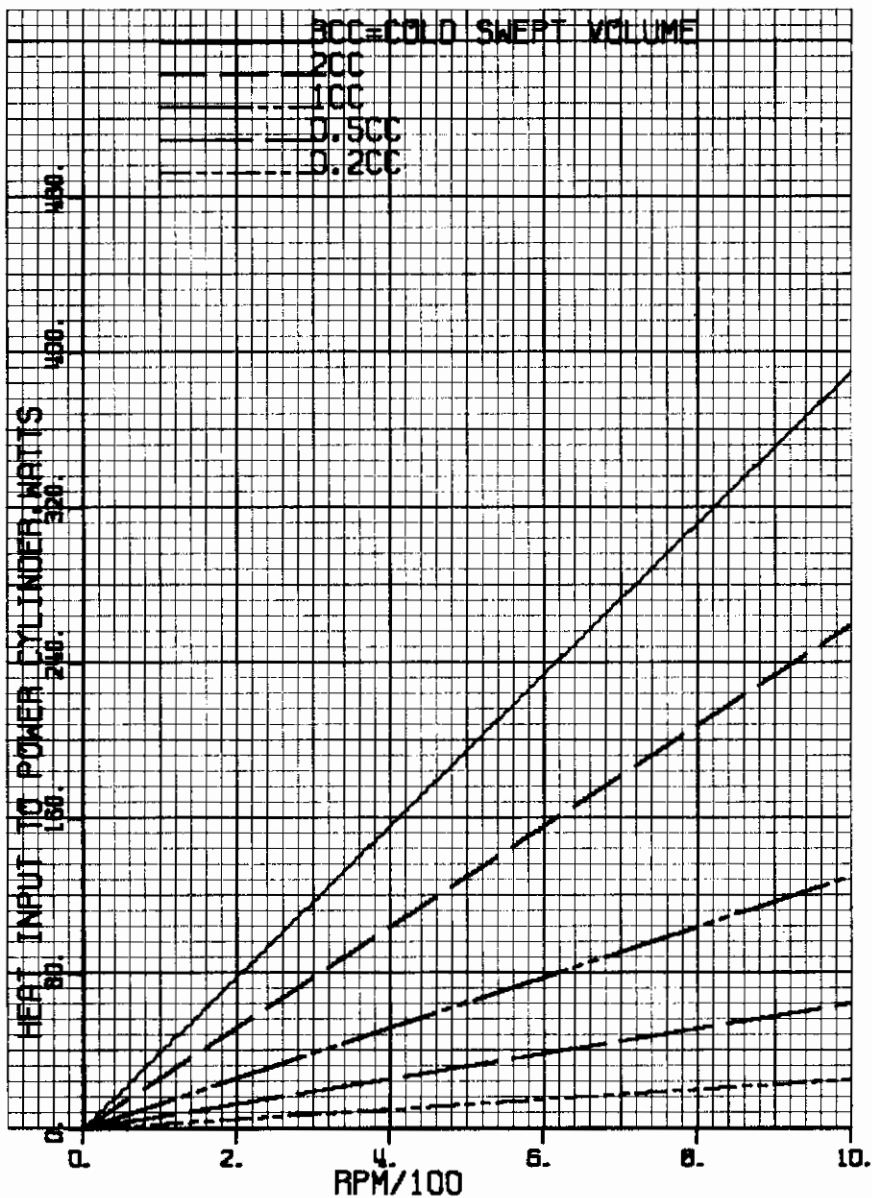


Figure 23. Required heat input to power cylinder as a function of refrigerator rpm with volume of cold cylinder as a parameter for VM machine of Figure 22.

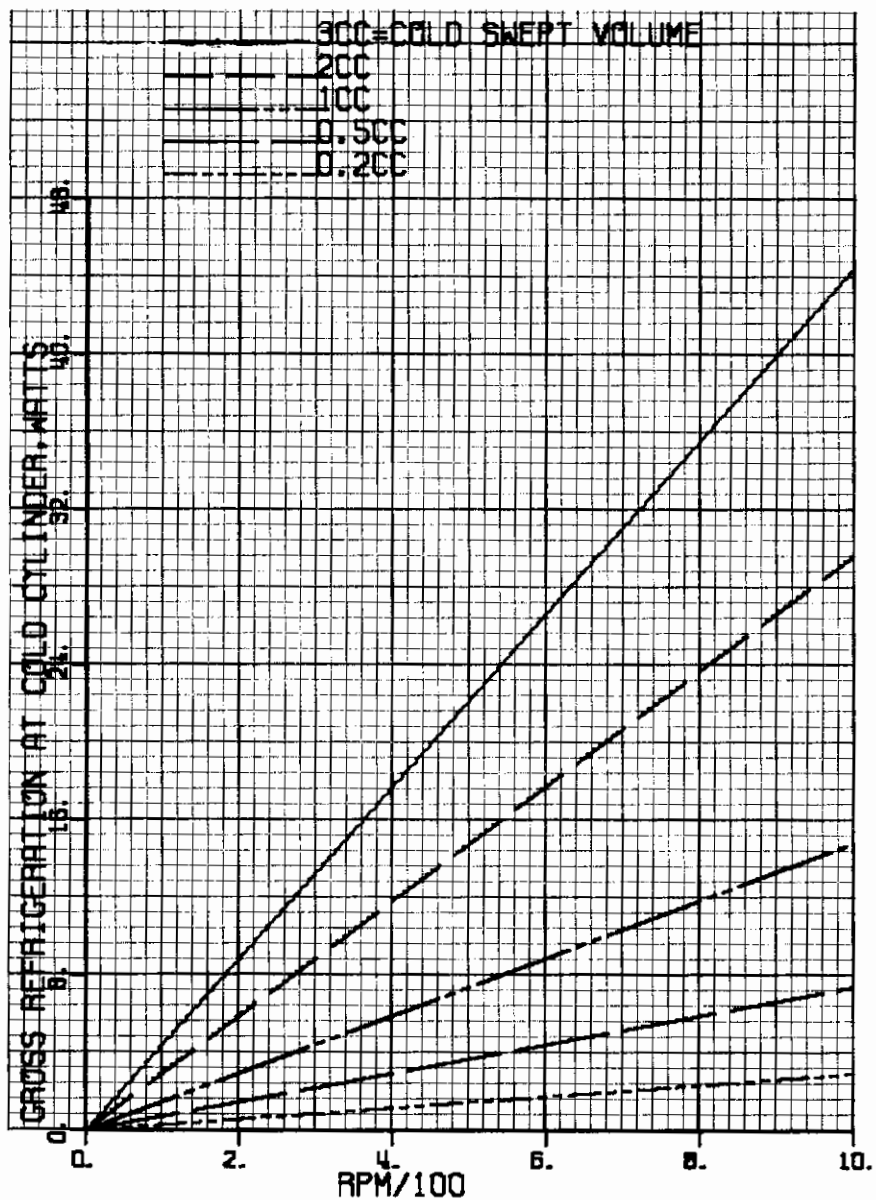


Figure 24. Gross refrigeration as a function of rpm when volume of cold cylinder is a parameter of VM refrigerating unit that produces no net power output when

refrigerating temperature limit = 70°K
 heat rejection limit = 160°F
 power cylinder temperature = 1200°F

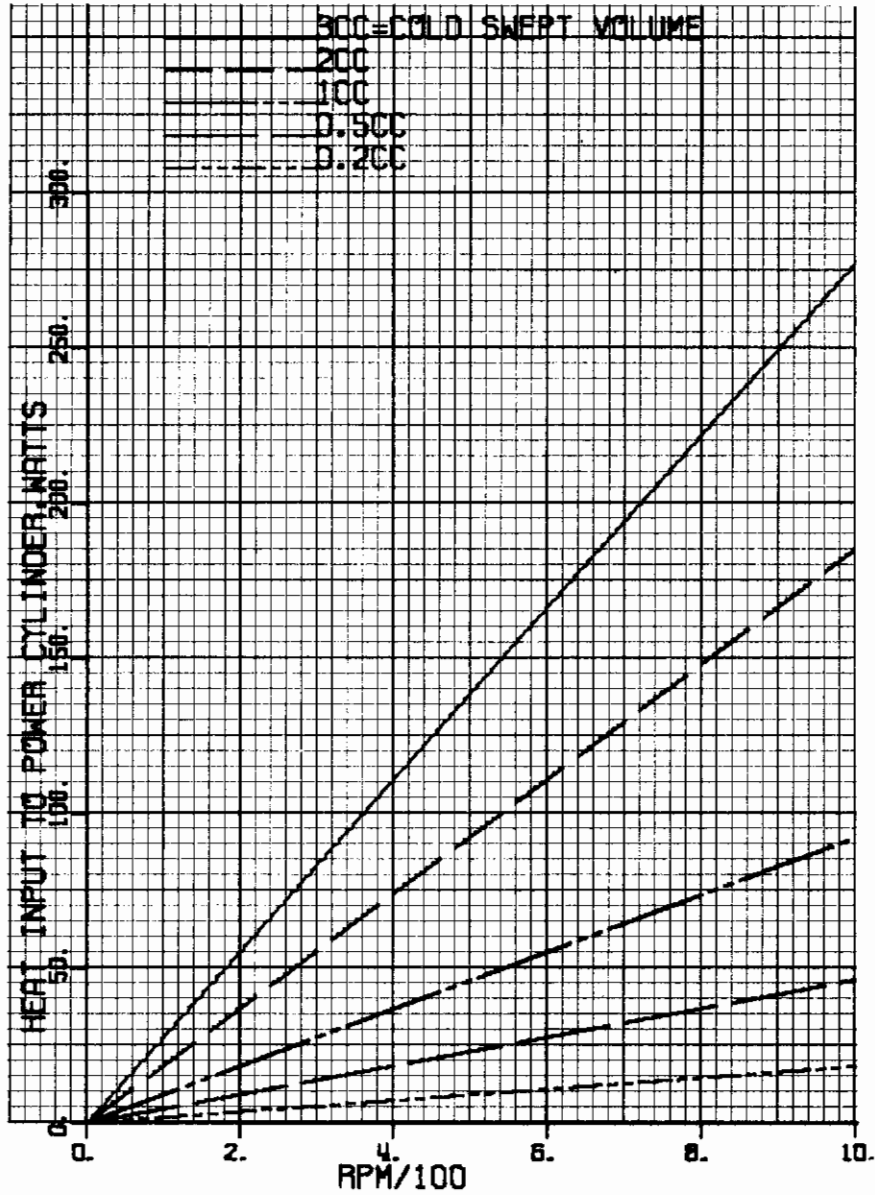


Figure 25. Required heat input to power cylinder as a function of refrigerator rpm with volume of cold cylinder as a parameter for VM machine of Figure 24.

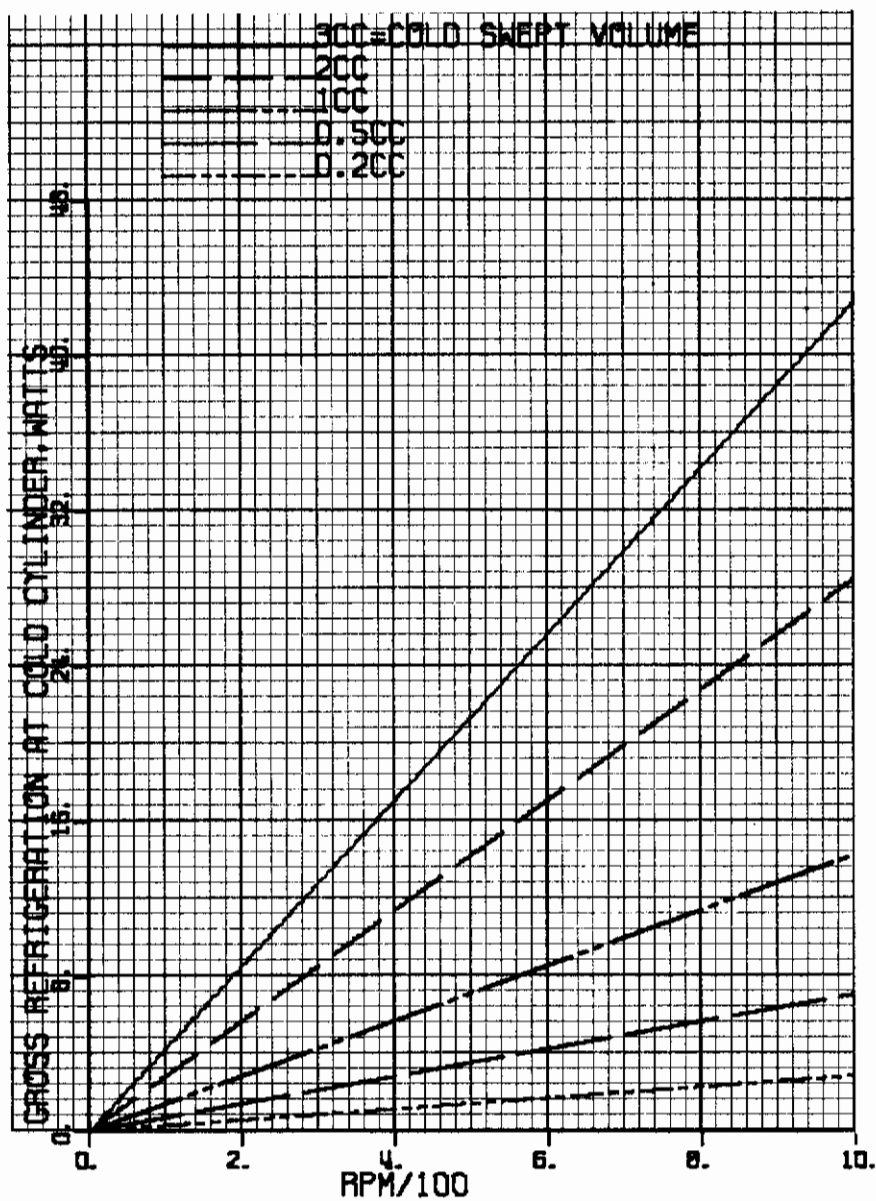


Figure 26. Gross refrigeration as a function of rpm when volume of cold cylinder is a parameter of VM refrigerating unit that produces no net power output when

refrigerating temperature limit = 70°K
 heat rejection limit = 70°F
 power cylinder temperature = 1200°F

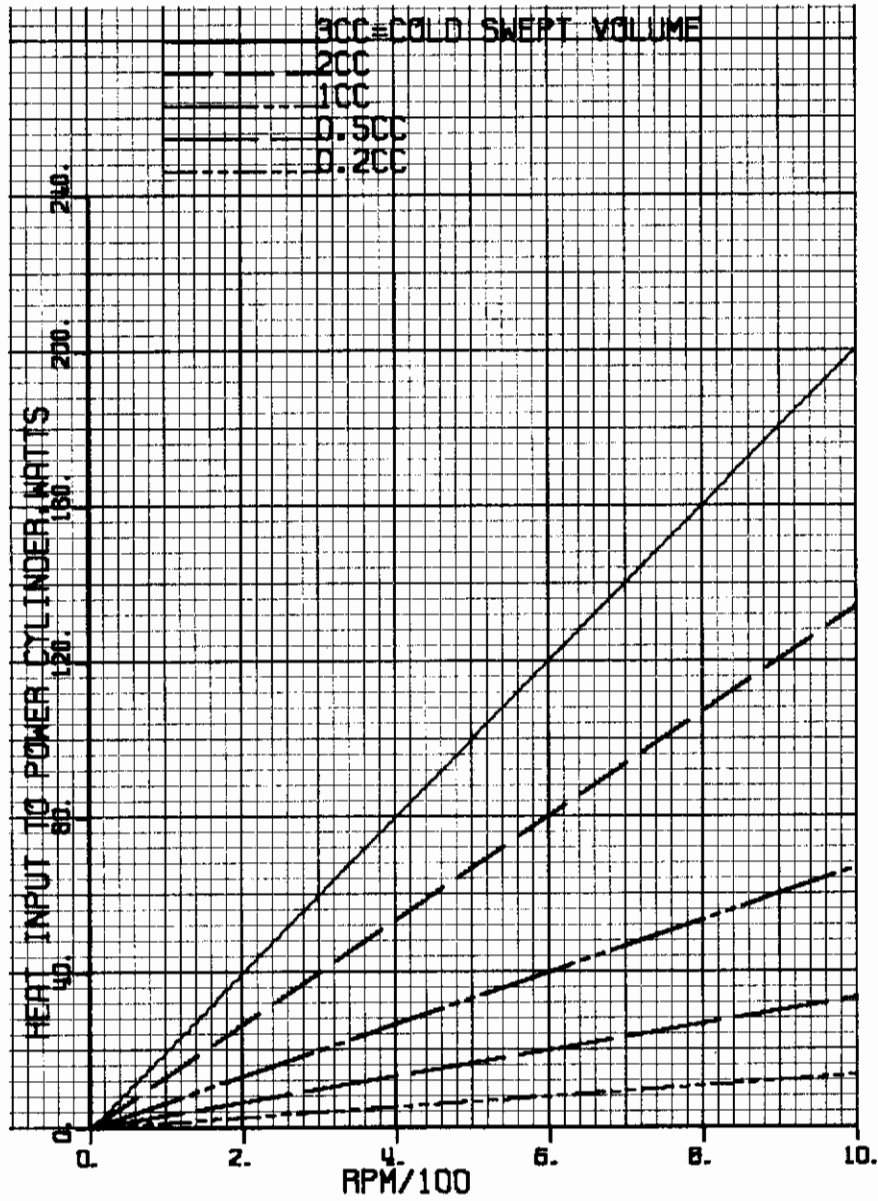


Figure 27. Required heat input to power cylinder as a function of refrigerator rpm with volume of cold cylinder as a parameter for VM machine of Figure 26.

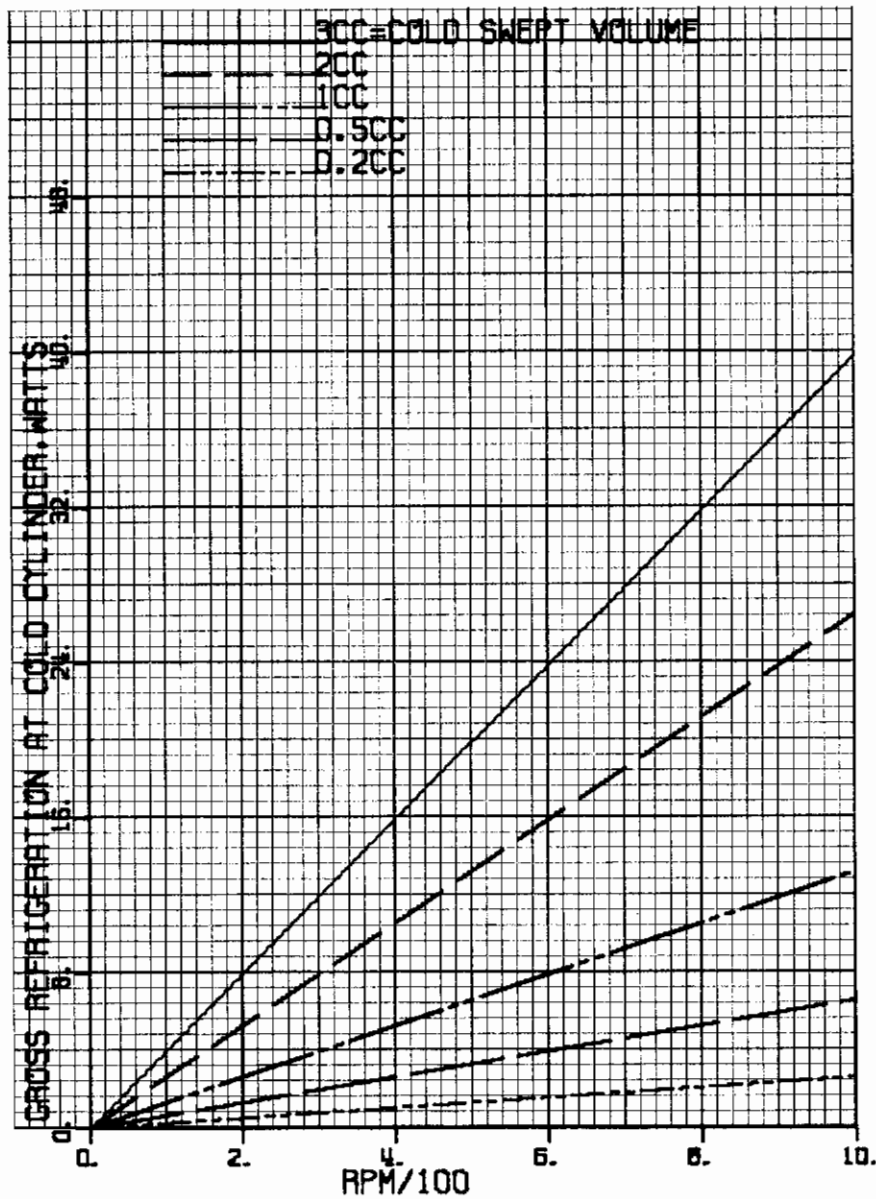


Figure 28. Gross refrigeration as a function of rpm when volume of cold cylinder is a parameter of VM refrigerating unit that produces no net power output when

refrigerating temperature limit = 70°K
 heat rejection limit = -65°F
 power cylinder temperature = 1200°F

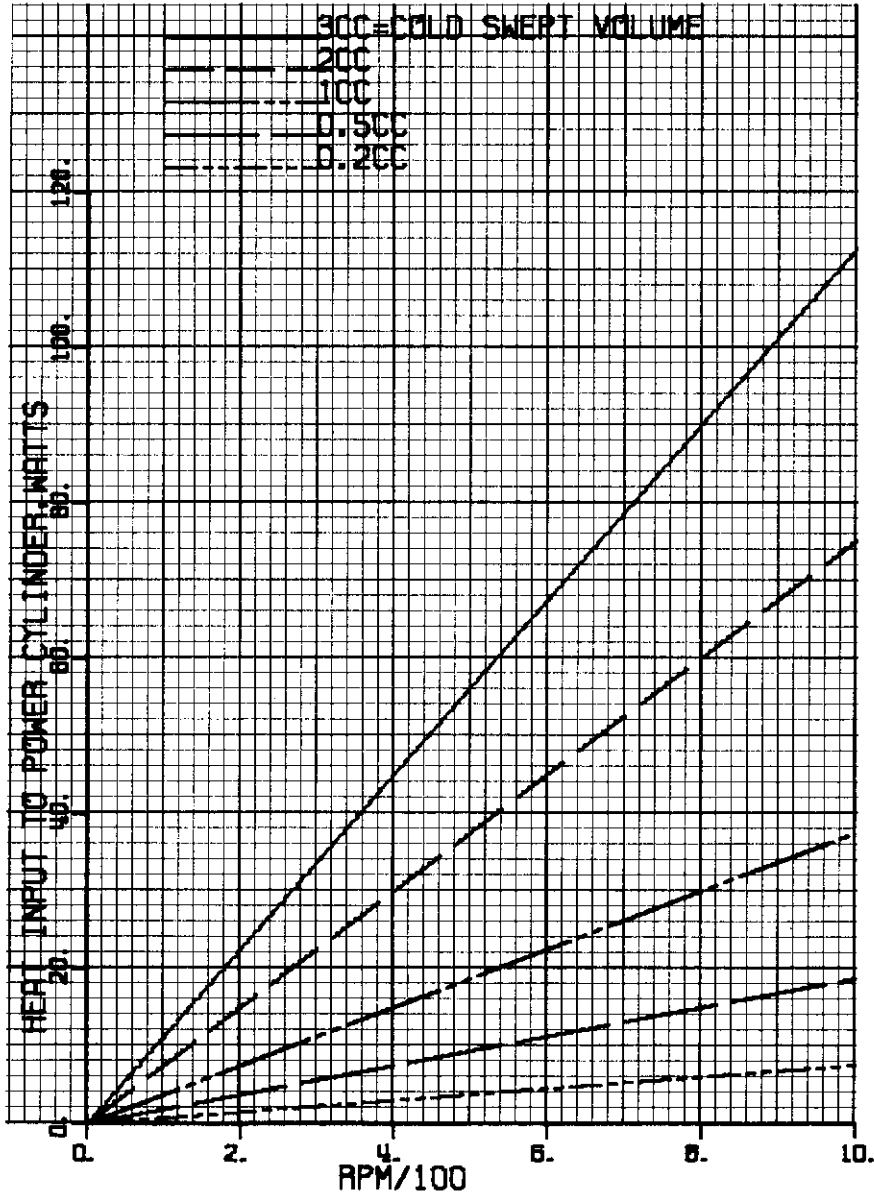


Figure 29. Required heat input to power cylinder as a function of refrigerator rpm with volume of cold cylinder as a parameter for VM machine of Figure 28.

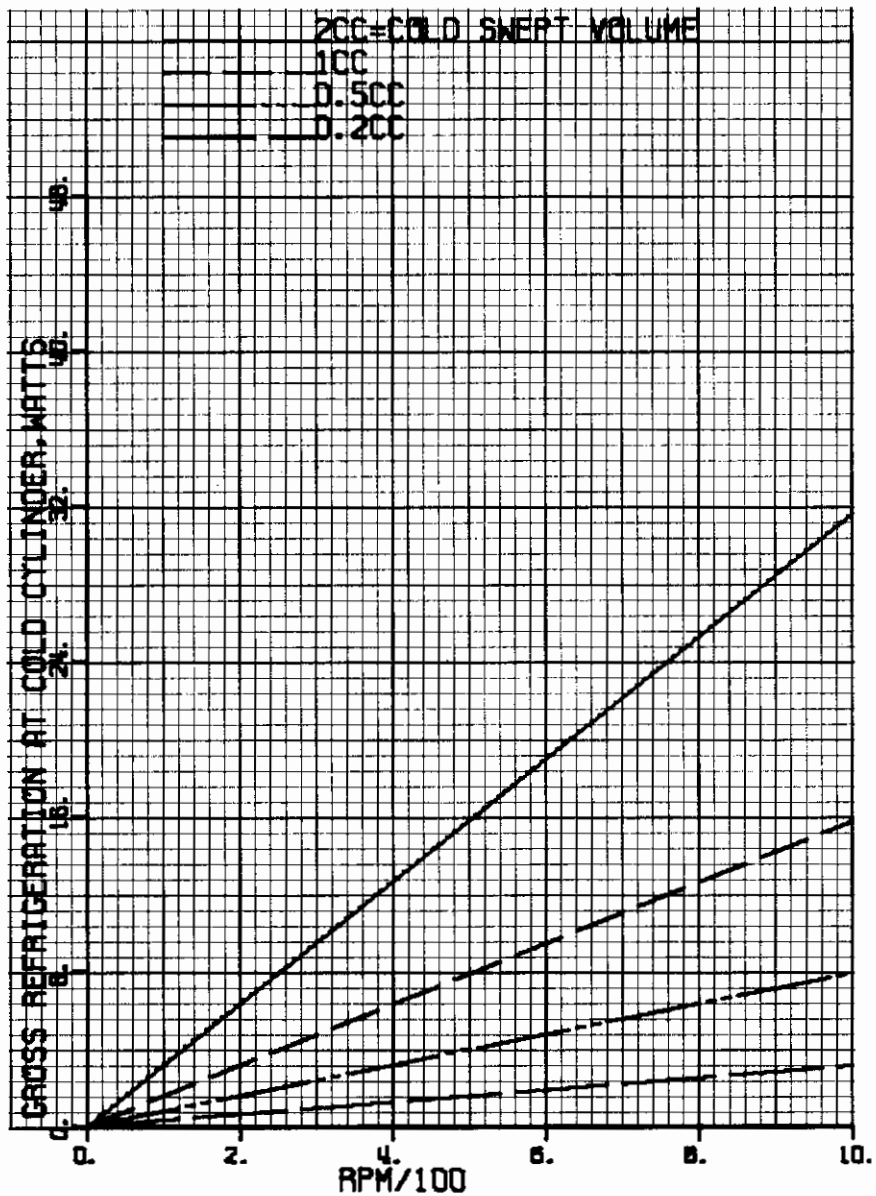


Figure 30. Gross refrigeration as a function of rpm when volume of cold cylinder is a parameter of VM refrigerating unit that produces no net power output when

refrigerating temperature limit = 30°K
 heat rejection limit = 300°F
 power cylinder temperature = 1200°F

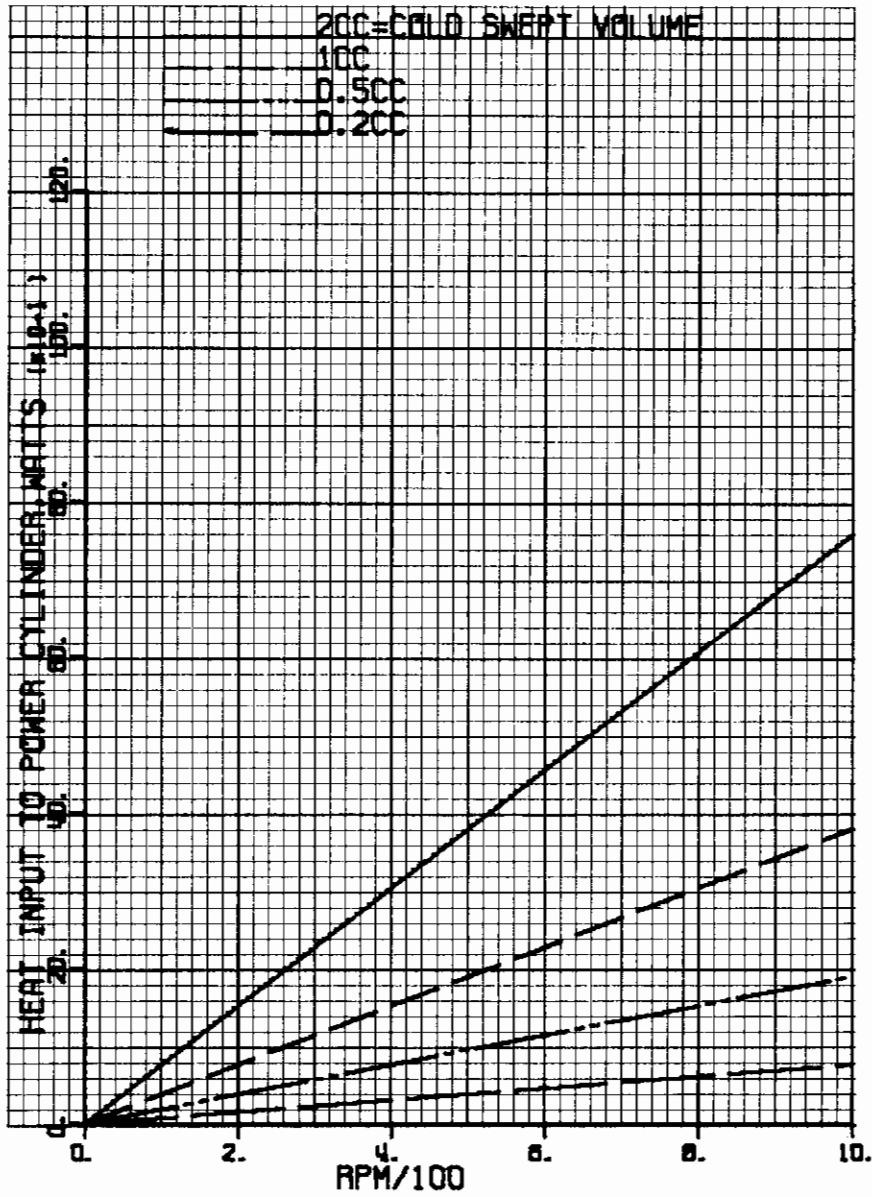


Figure 31. Required heat input to power cylinder as a function of refrigerator rpm with volume of cold cylinder as a parameter for VM machine of Figure 30.

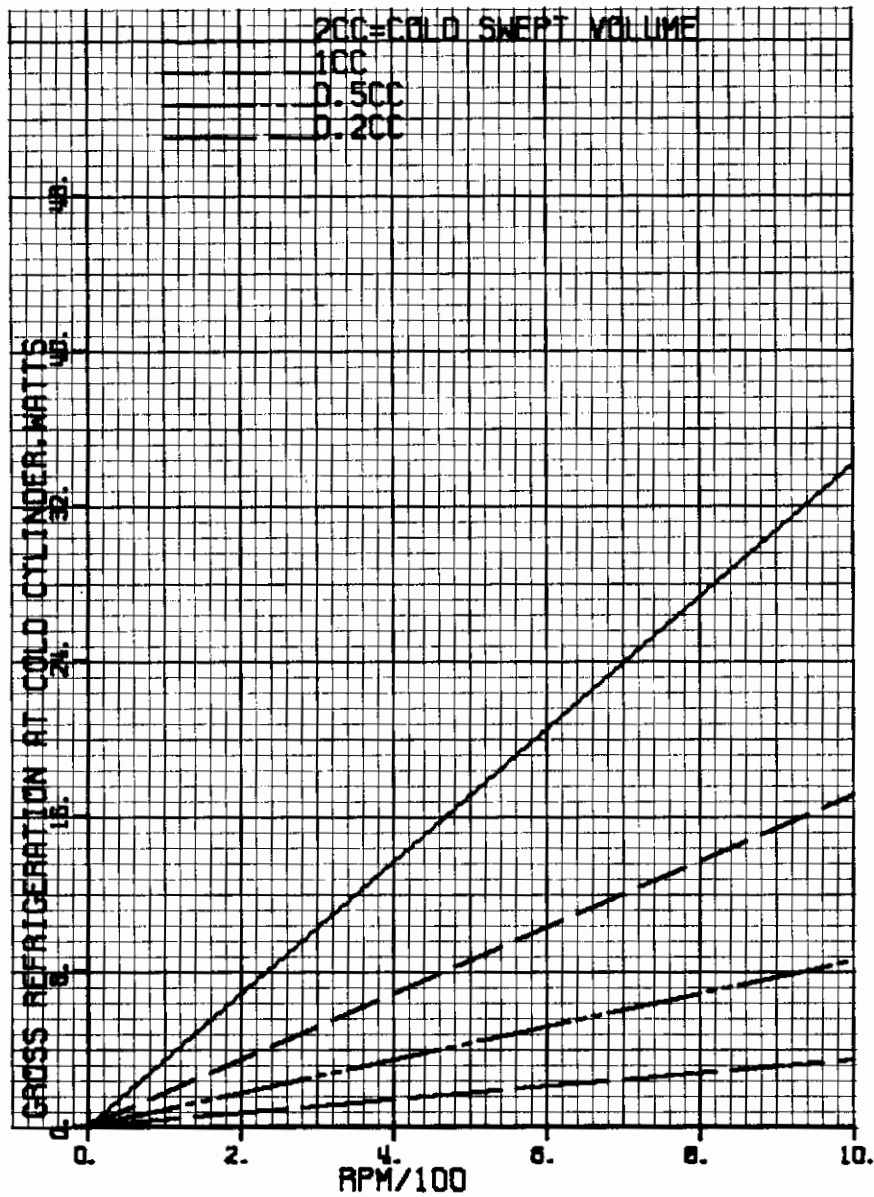


Figure 32. Gross refrigeration as a function of rpm when volume of cold cylinder is a parameter of VM refrigerating unit that produces no net power output when

refrigerating temperature limit = 30°K
 heat rejection limit = 160°F
 power cylinder temperature = 1200°F

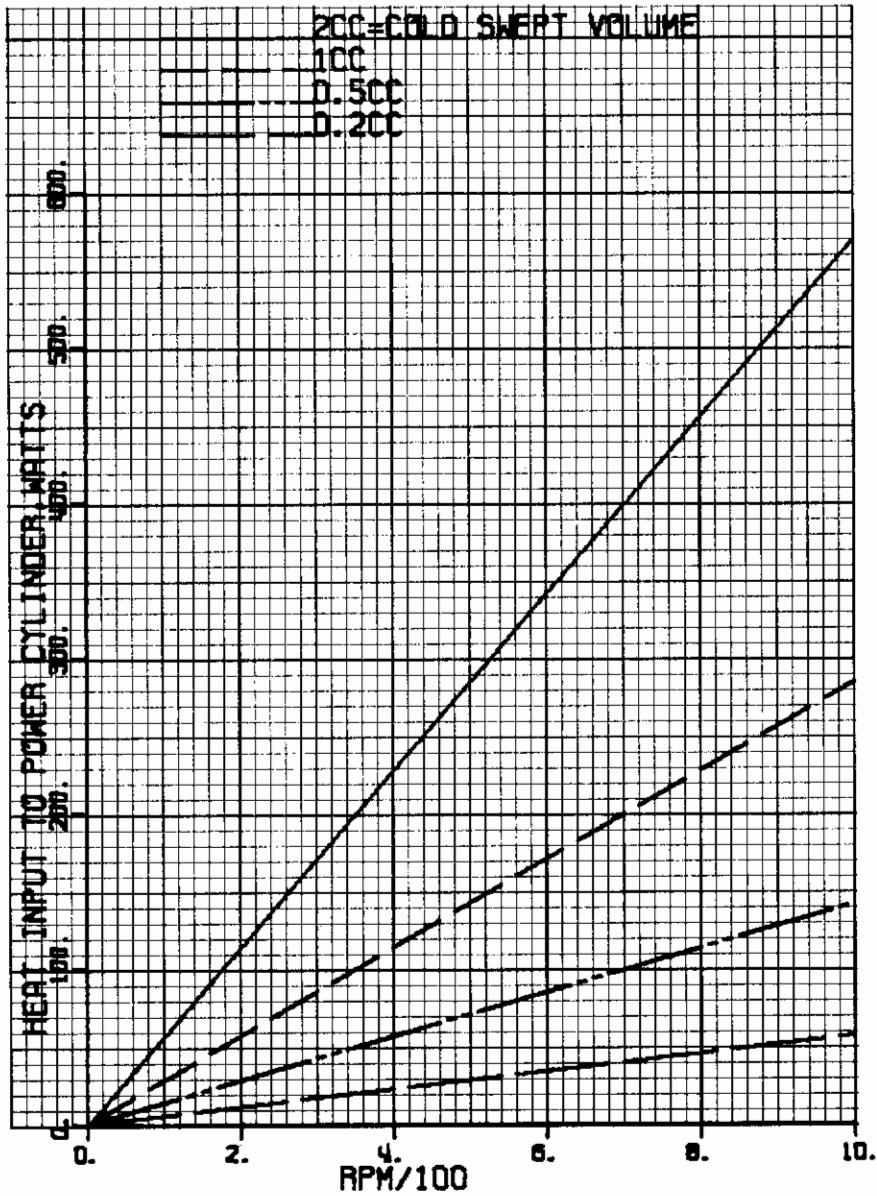


Figure 33. Required heat input to power cylinder as a function of refrigerator rpm with volume of cold cylinder as a parameter for VM machine of Figure 32.

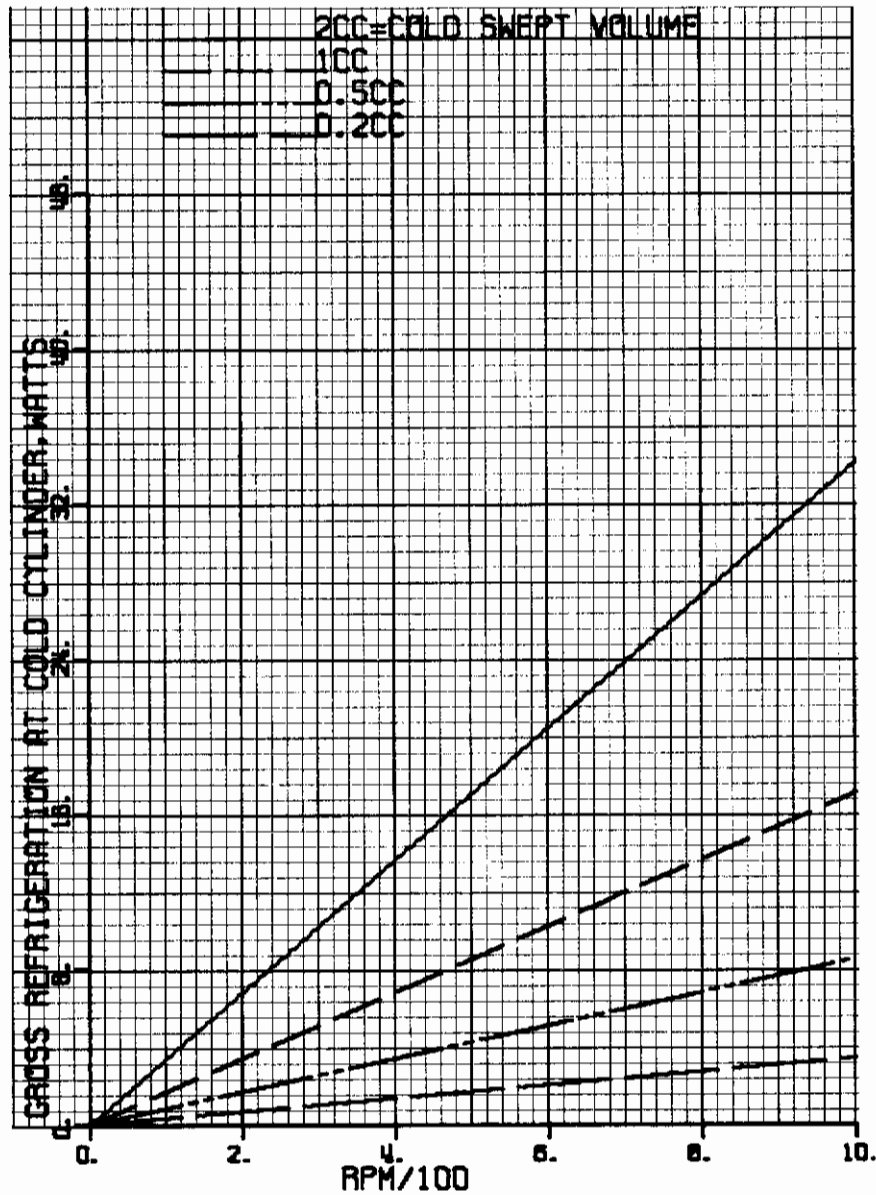


Figure 34. Gross refrigeration as a function of rpm when volume of cold cylinder is a parameter of VM refrigerating unit that produces no net power output when

refrigerating temperature limit = 30°K
 heat rejection limit = 70°F
 power cylinder temperature = 1200°F

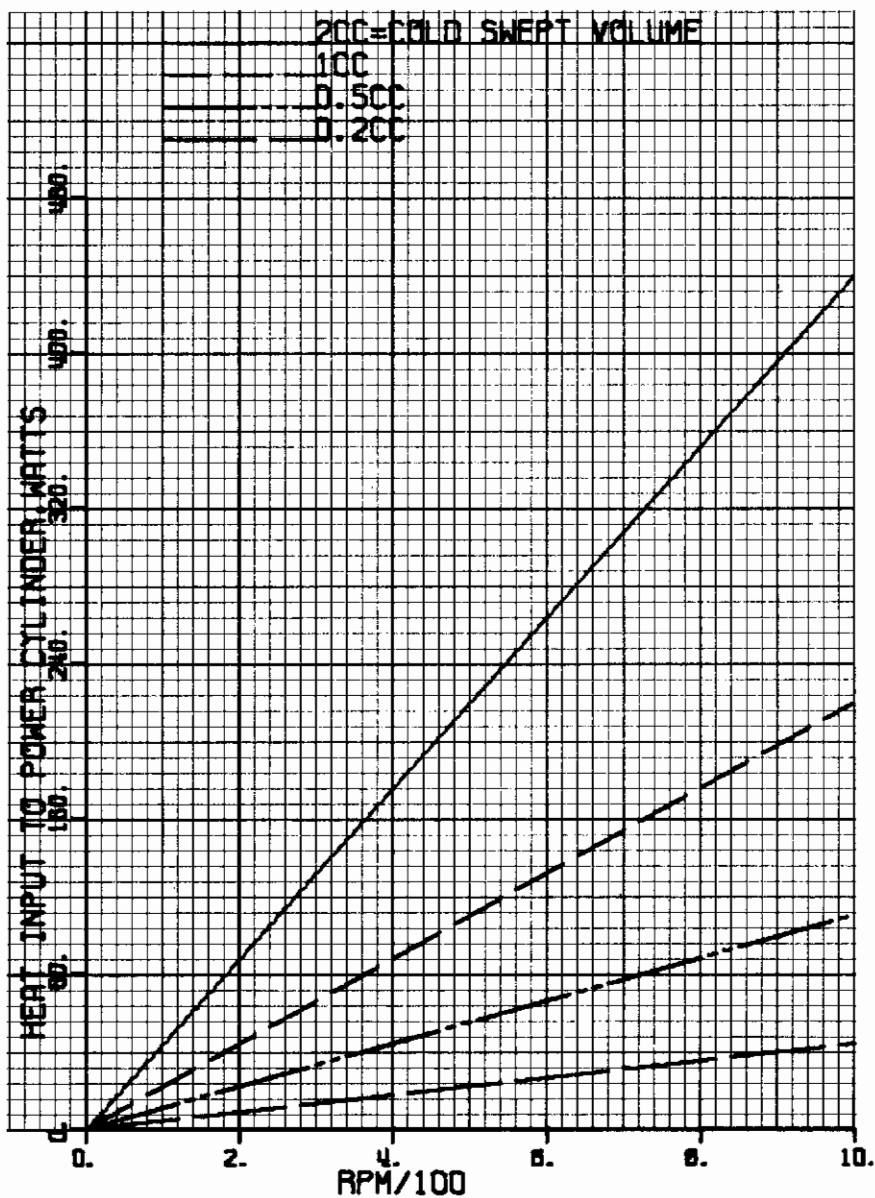


Figure 35. Required heat input to power cylinder as a function of refrigerator rpm with volume of cold cylinder as a parameter for VM machine of Figure 34.

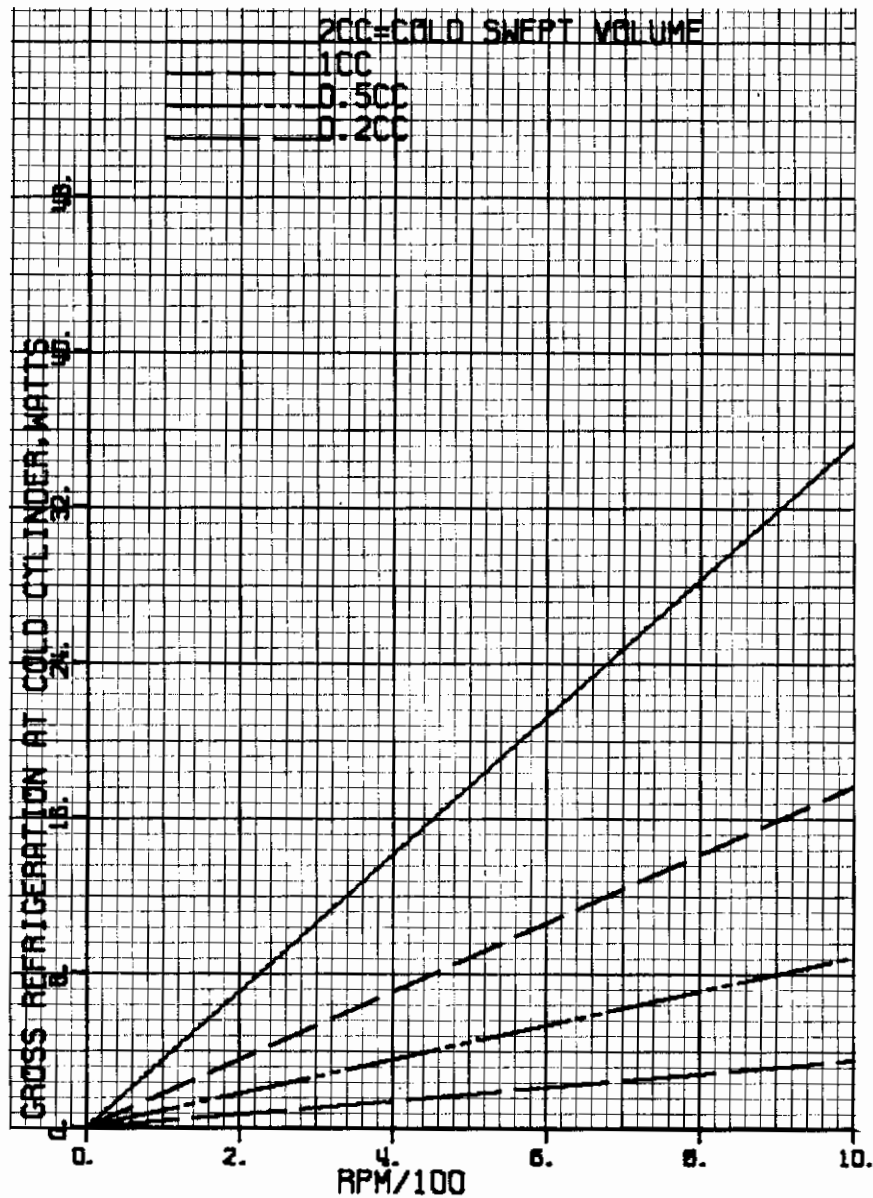


Figure 36. Gross refrigeration as a function of rpm when volume of cold cylinder is a parameter of VM refrigerating unit that produces no net power output when

refrigerating temperature limit = 30°K
 heat rejection limit = -65°F
 power cylinder temperature = 1200°F

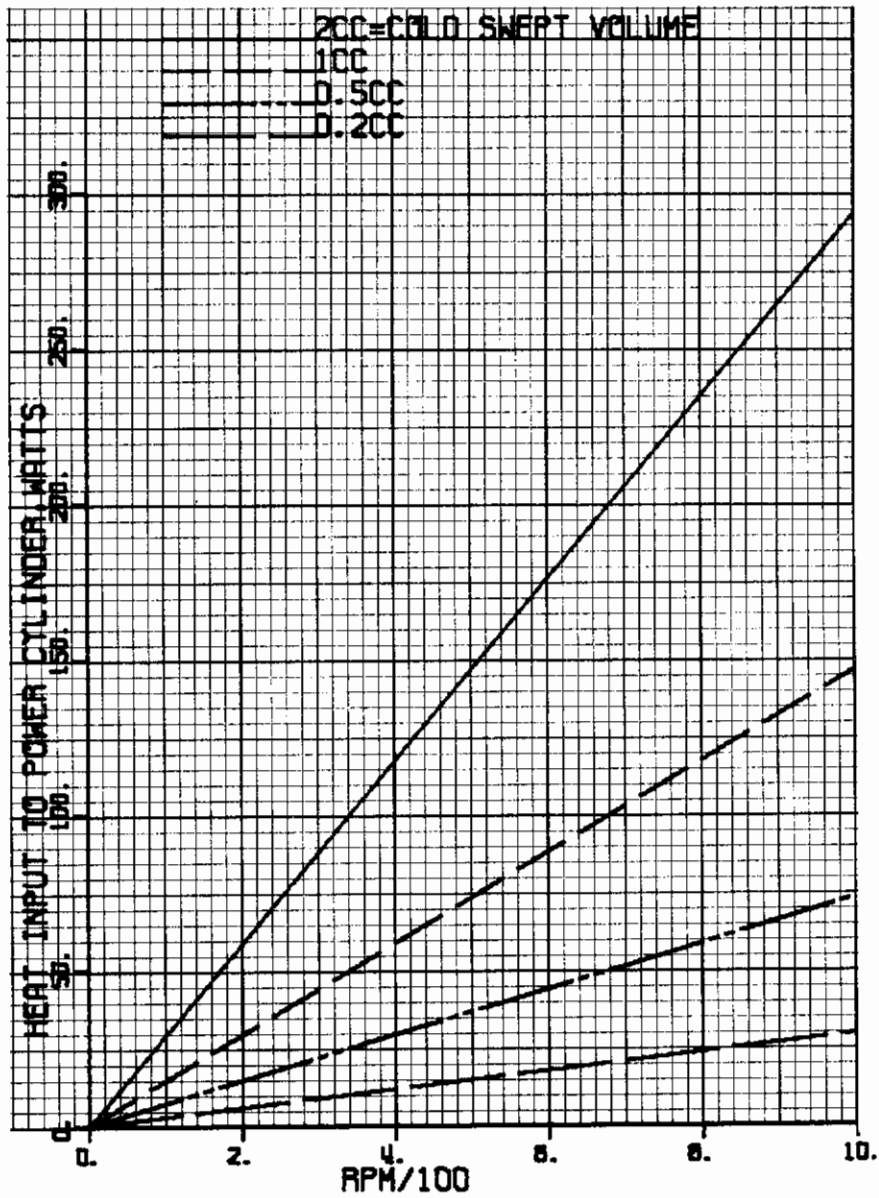


Figure 37. Required heat input to power cylinder as a function of refrigerator rpm with volume of cold cylinder as a parameter for VM machine of Figure 36.

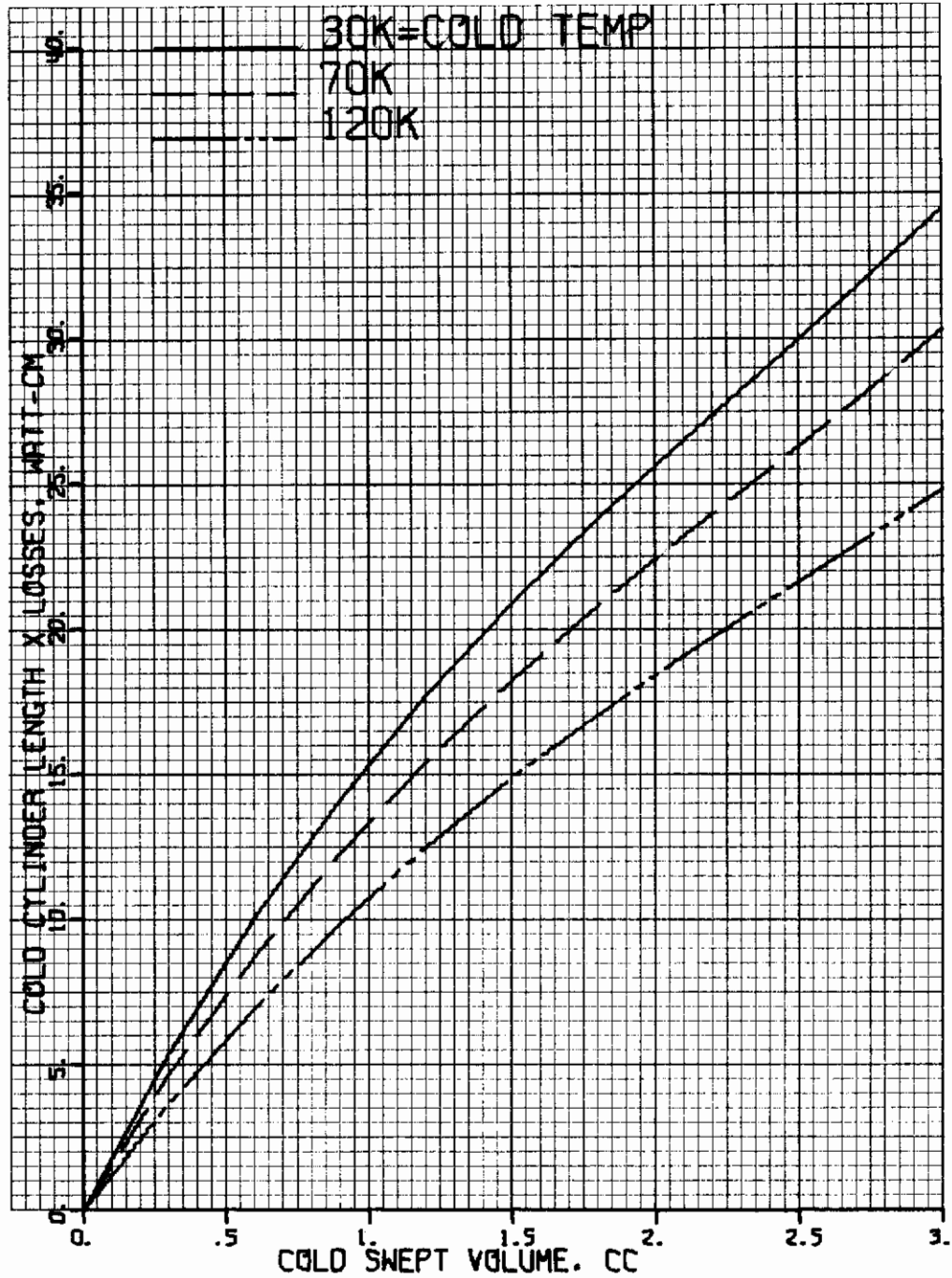


Figure 38. Cold loss as a function of volume and temperature.

Ambient temperature = 300°F.

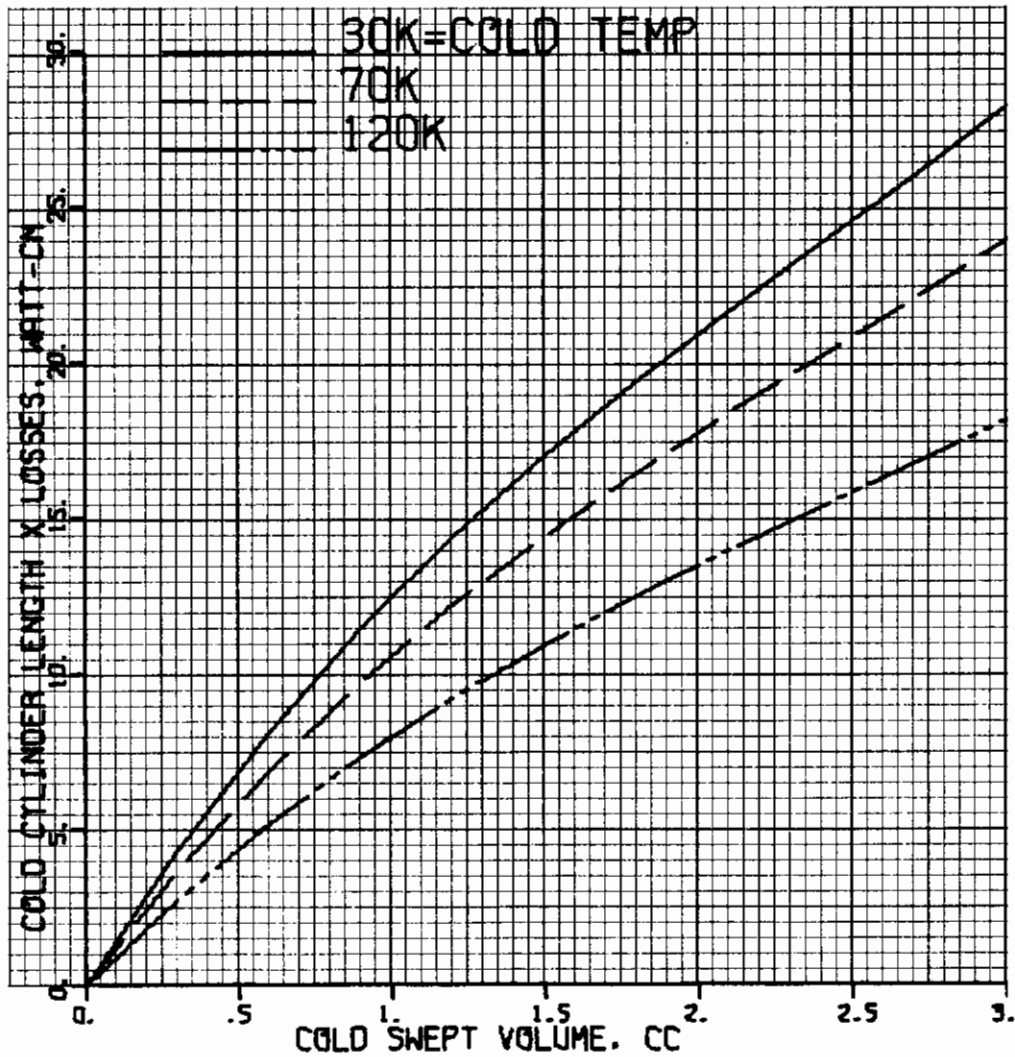


Figure 39. Cold loss as a function of volume and temperature.

Ambient temperature = 160°F

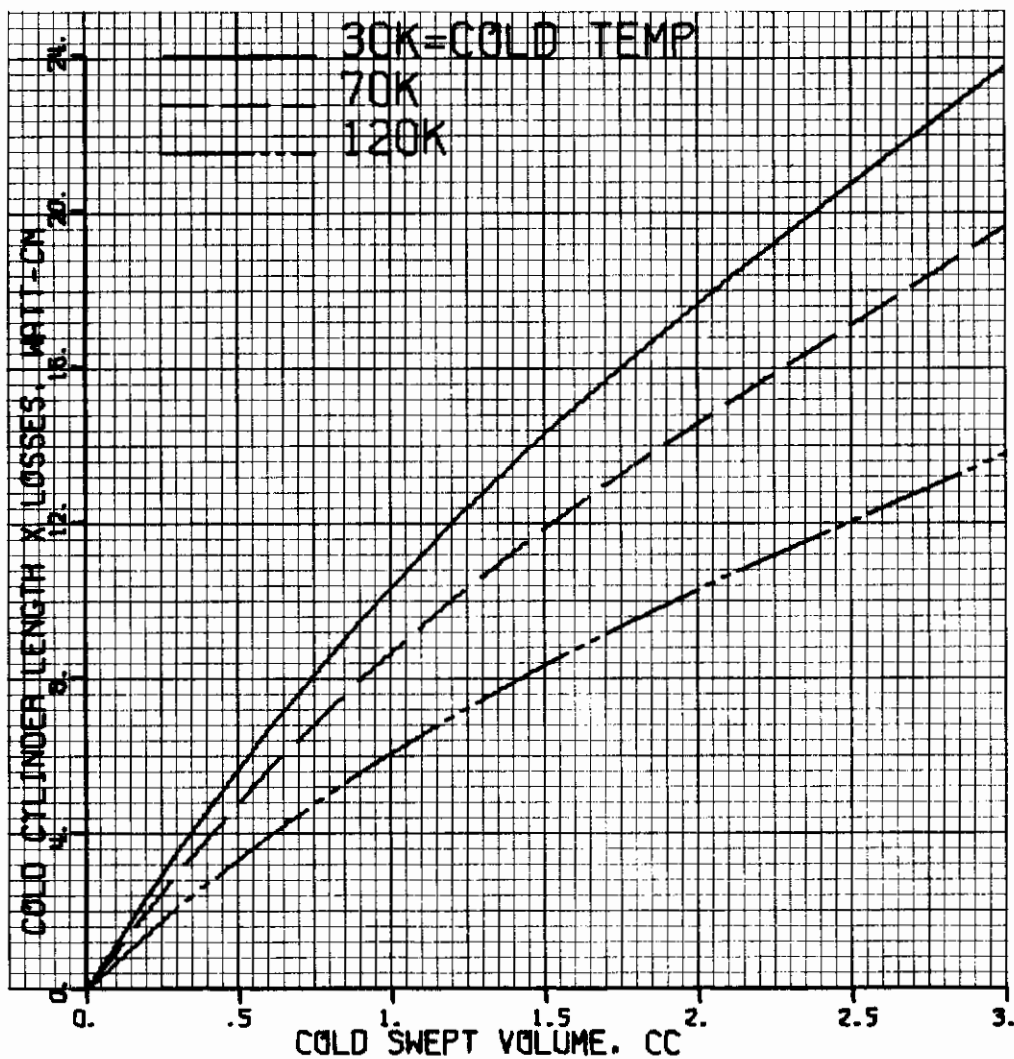


Figure 40. Cold loss as a function of volume and temperature.

Ambient temperature = 70°F.

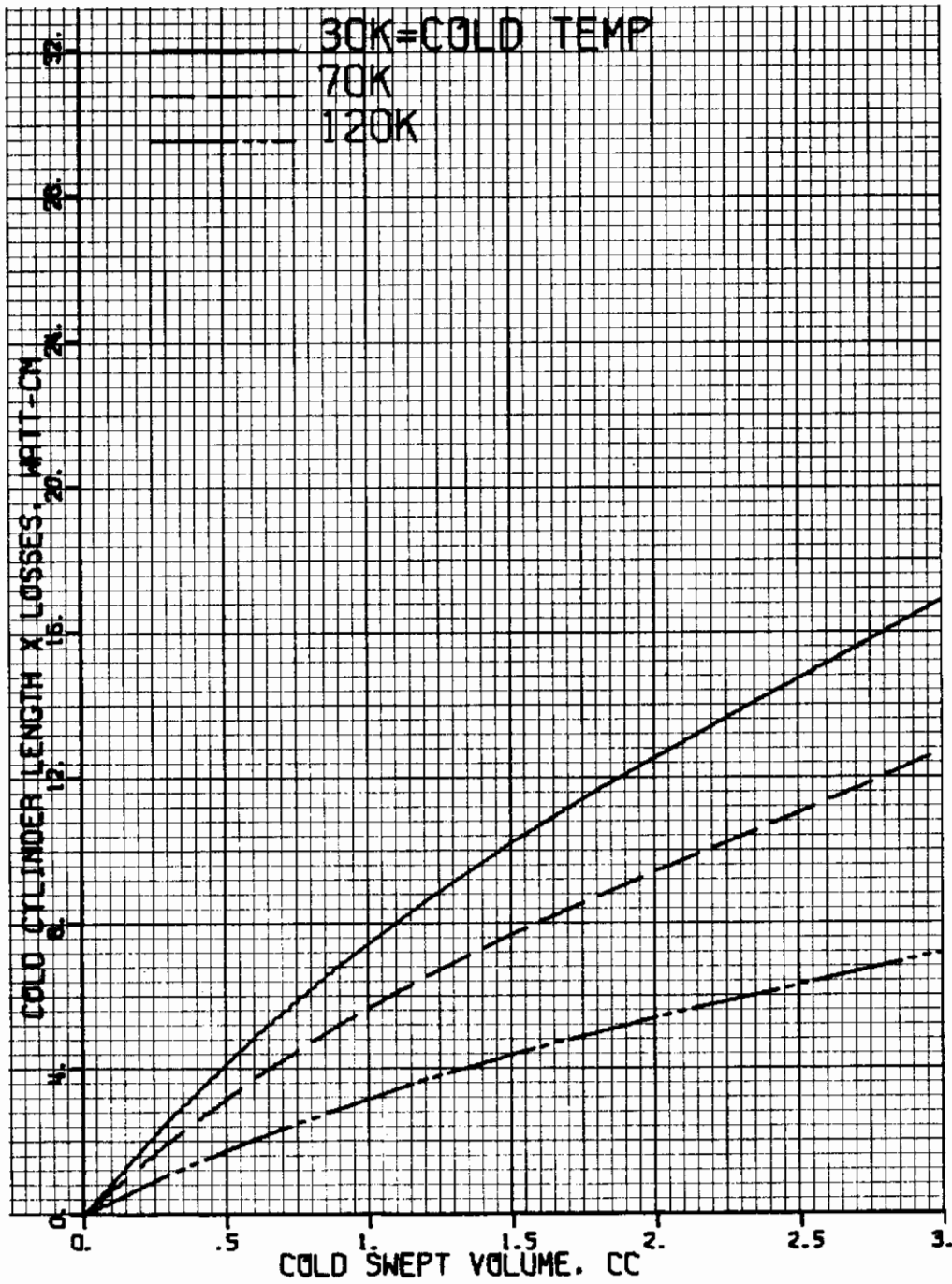


Figure 41. Cold loss as a function of volume and temperature.

Ambient temperature = -65°F.

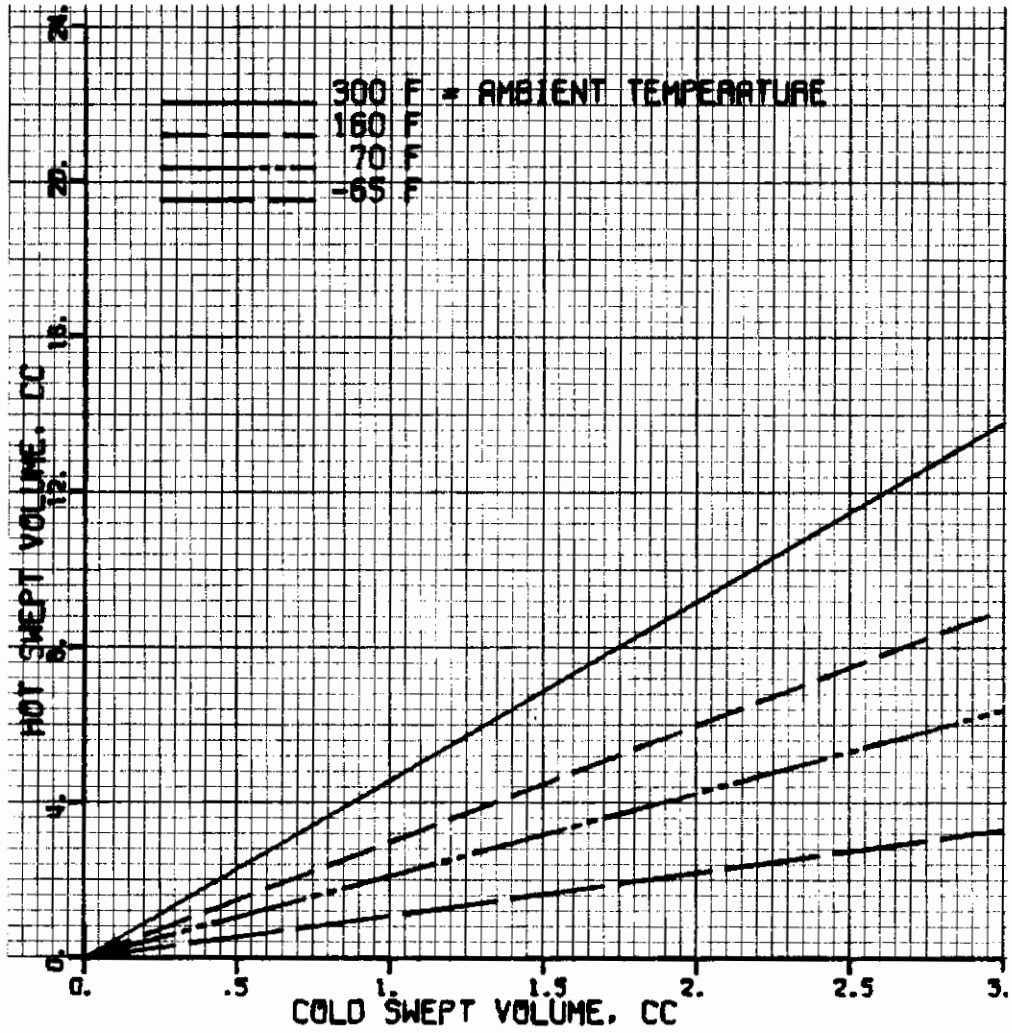


Figure 42. Hot volume as a function of cold volume for four temperatures.

Cold temperature = 120°K.

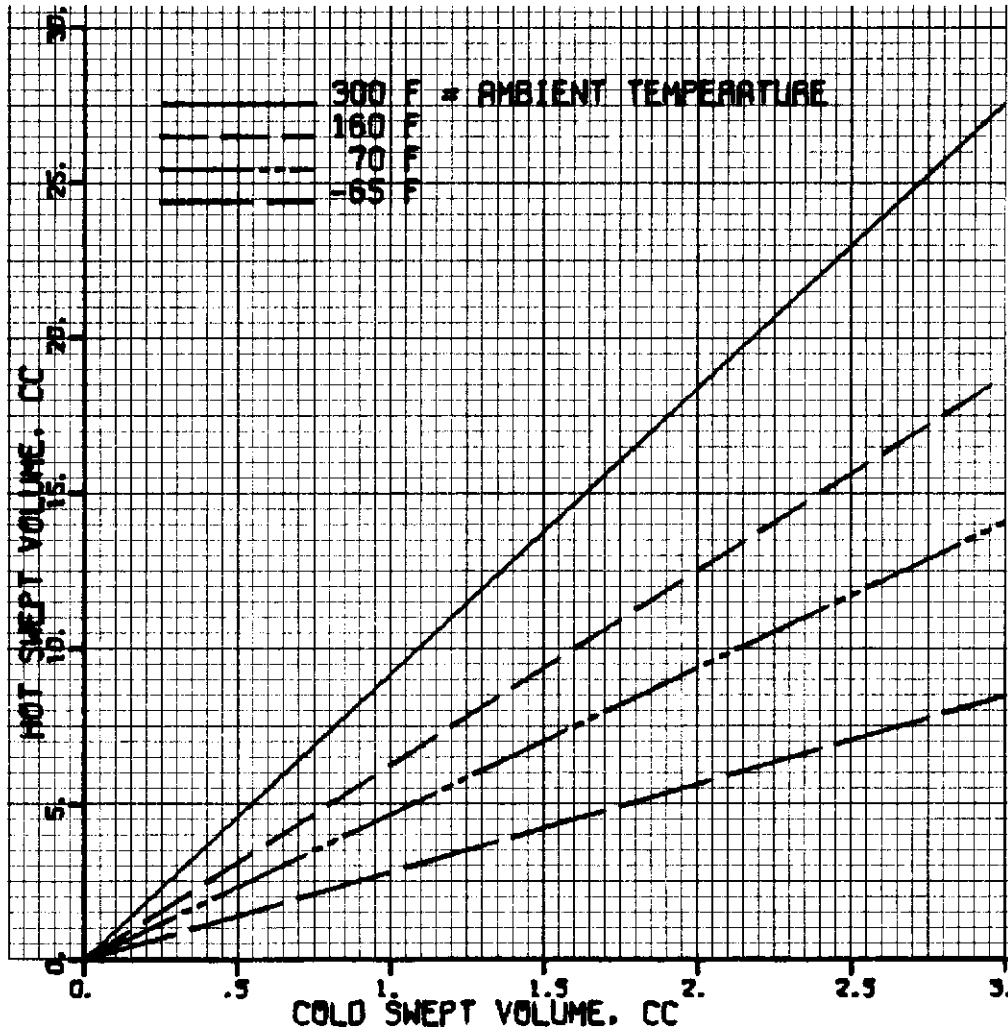


Figure 43. Hot volume as a function of cold volume for four temperatures.

Cold temperature = 70°K .

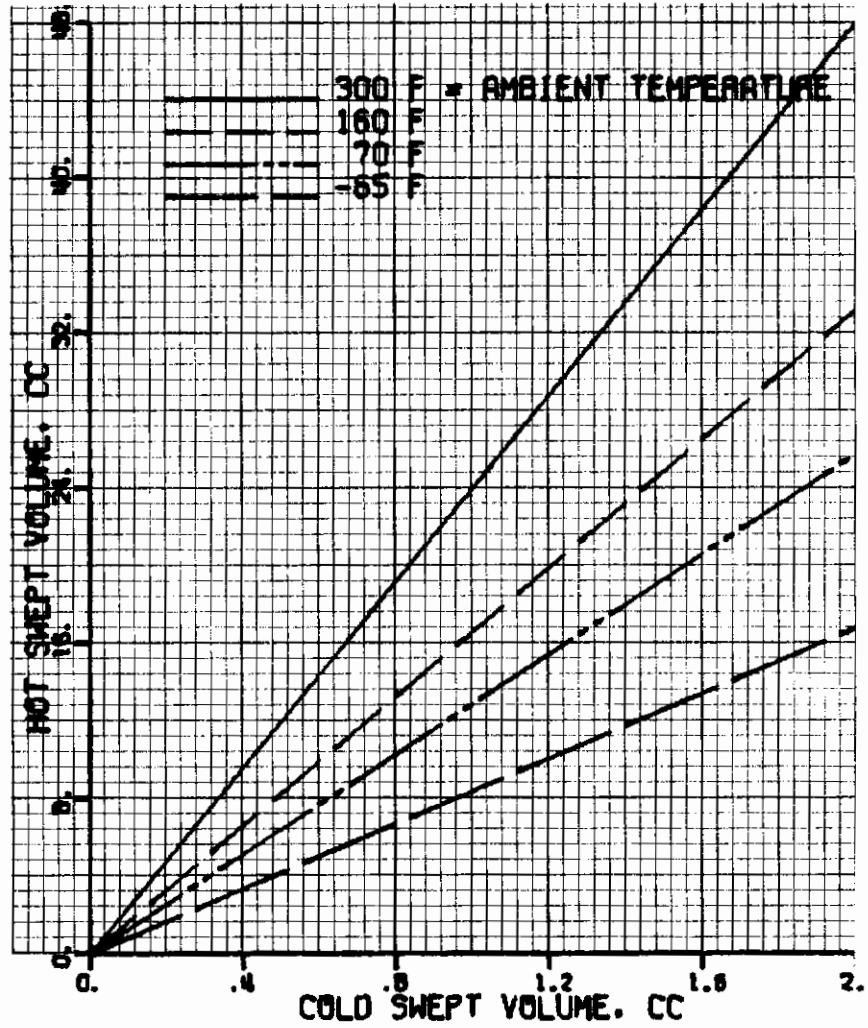


Figure 44. Hot volume as a function of cold volume for four temperatures.

Cold temperature = 30°K .

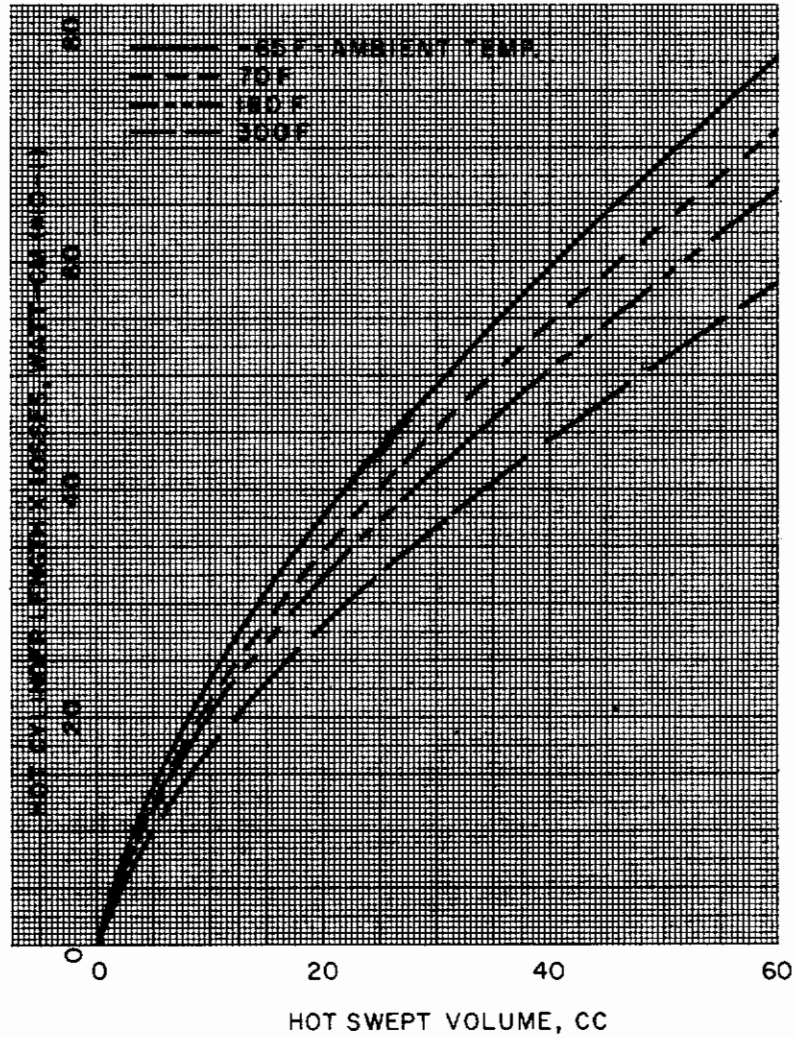


Figure 45A. Hot losses as a function of volume and temperature.

Hot temperature = 1200°F
Cold temperature = 70°K

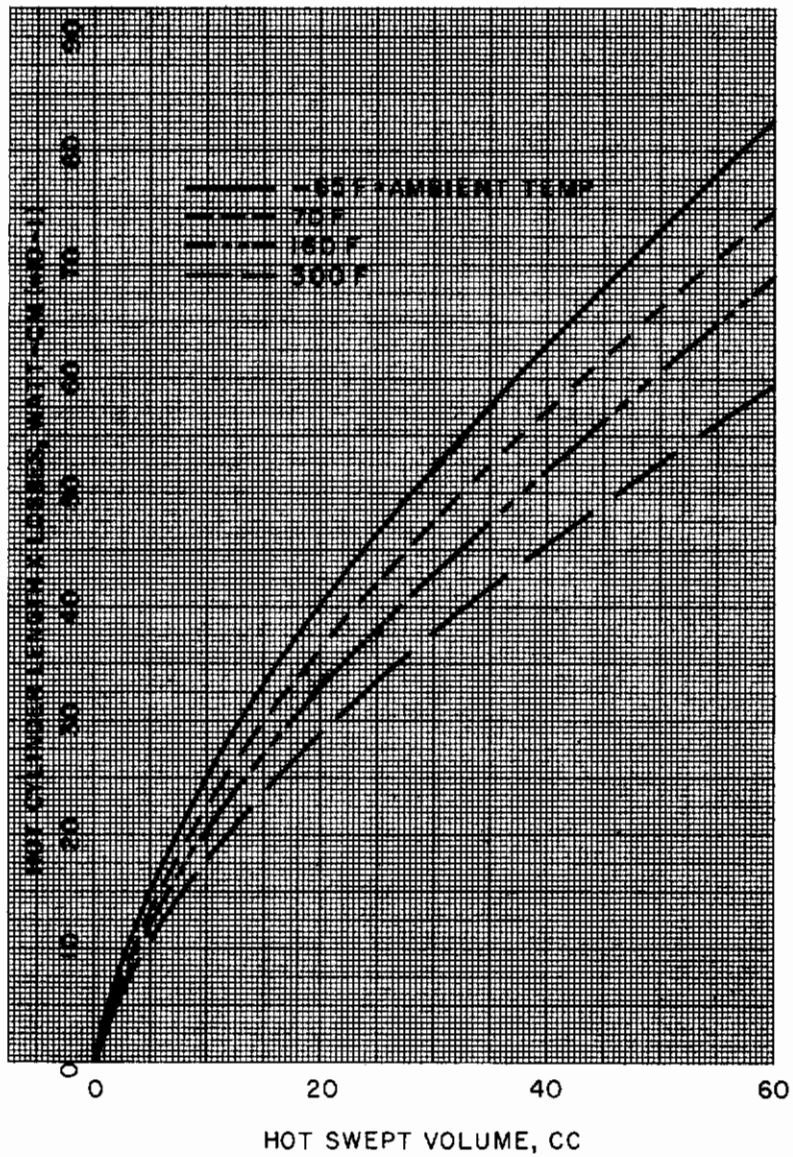


Figure 45B. Hot losses as a function of volume and temperature.

Hot temperature 1200°F
Cold temperature = 30° K

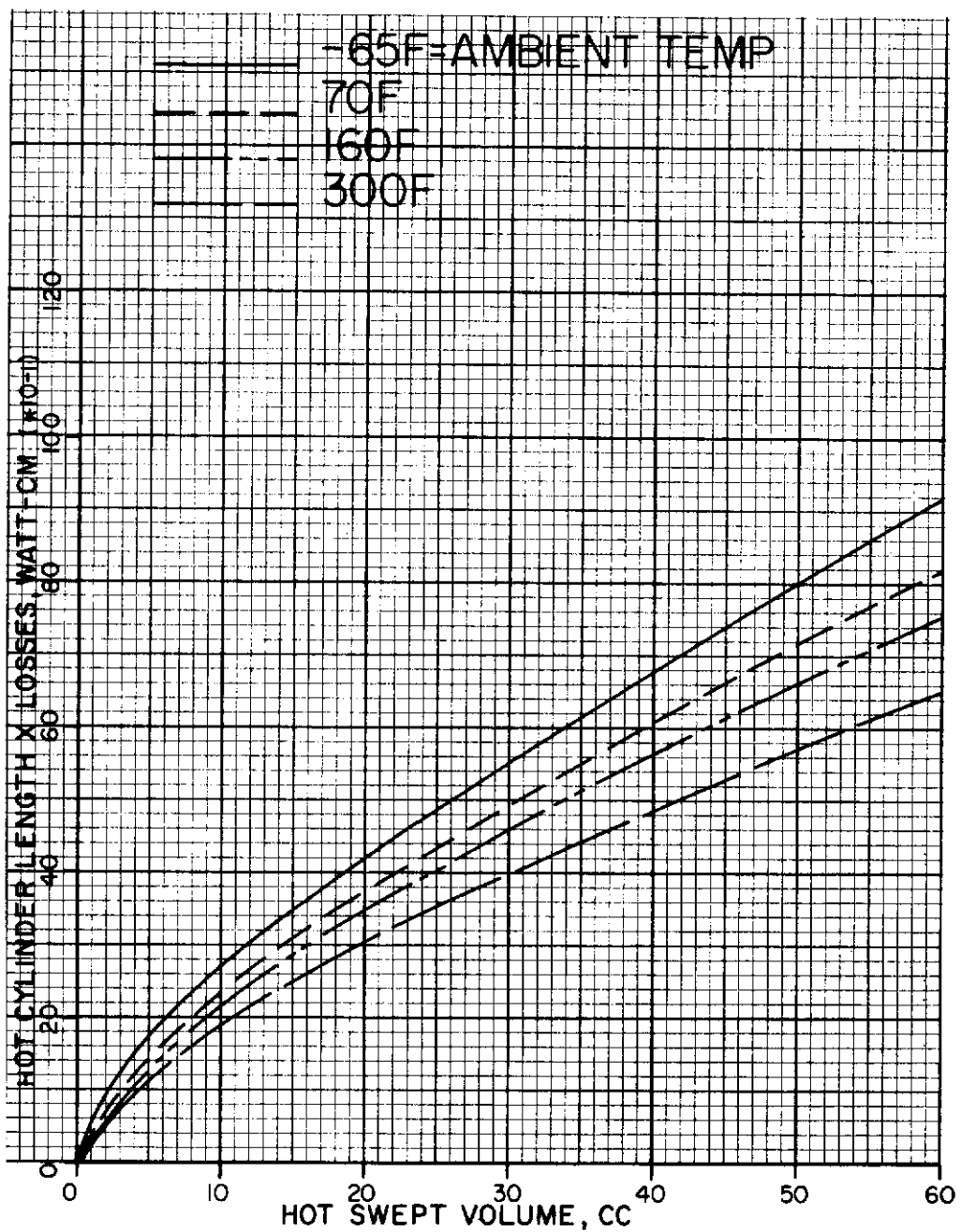


Figure 45. Hot losses as a function of volume and temperature.

Hot temperature = 1200^oF
Cold temperature = 120^oF

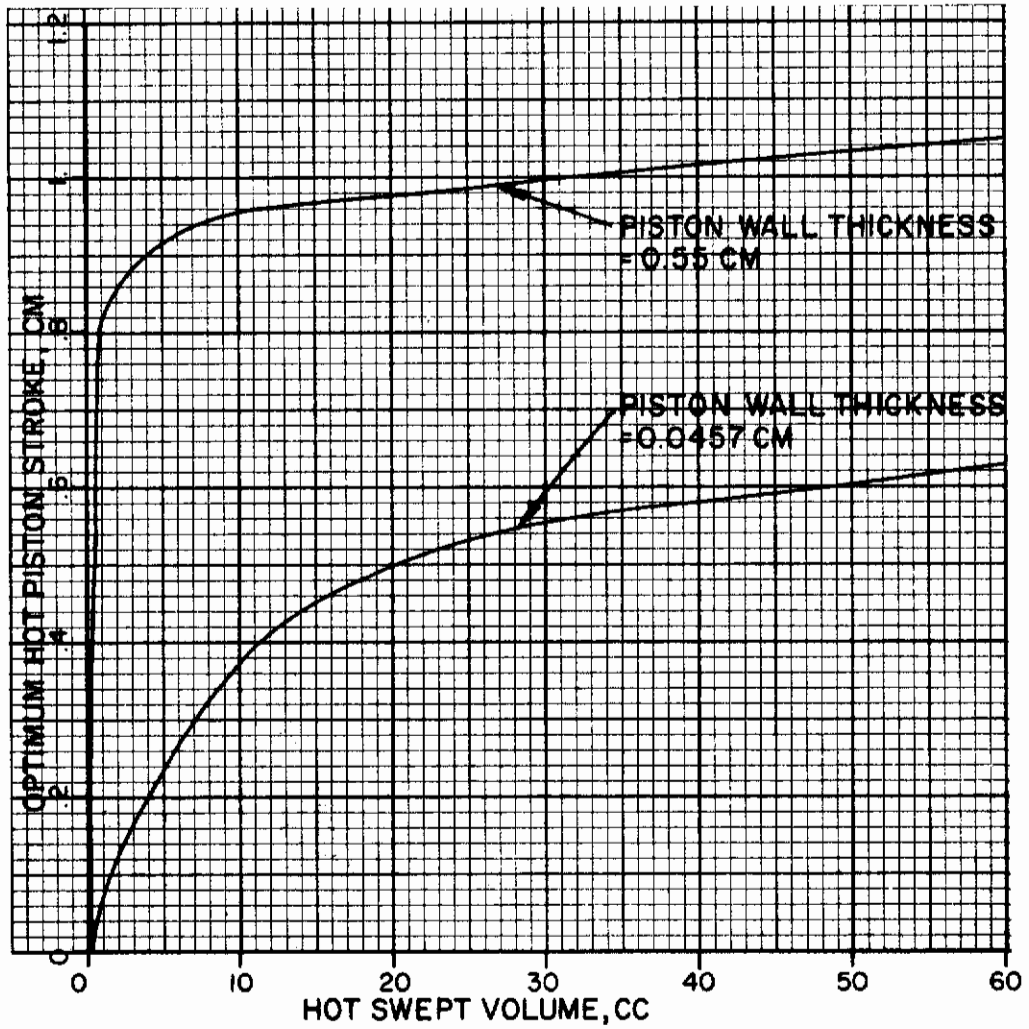


Figure 46. Optimum stroke of hot piston as a function of swept volume with thickness of piston wall as a parameter.

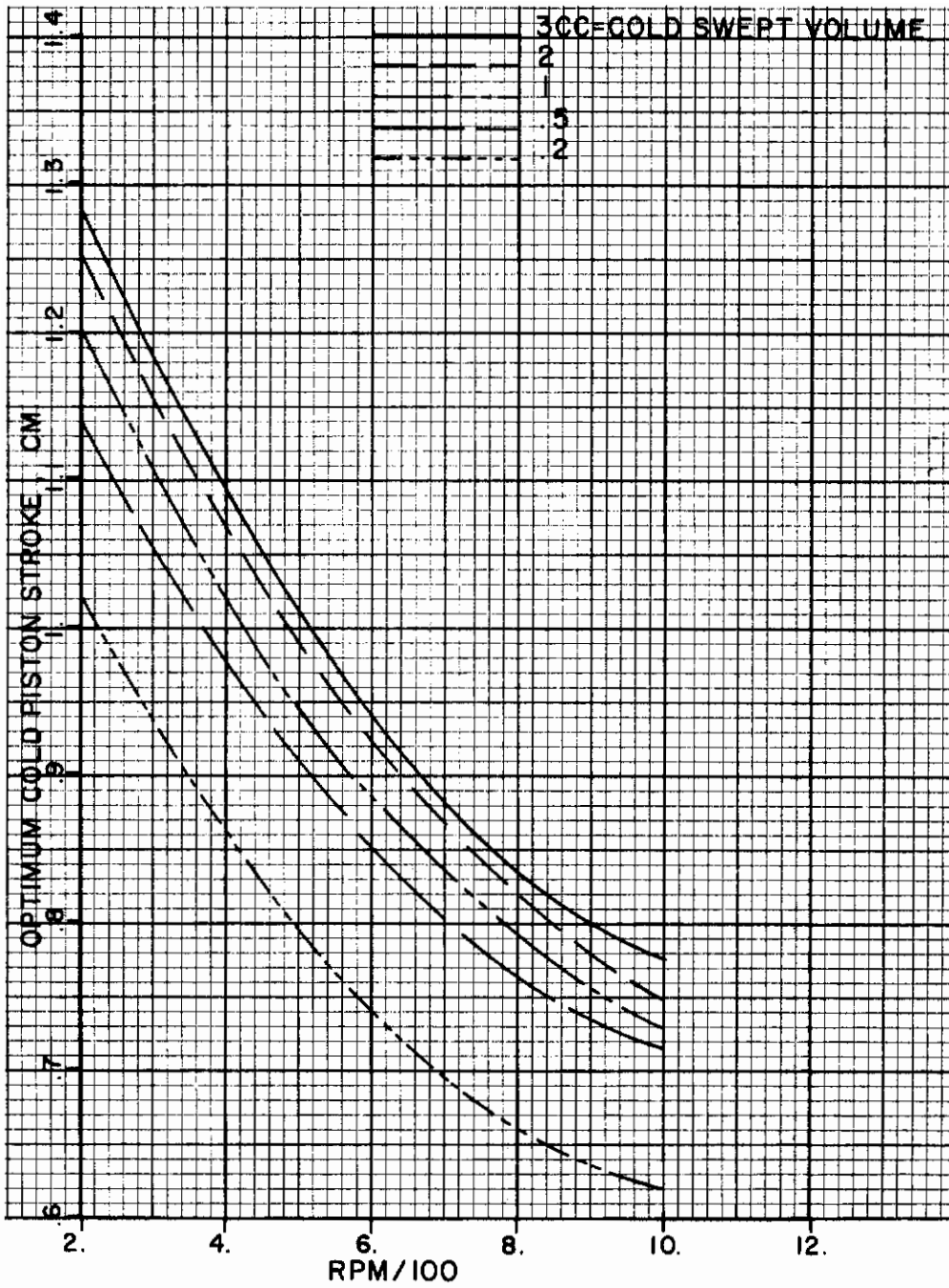


Figure 47. Optimum piston stroke as a function of rpm for five cold volumes.

Cold temperature = 120°K
 Ambient temperature = 300°F

7. The total required power input to the hot cylinder of the unit is found by adding the hot cylinder losses to the minimum required power input to the hot cylinder.
8. The optimum stroke of the piston in the hot cylinder at the required swept hot cylinder volume is found from Figure 46.
9. The optimum stroke of the piston in the cold cylinder at the chosen swept cold cylinder volume is found from Figures 47 through 58.
10. The weight of the refrigerator at the required swept hot cylinder volume and at the optimum stroke of the piston in the hot cylinder is found from Figure 59.
11. At the given refrigeration and ambient temperature, rpm, and swept volume in the cold cylinder, the coefficient performance of the refrigerator is found from Figures 60 through 71.

DISCUSSION OF GRAPHS

It is seen from the figures that a speed range of 0-1000 rpm was used in the various computations. The reason for choosing this speed range is mainly based on machine life and noise. The purpose of developing the VM refrigerator is to obtain a simple and practical unit that has a long life and a low noise level. At the present time, there is no test data available for life versus rpm at a fixed refrigeration load. However, a speed range up to 1000 rpm seems to fit the design and construction of the present VM units very well with respect to noise, pressure drops, and dimensions.

The losses that are accounted for in the computations include the shuttle, pumping, heat conduction, and regenerator losses. Thus, the following equations were used in minimizing the losses.

$$Q_{sh} = 0.186 Y_p^2 C \frac{k_g}{S} \frac{(T_h - T_c)}{L_{cy}} \quad (29)$$

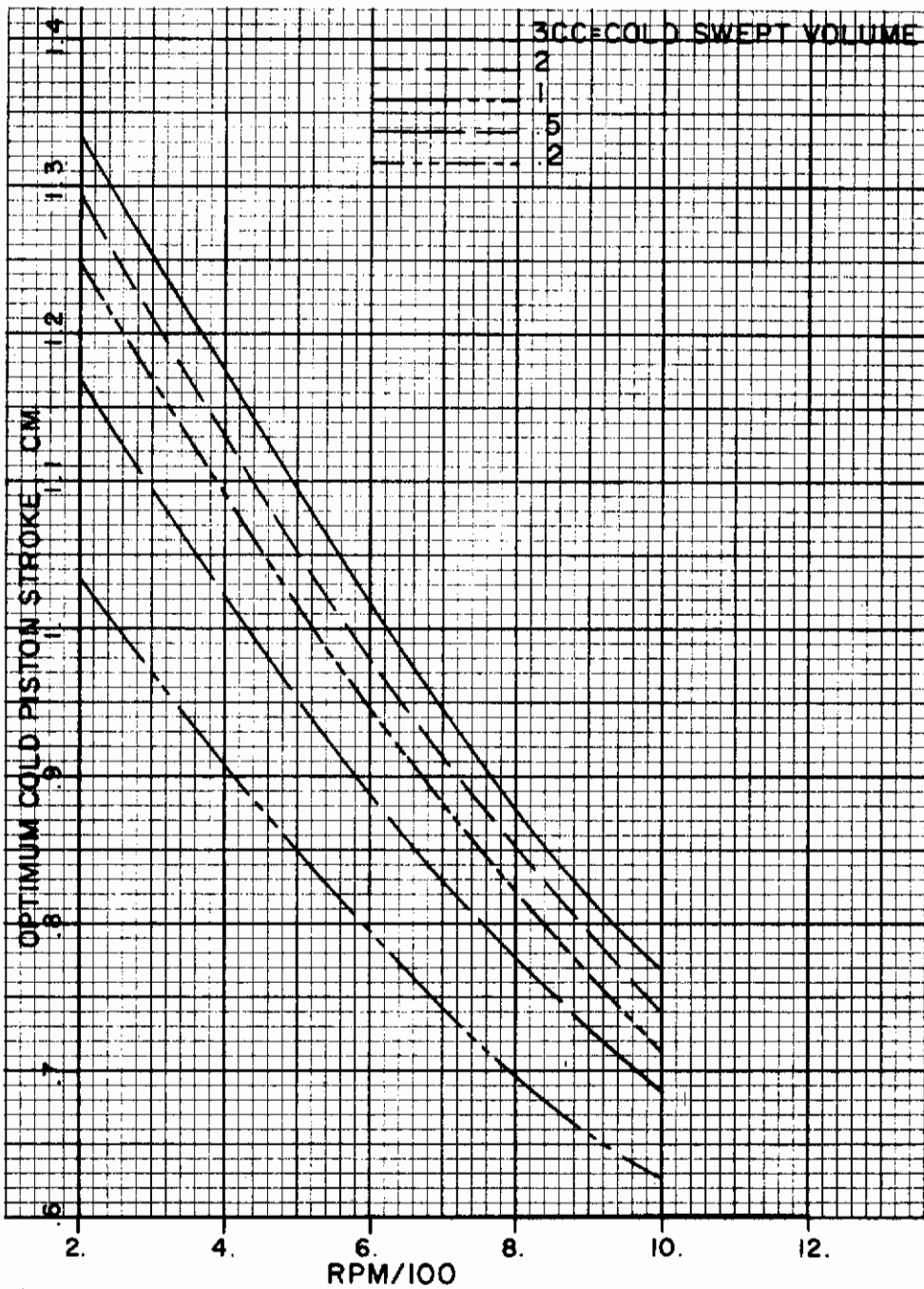


Figure 48. Optimum stroke of piston as a function of rpm for five cold volumes.

Cold temperature = 120°K
Ambient temperature = 160°F



Figure 49. Optimum piston stroke as a function of rpm for five cold volumes.

Cold temperature = 120°K
 Ambient temperature = 70°F

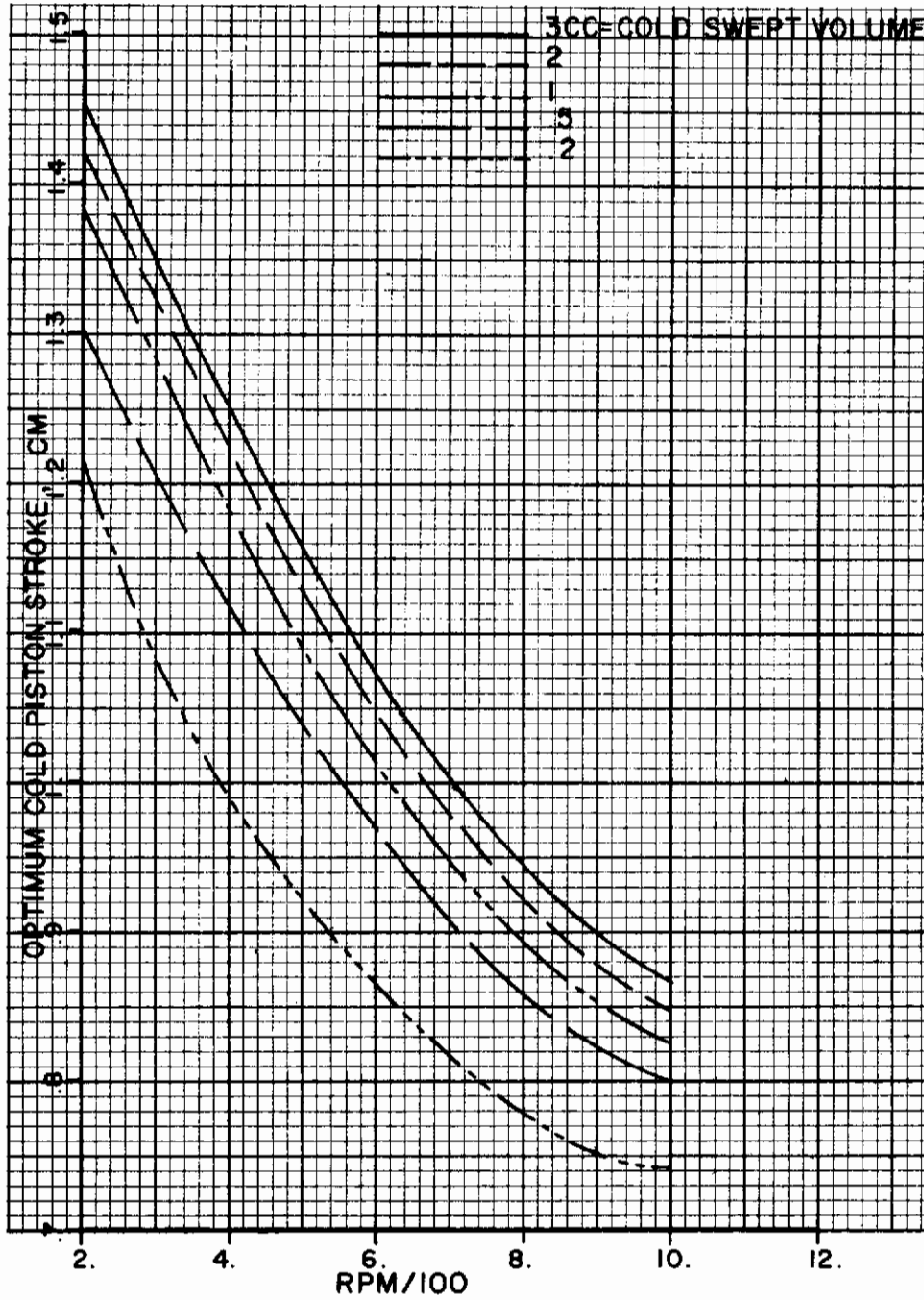


Figure 50. Optimum piston stroke as a function of rpm for five cold volumes.

Cold temperature = 120°K
 Ambient temperature = -65°F

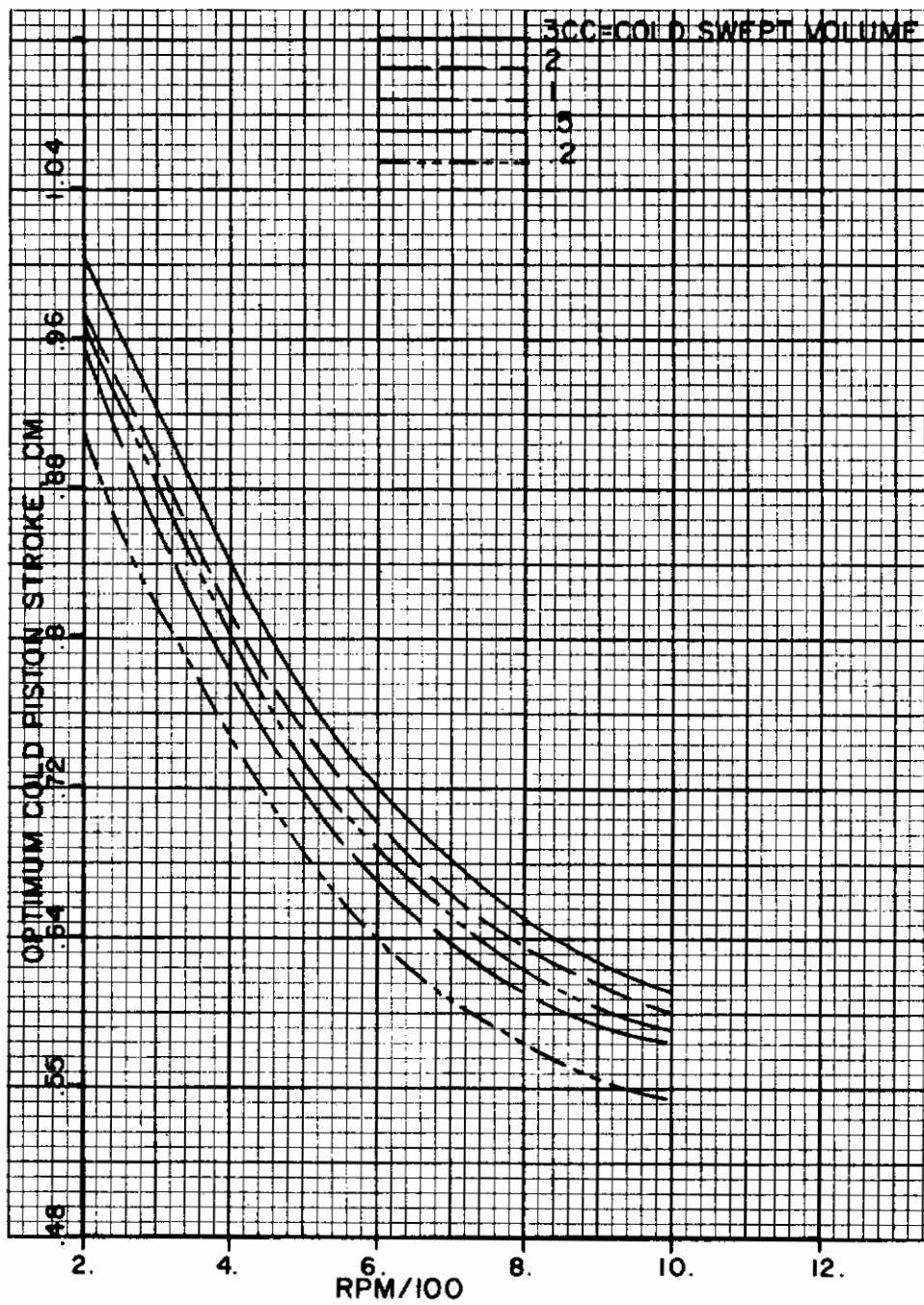


Figure 51. Optimum piston stroke as a function of rpm for five cold volumes.

Cold temperature = 70°K
 Ambient temperature = 300°F

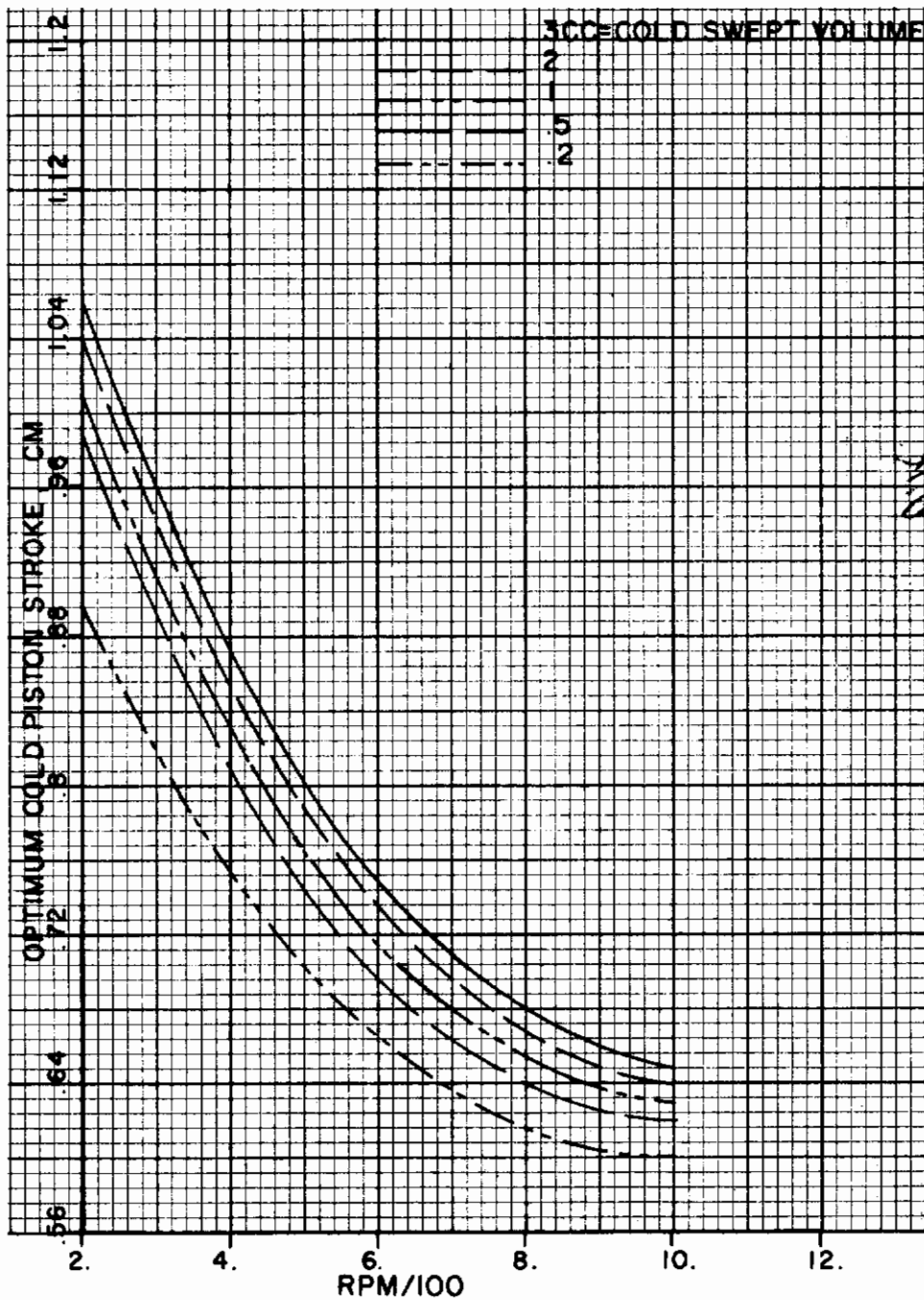


Figure 52. Optimum piston stroke as a function of rpm for five cold volumes.

Cold temperature = 70°K
 Ambient temperature = 160°F

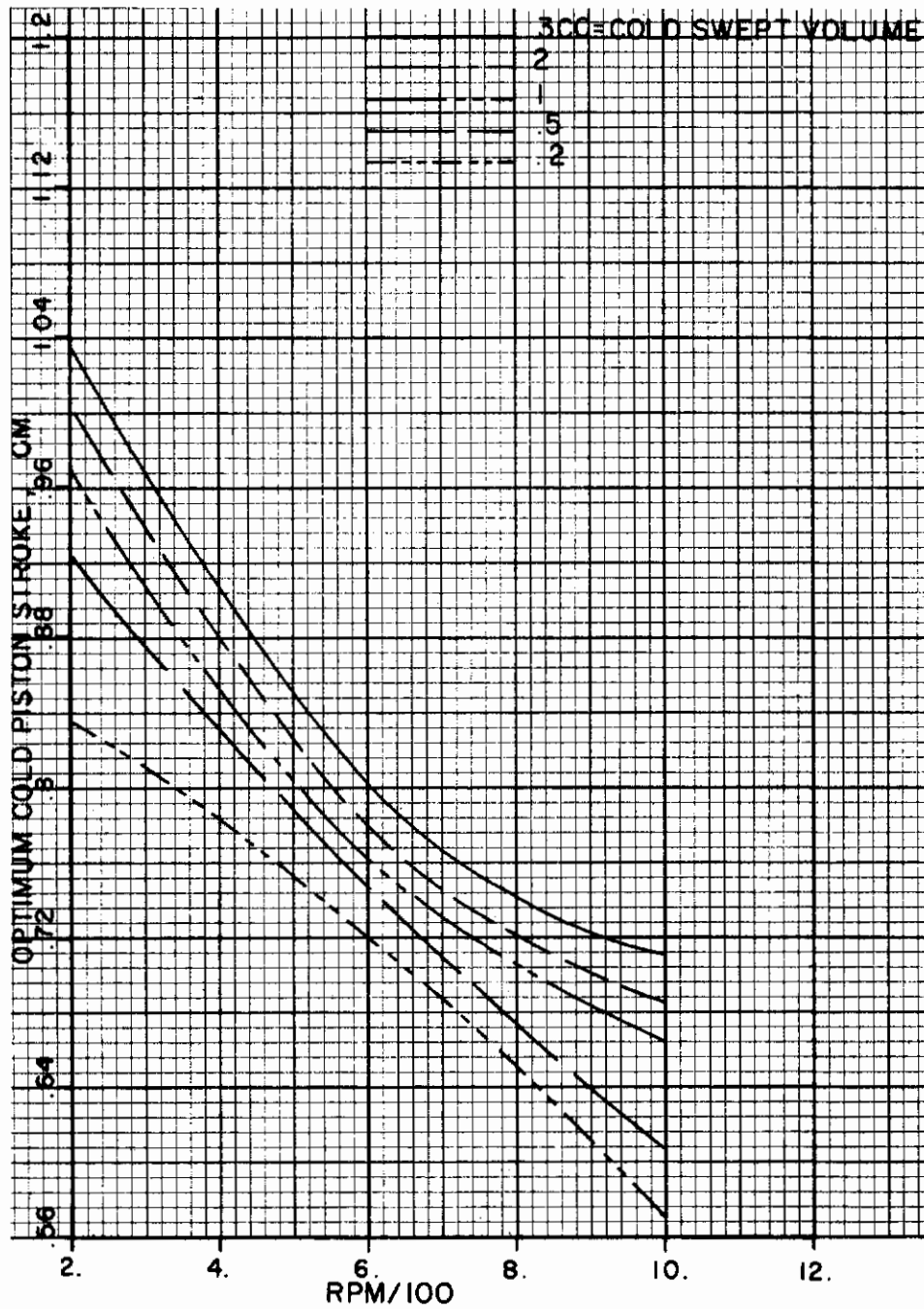


Figure 53. Optimum piston stroke as a function of rpm for five cold volumes.

Cold temperature = 70°K
 Ambient temperature = 70°F

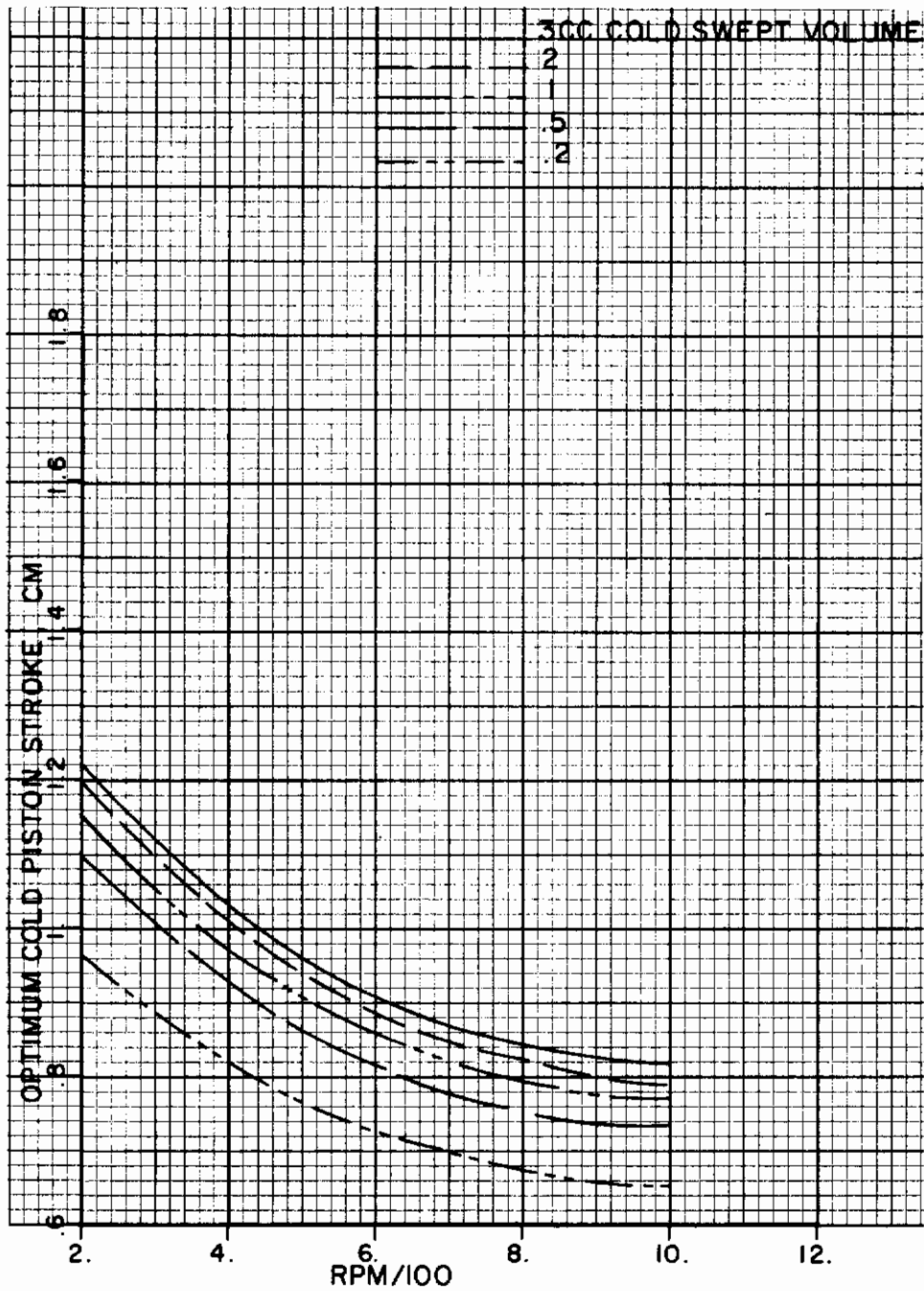


Figure 54. Optimum piston stroke as a function of rpm for five cold volumes.

Cold temperature = 70°K
Ambient temperature = -65°F

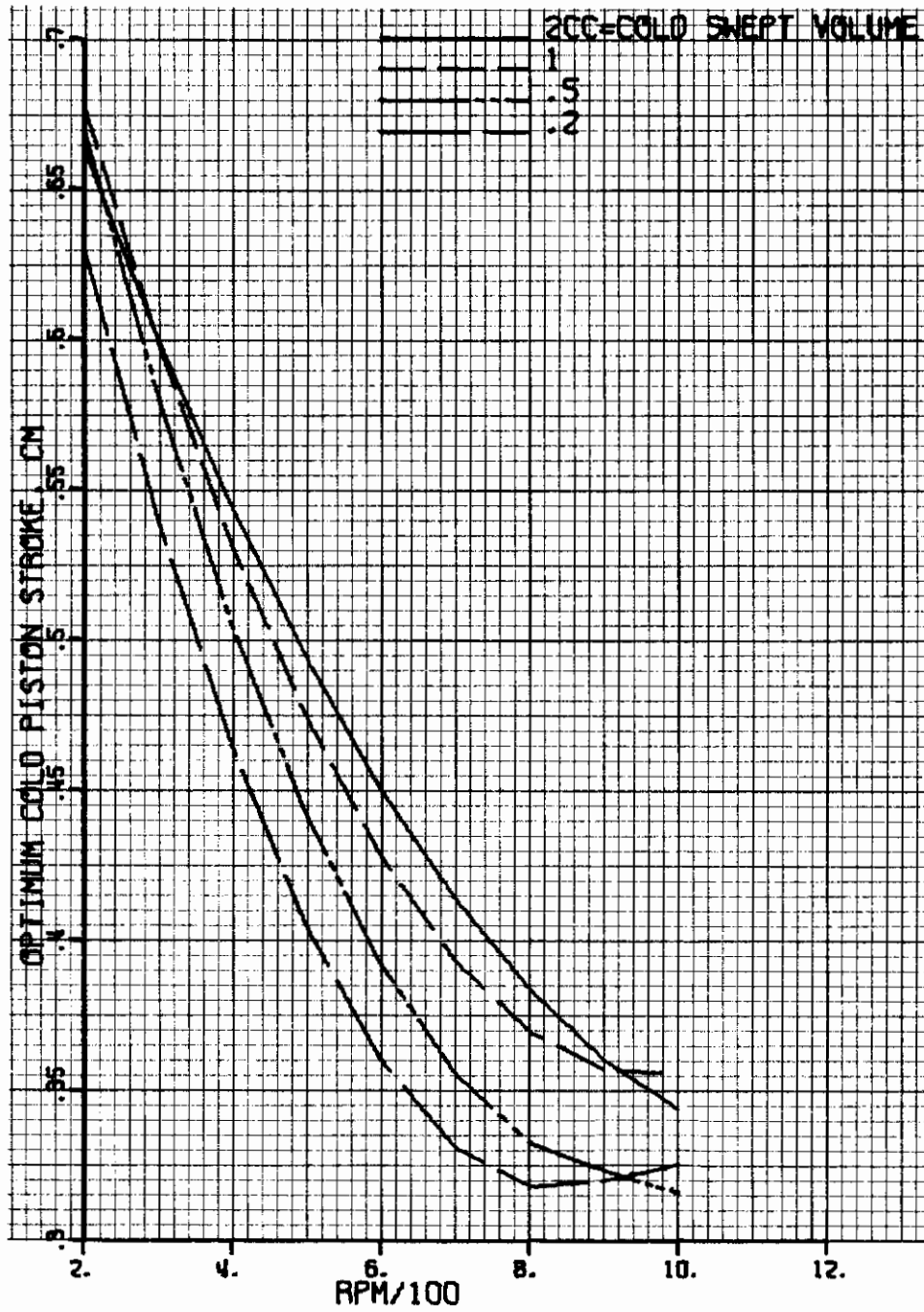


Figure 55. Optimum piston stroke as a function of rpm for five cold volumes.

Cold temperature = 30°K
Ambient temperature = 300°F

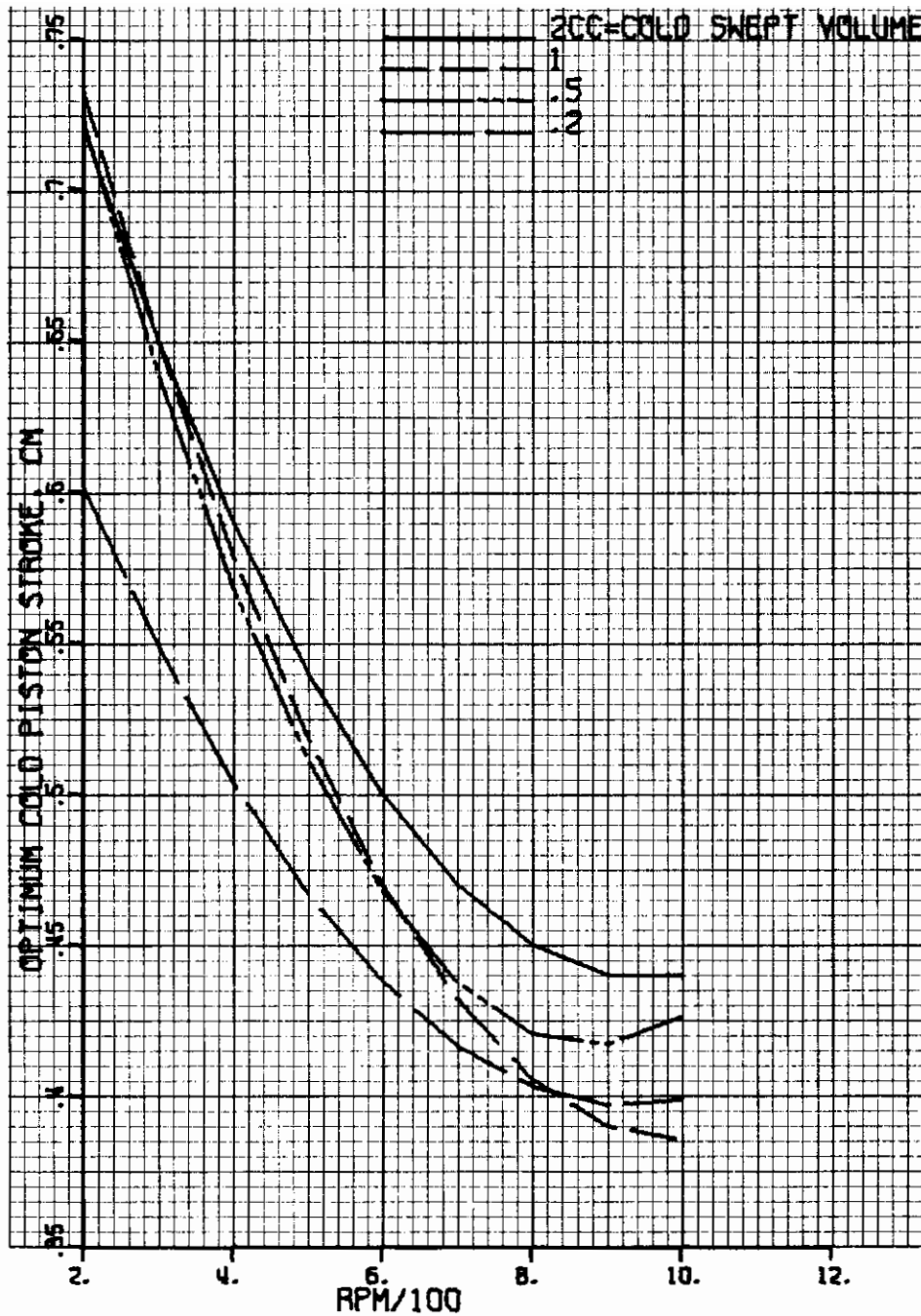


Figure 56. Optimum piston stroke as a function of rpm for five cold volumes.

Cold temperature = 30°K
Ambient temperature = 160°F

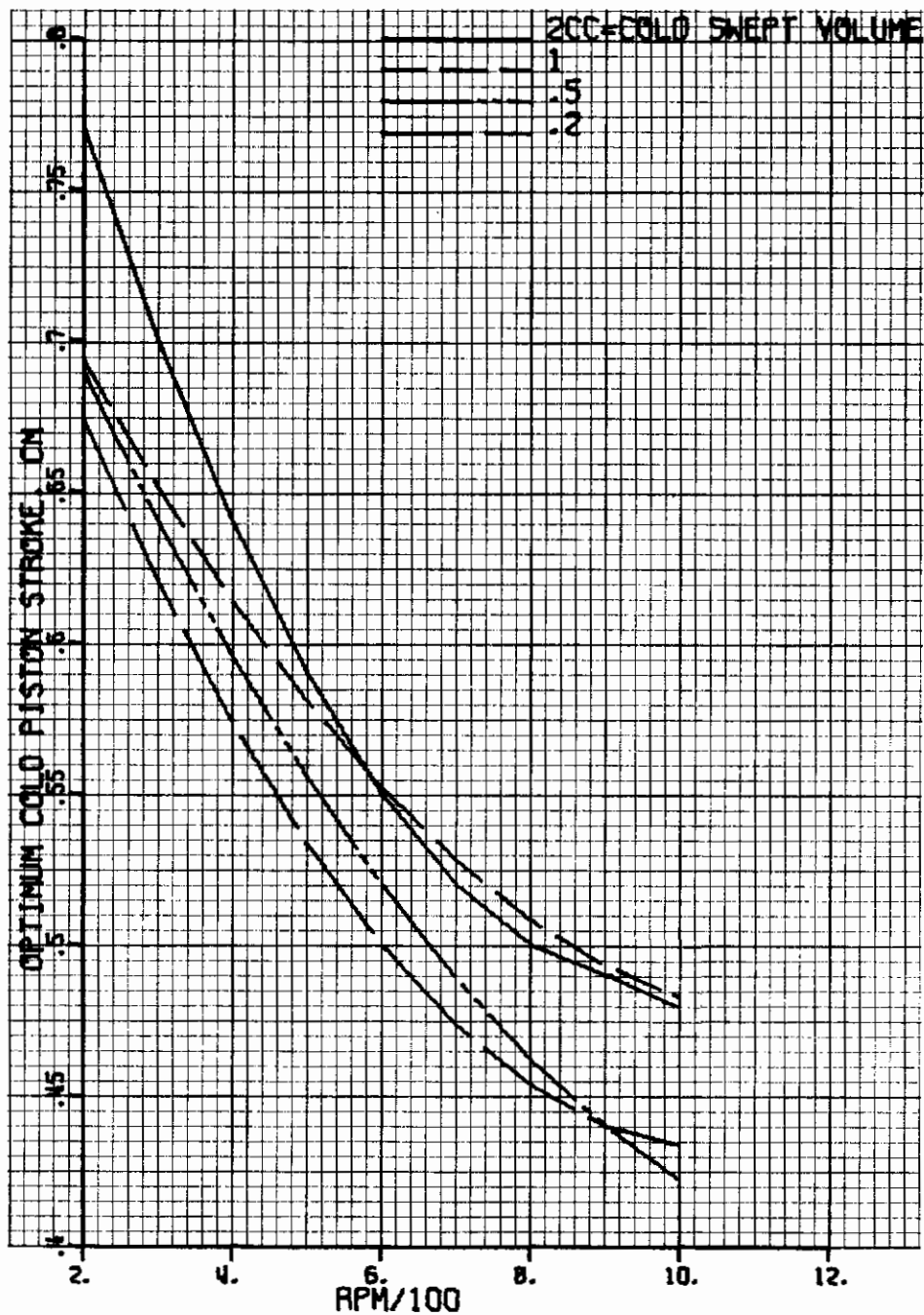


Figure 57. Optimum piston stroke as a function of rpm for five cold volumes.

Cold temperature = 30°K
 Ambient temperature = 70°F

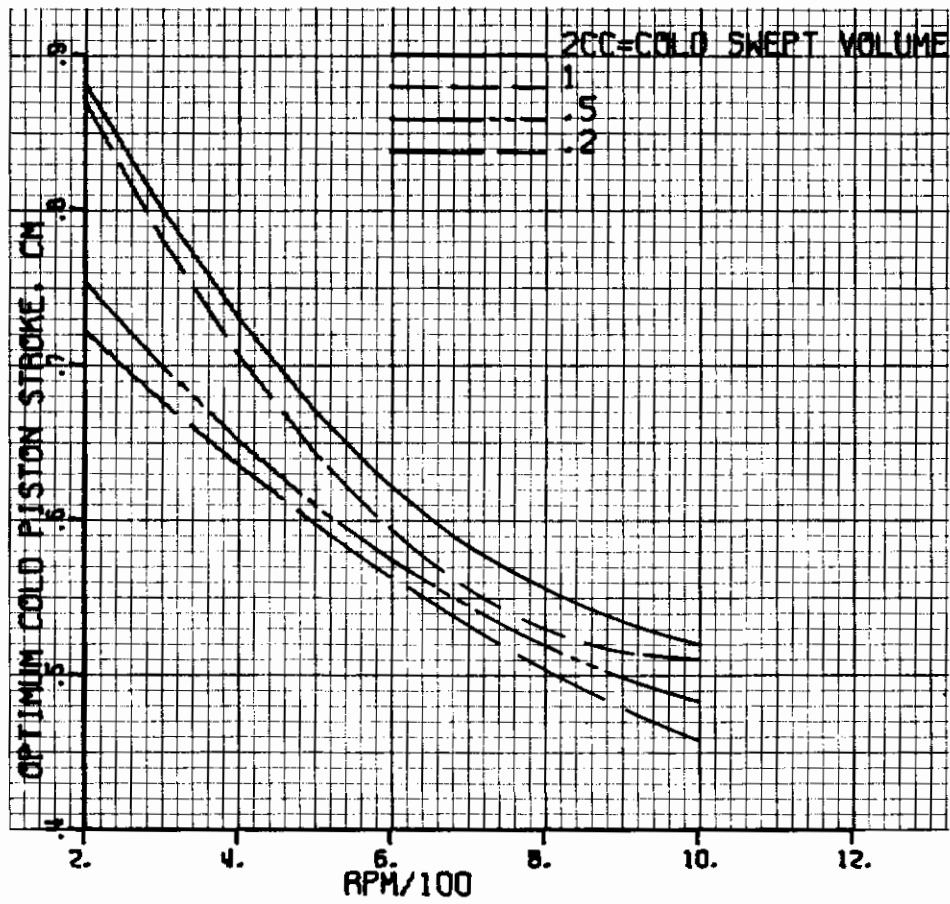


Figure 58. Optimum piston stroke as a function of rpm for five cold volumes.

Cold temperature = 30°K
Ambient temperature = -65°F

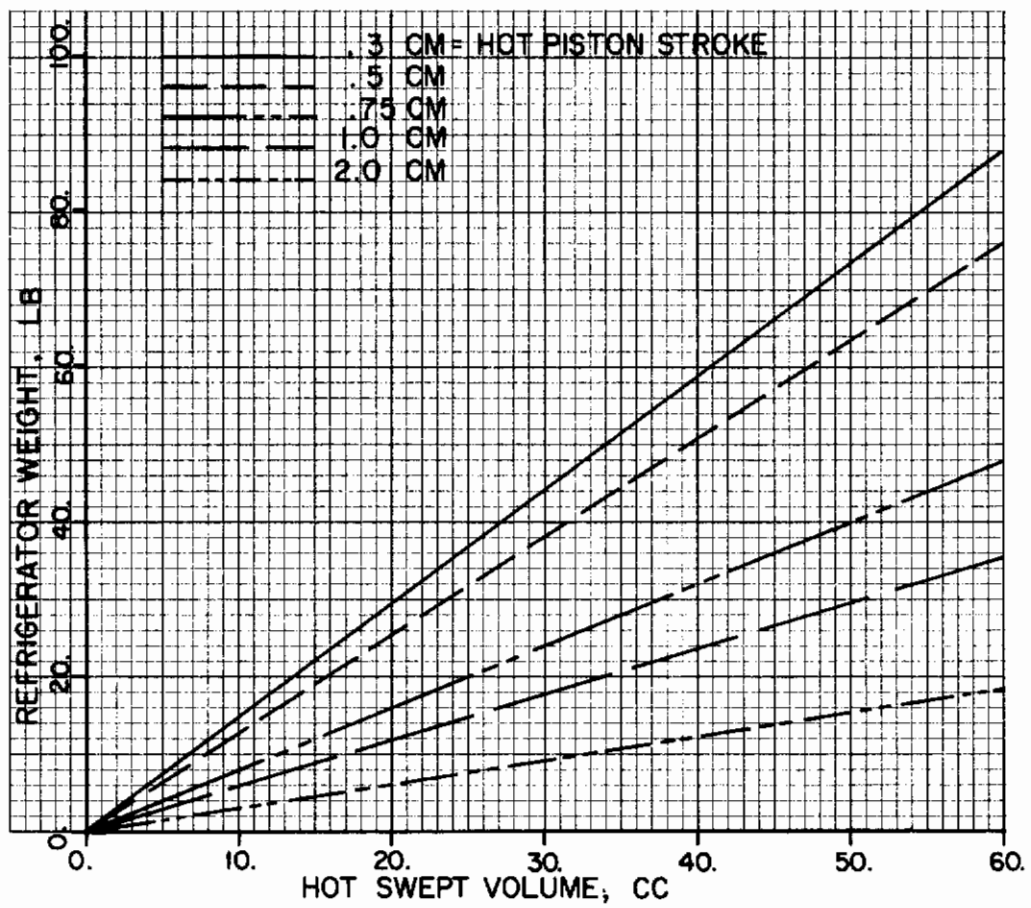


Figure 59. Weight as a function of hot volume and piston stroke.

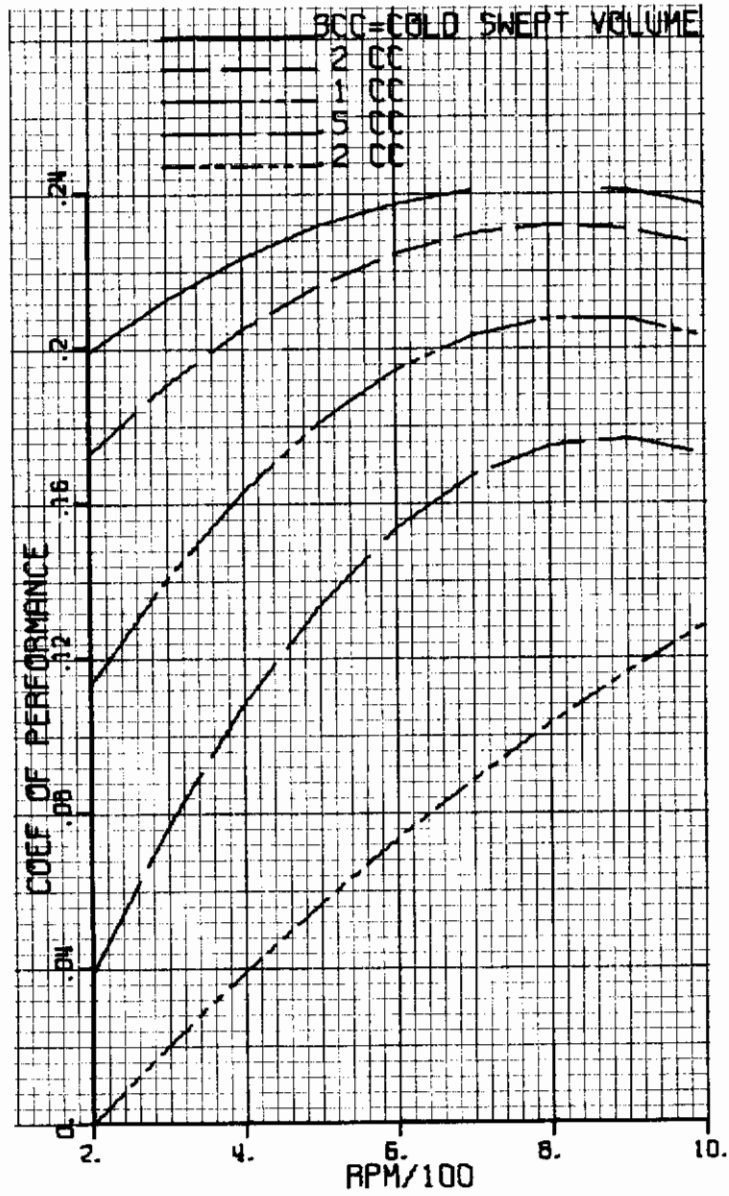


Figure 60. COP as a function of rpm for five cold volumes.

Cold temperature = 120°K
 Ambient temperature = 300°F

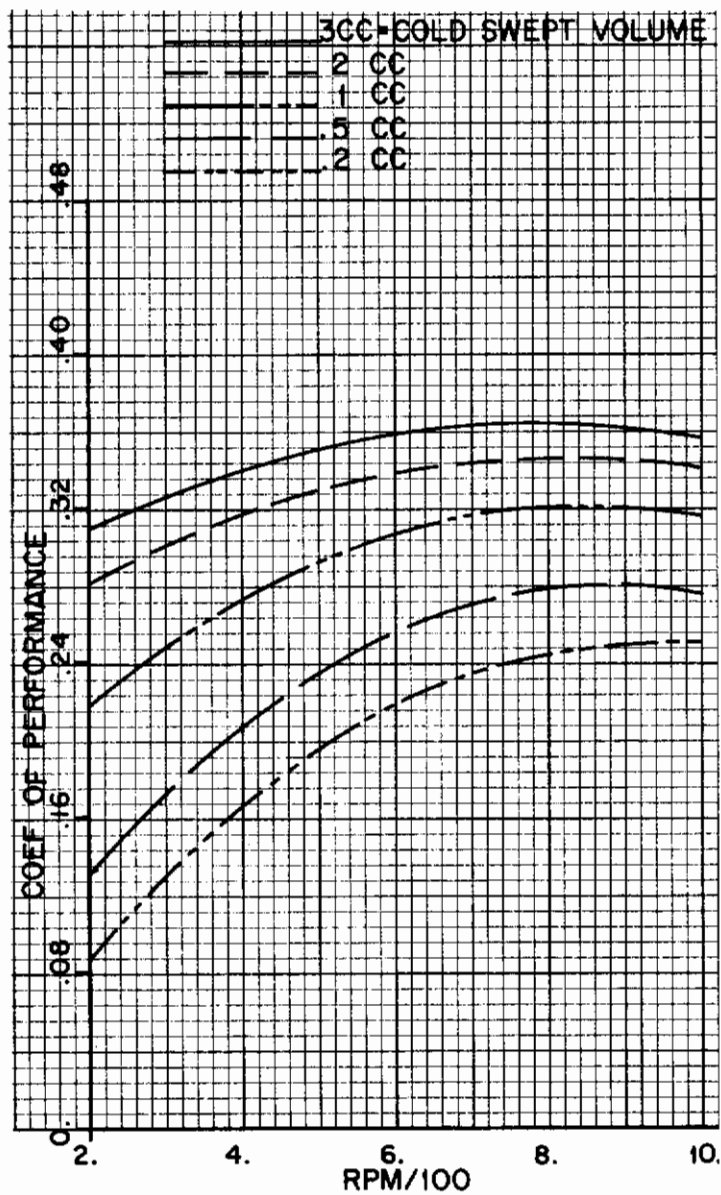


Figure 61. COP as a function of rpm for five cold volumes.

Cold temperature = 120°K
 Ambient temperature = 160°F

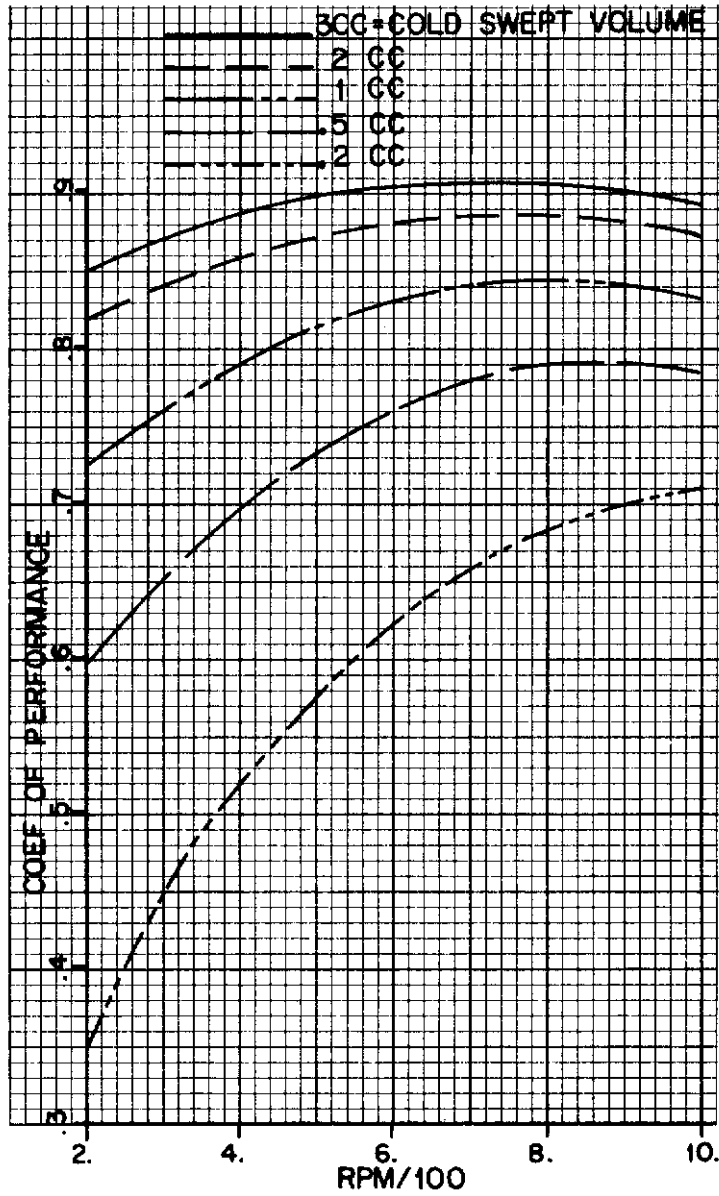


Figure 62. COP as a function of rpm for five cold volumes.

Cold temperature = 120°K
 Ambient temperature = 70°F

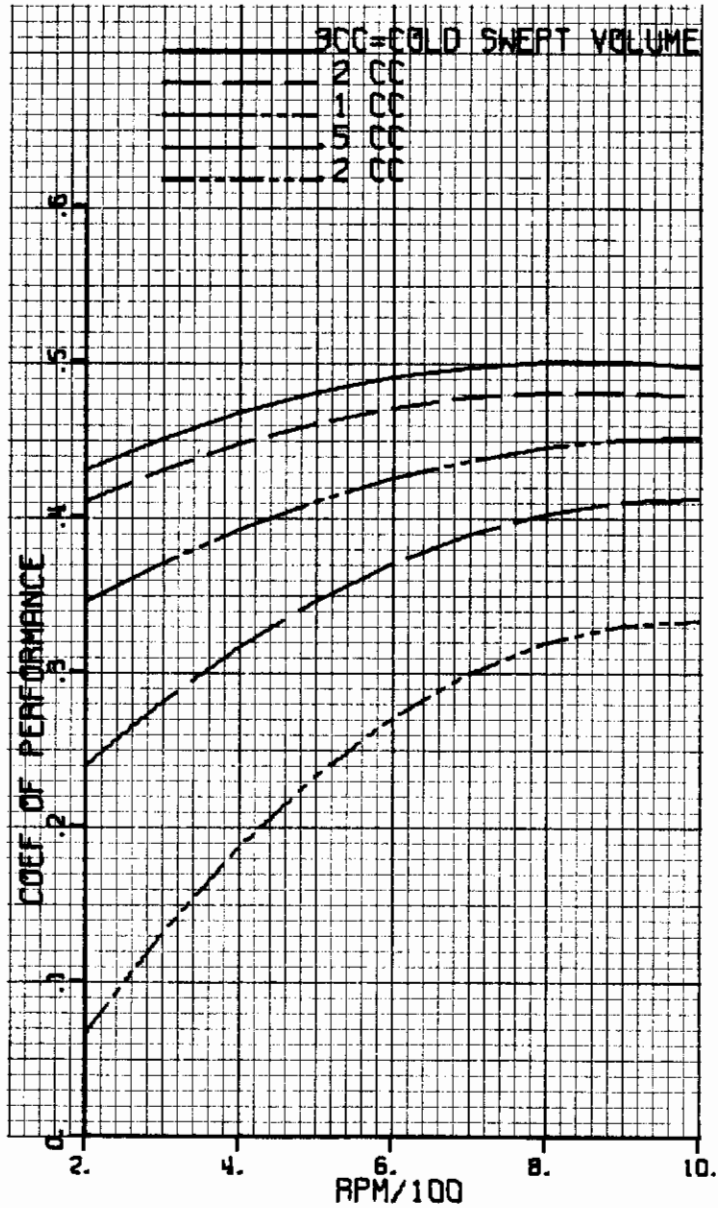


Figure 63. COP as a function of rpm for five cold volumes.

Cold temperature = 120°K
 Ambient temperature = -65°F

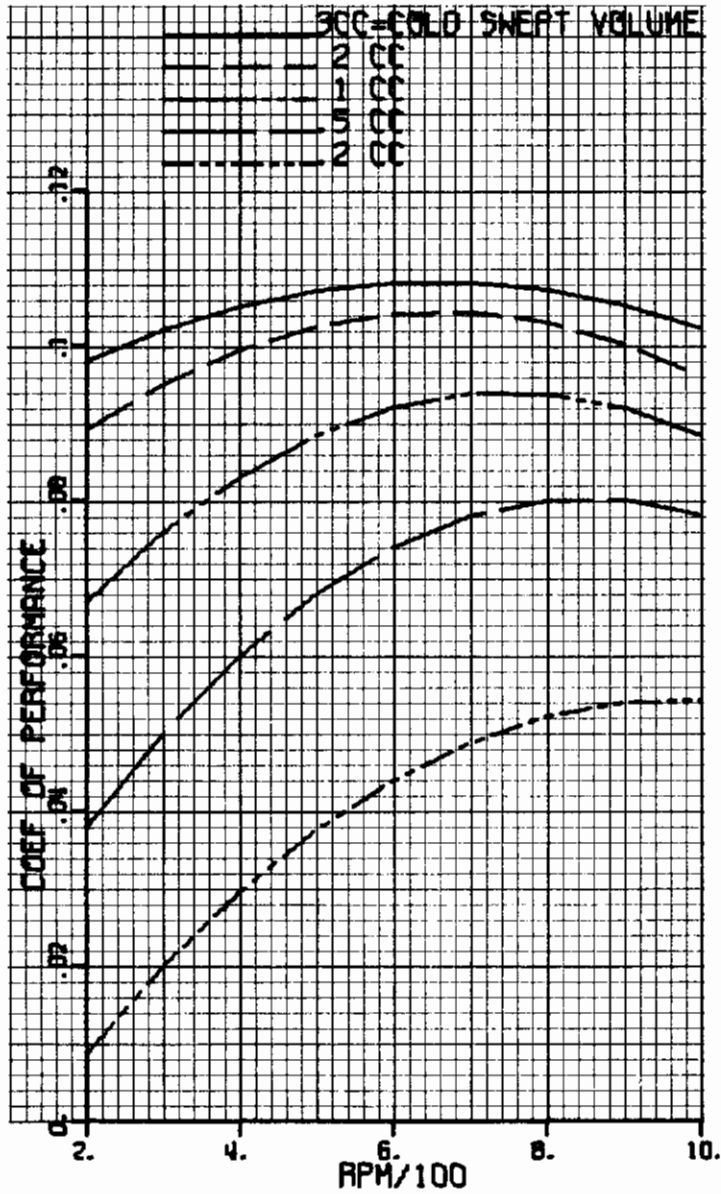


Figure 64. COP as a function of rpm for five cold volumes.

Cold temperature = 70°K
 Ambient temperature = 300°F

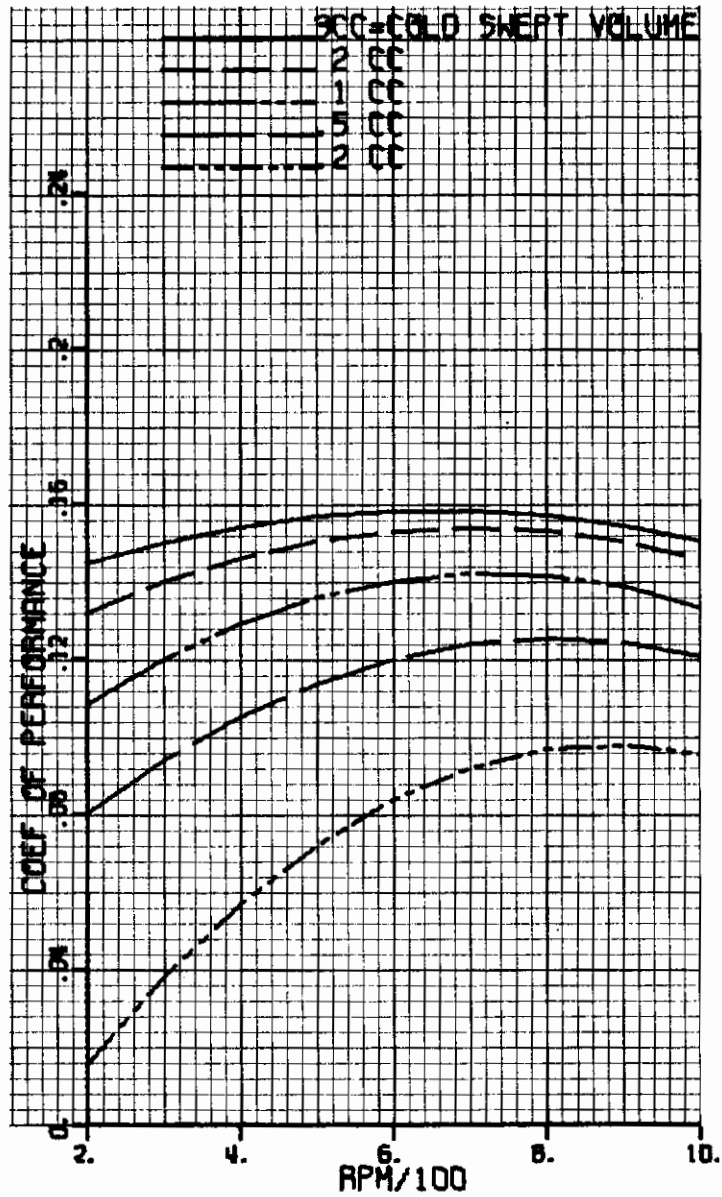


Figure 65. COP as a function of rpm for five cold volumes.

Cold temperature = 70°K
 Ambient temperature = 160°F

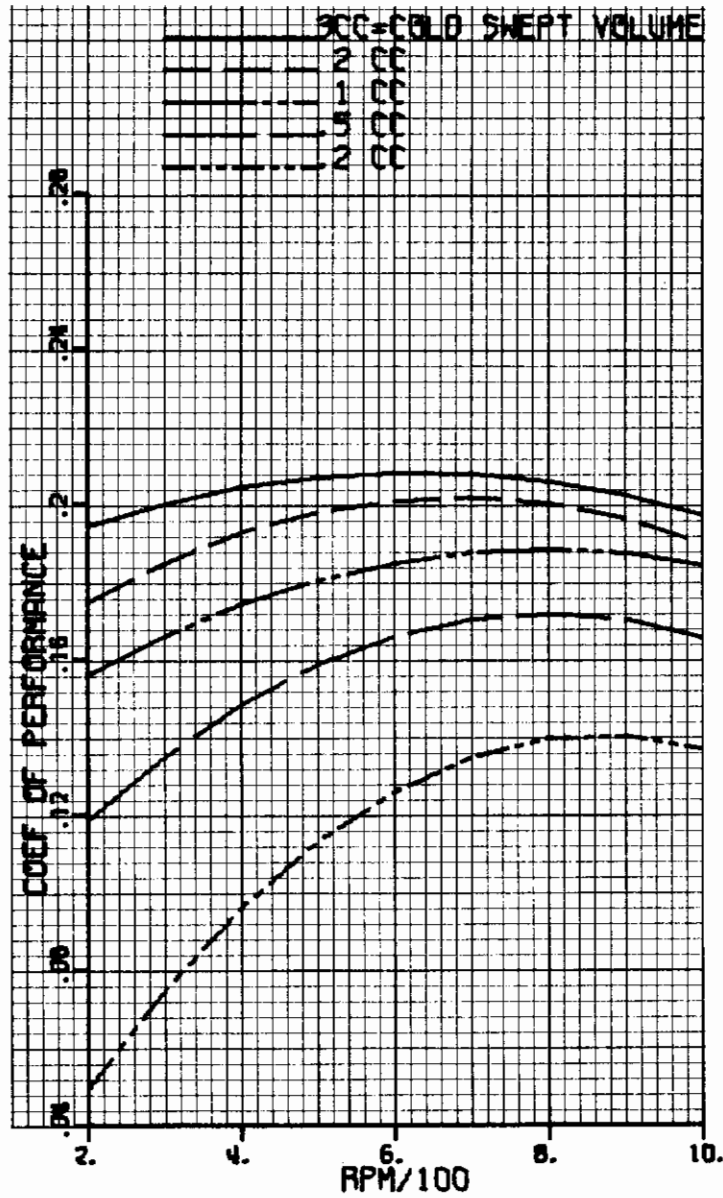


Figure 66. COP as a function of rpm for five cold volumes.

Cold temperature = 70°K
 Ambient temperature = 70°F

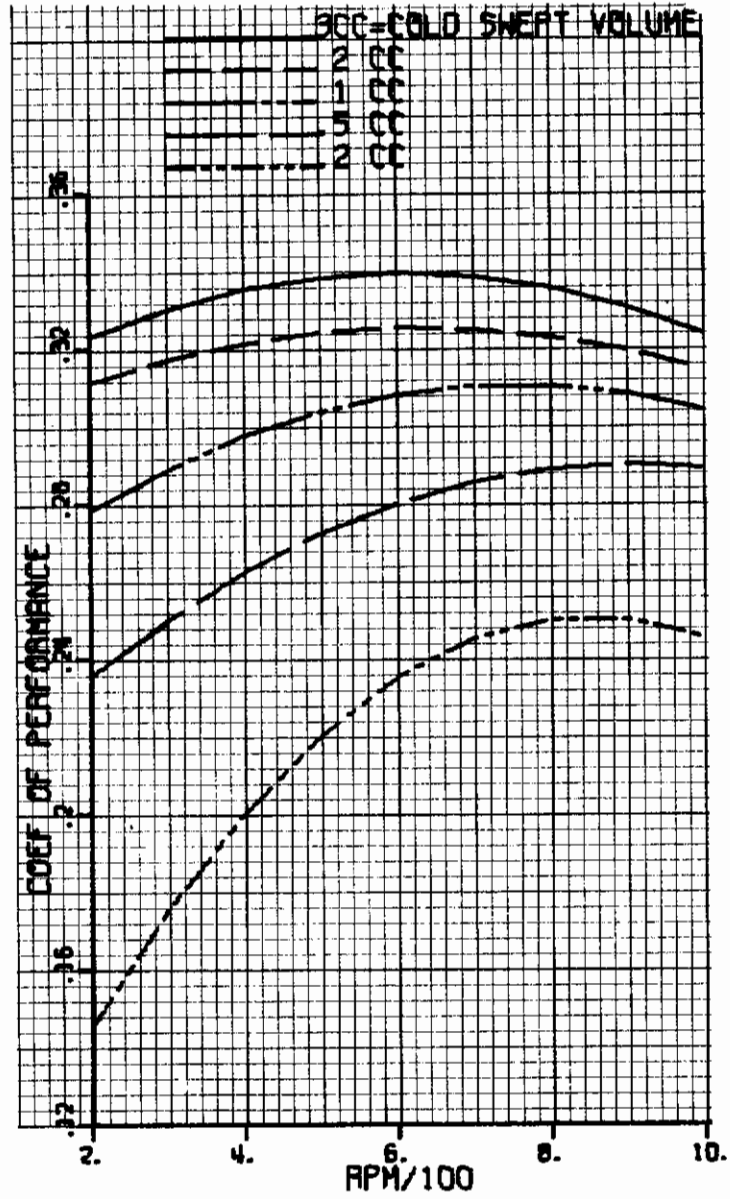


Figure 67. COP as a function of rpm for five cold volumes.

Cold temperature = 70°K
 Ambient temperature = -65°F

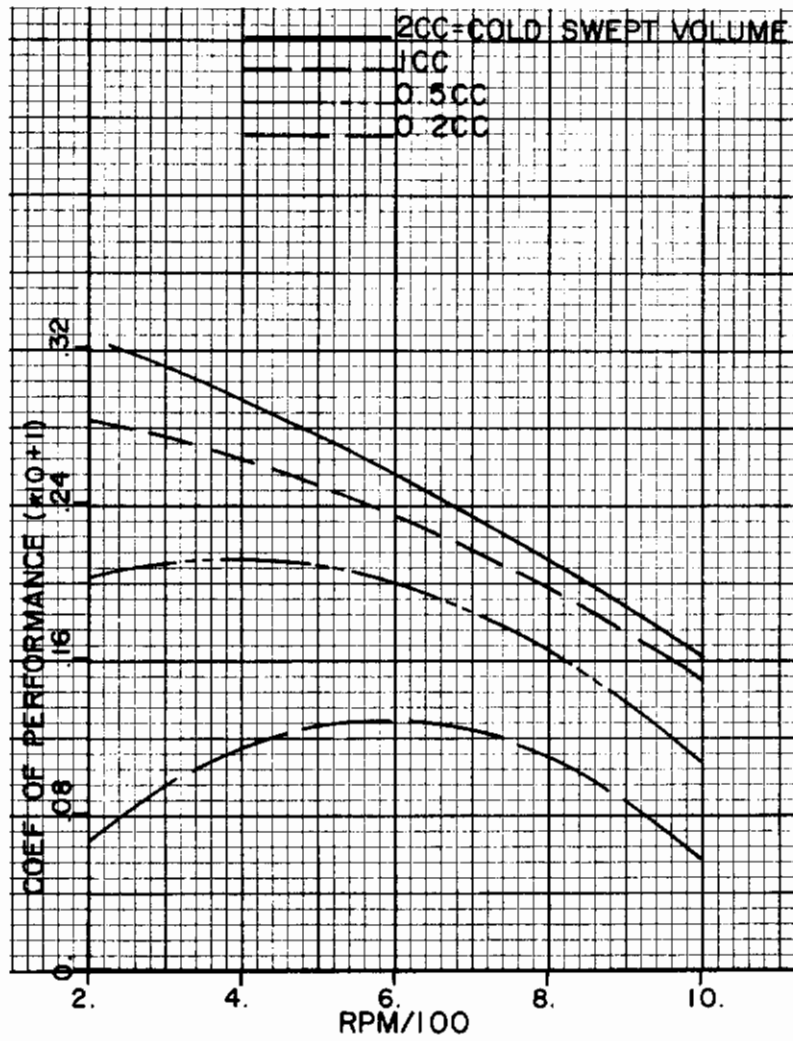


Figure 68. COP as a function of rpm for five cold volumes.

Cold temperature = 30°K
 Ambient temperature = 300°F

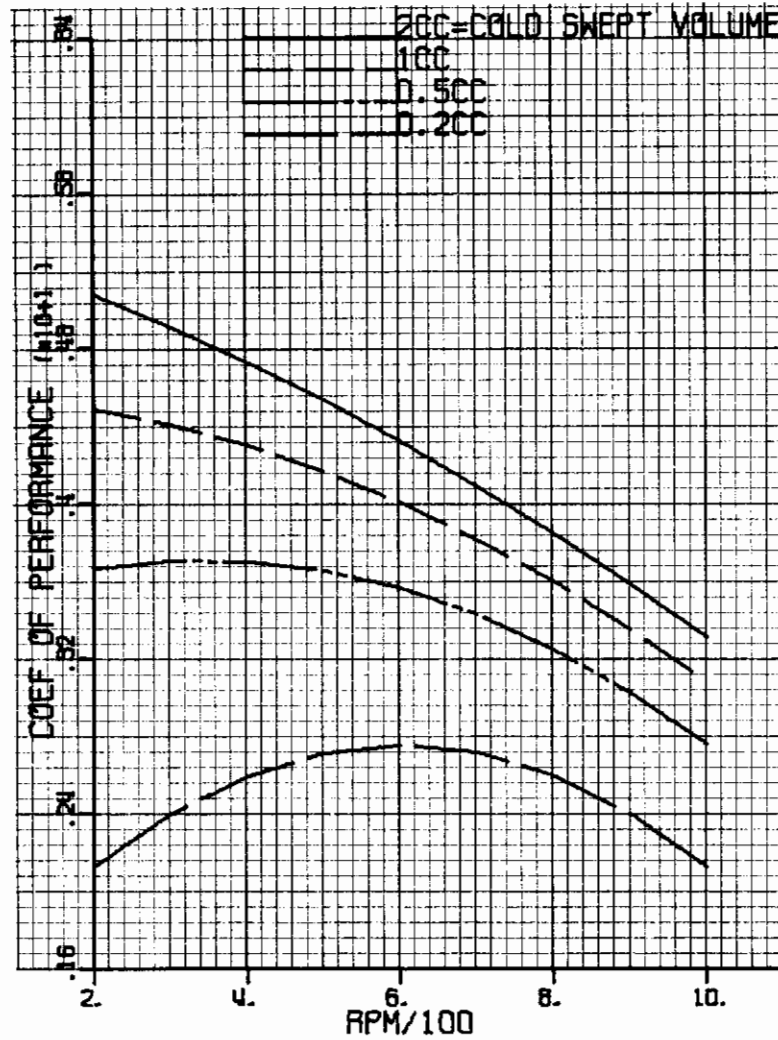


Figure 69. COP as a function of rpm for five cold volumes.

Cold temperature = 30°K
 Ambient temperature = 160°F

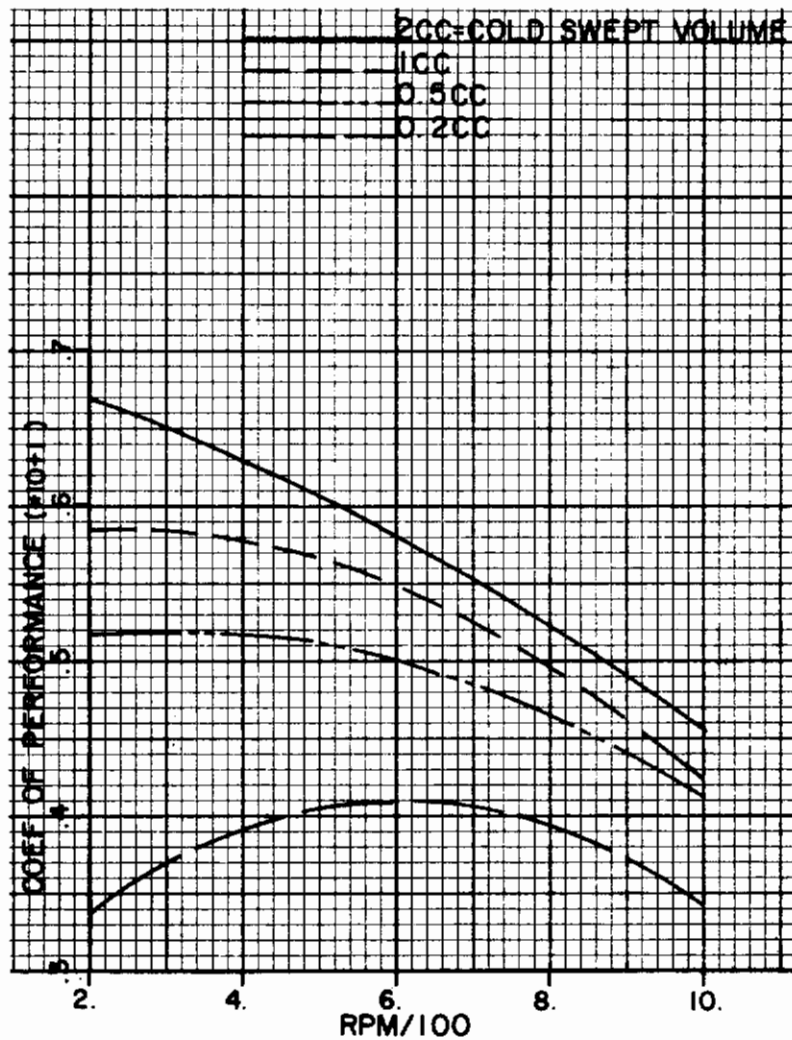


Figure 70. COP as a function of rpm for five cold volumes.

Cold temperature = 30°K
 Ambient temperature = 70°F

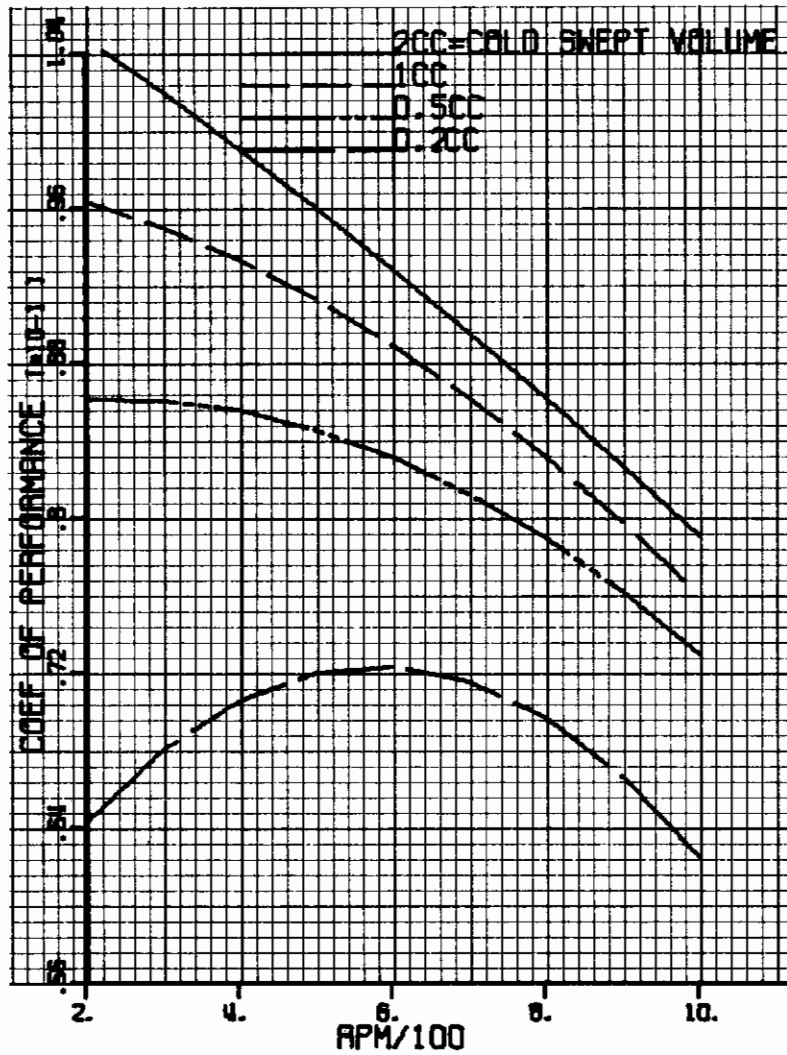


Figure 71. COP as a function of rpm for five cold volumes.

Cold temperature = 30°K
 Ambient temperature = -65°F

Contrails

$$Q_{pu} = \frac{2 (\pi D_c)^{0.6} L_{cy} (P_{max} - P_{min})^{1.6} N^{1.6} C_p^{1.6} (T_h - T_c) k_g^{-0.6}}{1.5 R^{1.6} \left(\frac{T_h + T_c}{2} \right)^{1.6}} S^{2.6} \quad (38)$$

$$Q_p = \frac{k_p \pi \left[(D_c - 2S)^2 - D_{ip}^2 \right] (T_h - T_c)}{4L_p} \quad (42)$$

$$Q_w = \frac{k_{cy} \pi P_{max} D_c^2}{L_{cy} \cdot 2 \cdot \sigma \left(1 - \frac{P_{max}}{2\sigma} \right)^2} (T_h - T_c) \quad (47)$$

$$\Delta P_{reg} = \frac{1}{2g_c} \rho U^2 f \frac{L_r}{D_e} = \frac{\dot{m}_f^2 L_r}{2g_c A_{reg}^2 D_e \rho} \quad (53)$$

$$Q_{rf} = \frac{\Delta P_{reg}}{\rho \cdot J} \dot{m} = \frac{\Delta P_{reg} (P_{max} + P_{min}) V_c \cdot 2 \cdot N}{\rho J 2 R T_c} \quad \begin{matrix} \text{(regenerator} \\ \text{friction loss)} \end{matrix} \quad (54)$$

$$\eta_r = \frac{1}{1 + \frac{1}{\lambda}} \quad \begin{matrix} \text{(regenerator heat transfer loss due} \\ \text{to film coefficient (h))} \end{matrix} \quad (20)$$

$$Q_{rh} = (1 - \eta_r) \dot{m} C_p (T_h - T_c) = (1 - \eta_r) C_p (T_h - T_c) \frac{(P_{max} + P_{min})}{2 R T_c} V_c N \quad (55)$$

Contrails

The above equations were added together and the partial derivative of the total loss with respect to the clearance S was put equal to zero.* A piston stroke was chosen and a solution was obtained for the clearance S at the assumed swept volume. The losses were then calculated using the computed value of S . A number of piston strokes were chosen until the losses reached a minimum. Piston strokes between 0.1 and 0.8 inch were applied until a curve was obtained that had a minimum point for the losses. Hence, this minimum point corresponds to an optimum cold piston stroke for an assumed swept cold volume and a fixed speed. A set of curves was computed in this manner since several swept cold volumes were applied. The speed was then changed and the computations repeated. The results are shown in Figures 47 through 58.

The curves in Figure 38 through 41 are based on shuttle, pumping, and heat conduction losses only and on a fixed cold cylinder length of 1 cm. The reason for this simplification was to generate a set of curves from which the sum of these three losses could readily be determined if the length of the cold cylinder is fixed at some chosen value. The accuracy of the curves increases as the pumping loss decreases since the shuttle and heat conduction losses are inversely proportional to the chosen cylinder length. Thus, a pumping loss that is less than 1/3 of the shuttle loss can generally be neglected and the losses become inversely proportional to the chosen length of the cylinder. The pumping loss becomes 1/3 of the shuttle loss at 1000 rpm if the two losses are added and the partial derivative taken with respect to the clearance S , and set equal to zero. The equation for the pumping loss shows that this loss decreases with rpm decreasing. The combination of high rpm and long cold cylinder length will increase the pumping loss sufficiently to introduce error into the cold cylinder length x losses graphs. Hence the curves in Figures 38 to 41 are accurate only if the cold cylinder regenerator is perfect and if the pumping loss is less than 1/3 of the shuttle loss.

Note: $L_{cy} = L_p = L_r = 1.4 \times \text{cold piston stroke} \times T_{avg} \text{ Regenerator} / T_c$.

The curves in Figure 45 are based on shuttle and head conduction losses only, since the hot cylinder does not have a pumping loss because of its regenerator design. The hot cylinder regenerator is assumed to be perfect.

Figure 60-71 show the C.O.P. for the VM machine. The curves in these figures are based on shuttle, pumping, heat conduction, regenerator friction and heat transfer losses; hence a total of five losses. The C.O.P. is defined as the ratio of the heat received by the refrigeration section from the body that is being cooled to the network received by the refrigeration section. Thus,

$$\text{C.O.P.} = \frac{Q_{\text{GROSS}} - Q_{\text{ut}}}{Q_{\text{GROSS}} \frac{(T_{\text{A}} - T_{\text{c}})}{T_{\text{c}}} + Q_{\text{rf}}} \quad (56)$$

The regenerator friction Q_{rf} was neglected in the computations, since it is small compared to the first term in the denominator.

In computing the C.O.P., all the above losses were minimized as described previously. The optimum cold piston stroke in Figures 47 through 58 was determined from these computations since the cold cylinder length is a function of the cold piston stroke. The cold cylinder length is equal to the regenerator length and the void volume in the regenerator is 70 percent of the swept cold cylinder volume that is computed at the average temperature of the regenerator. The cross sectional area of the regenerator is 50 percent of the cold piston cross sectional area. Hence, the cold cylinder length, applied in computing the C.O.P. is equal to $1.4 \times$ the cold piston stroke $\times T_{\text{avg regenerator}}/T_{\text{c}}$.

Only the equations for the shuttle and heat conduction losses in the hot cylinder were applied in constructing the curves of Figure 45. The sum of these losses was minimized by taking the partial derivate with respect to the piston stroke Y_{P} and setting this expression equal to zero. The clearance and the thickness of the piston wall were taken to be 0.005 inch and 0.018 inch, respectively, and a solution was

obtained for the piston stroke at a fixed swept volume. The curves were obtained by setting the length of the cylinder to equal 1 cm. The 0.005 inch clearance and the 0.018 inch thickness of the piston wall have been found to be practical values for the VM machines that have been built by Hughes up to date.

The equation for the heat losses in the hot cylinder is a function of the hot piston stroke and the inner diameter of the hot cylinder since all other parameters are fixed. The length of the piston is equal to the length of the cylinder. Since the piston stroke and the inner diameter are connected by the equation for the swept volume, the resulting minimum is a constrained minimum. A solution for the piston stroke at a fixed swept volume gives a minimum heat loss because the second derivative of the heat loss with respect to the piston stroke is positive. Thus, the computations, shown graphically in Figure 45, are carried out by solving for the inner cylinder diameter in the equation for the swept volume and substituting this value into the equation for the heat loss. The equation for the first derivative is a function of the piston stroke only and a solution is obtained for the piston stroke since the swept volume is fixed. By assuming another swept volume another optimum piston stroke is obtained and so on.

It is seen from Figure 46 that the optimum piston stroke depends on the fixed value for the thickness of the piston wall. The hot cylinder heat loss decreases when the thickness of the piston wall decreases and the thickness of the piston wall should, therefore, be as small as is practical with respect to refrigerator design.

Both the shuttle and conduction losses are independent of speed. The temperature limits and the hot cylinder length drop out in the expression for the partial derivation and, therefore, only a single curve for each piston wall thickness in Figure 46 shows the relationship between optimum hot piston stroke and swept hot volume at a fixed thickness for the piston wall.

The length of the regenerator in the hot cylinder equals the length of the piston. The piston is equal to the cylinder length and, hence, is fixed once a cylinder length has been chosen so that the losses in the hot cylinder are acceptable.

The relationship between the swept hot volume and the swept cold volume is computed from

$$\frac{V_{\text{hot}}}{V_{\text{cold}}} = \frac{T_h (T_A - T_c)}{T_c (T_h - T_A)} \quad (57)$$

This equation is derived from the ideal work and the ideal refrigeration production that takes place in the machine during a cycle when the pressure at crank position N is assumed equal to the pressure at crank position W as indicated in Figures 8 through 10.

The weights of the VM refrigerator, Figure 59, include the weight of the crank-case, and the weight of the electrical motor. Thus, the weight formula, $W = 0.6 \times \text{hot swept volume}/\text{hot piston stroke}$, for the refrigerator weight is based on actual crank-case dimensions that have been obtained from the machines that have been built up to date by Hughes. The weight, obtained by using the formula, agree well with real refrigerator weights. The weight of a VM refrigerator can also be obtained from Figure 46 and the weight computed by using the weight formula. Figure 59 was constructed in order to eliminate the computational work.

The weight of the electrical motor that is required to drive a long-life Vuilleumier refrigerator against friction is generally about 1/3 of the weight obtained for a particular unit from Figure 59. The friction and, hence, the weight of the electrical motor depends strongly on the alignment of the various parts of the refrigerator.

If the weight of a VM refrigerator is limited by a maximum value, the designer can start with Figures 59 and 46 and work backwards in order to obtain the necessary net refrigeration and machine dimensions. In applying the graphs in this manner, it should be remembered that the losses in the cold cylinder are inversely proportional to the cold cylinder length only if the pumping losses in the cylinder and the friction losses in the regenerator are negligible compared to the shuttle and heat conduction losses.

The maximum pressure in the machine is determined by trial and error until practical dimensions are obtained for regenerators, speed, and cylinders. It has been found that a maximum pressure of about 700 psi is a practical value for the machines that have been built up to date by Hughes. The 700 psi maximum pressure corresponds to a minimum or filling pressure of about 500 psi. The maximum pressure occurs when the major part of the working fluid is in the hot cylinder and in the ambient temperature spaces. The minimum pressure occurs when the major part of the working fluid is in the cold cylinder and in the ambient temperature spaces.

The maximum pressure of 700 psi gives a cylinder wall thickness that is acceptable with respect to heat conduction losses. It is desirable to use a material for the pistons and cylinders that has a thermal conductivity that is as low as possible. However, the material should also have properties that are acceptable from a design and construction viewpoint. In the computations, it is assumed that the cold and hot cylinders are made of 304 stainless steel and 718 inconel, respectively; the cold and hot cylinder displacers of glass loaded epoxy and 750 inconel, respectively, and the crank-case of brass with connecting rods of stainless steel.

The void or dead volume in the VM machine was taken to be 1.5 times the cold swept volume at the particular refrigeration temperature and this number was applied in computing the pressure ratio P_{\max}/P_{\min} .

The mass of gas in the refrigerator is computed, from the total volume, the temperature limits and the maximum or minimum pressure, by means of the perfect gas law.

The angular phasing in the machine was taken to be 90 degrees in the computation. Thus, in the refrigeration section of the machine, the cold temperature piston face in the cold cylinder is at TDC when the ambient temperature piston face in the hot cylinder is 90 degrees from BDC.

The friction factor and the heat transfer coefficient that were applied in the computations were taken from experimental data. This data is presented in Reference 5 by Figures III-1, III-2, III-3.

No losses are included in Figures 14 through 37, 42 through 44, and 59, but losses are included in all the other figures that present curves. Only the shuttle and heat conduction losses are included in Figures 45 and 46. The shuttle, pumping, and heat conduction losses are included in Figures 38 through 41. The shuttle, pumping, heat conduction, regenerator friction and heat transfer losses are included in Figures 47 through 58 and in Figures 60 through 71. It is pointed out again that the losses shown in Figures 38 through 41 are inversely proportional to cylinder length only when the pumping and regenerator losses can be neglected with respect to the shuttle and heat conduction losses. The percent error, by assuming that the losses given in Figures 38 through 41 are inversely proportional to the length of the cold cylinder, varies with the shuttle and conduction losses and with the chosen length of the cold cylinder. The percent error decreases as the difference between the pumping and the shuttle losses increases, but increases as the difference between the chosen length of the cold cylinder and 1 cm increases.

The refrigerator temperature limits of 120°K , 70°K , and 30°K were chosen as parameters because they can be reached by a single-stage Vuilleumier refrigerator and they are frequently the operating temperatures of infrared devices.

The heat-rejection temperatures of -65°F , 70°F , 160°F , and 300°F were chosen as parameters because the first three of these temperatures are generally encountered at sea-level operation and the fourth temperature is a practical temperature limit for heat rejection when the refrigerator is spaceborne.

A temperature limit of 1200°F for heat addition to the hot cylinder and a maximum pressure of about 700 psia are practical design values with respect to the metallurgical limit of the hot cylinder material.

Application of Graphs

In order to show how Figures 14 through 71 are applied in determining the weight of a Vuilleumier refrigerator, let it be assumed that an infrared device required 2 watts of refrigeration at 70°K . It is required to determine the size of the cylinders, the optimum piston strokes, the power input to the hot cylinder, the weight, and the coefficient of performance of the refrigerator when it is operating at 500 rpm and rejecting heat at 70°F .

The above dimensions and values are determined as follows:

1. From Figure 26, at 500 rpm and at a swept volume in the cold cylinder of 0.4 cc, the gross refrigeration is 2.9 watts.
2. From Figure 27, at 500 rpm and at a swept volume in the cold cylinder of 0.4 cc, the minimum required power input to the hot cylinder is 13.6 watts.
3. From Figure 40, at a swept volume in the cold cylinder of 0.4 cc, the losses at the cold cylinder are 4 watt cm. Taking the cold cylinder length to be 4.45 cm gives a loss of 0.9 watt and the net refrigeration is thus 2 watts.
4. The swept volume in the hot cylinder at a swept volume of 0.4 cc in the cold cylinder is read from Figure 43 and equals 2 cc.
5. The losses at the hot cylinder for a swept volume of 2 cc in the hot cylinder are read from Figure 45 and are 70 watt cm. Taking the length of the hot cylinder to be 5 cm, the losses at the hot cylinder are 14 watts and the required total power input to the hot cylinder is 27.6 watts.
6. From Figure 53, at a swept volume of 0.4 cc in the cold cylinder, the optimum piston stroke in the cold cylinder equals 0.78 cm.
7. From Figure 46, at a swept volume of 2 cc in the hot cylinder, the optimum piston stroke in the hot cylinder equals 0.12 cm.

Contrails

8. From Figure 59, at a swept volume of 2 cc in the hot cylinder, and at an optimum hot piston stroke of 0.12 cm, the weight of the refrigerator equals 3.8 pounds.
9. The coefficient of performance is determined from Figure 67 and equals 0.146 at 500 rpm and at a swept volume in the cold cylinder of 0.4 cc.

The graphs were also applied in checking the real VM design X447525-100; the results are shown in the sample calculation below.

SAMPLE CALCULATION

| | <u>Applications Envelope Calculation</u> | <u>X447525-100 Design</u> |
|--|--|--|
| Cold temperature, °K (assumed) | 70 | 77 |
| Rejection temperature, °K (assumed) | 300 | 260 |
| Hot temperature, °K | 1200 | 1200 |
| RPM | 510 | 510 |
| Cold swept volume, cc (assumed) | 0.5 | 0.48 |
| Gross cold, watts | 3.6 | 5 |
| Minimum heat input, watts | 33 | 35 |
| Length of cold cylinder x losses, watt cm | 7.9 | |
| Cold cylinder length, cm | 4.65 | 4.65 |
| Cold end losses, watts | 1.7 | 2.7 total 1.8 (neglecting regenerator losses) |
| Net refrigeration, watts | 2.08 | 2; 1.5 (actual) |

Contrails

| | <u>Applications Envelope Calculation</u> | <u>X447525-100 Design</u> |
|--|--|--|
| Hot swept volume, cc | 4.65 | 3.66 |
| Hot cylinder length x losses, watt cm | 112 | |
| Hot cylinder length, cm | 2.5 | 2.5 |
| Hot cylinder losses, watts | 45 (without insulation and regen- erator losses) | 124 total 116 (without insulation losses 49 (without insulation and regenerator losses) |
| Total input power, watts | 78 | 84 (without insulation and regenerator losses) |
| Hot piston stroke, cm | 0.22 | 0.65 |
| Cold piston stroke, cm | 0.69 | 0.65 |
| Weight, lb | 3.4 | 3; actual (including weight of fan) = 5 |
| .C.O.P. | 0.0445 | 0.0407 0.0121 Actual |

The difference in the above two cold and losses are due to the difference between the chosen cold cylinder length of 5.2 cm and 1 cm. The curves in Figures 38 through 41 are, as explained above, based on a cold cylinder length of 1 cm and the pumping loss is taken to be inversely proportional to cylinder length when reading the data from the curves. However, the real pumping loss is a direct function of the cylinder length and the curves, therefore, show a small cold end loss.

The difference between the hot swept volumes is due to the difference in temperature limits. The applied curve in Figure 43 is

based on the ambient temperature of 300°F, and a cold end temperature of 70°K, but the computed hot swept volume is based on 260°F and a cold end temperature of 77°K.

From the above discussion, it is seen that all of the important parameters of a Vuilleumier refrigerator can be determined from the figures once the boundary conditions have been fixed.

The technical fields (Reference 19) where cryogenic cooling is required and, hence, where the Vuilleumier refrigerator can be applied are shown in Figure 72. It is seen from this figure that there are seven important technical fields that have applications for the Vuilleumier refrigerator. Some of these applications require a one-stage refrigerator, some a two-stage refrigerator and some a two-stage refrigerator with a special loop that contains a compressor and a Joule-Thomson throttling valve.

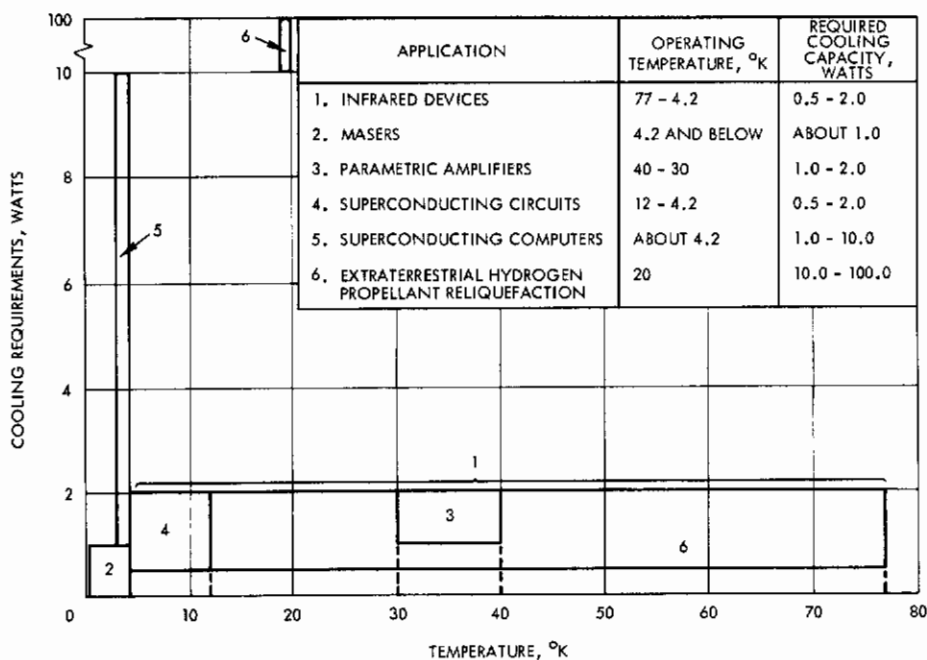


Figure 72. Technical areas in which Vuilleumier refrigerator can be applied.

Contrails

SECTION V

30°/75°K BREADBOARD REFRIGERATOR
(X447550-100)

INTRODUCTION

The X447550-100 refrigerator is an end item in Phase I of the development program to demonstrate the feasibility and applicability of the Vuilleumier two-stage refrigeration cycle. It was designed as a breadboard model for cooling a typical space based infrared receiver to investigate and define various interface problems associated with this type application. However, although designed as a space breadboard, it has the capability of operating in an application aboard a military aircraft.

DESIGN REQUIREMENTS

Design specifications required detailed design and integration of all components of the refrigerator including power conversion equipment. The end product was to fulfill three basic functions.

1. Act as a laboratory breadboard model to demonstrate feasibility of the Vuilleumier cycle and obtain new information which would permit refinement of the design.
2. Act as a laboratory breadboard model to investigate the interface problems between the Space Based Warning Receiver (SBWR), the cryogenic refrigerator and space vehicle installation.
3. Act as a flyable prototype to be used in aircraft to demonstrate performance feasibility and compatibility with potential airborne system applications.

The model must be capable of operating on 28 vdc input power and thus would incorporate all required power conversion equipment. It is designed to be liquid cooled and compatible with existing aircraft liquid cooling systems.

Specific contractual design requirements were:

"The breadboard model Space Based Warning Receiver Vuilleumier cycle refrigerator will be designed to produce 5 watts cooling at 75°K and 1/2 watt at less than 30°K. Although the breadboard model may be used to investigate interface problems or as a test bed to prove the solution of various refrigerator problems, the breadboard refrigerator will be delivered complete with any power conversion equipment in a form that would be representative of a lightweight, efficient electrically powered refrigerator that would be used in an aircraft application."

There were several specific requirements for test instrumentation to be delivered with the breadboard.

- Temperature measuring devices located on hot cylinder, cold cylinder and crankcase heat rejection area.
- An electrical resistance heater to simulate detector and optical loads at each cold stage.
- A pressure gage attached to indicate unit internal pressure.

UNIT SPECIFICATIONS

Working specifications for the unit and major components were generated from these requirements. Where requirements were incomplete, values were assumed to complete the specifications. Preliminary equipment specification XES-30528-010, pages 1 to 4 describes the X447550-100 breadboard refrigerator.

| | | | |
|---|---|----------------------|---------|
| HUGHES HUGHES AIRCRAFT COMPANY CULVER CITY CALIFORNIA AIR DEFENSE ELECTRO-OPTICAL LABORATORY | TITLE <i>Contracts</i> EQUIPMENT SPECIFICATION Vuilleumier Refrigerator P/N 447550 | NUMBER ES-30528-010 | |
| | | CODE IDENT NO. 82577 | |
| | | SH 1 OF 4 | REV LTR |

1. SCOPE

1.1 Scope - This specification covers a high efficiency, two stage Vuilleumier refrigerator utilizing an electrical heater for thermal power.

1.2 Refrigeration Capacity - The refrigerator shall deliver 0.5 watt at 30°K or less and 5.0 watts at 75°K.

1.3 Operating Temperatures

1.3.1 Hot Cylinder - The hot cylinder will be held at 1200 - 1400°F.

1.3.2 Crankcase - The crankcase will not exceed a maximum temperature of 260°F and shall not be less than -65°F.

1.3.3 Cold Cylinders - The secondstage cold sink will be at 30°K or below when its refrigeration load is 0.5 watt or less, and the first stage cold sink will be at 75°K or below when its refrigeration load is 5.0 watts or less. These loads are imposed concurrently.

1.4 Inputs

1.4.1 Thermal Energy - The thermal energy shall be supplied by an electric heater coil attached to the hot cylinder. The power required during operation is ___ watts at 28 vdc.

1.4.2 Drive Motor - The drive motor shall rotate the crankshaft at 240 rpm. The characteristics of the drive motor are specified in Motor Specification PS 30528-011.

1.4.3 Cooling Fluid - Cooling fluid (Coolanol 25 or equivalent) shall be supplied to the unit at a minimum flow rate and pressure of 0.5 gal/min and 50 psi and an input temperature not in excess of 380°K (225°F).

| INITIAL APPROVALS | DATE | REV LTR | DATE | APPROVAL | | |
|-----------------------|------|---------|------|----------|--|--|
| PREPARED R. L. Berry | | | | | | |
| CHECKED S. E. Spencer | | | | | | |
| APPROVED K. W. Cowans | | | | | | |

9802 CC REV. 2-64

2. APPLICABLE DOCUMENTS

The following documents form a part of this specification to extent specified.

Drawings

Hughes Aircraft Company

| | |
|-------------|---|
| X447550-500 | Outline and Mounting, VM Refrigerator -30°/75°K Breadboard Spaceborne |
| X447550 | Cryogenic Refrigerator, VM Refrigerator -30°/75°K Breadboard Spaceborne |
| X447550-200 | Schematic Diagram, 30°/75°K Refrigerator |

Specifications

| | |
|--------------|---|
| PS 30528-011 | Motor Specification – Induction, 2 phse Frameless |
| PS 30528-012 | Heater Specification |
| PS 30528-013 | Inverter Specification |

Other

3. REQUIREMENTS

3.1 Dimensions – The dimensions shall conform to Hughes Aircraft Company drawings X447550-500 and X447550.

3.2 Weight – The weight of the unit as shown on drawing X447550-500 shall not exceed 15 lb.

3.3 Performance

3.3.1 Heat Load – The refrigerator shall deliver a minimum of 0.5 watts of refrigeration at 30°K and 5.0 watts at 75°K when the crank-case is at ___°K and the hot cylinder is at ___°K.

| | | | | |
|---|--|-------------|---------|------------------------|
| AIR DEFENSE ELECTRO-OPTICAL LABORATORY | HUGHES AIRCRAFT CO. CULVER CITY, CALIF. CODE IDENT NO. 82577 | 2 SH NO. | REV LTR | ES-30528-010 NUMBER |
|---|--|-------------|---------|------------------------|

9803CC

3.3.2 Cooldown Time - The cooldown time for an unloaded refrigerator shall not exceed __ minutes when the refrigerator is stabilized at 80°F before starting operation. The cooldown temperatures are 35°K and 80°K.

3.3.3 Continuous Operation - After cooldown the refrigerator shall be capable of maintaining cooling for a minimum of 10,000 hours of continuous operation.

3.4 Power Supply

3.4.1 DC Power - The d-c power system shall be a two-wire grounded system having a nominal voltage of 28 vdc. The negative of the power supply shall be connected to ground.

3.5 Power Requirements

3.5.1 DC Power Requirements - The d-c power required for operation of the unit shall not exceed ____ watts at 28 vdc. This power is used to supply thermal energy (heater coil) and drive the drive motor. See motor specification PS 30528-011 for details of drive motor requirements.

3.6 Standard Conditions - The following conditions shall be used to establish normal performance characteristics under standard conditions and for making laboratory bench tests:

| | |
|---------------------|-------------------------|
| Temperature | Room Ambient (20 ±10°C) |
| Altitude | Normal Ground |
| Vibration | None |
| Relative Humidity | 90 percent or less |
| Input Power Voltage | 28 ±0.5 vdc |
| Barometric Pressure | 645-795 mm of Hg |

3.7 Operating Conditions

3.7.1 Temperature - The refrigerator shall be required to operate during extended exposure to surrounding temperatures within the range of -65°F to +160°F.

| | | | | |
|---|--|-------------|---------|------------------------|
| AIR DEFENSE ELECTRO-OPTICAL LABORATORY | HUGHES AIRCRAFT CO. CULVER CITY, CALIF. CODE IDENT NO. 82577 | 3 SH NO. | REV LTR | ES-30528-010 NUMBER |
|---|--|-------------|---------|------------------------|

3.7.2 Vibration – The refrigerator when normally mounted in the SBWR and in the same attitude that would be normal during the launch, shall perform as required when vibrated within the frequency range and amplitude (or g level) as shown in Figure 514-IV, test curve E of MIL-STD-810A of the latest issue. The cycling time shall be reduced to 50 percent of the values given in Table 514-IV of MIL-STD-810A. The vibration test shall consist of three (3) sweeps in each of two (2) mutually perpendicular axes, the axes to be selected by the unit engineer after the mounting orientation has been defined. In addition, the unit shall be subjected to resonance vibration at two (2) critical resonance frequencies in each of the two (2) axes chosen for vibration testing. The dwell time on each resonance frequency shall be five (5) minutes for a total time of twenty (20) minutes. The Q due to the mounting structures of the SBWR and any vibration fixtures shall not exceed ten (10). Test procedures shall be per MIL-STD-810A, except as noted in this specification.

3.7.3 Mechanical Shock – The refrigerator, when normally mounted in a structure simulating the SBWR and in the same attitude that would be normal during launch, shall perform as required, when vibrated within the frequency range and response indicated in Figure 516-II of MIL-STD-810A of the latest issue. The shock machine used will have the capability of producing the shock pulse configuration depicted in Figure 516-I of MIL-STD-810A, using the values listed for Procedure I. The only shock test that will be performed on the refrigerator shall be the basic design shock test. The unit, mounted on vibration isolators, shall be subjected to two (2) shocks in each direction, applied along two (2) perpendicular axes, for a total of eight (8) shocks. The axes shall be the same as the axes chosen for the vibration tests.

3.7.4 Acoustic Noise – The acoustic noise test for the refrigerator will be eliminated. The overall acoustic level is expected to be of a high level, but the unit has no parts that are critically susceptible to damage from high acoustic noise, such as diaphragms.

| | | | | |
|---|--|-------------|---------|------------------------|
| AIR DEFENSE ELECTRO-OPTICAL LABORATORY | HUGHES AIRCRAFT CO. CULVER CITY, CALIF. CODE IDENT NO. 82577 | 4 SH NO. | REV LTR | ES-30528-010 NUMBER |
|---|--|-------------|---------|------------------------|

PHYSICAL CONFIGURATION

The physical configuration of the unit can be described by referring to three basic drawings.

1. Outline and Mounting Drawing No. X447550-500 (Figure 73). The unit outline shows it to be 13-5/8 inches high by 10-1/2 inches long. These dimensions are along the cold cylinder-vacuum dewar axis and hot cylinder axis, respectively. The third dimension, 7-3/4 inches, is along the drive motor axis. A d-c to a-c power inverter (approximately 3-1/4 x 2-3/8 x 1-3/4 inches) for the drive motor is located remotely. The unit is liquid cooled and hence no cooling fan is included.

Four diameter mounting holes have been located on the crankcase flange 1.75 inches from unit centerline. A sheet metal enclosure of the crankcase houses electrical component and serves as mounting support for cooling lines and electrical power terminations, pressure gage and running time meter. Figure 74 is a picture of the unit setup for a laboratory test run.

2. Electrical Schematic Drawing X447550-200 (Figure 75). Total electrical input power to the unit is 480 watts of 28 vdc. Approximately 450 watts are required by the hot cylinder resistance heater. The remaining 30 watts vdc power is converted to vac by a separate power inverter for operating the drive motor. All power is received by the unit through a Deutsch receptacle.

Functionally this circuit would perform as follows: to start the unit the on-off switch has to be actuated and the start button depressed. The 28 vdc power then will pass into the unit to power the heater, drive motor, elapsed time indicator the relay coil to close the holding switch. Protective switches are located in the line to the overload relay. If the stator overheats or the coolant supply is lost, a protective switch will open to de-energize the relay coil and break

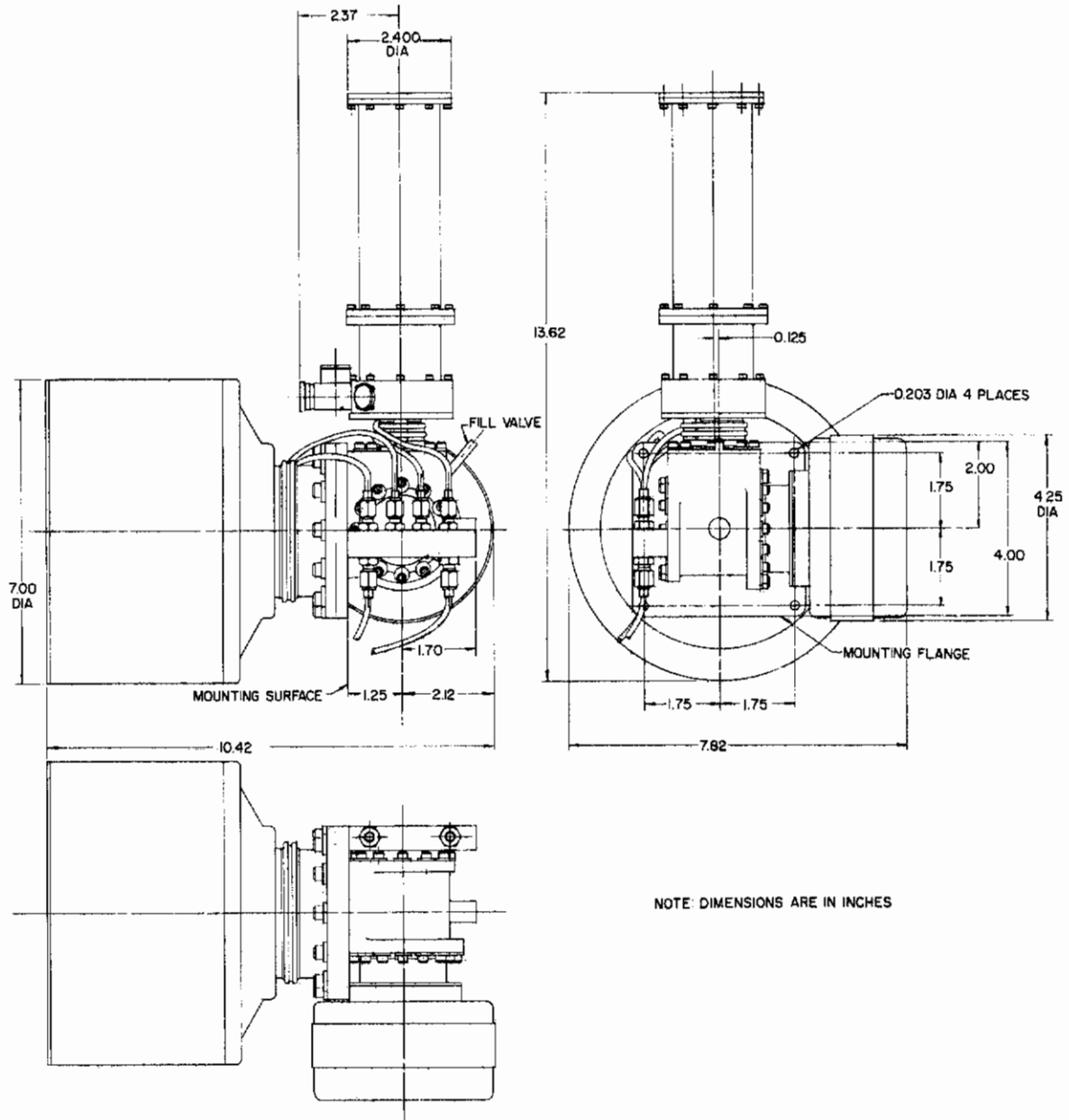


Figure 73. Outline and mounting drawing of 30°/75°K VM refrigerator

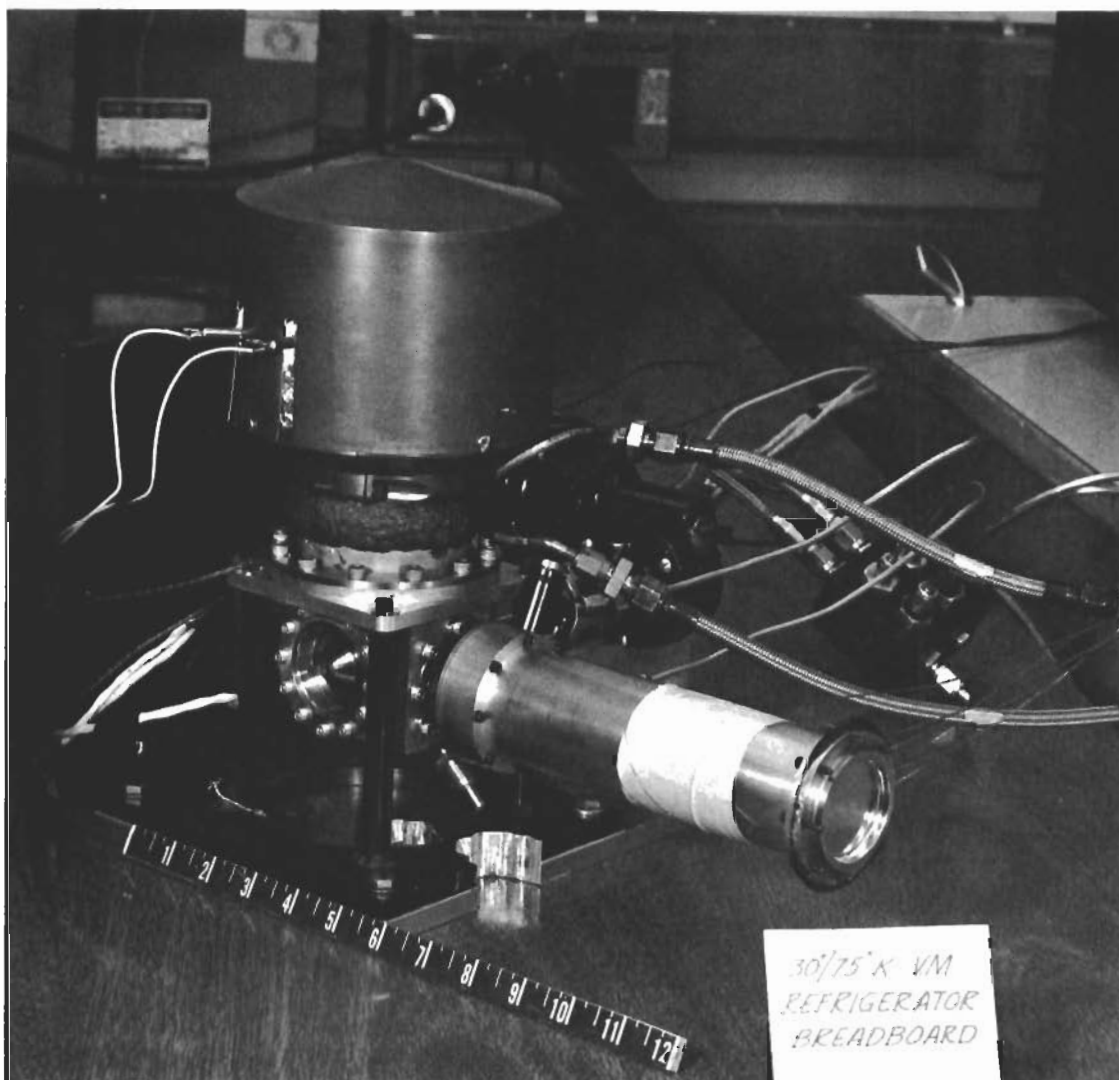


Figure 74. 30°/75°K breadboard unit 447550-100 assembled for test (HAC Photo 5R02716)

the power connection to the unit. The unit cannot be restarted until the start button is again depressed.

3. Refrigerator Assembly Drawing 447550-100 (Figure 76). This cut-away view shows internal details of the refrigerator. To minimize helium contamination, the drive motor stator is mounted on a thin wall nonmagnetic can outside the working volume of the refrigerator.

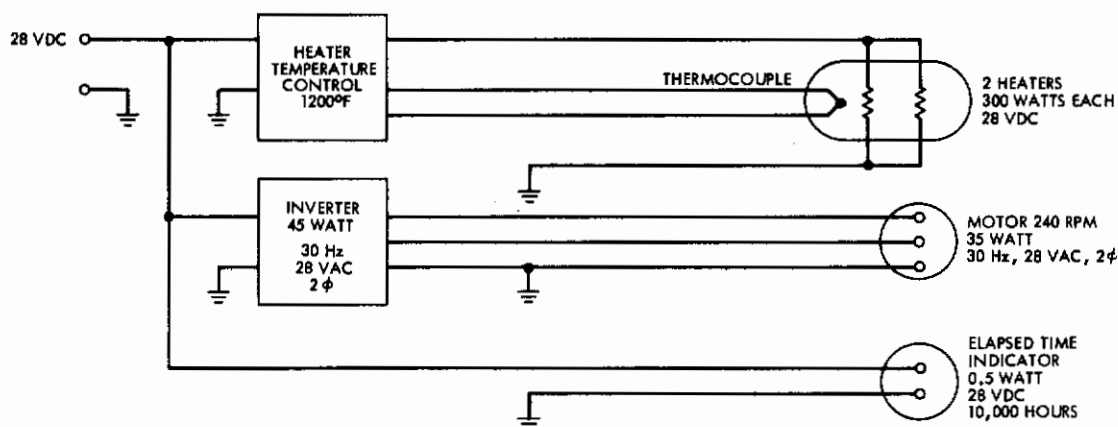
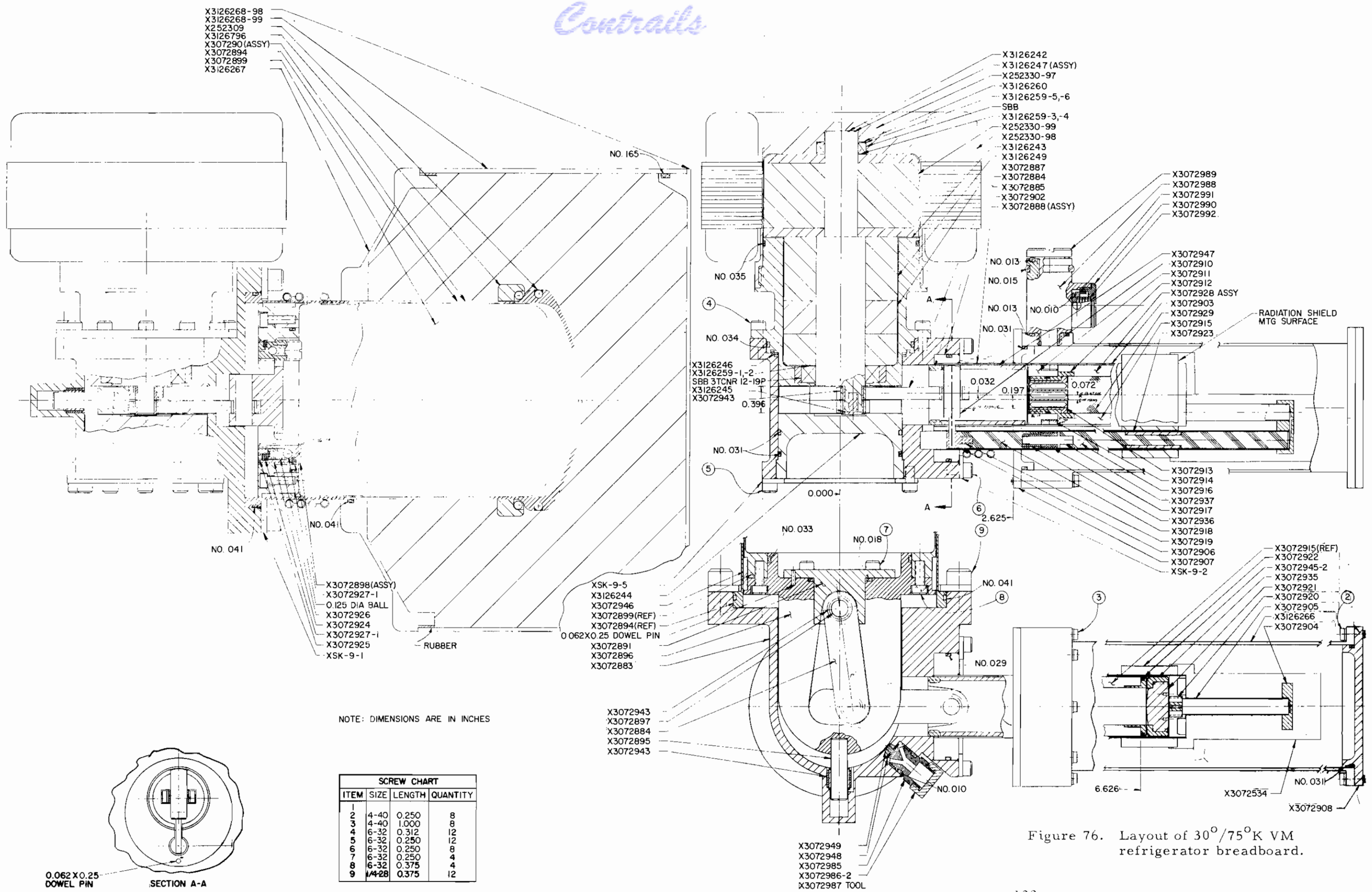


Figure 75. Schematic diagram of 30°/75°K VM refrigerator P/N 447550

The rotor is located inside the nonmagnetic can and is rigidly connected to the crankshaft. Two crankshaft bearings are located at extreme ends of the shaft. The connecting rods are attached to the crankshaft between the rotor and the outboard bearing of the crankshaft. Two flywheels which also serve as counterweights are located between the connecting rods on the crankshaft.

One connecting rod drives both the 75°K and the 30°K expansion displacers; these operate in separate, parallel cold cylinders. A thermal shorting block from 75°K stage is attached to the 30°K cylinder to intercept heat load in 30°K cylinder from the crankcase. The 30°K stage must then absorb heat leakage only from the 75°K stage. The first stage regenerator is located within the 75°K displacer. The second stage regenerator is located downstream of the first stage in the 75°K cylinder and the 30°K displacer is used only for expansion. Both cold cylinders are enclosed in a vacuum dewar for thermal insulation.

As can be seen from the center view, the hot piston is driven 90 degrees out of phase with the 75°K and 30°K expansion piston. A uniform clearance between the hot piston and the cylinder walls is maintained with the help of guide rings on the piston. Mechanism rotation is in a clockwise direction as viewed.



- X3126268-98
- X3126268-99
- X252309
- X3126796
- X307290 (ASSY)
- X3072894
- X3072899
- X3126267

- X3126242
- X3126247 (ASSY)
- X252330-97
- X3126260
- X3126259-5,-6
- SBB
- X3126259-3,-4
- X252330-99
- X252330-98
- X3126243
- X3126249
- X3072887
- X3072884
- X3072885
- X3072902
- X3072888 (ASSY)

- X3072989
- X3072988
- X3072991
- X3072990
- X3072992

- X3072947
- X3072910
- X3072911
- X3072912
- X3072928 ASSY
- X3072903
- X3072929
- X3072915
- X3072923

- X3072913
- X3072914
- X3072916
- X3072937
- X3072917
- X3072936
- X3072918
- X3072919
- X3072906
- X3072907
- XSK-9-2

- X3072915 (REF)
- X3072922
- X3072945-2
- X3072935
- X3072921
- X3072920
- X3072905
- X3126266
- X3072904

- XSK-9-5
- X3126244
- X3072946
- X3072899 (REF)
- X3072894 (REF)
- X3072891
- X3072896
- X3072883

- X3072943
- X3072897
- X3072884
- X3072895
- X3072943

- X3072949
- X3072948
- X3072985
- X3072986-2
- X3072987 TOOL

NOTE: DIMENSIONS ARE IN INCHES

| SCREW CHART | | | |
|-------------|--------|--------|----------|
| ITEM | SIZE | LENGTH | QUANTITY |
| 1 | 4-40 | 0.250 | 8 |
| 2 | 4-40 | 1.000 | 8 |
| 3 | 6-32 | 0.312 | 12 |
| 4 | 6-32 | 0.250 | 12 |
| 5 | 6-32 | 0.250 | 8 |
| 6 | 6-32 | 0.250 | 4 |
| 7 | 6-32 | 0.250 | 4 |
| 8 | 6-32 | 0.375 | 4 |
| 9 | 1/4-28 | 0.375 | 12 |

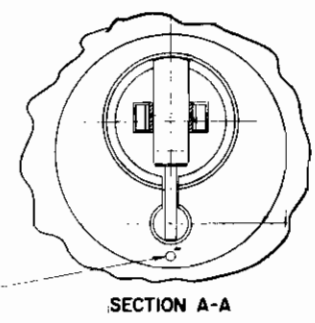


Figure 76. Layout of 30°/75°K VM refrigerator breadboard.

THERMODYNAMIC DESIGN

The principles of thermodynamic design of a Vuilleumier refrigerator were previously described in some detail. Accordingly this discussion will be limited to specific aspects of the 30°/75°K refrigerator design.

There are three individual P-V curves to be considered in the thermodynamic design; one hot volume, one ambient volume, and two cold volumes. A typical cold volume P-V diagram is shown in Figure 77. The P-V curves plotted for the cold volumes give the gross power capacity that is generated at the refrigeration temperature. All of this power however is not available for useful refrigeration work since some must be used to overcome losses.

Table 4 shows calculated losses for the 30°K state. Since the sources of these losses were described previously, they will not be discussed here and only the total 0.54 watt is noted. The gross power available under the P-V curve is 1.06 watts so that the load capacity is 0.52 watt at the worst case condition of 400°K crankcase temperature, approximately 260°F. This

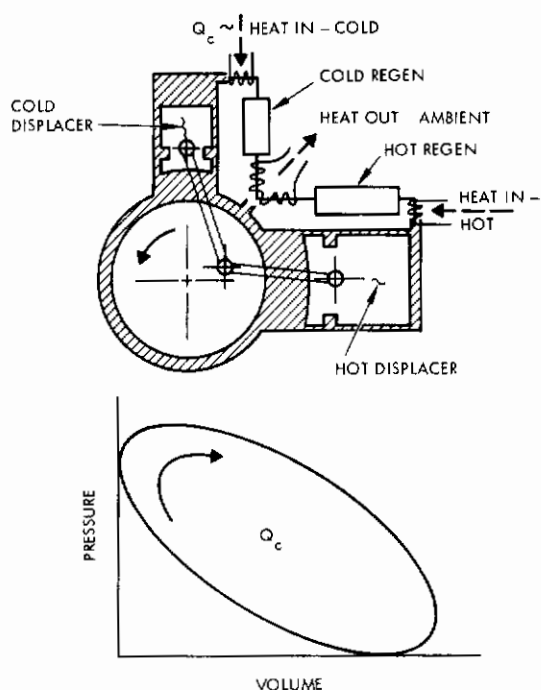


Figure 77. Schematic of a VM cryogenic refrigerator

evaluation also assumes the specified hot temperature input of 920°K which is approximately 1200°F.

Calculated losses for the 75°K stage are shown in Table 5. A gross power capacity denoted by the P-V curve of 13.34 watts leaves a load capacity of 5.03 watts under the worst case conditions of 400°K crankcase temperature (approximately 260°F). Again this is evaluated with a hot input temperature of 920°K or approximately 1200°F. Included in these losses is one additional loss not shown in the 30°K summary; this is the Joule-Thomson loss.

The Joule-Thomson loss is caused by the imperfection of the gas, i. e.,

Table 4. Design losses and load capacity of 30°K stage

| | |
|------------------------------------|------------|
| Regenerator | 0.14 watt |
| Pressure Drop | 0.03 watt |
| Shuttle | 0.09 watt |
| Pumping | 0.21 watt |
| Conduction | |
| Cylinder wall | 0.04 watt |
| Displacer wall | 0.01 watt |
| Regenerator | 0.02 watt |
| | 0.54 watt |
| Gross Power | 1.06 watts |
| Load Capacity (400°K Crankcase) | 0.52 watt |

Table 5. Design losses and load capacity of 75°K stage

| | |
|------------------------------------|-------------|
| Regenerator | 3.04 watts |
| Pressure Drop | 0.26 watt |
| Joule-Thomson | 0.02 watt |
| Shuttle | 2.19 watts |
| Pumping | 1.49 watts |
| Conduction | |
| Cylinder wall | 0.87 watt |
| Displacer wall | 0.27 watt |
| Regenerator | 0.17 watt |
| | 8.31 watts |
| Gross Power | 13.34 watts |
| Load Capacity (400°K Crankcase) | 5.03 watts |

its deviation from the ideal gas. Because it is less than ideal, as the gas passes through a porous plug or through a pressure drop it will either rise or lower in temperature depending upon its Joule-Thomson coefficient. In the range in which this regenerator operates, the Joule-Thomson coefficient causes an increase in temperature of gas as it passes through a pressure drop, and this results in our Joule-Thomson loss of 0.02 watt. This loss was omitted from 30°K stage because in the range of 75°K to 30°K for that regenerator the Joule-Thomson coefficient reverses itself and the over-all effect is zero.

The remaining 920°K stage is summarized on Table 6. This is where the major energy input takes place. With the summary of these losses, the motor loss has been included so that we can evaluate the total power input, although it is not really a loss to the 920°K stage. The insulation losses to this stage are 56 watts. This is the insulation around the hot cylinder, which prevents heat from escaping in a radial or axial direction. Heat input to the gas is 140 watts, and finally the power to the motor is 10 watts for a total input of 299.3 watts. This is at a crankcase temperature of 400°K.

The displacer filler loss results from the filler placed in the hot displacer. The hot displacer is designed as a very thin walled cylinder for two reasons: first to prevent large conduction losses from hot to ambient end, and second to minimize its weight so that good dynamic balance can be achieved between hot and cold displacers. To minimize the displacer wall thickness it is equipped with inlet and outlet valves to minimize the pressure differential across the wall. If it were filled only with gas there would be a conduction current set up due to the shuttling back and forth of the displacer and the extreme temperature differences and high gas conduction losses would result. To prevent this the hot displacer was filled with a very porous, fibrous insulation that prevents conduction currents from taking place.

Table 6. Design power requirements of the 920°K stage (1200°F)

| | |
|----------------------------------|--------------------|
| Insulation | 56.0 watts |
| Regenerator | 20.0 watts |
| Shuttle | 37.5 watts |
| Conduction | |
| Cylinder wall | 19.1 watts |
| Displacer wall | 9.2 watts |
| Displacer filler | 7.5 watts |
| Heat Input to Gas | 140.0 watts |
| Power to Motor | 10.0 watts |
| Total Input (400°K Crankcase) | <u>299.3 watts</u> |

MECHANICAL DESIGN

As pointed out earlier the Vuilleumier refrigerator presents a relatively simple mechanical design problem. In addition to the inherently low dynamic loadings and relatively slow speed of the mechanism, special emphasis was devoted to design factors to maximize operation time between maintenance cycles on this unit.

1. The machine design speed is low, 4 cycles/second or approximately 240 rpm.
2. Materials contributing possible contaminants to the working volume have been minimized.
3. The internal mechanism can be subjected to high temperature vacuum bakeout.
4. Bearings are dry lubricated type and can be replaced by carbon sleeve type bearings.

These design factors imposed additional mechanical design problems, especially when combined with the requirement to minimize internal dead

volume through extremely close tolerances. The other major problem is introduced by the temperature extremes in which the mechanism must operate.

Primary load factors were derived from knowledge of the unit requirements. A maximum internal pressure of 700 psi was used to calculate the limiting pressure vessel type stresses. Simultaneous temperature requirements were 1200^oF hot cylinder, 260^oF crankcase and 25^oK cold cylinder. To these basic stress requirements must be added the dynamic stresses introduced by machine operation and shock and vibration environment. Maximum 50 g shock and 30 g vibration loads were used.

The following is a summary of major component design analysis.

Cold Cylinder - Inconel 718

Temperature varies from +260^oF to 25^oK over length of the cylinder. Combination of axial hoop and bending stress resulted in maximum stress of 47,000 psi at base of cold cylinder. Cylinder has lead ball regenerator mounted at upper end.

Cold Pistons - Glass Loaded Nylon and 303 Stainless

Temperature varies from +260^oF to 25^oK over length of piston. Piston shell loaded with stainless steel 75^oK regenerator screens. Stress loading minimum on all parts.

Crankshaft 17-4 PH

The crankshaft is a simply supported beam with bearings at either end and rotor and connecting rods between. Two flywheels are mounted on the crankshaft and motor rotor and rotor spacer are shrunk onto one end of the shaft. Bearing surfaces are chrome plated. Maximum shaft bending stress was 342 psi.

Drive Motor Rotor Enclosure - 303 Stainless

Temperature varies from ambient to 260^oF. Wall thickness used for calculation was 0.0075 inch. Based on a pressure of 1000 psi the axial stress is 60,000 psi and hoop stress is 120,000 psi. This is based on

assumption that motor stator does not strengthen the enclosure. The radial displacement calculated is 0.002 inch.

Crank Main and Wrist Pin - Carbon P5N Journal

This material was selected because of its good properties in a dry helium atmosphere. For a 30 g loading the force exerted by each piston, which is balanced, is 35 lbs and since the compression strength of P5N is 35,000 psi, there is no problem in withstanding this force. From the IBM Zero Wear Study two methods of calculations were used, both of which have indicated that the bearing should easily exceed 10,000 hours life.

Hot Cylinder - Inconel 718

This material has a yield strength at room temperature of 172,000 psi. At operating conditions, the maximum stress will occur a small distance from the end of the piston which would be at approximately 1000°F. The stress at this point is 48,000 psi, and the rupture strength of Inconel 718 is 65,000 psi for 10,000 hour life.

Hot Displacer - Inconel 750

The displacer is hydroformed to obtain a rough blank which is then machined. Two check valves are mounted in the base of Displacer, one inlet and one exit to minimize pressure differential across wall. Two stainless rings are brazed inside the displacer diameter to give added strength against implosion. The displacer is filled with Refrasil to reduce dead volume. Wall thickness is 0.025 inch and temperature varies over length from ambient to 1200°F. Unsupported collapsing pressure is 180 psi; reinforced it is 750 psi. A 0.0024 inch radial change in diameter was calculated.

Thermal Expansion

For thermal expansion, the point of major consideration would be the difference in expansion between the hot connecting rod and the hot displacer base. The connecting rod is stainless and the base is made of aluminum. The difference in expansion for a rise in temperature from room temperature

to 260°F was found to be 0.001 inch which presents no problem since the clearance allowed at this point is 0.008 inch. For the cold displacer glass loaded nylon is used for the displacer material and at cold temperature this material will contract, thus no problem with rubbing between the Inconel cylinder and nylon displacer should occur. Also there will be no significant change in the annulus thickness.

Unit Mounting

The unit is mounted with four equidistant 10-32 bolts. The center of gravity of the unit is approximately one inch from the plane of the bolt pattern. The tensile load per bolt for a 50 g condition is 69.5 pounds, while the shear load per bolt is 125 pounds. This falls well within the limits for the bolt of 1100 pounds tensile allowable and 550 pounds shear allowable.

Unit Weight

Table 7 summarizes unit weight by major part. It is noted that weight of a number of heavier parts can be substantially reduced through use of lighter materials or fabrication and greater attention to configuration detail.

PERFORMANCE

Initial testing of the unit was plagued with interference problems and premature heater failures. Despite these problems which required the initial tests be run at approximately half design charge pressure and speed, the unit attained cold temperatures of 117°K and 86°K at first and second stages respectively. Subsequent development work resulted in a unit capable of 0.5 watt at 30°K and 6.0 watts at 75°K.

Table 8 presents a comparative summary of specific performance data for the X447550-100 refrigerator.

The developmental testing confirmed that the unit was relatively straightforward relative to thermodynamic design. It was possible to predict unit performance when thermodynamic conditions had been established from the data.

Table 7. Weight summary, 30°/75°K Vuilleumier cryogenic refrigerator (X447550-100).

| | Design Weight, lb | Actual Weight, lb |
|--|----------------------|----------------------|
| Crankcase assembly | 2.77 | 3.29 |
| Crankshaft and conn. rod assembly | 0.91 | 0.83 |
| Counterweights | 0.25 | 0.24 |
| Motor assembly | -- | 0.83 |
| Hot displacer assembly | 0.70 | 1.08 |
| Hot cylinder assembly | 0.99 | 0.91 |
| Cold displacers and cylinder assembly (75°K) | -- | 0.79 |
| Cold displacers and cylinder (30°K) | -- | 0.74 |
| Dewar assembly | -- | 0.06 |
| Miscellaneous | -- | 0.83 |
| Total | | <u>9.60</u> |

Development problems were primarily concerned with mechanical aspects of the unit. Major areas of design revision resulted from reduction of excessive internal friction and prevention of hot displacer distortion.

Significant areas of developmental progress could be categorized as follows:

1. Excessive Internal Friction

Internal friction encompasses all types of friction inherent in the unit - rubbing of seals, interference of parts and pressure drop in regenerators and flow passages.

Table 8. Performance summary for X447550-100 cryogenic system

| | Breadboard (A/C)** | | Flight Weight (Space)** | |
|-----------------------------|--------------------|------------------------------|-------------------------|--------|
| | Contract Spec. | Actual | Contract Spec. | Actual |
| A. Refrigerator | | | | |
| 1. Weight | - | 18 lb | - | |
| 2. Power Input | - | 450 | - | |
| Heater | - | 30 | - | |
| Motor | - | 480 (approx) | 200 W | |
| Total | | | | |
| 3. Temperature/Capacity | | | | |
| 75°K Stage | 5.0 W | 75°K/6.0W | 5.0 W | |
| 30°K Stage | 0.5 W | 30°K/0.5W | 0.5 W | |
| 4. Cooldown | - | 75°K/20 min. 30°K/23 min. | - | |
| 5. Engine Speed | - | 240 RPM | - | |
| 6. Charge Pressure | - | 400 psi | - | |
| 7. Life (hours) | 10 ⁴ hr | 200 hr to date | - | |
| B. Inverter | | | | |
| 1. Size | - | 3-1/4 x 2-3/8 x 1-3/4 in. | - | |
| 2. Weight | - | 1.1 lb | - | |
| *Liquid cooled | | | | |
| **Will not be liquid cooled | | | | |

2. Hot Displacer Structural

Structural design of the hot displacer involved a tradeoff of wall thickness, internal pressure control and heat transfer losses.

3. Heat Transfer

Parameters pertaining to maximum efficiency of heat energy input to the unit had to be identified and used to design a suitable heater-hot cylinder-hot displacer subassembly.

4. Drive Motor

The task of developing a small speed controllable canned a-c motor with sufficient torque proved to be a major problem.

5. Bearings

Considerable development effort was directed toward obtaining laboratory data on performance of carbon sleeve and flex pivot bearings in refrigerator applications especially for long-life units.

6. Working Gas Contamination

This item involved both identification of possible contaminants introduced by charge gas or generated by operation of the machine.

Although the refrigerators development effort could be discussed in general, chronological progress it is felt that a more informative approach would be a description of specific areas similar to those outlined above.

CRANKCASE AND MECHANISM DEVELOPMENT

The crankcase material selection was based on the requirements that a material used should be easy to machine and solder and have a thermal expansion coefficient close that of steel; brass was chosen. Material thickness was held to a minimum of 0.125 inch to keep stress levels from pressure induced forces and component loading to less than 25,000 psi. The drive mechanism which includes the two piece crankshaft, counter weights,

bearings and drive motor rotor is enclosed in the crankcase. These parts are shown in Figure 78.

For ease of maintenance a two-piece crankshaft was designed. To keep shaft deflections down to less than 0.001 inch, cross sectional areas were maintained at >0.50 inch in diameter except for the bearings areas. Bearing surfaces were hard chrome plated to keep wear from the sleeve bearings down to minimal levels.

Two counter weights slip on the crankshaft and are then fastened into place on either side of the reciprocating parts. The balance weights are made of Mallory 2000 pinned to the magnesium body of the counter weights.

Presently the unit is being tested with Fafnir Fabroid sleeve bearings pressed into the connecting rods and Barden SR 4SSTB Bartemp bearings on the crankshaft. Sleeve bearings of a carbon material, i. e., pure carbon grade P5N are presently being evaluated in the bearing life test fixture described in following section.

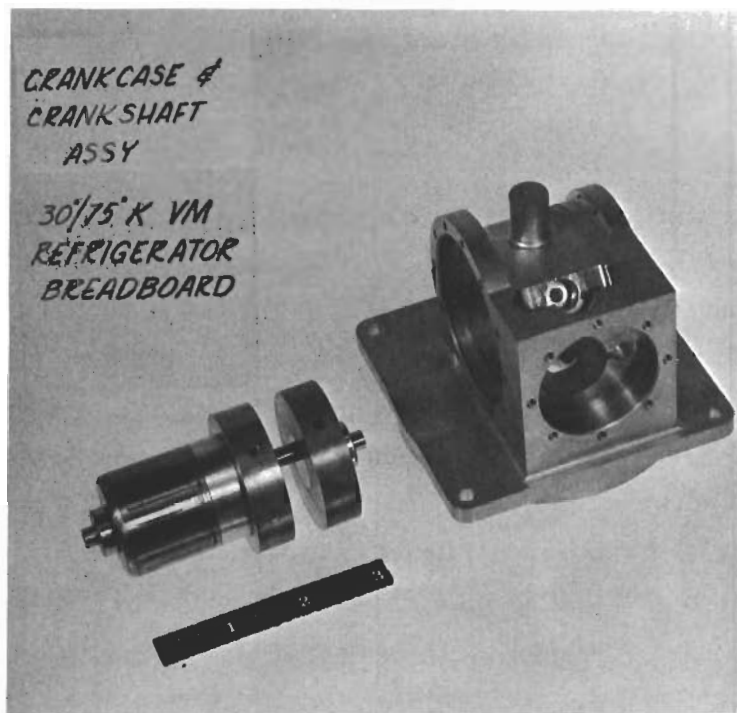


Figure 78. Crankcase and drive mechanism of unit 447550-100 (Hughes photo 4R02918)

Alignment between the parts is accomplished by the use of glass filled teflon washers on the crankshaft between the reciprocating parts. Side loads on the washers is calculated to be 0.05 lb, which is well within the load carrying capacity of the washers.

Eccentricity of the crankshaft assembly should be minimized to facilitate minimization of dead volume within the crankcase. The piece parts were therefore assembled to the crankshaft and the whole assembly machined concentric to the bearings. To eliminate eccentricity due to bearing wear Barden bearings with a slight pre load were used as the main crankshaft bearings. As a result running clearance of 0.008 inch is feasible and is presently being maintained within the unit.

Design calculations indicated that with nominal clearances of 0.008 inch a pressure ratio of 1.44 could be achieved. Total dead volume within the unit would then be 23.4 cm^3 . On initial startup interferences between the rotating parts and the crankcase required remachining the affected parts to a clearance of 0.010 to 0.015; however in spite of the increased clearance, pressure ratios of 1.4 to 1.45 have been recorded during the unit test runs.

Bearing Life Test

A life test was conducted on the carbon bearings seals and riders intended for use in the flight weight unit. The bearing material used was P5N carbon, manufactured by Pure Carbon Company.

The life test fixture was assembled from spare parts and driven by the Gaylord Rives Motor which was mounted on the crankcase as shown in the unit O&M drawing. The test unit incorporated two carbon crankshaft sleeve bearings, both placed over each end of the crankshaft, and a carbon crankshaft thrust bearing at each end of the crankshaft.

The crankshaft assembly included both flywheels per design configuration. The opening for hot piston on the crankcase however was sealed using a "hot end" plate, especially designed for the life test since no spare hot cylinder and displacer were available.

In place of the normal cold cylinder assembly in the unit, a new life test cold cylinder was fabricated. This included only the 75°K piston; the 30°K piston was excluded from the life test again because spare parts were unavailable. Thus the unit was dynamically unbalanced and had somewhat less pressure drop than an actual unit.

The unit was driven by a d-c power supply and an inverter. The voltage input to the motor was maintained at 42 volts, to increase motor torque and minimize the possibility of unit stalling due to wear particles. The inverter frequency was 62.5 cps. The pressure inside the unit was held at approximately 400 psi. The speed of the unit was 545 rpm. Pictures of the unit are shown in Figures 79 and 80.

The unit ran in this configuration for a total of 96 hours. At this point the life fixture was disassembled. The carbon bearing inside diameters were measured and then the unit was reassembled and underwent an overnight oven bakeout. On inspection of the bearings, there was no noticeable wear present. The unit then purged and filled with helium. The unit was restarted equipped with instrumentation to permit continuous 24-hour/day operation.

HOT CYLINDER ASSEMBLY

The hot cylinder assembly consists of hot cylinder, hot displacer, and input heater. The hot cylinder is made from Inconel 718, while the hot displacer is made from Inconel 750. Carbon hot riders are used at both ends of the displacer to form a bearing surface and insure concentric movement in the cylinder. Figure 81 is a picture of the major parts of the assembly.

In order to maintain the design heater input of 300 watts, no more than 60 watts could be lost in radiation and convection from the heater. In order to assure this, an insulation wrap of Refrasil A-100 was selected to form the basic insulation. At a mean temperature range of about 820°F, this insulation has a thermal conductivity of 0.66 BTU/hr sq ft °F/inch at ambient pressure, and 0.22 BTU/hr sq ft/°F/in. at pressures of one micron and below.

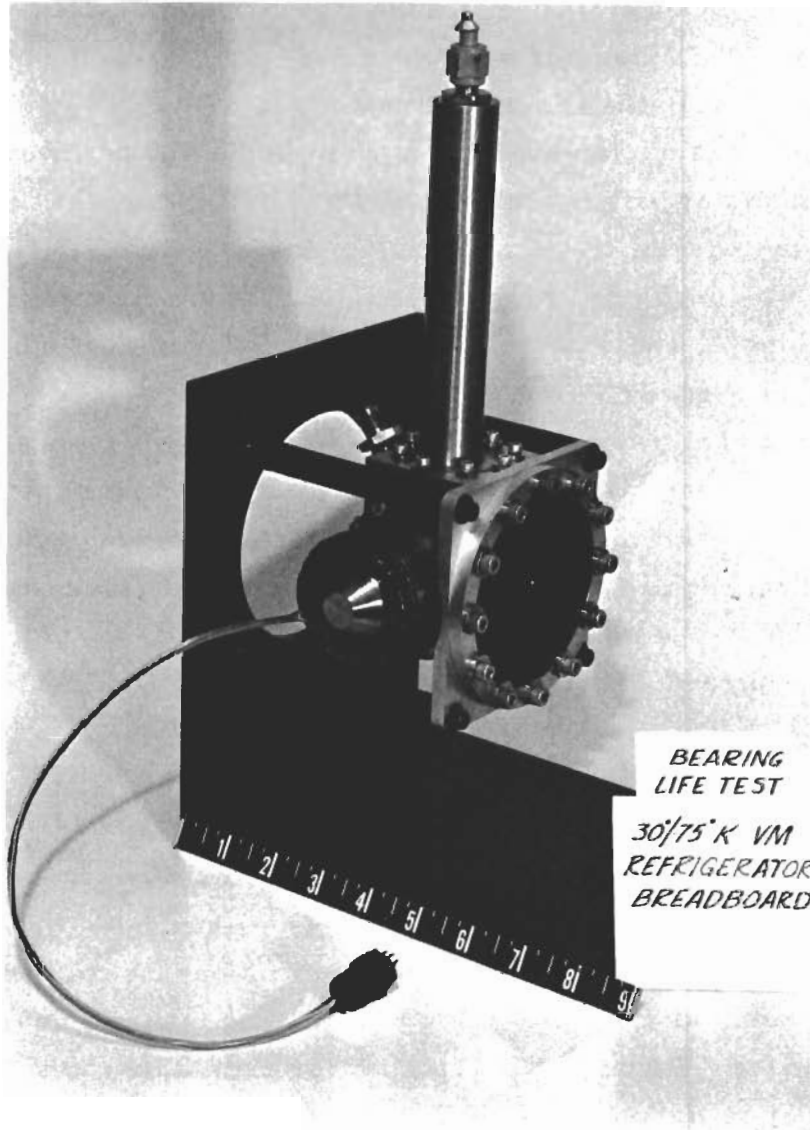


Figure 79. Fixture for testing bearing life of unit 447550-100 (HAC photo 5R02720)



Figure 80. Setup for bearing life test of unit 447550-100 (HAC photo 5R02719)

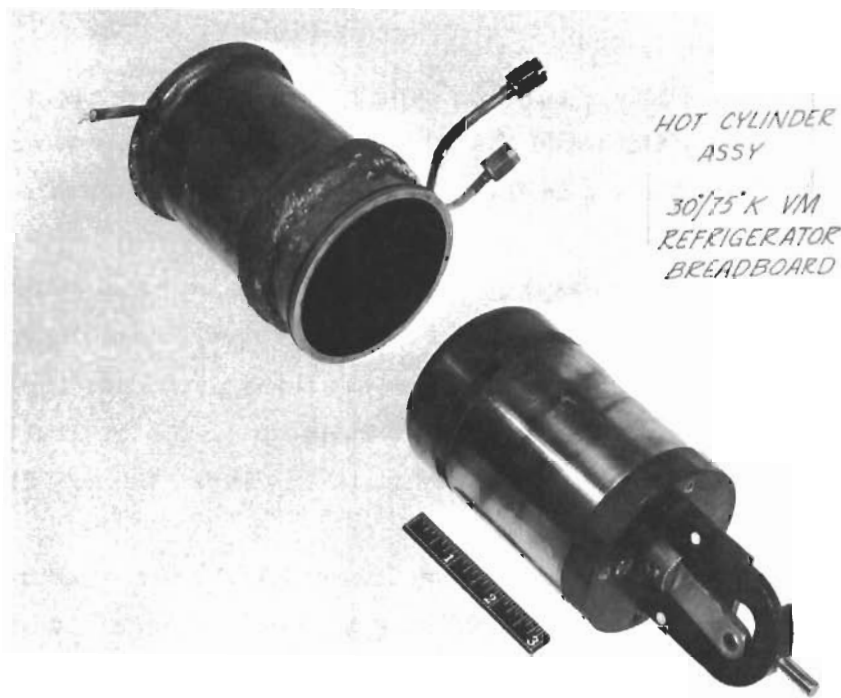


Figure 81. Hot cylinder assembly parts of unit 447550-100 (HAC photo 4R02920)

The wraps are formed around the hot cylinder, and interspaced with a wrap of 0.002-inch-thick aluminum foil to serve as radiation shields. The final wrap is aluminum foil which is carefully placed to prevent thermally shorting to the anodized aluminum can, which is placed over the final insulation for protection.

Conduction heat loss down the length of the cylinder wall was calculated to be about 19 watts.

During course of development it was found that by brazing the heater onto the hot cylinder instead of mounting it with thermal cement as originally planned, the heat could more readily be directed into the hot cylinder. By brazing the heater, the heat input necessary to maintain the hot end at 1200°F was reduced by about 100 watts.

In a test on the unit with the inside evacuated, coolanol flowing through the heat exchanger, and the heater turned on to maintain a temperature of 1200°F, the power into the heater was determined to be 102 watts. This would include conduction down the cylinder wall, radiation and free convection from the insulation surface.

The regenerator is a simple annulus type between the hot cylinder and the hot displacer. It was calculated that the most effective clearance would be 0.0075 inch. The heat losses in the gas within the clearance was estimated to be about 58 watts.

It was found necessary to combine a rider surface and a heat exchange volume at the base of the hot displacer. This was solved by using a scalloped rider made of P5N carbon material, with the scallops providing the flow area for the gas and exchange heat load to the hot cylinder which in turn is cooled by the coolanol flowing in the tubing brazed to the cylinder base. The rider was split to provide ease of assembly.

The hot displacer is hydroformed from Inconel 750 sheet material and then brazed to a Stainless steel type 321 flange. The displacer is stuffed with shredded Refrasil A-100 insulation to minimize internal convection losses. The total estimated conduction loss through the hot displacer wall and insulation is about 17 watts. Figure 82 shows a hydroformed hot displacer blank.



Figure 82. Hydroformed hot displacer shell of unit 447550-100 (HAC photo 4R02922)

The displacer base is mounted to the hot piston flange with four bolts. Two check valves are mounted in the base to control the pressure within the hot displacer to minimize pressure differential between the helium inside and outside of the displacer. The inlet check valve is set to allow it to open when there is a difference of more than 200 psi between inside and outside of the hot displacer, while the exit valve is set to open when the difference is more than 50 psi.

The check valves are mounted in the displacer base to eliminate the volume inside the displacer as dead volume, and at the same time to prevent an overload collapse of the displacer. During one test the displacer was collapsed (see Figure 83 and Figure 84). This was attributed to too rapid filling of the unit with helium in preparation for a test run. Apparently, the check valves could not respond fast enough to prevent an overpressure of the displacer and the failure resulted. This was corrected by placing a restrictor



Figure 83. Side view of failed hot displacer of unit 447550-100 (HAC photo 4R02723)



Figure 84. End view of failed hot displacer of unit 447550-100 (HAC photo 4R02724)

in the fill line, so that the unit can only be charged at a safe rate. As an added safety precaution two stainless steel rings were brazed inside the displacer to give added strength.

After running the unit, it was found that there was considerable rubbing of the hot displacer inside the hot cylinder, near to the 1200^oF end of the cylinder. To prevent this, a slot was machined in the displacer near to the hot end and a shortened version of the hot displacer rider (with scallops) was added, to function as a rider at the hot end.

Subsequent testing has shown that hot end carbon rider prevents the displacer from touching the cylinder wall, thus preventing friction, rubbing, and wearing away of the material. It also helped to lower the heat input to the unit, since the displacer no longer touched the cylinder wall, and removed heat by conduction from the hot cylinder. Tests showed that a reduction of over 50 watts was effected in input power requirements. The rider also centered the piston within the cylinder, creating an annulus with equal clearance around the displacer, thus increasing the hot regenerator efficiency.

HEATER

The heat input power design requirement for the breadboard unit was 300 watts. This was to be delivered by an electrical resistance heater brazed to the hot cylinder which was to have a life capability of at least 10,000 hours.

The initial heater selected was made by American Standard Aero Research Instrument Department. The heater was 10 inches long with an overall diameter of 0.125 inch. The heater provided a single wrap around the end of hot cylinder on the unit in the slot provided for it. The heater wire was made of nichrome and was mounted biaxially, providing both terminations of the nichrome wire at one end of the heater. The heater wire was enclosed in a magnesium oxide insulation which was covered with an inconel sheath. The heater was mounted initially on the hot cylinder with a high conductivity thermal cement to facilitate removal in event of failure.

It became apparent during initial unit testing, that there was a problem with the lead terminations on the heater. The heater would fail at the point

where the leads emerged from the sheathing, anywhere from immediately, to one hour after the current was applied to the heater. The heater power was controlled by a Variac autotransformer.

Life tests on the heater were therefore run on a specially constructed fixture. The longest period of continuous operation achieved on any of the original heaters was fifty-two hours. It was determined that the heat was not being removed fast enough at the termination to the heater, apparently because of insufficient heat transfer surface area.

Two variations to the original heater were tested; in both cases the heater was identical, but the terminations were different. On one heater there was a one inch length, in which the sheath diameter increased from 0.125 inch to 0.250 inch, before the nichrome wire emerged from the heater. In the other heater, a one inch length was added where the sheath diameter increased from 0.125 inch to 0.1875 inch, but in this case, the nichrome wire was joined to nickel leads inside the termination, and therefore nickel lead wires emerged from inside the heater.

The first of these heaters was incorporated into the breadboard unit and the results proved to be excellent. None of these heaters have failed to date. The heater was also placed on the life test fixture and has logged over 1500 hours of continuous operation.

The second configuration of the heater, with nickel leads, has proved to be equally as dependable as the first type.

The life test fixture is shown in Figures 85 and 86 which are photographs of test equipment. The heater was wrapped in a single turn around a specially constructed hot cylinder made of bar steel with a large brass tin at the base. The heater was fastened to the fixture using thermal cement.

The heater and fixture was wrapped with Refrasil A-100 Batt insulation to a thickness of 1.25 inches and covered with a layer of 0.002 inch aluminum foil.

A thermocouple mounted near to the heater was used with a galvanometer to measure the temperature. Electrical input power was controlled by a Variac autotransformer, and current and voltage were measured with an ammeter and voltmeter.

A temperature of 1200°F, with a heat input of 300 watts was maintained for 1500 hours without failure.

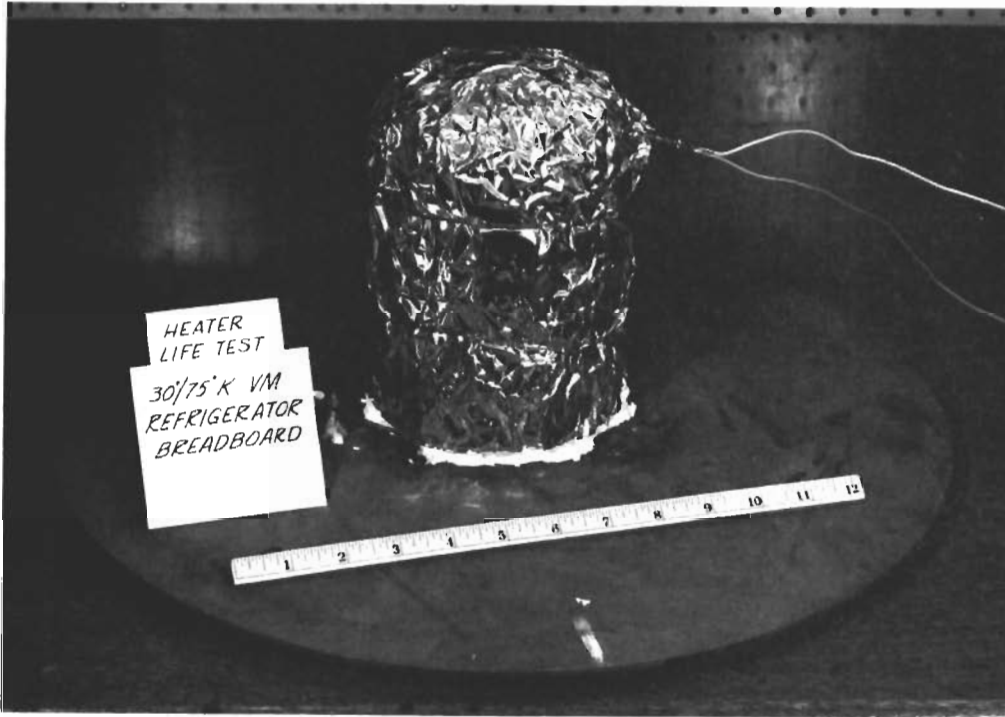


Figure 85. Heater life test fixture for unit 447550-100 (HAC photo 5R02718)



Figure 86. Heater life test setup for unit 447550-100 (HAC Photo 5R02717)

DRIVE MOTOR AND INVERTER

The mechanical power required to overcome gas friction, bearing losses, and mechanical rubbing interference of the reciprocating and rotating parts is supplied by a small induction motor. A canned design, one in which the field windings are hermetically sealed from the rotor, was used to prevent contamination of the working gas and to keep the crankcase volume small without the use of seals.

The power available for the refrigerator was 28 vdc. Thus, it was necessary to use either a dc motor or include a device to convert the dc to ac power. Numerous dc motors are available that could supply the required power in an acceptably sized package, but for the most part they employ brushes for commutation. These brushes would be used in a dry, unlubricated, helium atmosphere for which there was little past history of successful application. Since it was a design goal to develop a machine with a 10,000 hour life it was decided not to use a brush type motor for which there was little history of successful application in this type of environment.

A review of brushless types of dc motors using commutation by optical or magnetic switching showed that in general these motors were not readily available, they were costly, and there was not data to show that they could withstand the probable environmental conditions imposed by vibration and temperature.

An induction motor was therefore considered. Hughes Aircraft Company has had considerable experience with the use of induction motors in development of other cryogenic refrigerators which indicated that there were no basic problems operating in the dry helium atmosphere. However the experience did show that the field winding was a major source of contamination of the working helium gas and could cause the refrigerator to lose capacity over an extended time period. To prevent any possibility of contamination the sealed induction motor was selected since it offered the following advantages:

1. The field winding could not contaminate the working gas and did not have to be specially treated or cleaned.

2. The dead volume of the machine was minimized in the crankcase-motor region without the use of seals. This allowed use of a simple mechanical design of the drive-crankshaft subassembly.

The investigation of induction motors presumed an acceptable means of converting from d-c to a-c power. Many of the manufacturers of special purpose motors also supply inverters so that their motors can be used with either ac or dc power. The inverter is usually composed of highly reliable electronic components, is small, lightweight, and can be adjusted to deliver a wide range of frequency output which can be used to vary motor speed. It was only necessary to specify that the inverter not use saturating magnetic components that might later cause systems problems in the event that the refrigerator should be used as a part of some electronics system. Figure 87 is a photograph of the final driver motor and power inverter.

As a result of the decision to use a canned induction motor the mechanical design of the drive-crankshaft and the crankcase was simplified. There have been no problems associated with the motor and inverter drive concept



Figure 87. Drive motor and inverter of unit 447550-100 (HAC photo 4R02921)

after the initial debugging of the assembly. Frictional losses however were higher than predicted. However, it was found that the torque required to operate the unit was larger than had been anticipated so that it was necessary to install a larger drive motor. At this time it appears that most of the motor power is going into the seals on the two cold displacers so there is a high probability that the motor power will be decreased in the future. At present, the input power to the inverter is 30 watts.

The inverter supplied with the unit is MIL Spec design. It is equipped with a speed control to permit continuous variation of output frequency from 25 to 75 Hz. This varies the motor speed from 180 to 540 rpm.

COLD CYLINDER ASSEMBLY

Basically the cold cylinder assembly consists of two thin wall Inconel 718 cylinders with coil heat exchanger brazed at the ambient end, a copper thermal shorting block from 75°K stage to 30°K cylinder to intercept conduction losses from crankcase and copper cold head for 30°K load mounting. By keeping cylinder wall thickness to 0.008 inch heat conduction down the cylinders was calculated to be 0.71 watt. Figure 88 is a photograph of the cylinder assembly. The cold head consists of a crossover manifold and has the dual purpose of providing a helium flow path to the second stage cylinder and sufficient heat transfer area to thermally couple the gas to the second stage load. It couples the top of the two cold cylinders together.

The second stage regenerator thermal mass consists of lead balls 0.005 inch in diameter that are held in place by 400 mesh screens at both ends of the regenerator shell. It is mounted in the cold cylinder between the 75°K stage and cold head.

The first stage displacer is a two piece assembly consisting of the 75°K regenerator and the base which contains seal and ambient heat exchanger. The regenerator consists of a glass epoxy shell stacked with 250 mesh stainless steel screens with a manifold at either end to direct helium flow in and out of the regenerator. To achieve better dynamic balance the base of the displacer has been machined out of Mallory metal to increase the weight to more nearly equal that of the hot displacer.

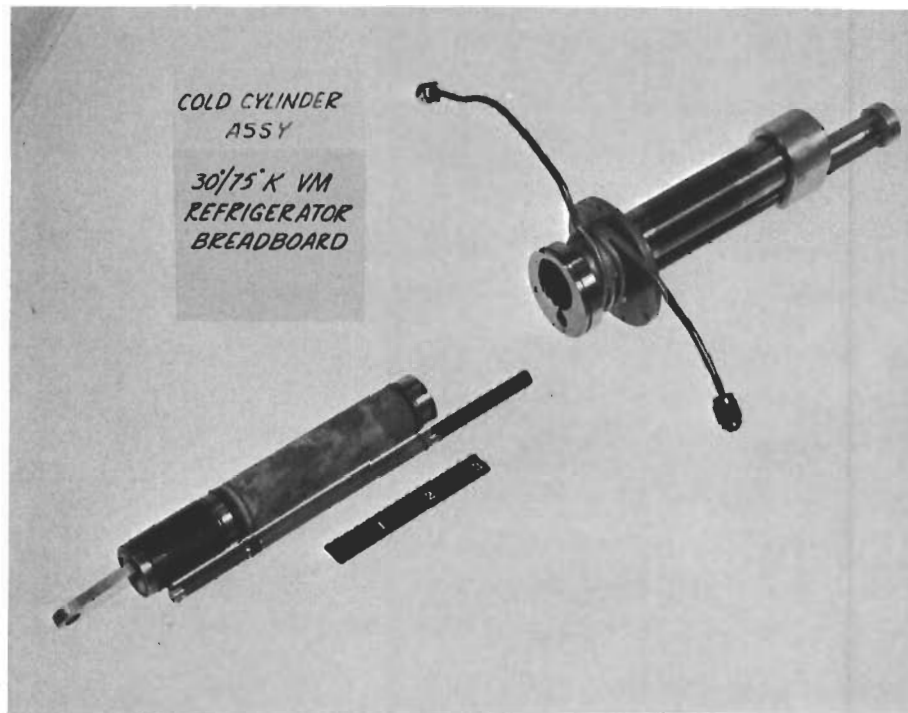


Figure 88. Cold cylinder assembly parts of unit 447550-100 (HAC Photo 4R02919)

The displacer for the second stage is a two piece assembly with a heat exchanger at the 75°K section, and a seal at the ambient end. By machining the displacer out of glass loaded epoxy heat conduction was minimized.

The vacuum dewar is fastened to the dewar flange around the cold cylinder. To evacuate the dewar, a connection is made to a Richards type valve which is mounted on the side of the dewar. Heater wires and thermocouple leads from the cold end are presently being brought out through a gasket in the dewar cover.

Seals presently being tested on the first and second stage displacers are made of 15% glass loaded teflon. Spring loading against the cylinder is accomplished by the use of "O" rings assembled in the seals. The seals have proven to be effective, however, seal drag is relatively high and motor torque levels of 20-30 in. oz. have been required to drive the unit. Other seal designs using different materials and spring loadings are being evaluated.

TEST STATION

Figure 89 is a photograph of the test area showing a technician at the temperature recording station. During actual operation a second operator was required to monitor and control the speed, pressure ratio and heater input.

Test instrumentation could generally be characterized as conventional off-the-shelf hardware. Figure 90 is a flow diagram of the equipment set up for a typical development test.

During early testing the unit was driven by a Bodine fractional horsepower motor which was controlled by a Minatrol motor speed control. The RPM of the unit was measured by a magnetic pickup coil mounted to the outside of the crankcase, and a magnet mounted on one of the flywheels, inside the unit. A trace of the RPM was recorded on a Honeywell Visicorder through use of an eight-channel dc amplifier that was driven by a dc power supply manufactured by Electronic Research.



Figure 89. View of 30⁰/75⁰K VM test area
(HAC Photo 5R02721)

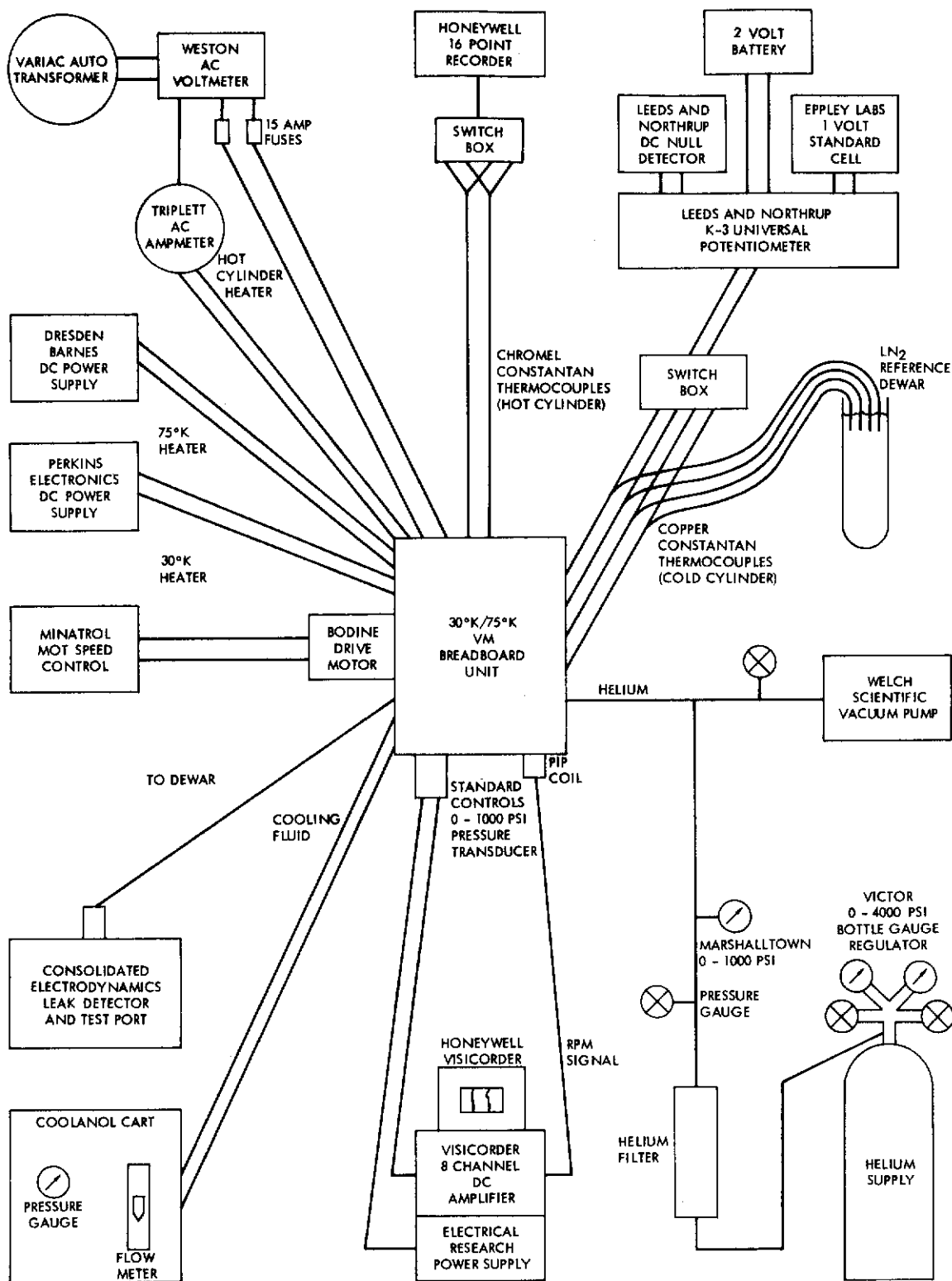


Figure 90. Test equipment flow chart for 30°/75°K VM breadboard refrigerator.

Contrails

The pressure measurement inside the unit was also recorded on the Visicorder. The input was obtained from the unit through the use of a Standard Controls 0-1000 psi pressure transducer, mounted on the crankcase.

Research grade helium was provided for the unit, with supply controlled by a Victor regulator. The charge gas was passed through a filter to eliminate moisture. A Marshalltown 0-1000 psi pressure gauge was used to monitor the pressure in the line. Mounted to the same line was a Welch Scientific vacuum pump, used to evacuate the unit, prior to the changing operation.

A high vacuum was maintained in the dewar surrounding the cold cylinder, through use of a Consolidated Electrodynamics vacuum pumping station.

Coolanol 25 fluid was circulated in the heat exchanger coils at the bases of the cold and hot cylinders. The system was equipped with a thermometer pressure gauge and flow meter to monitor the coolant flow.

The power to the 1/2 watt load heater mounted at the top of the cold cylinder at the 30°K stage was provided by a Perkins Electronics dc power supply. The power to the 5 watt load resistance heater for the 75°K stage, was supplied by a Dresden-Barnes dc power supply. The heater power to maintain a temperature of 1200°F at the top of the hot cylinder, was controlled by a Variac autotransformer. Voltage was monitored by a Western ac voltmeter and the current by a Triplet ac ammeter. Two 15 amp fuses were wired in the circuit to prevent damage if the heaters were accidentally overloaded.

The temperature was monitored at two places on the hot cylinder, at the side and at the top of the dome, by use of chromel-constantan thermocouples. A Honeywell 16 channel recorder was used to display the temperature readout, and a switch box was used to select either of the two thermocouples. Two thermocouples were used at each point to obtain a redundant check of the readout temperature.

The 30°K and 75°K cold cylinder temperatures were monitored by a Leeds and Northrup K-3 universal potentiometer. The potentiometer circuit included a Leeds and Northrup dc null detector, an Eppley Laboratories

one-volt standard cell, and a two volt storage battery. A switch box was again used to select the thermocouple which in this instance was copper-constantan. A dewar of liquid nitrogen was used as a cold junction reference.

CONCLUSIONS

During the development test phase several problem areas were identified where future exploratory effort concentration should yield good dividends in improved unit reliability and performance.

1. Heater input power requirements were much higher than could be supported by design calculations. Final test data show 550-650 watts required as compared with calculated value of 300 watts. Some of this discrepancy was resolved by tests determining that non operating losses-heat conduction through insulation and displacer/cylinder assembly were higher than anticipated (125 watts actual versus 90 watts design). The majority of the loss however could only be classified as unaccounted and grossly assigned to regenerator and heat transfer effectiveness in the hot cylinder assembly. Design changes to explore this problem and improve unit performance might consist of: a) a study of the performance of the rider on the hot end of the displacer; and b) increasing hot displacer and hot cylinder length to improve regenerator performance and decrease conduction losses.
2. The cold-cylinder-displacer seal effectivity was a continuing problem. It was observed that the thin wall Inconel cylinders exhibited various degrees of non uniformity and out of roundness (0.002 to 0.004 inch T.I.R.) within the seal area. This placed a heavy responsibility on the seal to obtain effective performance. During development testing the problem was

minimized by variously making the seal more compliant and increasing the sealing force. This solution however increases the seal drag with resulting increased drive motor torque required. The system aspects of cylinder fabrication, seal type and required torque should be explored in detail.

3. The required running torque level for the drive motor is 40 in. oz. approximately 5 times the original design value of 8 in. oz. The problem outlined in (2) above accounts for some of this increase; obviously however there are other areas which should be explored toward reducing the torque requirement. These include bearing type and drag, pressure drop and parts interference.
4. To achieve the long life of which this machine is capable will require additional information on bearing performance in a dry helium environment. Carbon (P5N) journal bearings were briefly explored in a special test fixture resembling the refrigerator crankcase. Other carbon materials and other type bearings such as fabroid bearings should be tested over an extended operating period.
5. The long term effects of contamination on thermodynamic performance of the unit must be investigated. The development schedule precluded extended runs with result that longest continuous run to date is approximately 34 hours. Although the unit is designed to minimize any contamination problems, additional evaluation work is in order to ascertain the performance limits of the unit.

Figures 91 and 92 illustrate the mean final performance capability of the refrigerator as delivered.

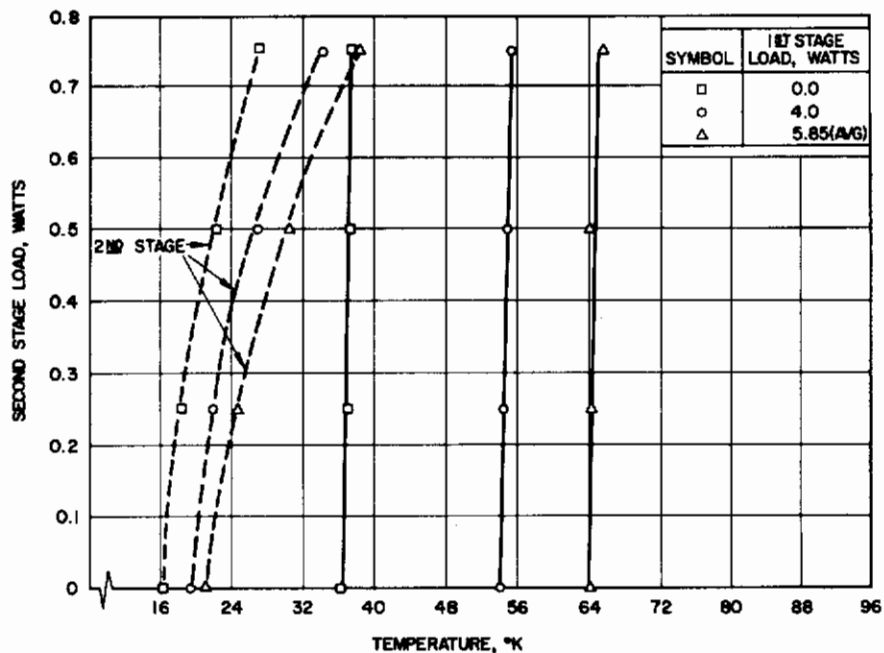


Figure 91. Load capacity curves for 30°/75°K VM refrigerator unit X447550-100

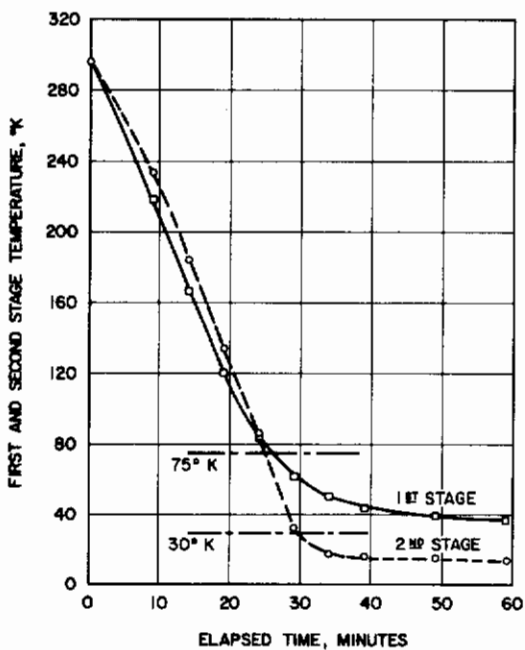


Figure 92. Cooldown time for 30°/75°K VM refrigerator

Contrails

SECTION VI

77°K BREADBOARD REFRIGERATORS (X447525-100)

INTRODUCTION

The X447525-100 refrigerator is an end item in Phase I of the development program to demonstrate the feasibility and applicability of the Vuilleumier refrigeration cycle. It was designed as a breadboard model capable of direct mount cooling an infrared detector package for typical aircraft application. Although designed as a breadboard the unit was delivered capable of operating and application aboard a military aircraft. After initial development on the first X447525-100 unit proved the design, a second breadboard was fabricated, tested and delivered.

DESIGN REQUIREMENTS

Design specifications required detailed design and integration of all components of the refrigerator including power equipment. The end product was to fulfill two basic functions.

1. Act as a laboratory breadboard model to demonstrate the feasibility of the Vuilleumier cycle and obtain new information which would permit refinement of the design optimization process.
2. Act as a flyable prototype to be used in aircraft to demonstrate performance feasibility and compatibility with infrared sensors and other potential system applications.

To have the capability of operating in existing aircraft, the refrigerator must be complete with air cooling blower and input power conversion equipment. The blower must have capacity to deliver sufficient cooling air at ambient temperature of +160°F at altitudes up to 50,000 feet. The system must be capable of operating on 28 vdc input power.

Specific contractual design requirements were: "The goal of the X447525-100 breadboard is a minimum size, minimum weight, direct

mount type aircraft refrigerator with maintenance-free life of 3000 hours. ¹¹ It is also stated that the refrigerator will be a miniature aircraft model based on the Vuilleumier cycle and designed to produce 2 watts of cooling at 77°K.

There were specific requirements for test instrumentation to be delivered with each breadboard.

The instrumentation was to consist of:

- Temperature measuring devices located on the hot cylinder, cold cylinder and crankcase heat rejection area.
- An electrical resistance heater to simulate detector load at cold end.
- A pressure gage attached to indicate unit internal pressure changes.

UNIT SPECIFICATIONS

The requirements were translated into working specifications for the unit and major components to form a basis for the design. Where requirements were lacking, assumed values were included to complete the specifications. Preliminary equipment specification XES 30527-010 sheet 1, 2, 3 describes the X447525-100 breadboard refrigerator.

| | | | |
|--|--------------|---|--|
| <div style="border: 1px dashed black; padding: 2px; display: inline-block;">HUGHES</div> <small>HUGHES AIRCRAFT COMPANY CULVER CITY, CALIFORNIA</small> AIR DEFENSE ELECTRO-OPTICAL LABORATORY | TITLE | Equipment Specification Vuilleumier Refrigerator P/N 447525 | XES 30527-010 <small>NUMBER</small> |
| | | | CODE IDENT NO. 82577 |
| | | | SH 1 OF 3 |

1. SCOPE

1.1 Scope – This specification covers a miniature Vuilleumier refrigerator utilizing an electrical heater for thermal power.

1.2 Refrigeration Capacity – The refrigerator shall deliver 2 watts minimum at 77°K.

1.3 Operating Temperatures

1.3.1 Hot Cylinder – The hot cylinder will be held at 1200° F - 1400° F.

1.3.2 Crankcase – The crankcase will not exceed a maximum temperature of 260° F and shall not be less than -65° F.

1.3.3 Cold Cylinder – The cold sink will be at 77° K or below when the refrigeration load is 1.6 watts or less.

1.4 Inputs

1.4.1 Thermal Energy – The thermal energy shall be supplied by an electric heater coil attached to the hot cylinder. The power required during operation is 150 watts at 28 vdc.

1.4.2 Drive Motor – The drive motor shall rotate the crankshaft at 600 rpm. The characteristics of the drive motor are specified in Motor Specification XPS 30527-011.

1.4.3 Cooling Air – The integral blower to supply cooling air at a minimum flow rate and pressure of 40 CFM and 2.0 in water static pressure and an input temperature not in excess of 160° F (S/L condition). The blower to provide sufficient cooling at 50,000 feet altitude at 160° F air temperature.

| INITIAL APPROVALS | DATE | REV LTR | DATE | APPROVAL | | |
|----------------------|------|---------|------|----------|--|--|
| PREPARED R. L. Berry | | | | | | |
| CHECKED | | | | | | |
| APPROVED R. L. Berry | | | | | | |
| | | | | | | |
| | | | | | | |
| | | | | | | |

2. APPLICABLE DOCUMENTS

The following documents form a part of this specification to extent specified.

Drawings

Hughes Aircraft Company

X447525-500 Outline and Mounting, Vuilleumier Refrigerator VM-4/77

X447525 Cryogenic Refrigerator, VM-4/77

Specifications

XPS 30527-011 Motor Specification

XPS 30527-012 Heater Specification

XPS 30527-013 Inverter Specification

Other

3. REQUIREMENTS

3.1 Dimensions - The dimensions shall conform to Hughes Aircraft Company drawings X447525-500 and X447525.

3.2 Weight - The weight of the unit as shown on drawing X447525-500 shall not exceed 4.0 pounds.

3.3 Performance

3.3.1 Heat Load - The refrigerator shall deliver a minimum of 1.6 watts of refrigeration at 77°K when the crankcase is at 130°F and the hot cylinder is at 1300°F.

3.3.2 Cooldown Time - The cooldown time shall be less than 10 minutes when the refrigerator is stabilized at 80°F before starting operation. The cooldown temperature is 100°K.

3.3.3 Life - 3000 hours with no maintenance.

3.4 Power Supply

3.4.1 D-C Power - The d-c power system shall be a two-wire grounded system having a voltage of 28 ±4 vdc. The negative of the power supply shall be connected to ground.

| | | | | |
|--|--|-------------|---------|------------------------|
| AIR DEFENSE ELECTRO- OPTICAL LABORATORY | HUGHES AIRCRAFT CO. CULVER CITY, CALIF. CODE IDENT NO. 82577 | 2 SH NO. | REV LTR | XES30527-010 NUMBER |
|--|--|-------------|---------|------------------------|

3.4.2 A-C Power — Not required.

3.5 Power Requirements

3.5.1 D-C Power Requirements — The d-c power required for operation of the unit shall not exceed 200 watts at 28 vdc. This power is used to supply thermal energy (heater coil) and drive the drive motor and fan. See Motor Specification XPS 30527-011 for details of drive motor requirements.

3.5.2 A-C Power Requirements — None

3.6 Standard Conditions — The following conditions shall be used to establish normal performance characteristics under standard conditions and for making laboratory bench tests:

| | |
|---------------------|-------------------------|
| Temperature | Room Ambient (68 ±20°F) |
| Altitude | Sea Level |
| Vibration | None |
| Relative | 90 percent or less |
| Input Power Voltage | 28 ±4 vdc |
| Barometric Pressure | 645-795 mm of Hg |

3.7 Operating Conditions

3.7.1 Temperature — Per MIL-E-5400, Class 2.

3.7.2 Vibration — Per MIL-E-5400 Curve I — 0.08 DA to 10 cps, 0.42 G 10 to 14 cps, 0.036 DA 14 to 71 cps, 10 G 71 to 500 cps.

3.7.3 Mechanical Shock — Per MIL-E-5400 Paragraph 3.2.21.6 — Must operate after three shocks of 15 g's in three mutually perpendicular axes, duration 11 ±1 millisecond. Must remain in place after two shocks of 50 g's in three mutually perpendicular axes, duration 11 ±1 millisecond.

3.7.4 Storage Requirements — Five years.

| | | | | |
|--|--|-------------|---------|------------------------|
| AIR DEFENSE ELECTRO- OPTICAL LABORATORY | HUGHES AIRCRAFT CO. CULVER CITY, CALIF. CODE IDENT NO. 82577 | 3 SH NO. | REV LTR | XES30527-010 NUMBER |
|--|--|-------------|---------|------------------------|

PHYSICAL CONFIGURATION

The physical configuration of the unit can be described by reference to three basic drawings:

1. Outline and Mounting Drawing No. X447525-500 (Figure 93). This drawing shows maximum dimension for the unit to be 5.7 or 6.3 inches including the cooling fan in the axis orthogonal to the cold finger. The other two dimensions are between 5 and 5.5 inches. A dc to ac power inverter (3-1/4 x 2-3/8 x 1-3/4 inches) for the drive motor is located remotely. Mounting provision is on underside of crankcase and consists of 4-40 press nut inserts on 1.200 x 1.350-inch rectangular pattern.
2. Electrical Schematic Drawing No. X447525-200 (Figure 94) Electrical input to the unit is 200 watts of 28 vdc. Approximately 150 watts of this is required by the hot cylinder resistance heater. The remaining dc power is converted to ac through power inverter to power the refrigerator drive motor. The inverters are located remotely and all power is received by the unit through a Deutsch (DM 9601, 12P) receptacle. An elapsed time meter located on the unit records the refrigerator running hours.
3. Refrigerator Assembly Drawing No. X447525-100 (Figure 95). This drawing shows internal details of the refrigerator. To minimize dead volume and helium contamination, the stator for the drive motor is mounted outside the working volume on a thin wall stainless steel enclosure. The rotor is mounted inside and supported by two crankshaft bearings. The crankshaft is a cantilevered type driving the hot and cold displacers. (Counterweights are used on one side of the displacer connecting rods) and all crankcase dead volume has been minimized by including filler parts where possible. The cold regenerator is located internally in the cold displacer which has a seal at the crankcase end. The hot regenerator consists of the hot displacer and hot

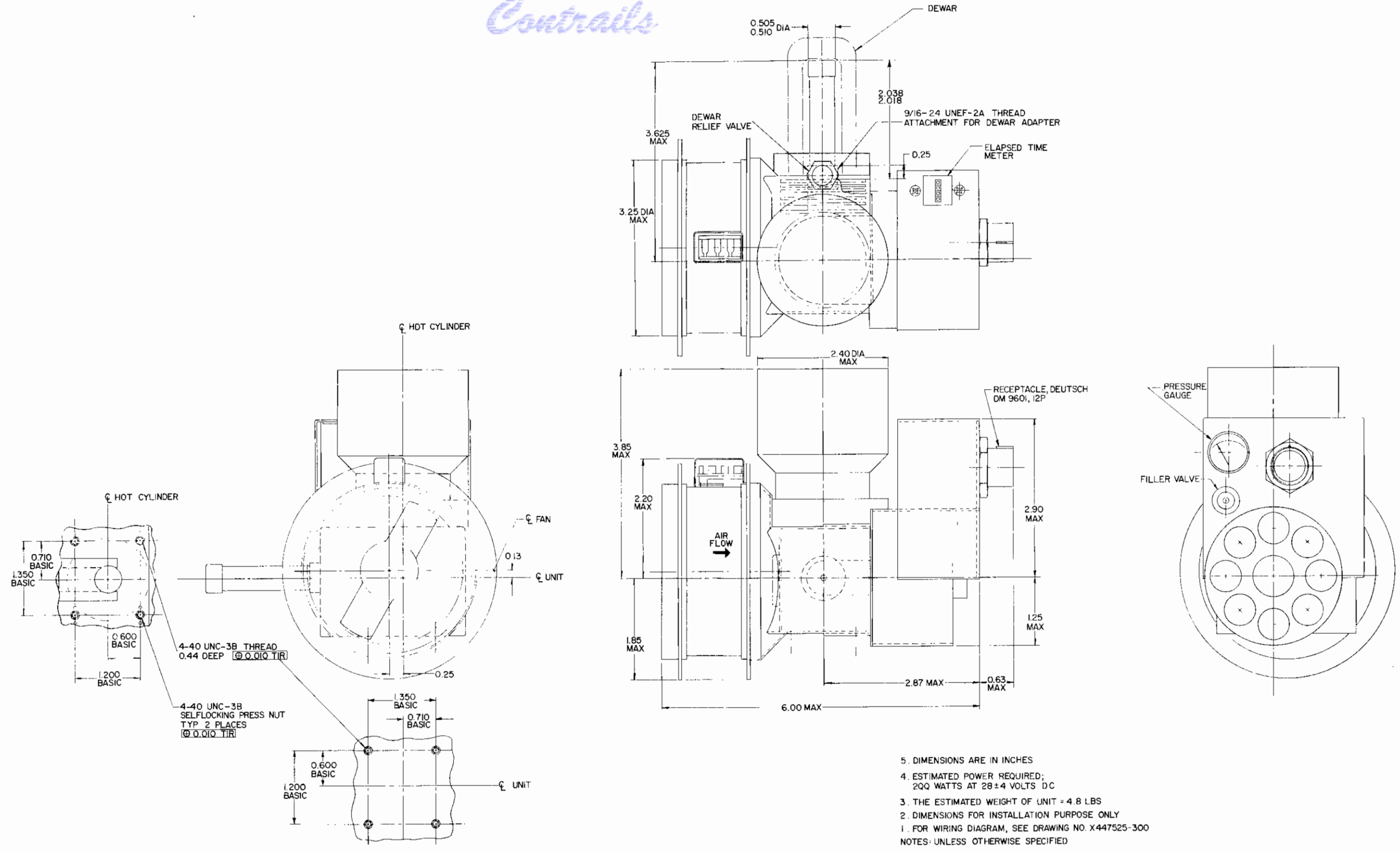


Figure 93. Outline and mounting drawing of VM refrigerator X447525-100

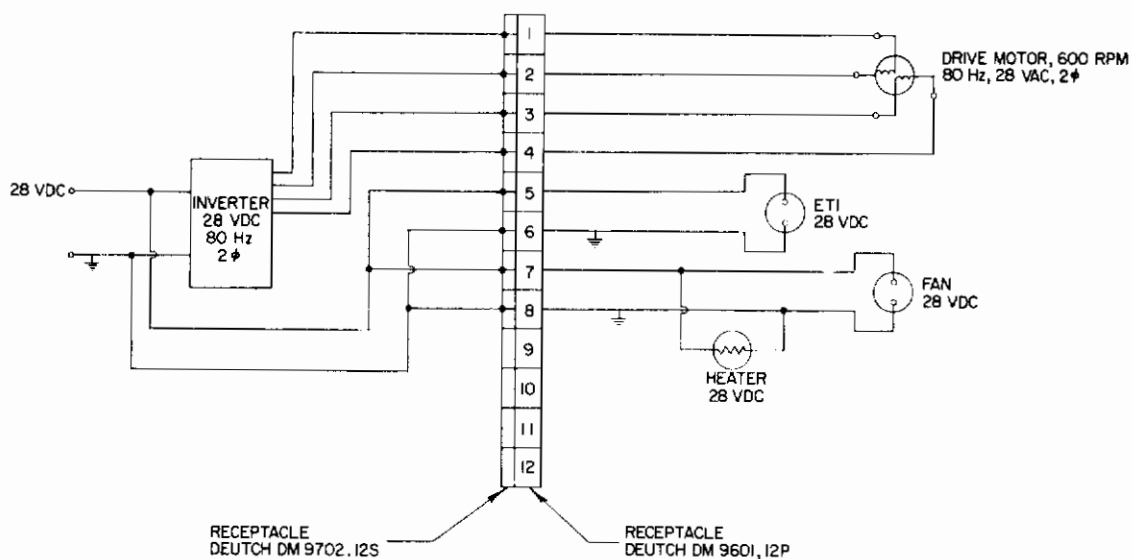


Figure 94. Electrical schematic of 77°K VM refrigerator P/N 447525

cylinder wall. The hot cylinder heater is brazed on the upper portion of the cylinder and insulated from ambient by special insulation protected by a metal enclosure.

THERMODYNAMIC DESIGN

The thermodynamic design is concerned primarily with the prediction of the losses that cause the refrigerator to deviate from the Carnot relationship. Table 9 shows the calculated losses for both hot and cold cylinders.

A regenerator is a heat storage device. The gas which oscillates through the regenerator alternately stores and absorbs heat. A temperature differential must exist between the gas and the regenerator matrix to accomplish this heat exchange. During the inflow cycle the gas entering the regenerator is at a temperature greater than the temperature of the ambient end of the regenerator. During outflow the gas is at a temperature

Table 9. Summary of heat losses for unit X447525-100

| | Design | Development |
|---------------------------------------|--------|-------------|
| Heat Losses from Cold Cylinder, Watts | | |
| Regenerator | 0.715 | 0.765 |
| ΔP | 0.057 | 0.092 |
| Joule Thomson | 0.017 | 0.017 |
| Shuttle | 1.158 | 0.860 |
| Pumping | 0.388 | 0.435 |
| Conduction | 0.646 | 0.535 |
| Total | 2.981 | 2.704 |
| Heat Losses from Hot Cylinder, Watts | | |
| Regenerator | 9.38 | 67.0 |
| ΔP | 0.01 | 0.1 |
| Shuttle | 26.000 | 20.6 |
| Conduction: | | |
| Cyl. Wall | 8.820 | 14.4 |
| Displacer | 8.100 | 9.4 |
| Insulation | 8.050 | 8.4 |
| Total | 60.360 | 119.9 |

lower than cold end of the matrix. The temperature differentials represent an energy deficit called the regenerator loss.

The second loss noted here is that due to pressure drop. The pressure drop loss results from the ΔP required to force the gas through the various flow passages. Most of this loss occurs in the regenerators themselves.

The Joule-Thomson loss is caused by the imperfection of the gas, i. e., its deviation from the ideal gas. Because it is less than ideal, as the gas

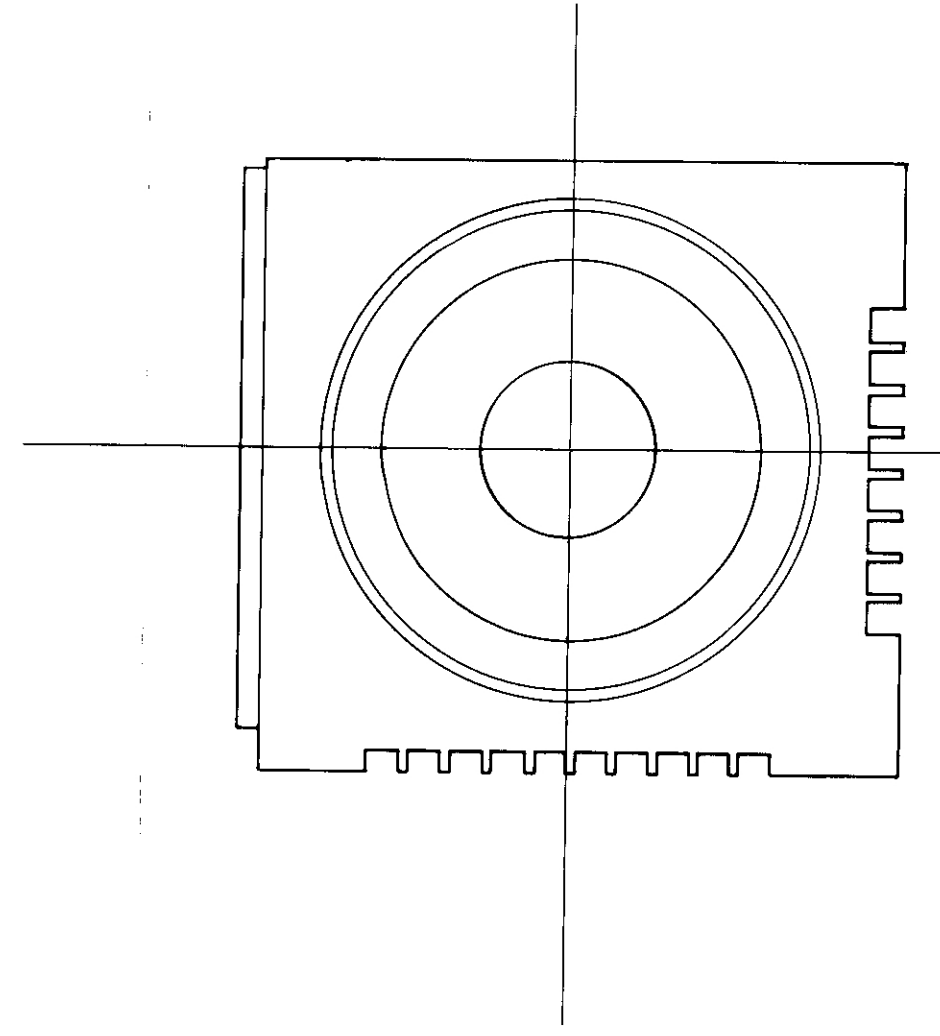
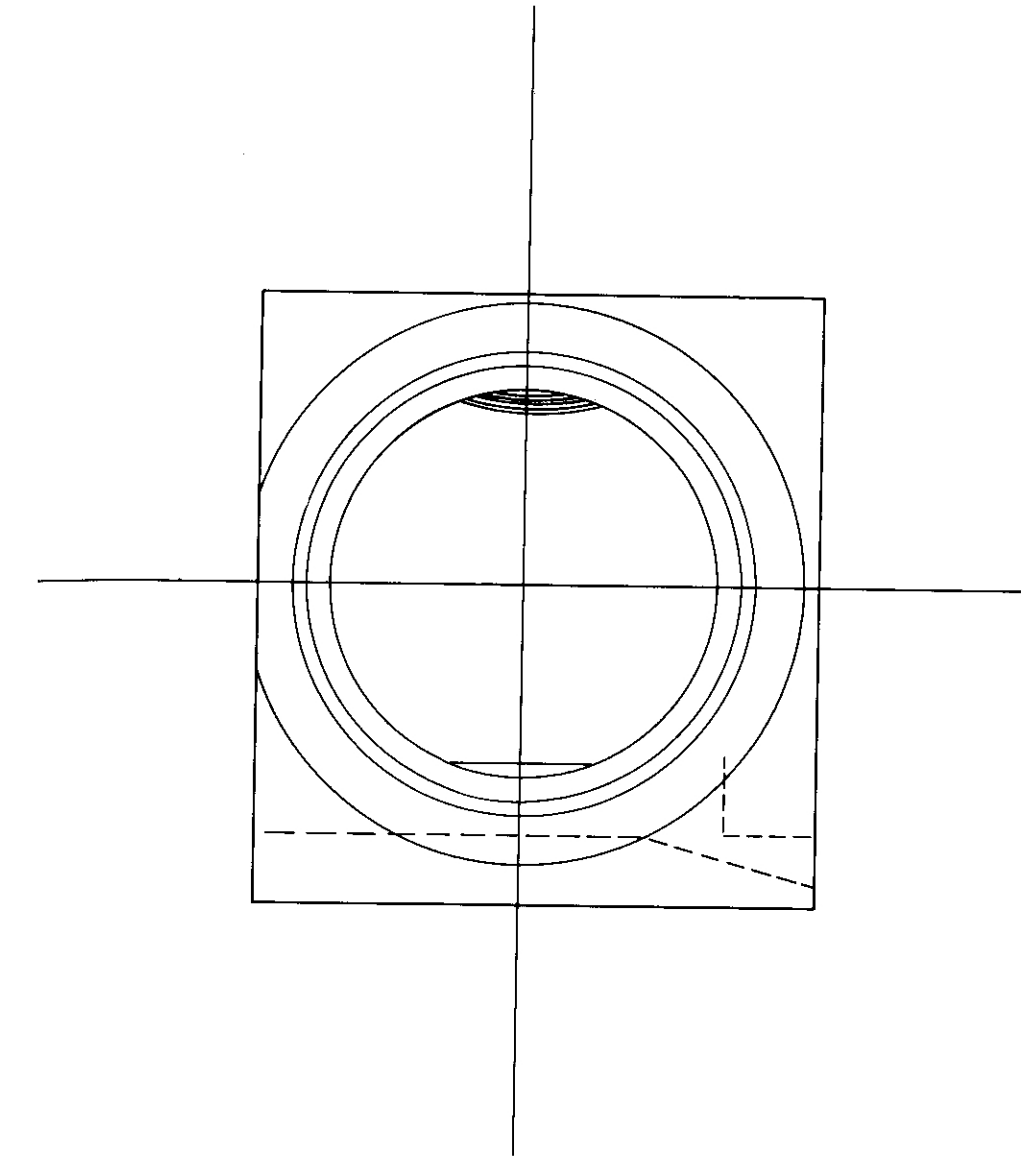
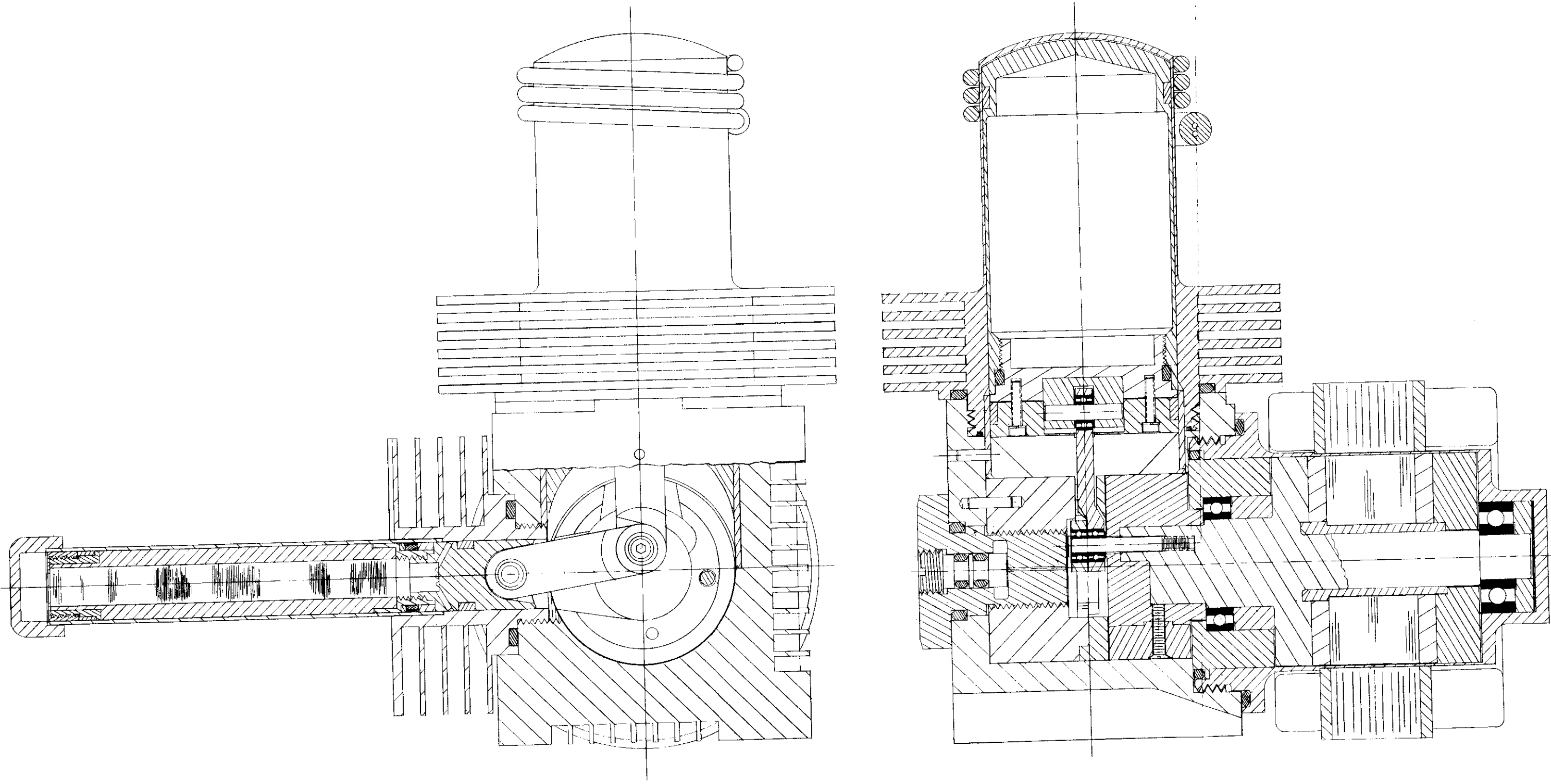


Figure 95. Cutaway of 77°K VM refrigerator

passes through a porous plug or through a pressure drop it will either rise or lower in temperature depending upon its Joule-Thomson coefficient. In the range (77-300^oK) in which this regenerator operates, the Joule-Thomson coefficient causes an increase in temperature of gas as it passes through a pressure drop, and this results in the Joule-Thomson loss shown.

The next loss is termed shuttle loss. Shuttle loss is caused by the mismatch of thermal gradients between the cylinder and the piston. Looking at the schematic diagram of the machine in Figure 77, it can be seen that the cylinder wall which is at ambient temperature at one end is at cryogenic temperature at the other. It has a fixed length and a gradient from warm to cold that is approximately linear. The piston is somewhat shorter than the cylinder wall by the length of the stroke, however, it has the same temperature extremes; warm at one end and cryogenic at the other. When the piston is at one extreme the temperature gradients are somewhat mismatched. As it passes through its stroke and reaches the other extreme the gradients are again mismatched, but now they are mismatched in the opposite direction so that the piston picks up heat from the cylinder when it is at the warm end and it gives off heat to the cylinder when it is at the cold end of its stroke. Hence, there is a picking up of heat at the warm end, a shuttling of the displacer to the cold end where it drops off the energy to the cylinder. It is thus termed a shuttle loss.

The pumping loss is due to the fixed clearance volume that must exist between the piston and the cylinder so that the piston can move without rubbing. Because this volume around the cylinder allowed for running clearance is fixed, the mass of gas in this volume at any one time is proportional to the pressure and the pressure in the machine is cycling from a maximum to a minimum. At the minimum pressure point there is a minimum mass of gas in this volume. Moving toward the maximum pressure point, gas must flow into this volume in order to increase the amount of gas there, proportional to the pressure. Hence, cold gas flows into this volume and up into the warm areas where it picks up energy. Then as the gas

pressure falls from the maximum pressure back to the minimum pressure, some warm gas must flow out of this volume into the cold regions. This causes a loss of refrigeration.

The conduction losses are conventional and represent the conduction loss due to thermal conductivity of the materials operating between two temperature extremes.

The theoretical PV curve shows a gross power capacity in the cold stage of 4.70 watts. Deducting the total losses of 2.70 watts leaves 2.00 watts of usable refrigeration. This is at the worst condition with a 400°K crankcase temperature or approximately 260°F . Figure 96 shows the expected increase in net refrigeration capacity as the crankcase operating temperature decreases.

The hot stage requirement is calculated at 920°K (1200°F) where energy input is introduced. The losses listed are similar to those shown for the cold stage with exception that the Joule-Thomson loss is omitted since it contributes to heat input. In addition to listing the losses, the summary on

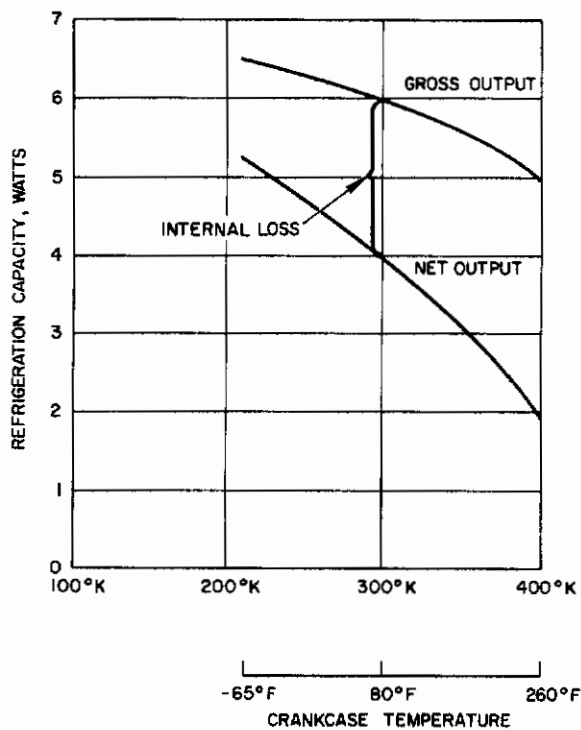


Figure 96. Refrigeration capacity as a function of crankcase temperature for unit X447525-100

Table 9 includes power input to drive motor and working gas. The heat input to the working gas is calculated from the P-V diagram for this stage. It should be noted again that these design results are for 400°K (260°F) reference crankcase temperature. Total design power input to the refrigerator under these conditions is 95 watts. Figure 97 shows the calculated effect of crankcase temperature on input power and cooling capacity.

MECHANICAL DESIGN

Mechanically the Vuilleumier is relatively simple to design since internal loading on bearings and seals are low, on the order of 1/20 of the loads encountered in a conventional Stirling refrigerator. This characteristic coupled with its inherent slow speed make the VM refrigerator a natural candidate for a long life machine if wear particles and gas contamination can be controlled. This of course imposes additional mechanical problems which combine with the close tolerance requirements imposed on internal parts to minimize the

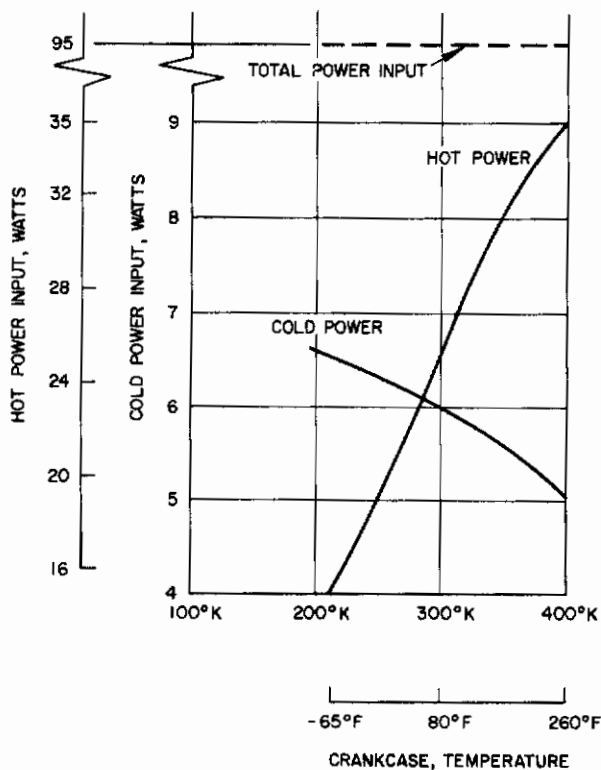


Figure 97. Input power and cooling capacity as a function of crankcase temperature for unit X447525-100

dead volume in the machine. The other major area is one of stress deriving from the temperature and pressure extremes in the unit.

Primary load factors were derived from knowledge of the unit requirements. A maximum internal pressure of 950 psi was used to calculate the limiting pressure vessel type stresses. Simultaneous temperature requirements were 1200°F hot cylinder, 260°F crankcase and -320°F cold cylinder. To these basic stress requirements must be added the dynamic stresses introduced by machine operation and shock and vibration loads (50 g shock and/or 30 g vibration) were chosen to reflect gimbals mounting and are well above MIL-E-5400 specification (30 g shock, 10 g vibration).

Although all considerations and calculations obviously cannot be presented, the following is a brief summary of major component stress analyses.

Hot Cylinder - Inconel 718

At 1200°F the stress due to internal pressure is 36,530 psi and the MS (margin of safety) is greater than 1. The Margin of Safety is the percentage by which the allowable strength of the material exceeds the design load. For fatigue due to pressure cycling, extrapolating a constant life diagram shows a life in excess of 5000 hours. The shear load on the threads is 3500 psi. The bending stress due to shock on the upper cylinder components is considered negligible.

Cold Cylinder - 304 Stainless

Temperature varies from +260°F to -320°F over length of the cylinder. Wall thickness is 0.0075 inch. The tensile stress on the wall due to the internal pressure is 25,350 psi, and on the head 26,740 psi. The bending stress produced by the weight of the piston at 50 g's is less than 1000 psi.

Cold Piston - Fiberglass and 303 Stainless Steel

The cold end of the piston experiences a temperature decrease of 240°K during cooldown. The stress produced in the wall due to the difference in coefficient of thermal expansion of the two materials is 5,350 psi and MS > 1.

The center of the piston cools about 120°K . The change in clearance due to contraction is 0.00025 inch.

Crankshaft - 17-4 PH

The crank design is basically a small shaft simply supported between two bearings with a load cantilevered from one end. The stress in the shaft due to the operating pressure, friction, and inertia loads is 8,600 psi at 260°F . After including a stress concentration factor of 1.45 for the section change, the stress is still well below the endurance limit of the material; therefore, there is no fatigue problem.

The stress in the shaft due to the shock of 50 g's on the piston-rod-counterweight mass is 108,800 psi. This gives an MS of 0.64. For unamplified 30 g vibration, the stress at the fillet is 94,600 psi which is still below the endurance limit.

This design, however, was unacceptable from a deflection standpoint. Assuming the motor rotor is non-structural, deflection at the inner end is 0.024 inch at 30 g's. This would require an excessive clearance around the counterweights and consequently excessive dead volume. In addition, the natural frequency of the system would be 135 cps. Any vibration input greater than about 5 g's at this frequency would therefore cause failure. This condition was eliminated in the development model by increasing the shaft diameter to achieve acceptable deflection.

Drive Motor Rotor Enclosure - 416 Stainless Steel

To achieve good motor efficiency the wall thickness separating the rotor end field must not exceed a maximum of 0.008 inch. The bending stress due to the outer bearing load is 2,910 psi. Buckling of this shell is not a problem. The tensile load due to internal pressure is 33,250 psi and the MS is > 1 . Operating temperature was assumed to be 260°F .

Bearings

All bearings used in the refrigerator are dry-lubricated ball type similar to those made by Barden Company. These are steel balls which are lubricated by a filled teflon retainer. Life calculations are based on published load ratings and margin safety for shock loading on the maximum radial static loading.

Wrist Pin - Bar Temp SR 133SSTB

The maximum radial load from the piston mass at 50 g's is 4.85 pounds. The cyclic load from pressure, inertia, and friction, is 0.50 pound, and the life is 20,000 hours.

The above assumes rotation, however, and this bearing oscillates through a relatively small angle. No data was available for this case.

Crank Pin - Bar Temp SR166SSTB

This bearing carries the additional weight of the rod; MS > 1, life 20,000 hours.

Crank Main - Bar Temp

This bearing carries a load of 20.0 pounds at 50 g's; MS > 1. The load due to cycling pressure etc. is 1.47 pounds and the life is 20,000 hours.

Electric Motor Bearing - Bar Temp

The loads are less than the wrist pin, therefore it is considered adequate.

UNIT MOUNTING

The unit is mounted on 4 screws through the panel at the cold cylinder end. The CG of the unit is approximately 2 inches inboard and on the centerline. The tensile and shear loads per screw are 50 and 25 pounds respectively at 50 g's. The allowables for 4-40 screws are 345 pounds and

280 pounds respectively, therefore $MS > 1$ for combined loading. These loads are carried through an 0.040 inch 6061-T6 aluminum sheet to the unit. Maximum stress in these panels is 595 psi. Figure 98 shows the cooling fan and sheet metal trim which encloses the basic unit.

DESIGN FEATURES

The mechanical design incorporates several basic features which were dictated by requirement to maximize the time between maintenance cycles. Since the machine operates at a relatively slow speed (600 RPM), the primary design contribution to long life lies in minimization of contamination of the working gas. One of the main sources of contamination of the gas identified from past experience with Stirling refrigerators is the electric motor. The windings therefore have been located outside of the crankcase so that they cannot contaminate the gas. The motor rotor is of all metal construction; attention was focused on elimination of all varnish and plastic materials.

All grease and oil type lubricants have been eliminated in design of the mechanism. The bearings are dry lubricated type which use a Teflon retainer to wipe the required lubricant on the ball.

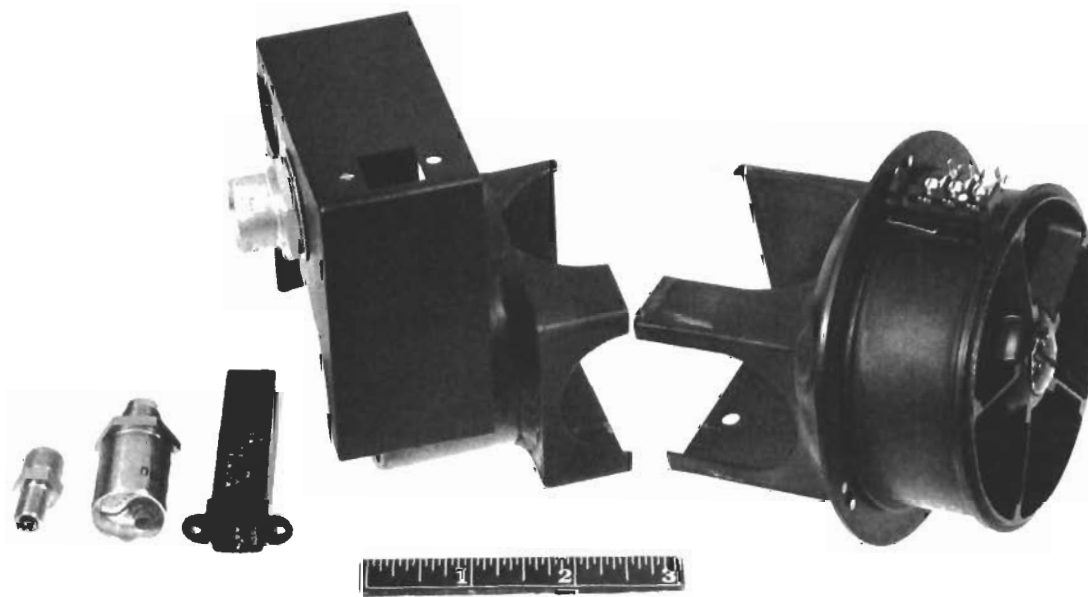


Figure 98. Cooling fan and sheet metal trim of unit 447525-100 (HAC photo 4R02913)

It would obviously be impractical to remove all possible sources of contamination from the working volume. However, the mechanism design is such that it permits a high temperature vacuum bake out which should further reduce the problem of long term contamination.

Table 10 summarizes the weight of the major parts of the unit. Weight of a number of the heavier parts could be substantially reduced through use of lighter weight material and some reconfiguration. An example is the crankcase which is made of brass to facilitate developmental changes; in the final design it could be made from aluminum.

PERFORMANCE

Performance of the unit matured from initial test run results of 215°K at no load to in excess of 1.6 watts at 77°K. During development

Table 10. Weight summary for 77°K VM cryogenic refrigerator
P/N 447525-100

| | Design Goal Weight, lb | Actual Weight, lb |
|--|---------------------------|----------------------|
| Crankcase Assembly (*Includes Hot and Cold Cylinders) | 0.383 0.564 | 1.13* |
| Crankshaft and C'Weight Assembly | 0.132 | 0.26 |
| Internal Parts and Miscellaneous | 0.334 | 0.14 |
| Motor Assy. | 0.383 | 0.82 |
| Hot Displacer Assembly | 0.087 | 0.13 |
| Cold Displacer Assembly | 0.040 | 0.04 |
| Shroud Assembly and Connector | 0.215 | 0.46 |
| Blower | 0.406 | 0.41 |
| TOTAL | | 3.39 |

testing one major design revision was effected. This involved primary rework of the internal crankcase and mechanism parts to minimize interferences and dead volume in the machine.

Table 11 presents a comparative summary of specific performance data for the X447525-100 refrigerator.

The test data proved also that the unit was relatively simple and straightforward to design. This was especially true in the thermodynamic area. In all cases it was possible to predict unit performance thermodynamically once conditions had been identified through use of PV diagrams, dead volume, temperatures, etc. Primarily, development problems were associated with the mechanical and mechanism features of the unit.

Table 11. Performance summary for VM cryogenic refrigerator P/N X447525-100

| | Performance Achieved Room Temperature Sea Level | | Contract Performance Goals 160°F 50 kft |
|--|---|--|---|
| Refrigerator | | | |
| 1. Weight, lb | 3.1 (without fan) | | Not specified |
| 2. Power input, watts | | | Not specified |
| Heater | 150 | | Not specified |
| Motor | 30 | | Not specified |
| Fan | 17 | | Not specified |
| Total (without fan) | 180 | | Not specified |
| 3. Temperature/capacity at 77°K, watts | 1.6 | | 2 |
| 4. Cooldown time, minutes | 7** | | 10 minutes |
| 5. Engine speed, rpm | 600 | | Not specified |
| 6. Maintenance free life, hrs | 744 To date | | 3000 hours |
| 7. Charge pressure, psi | 600 | | Not specified |
| Inverter | | | |
| 1. Size | 3-1/4 x 2-3/8 x 1-3/4 in. | | Not specified |
| 2. Weight | 1.1 lb (Breadboard) | | - |
| *To 100°K | | | |

Major developmental problem areas where significant developmental progress was made might be categorized as follows:

1) Excessive Internal Friction

This item includes all types of friction inherent in the unit — rubbing of seals, interference of parts, and pressure drop in regenerators and flow passages.

2) Excessive Dead Volume

This is closely related to Item 1 because minimizing dead volume increased the problems associated with mechanical interferences and internal friction.

3) Heat Transfer Efficiency

Parameters pertaining to maximizing efficiency of heat energy input to the unit had to be identified. Likewise heat rejection at the crankcase required considerable effort to define and improve performance.

4) Drive Motor

The task of designing and building a low speed ac motor having a metallic interruption in the air gap with sufficient torque to overcome starting friction proved to be a major problem. However, this was due in large degree to the schedule restriction which forced an early freeze on motor design.

5) Working Gas Contamination

Major development effort on this item was the identifying of possible contaminants introduced by the charge gas and the internal elements of the refrigerator. The design was executed to eliminate all of these from the working volume.

Rather than discuss the development of the refrigerator in general chronological activities, it is felt that a more informative approach would be descriptive of the specific areas outlined above.

CRANKCASE AND MECHANISM

The crankcase is basically a finned brass block as shown in Figure 99. It is bored to one inch on the crankshaft axis, and threaded to accept the hot and cold cylinders, the Helium fill valve, and the drive motor housing. All components are sealed to the crankcase with O-rings. A slotted sleeve is pressed into the hot cylinder port to provide more efficient ambient heat transfer to remove heat from the gas returning from the hot regenerator.

A brass filler with milled slots for connecting rod clearance is inserted into the crankcase for approximately half of its length. A dowel pin locates it and the helium fill plug is screwed into it thus clamping it against the crankcase wall. Another brass filler, about 1/8 inches thick and with matching slots for connecting rod clearance, is attached to this part when the rods are inserted.

The crankshaft, also shown in Figure 100 carries the drive motor rotor, a counterweight, and the two connecting rods. It is supported by two ball bearings. A Barden Bar Temp SR4SSTB is mounted in the end of the motor

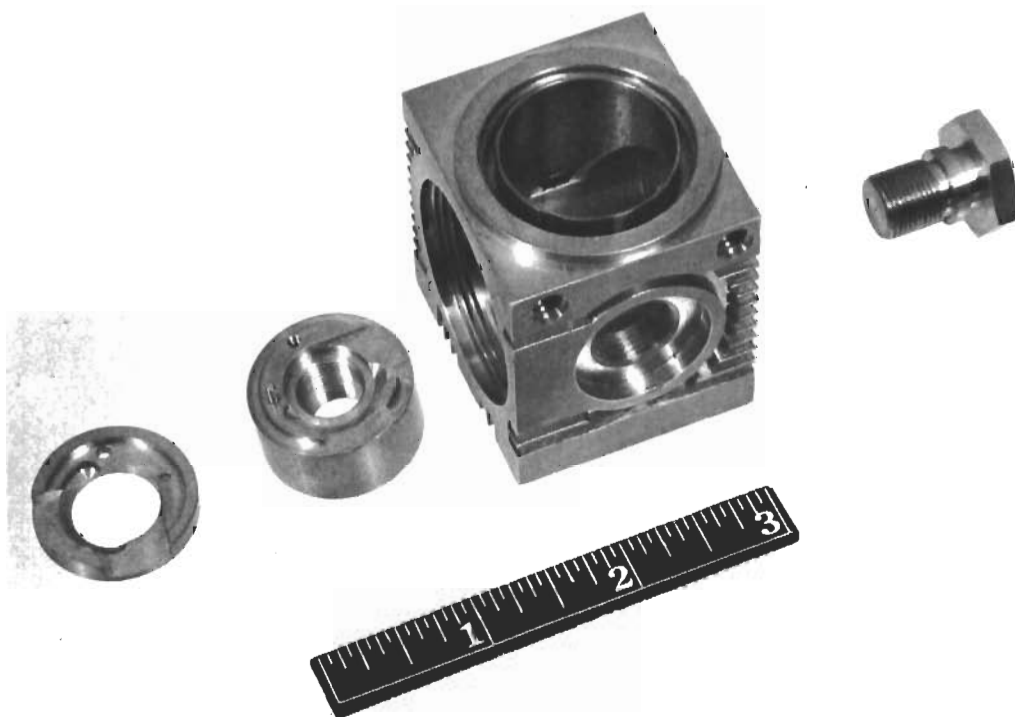


Figure 99. Crankcase of unit 447525-100
(HAC photo 4R02917)

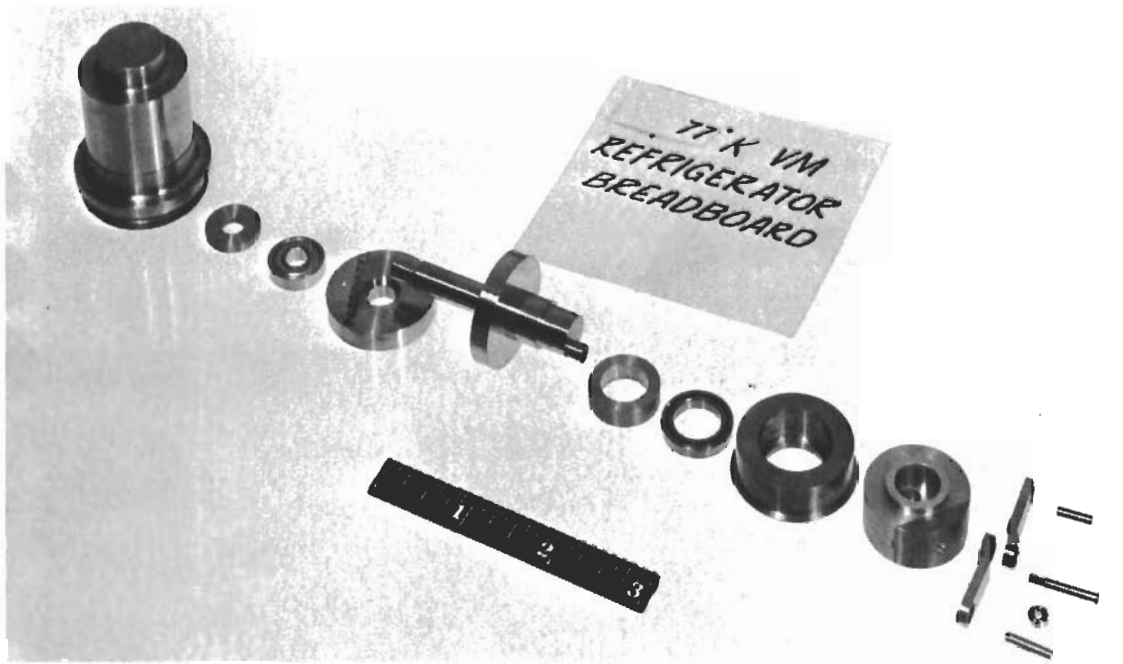


Figure 100. Crankshaft assembly parts of unit X447525-100 (HAC photo 4R02915)

housing, and a Split Ball Bearing Company 3TCNR8-12 is mounted in the front of the motor housing. The motor rotor and two steel filler sections are positioned between the bearings.

The counterweight and crankpin are cantilevered from the main bearing. The counterweight, a disc of aluminum and Mallory metal, is slipped over the end of the shaft and rotated by the offset crankpin. The crankpin itself is a 0.094 diameter pin with 2-56 NC threads on one end and a flange on the other. The flanged end contains an Allen socket. The pin is inserted through the rod bearing and screwed into the end of the crankshaft. Access is through the helium fill valve. The pin holds the two rod bearings and the counterweight against the end of the shaft. Shims are used to maintain proper length dimensions. Because loadings in this machine are light, stresses on the crankshaft are minimal. The shaft is made from 17-4-PH stainless, however, to insure a good surface for the bearings.

The connecting rods are 0.093 inch thick, 0.275 inch wide, and 1 inch long and are made from 416 stainless steel. They are offset on the crank end so that they may operate on the same cylinder axis with side by side bearings. Barden SR133SSTB bearings are used in each end of the rods. Steel pins are inserted through the bearings and into the base of each piston. The piston bases are slotted to accept the rod end with minimal dead volume.

An aluminum extension is attached to the base of the hot piston by screws. This part straddles the crankcase fillers and counterweight, and is used for filling dead volume only.

All six bearings in the machine are lubricated by the small amount of dry lubricant contained in the ball cage, and therefore require no oil or grease. This also affords low friction torque and minimizes gas contamination. Loadings on the two crankshaft bearings are relatively low, and no problems are anticipated. The rod bearings however are loaded near their maximum dynamic rating, particularly on the cold cylinder side. In addition, the piston end bearings oscillate rather than rotate, thus depositing less lubricant. No failures have occurred in several hundred hours of running, but it was planned that carbon sleeve bearings be tested in this application. There is no preloading, and therefore no thrust loads, on any bearing.

A prime consideration in the design of all mechanism components was the reduction of dead volume. In the design calculations, the dead volume was assumed to be $1.5 \times V_c$ (reduced), or 0.78 cc. Of this, 0.34 cc was in the cold regenerator, and 0.04 cc in the hot regenerator. The remainder, 0.40 cc, or 2.0 cc at 400°K , could be in the crankcase area. In the original machine, crankcase volume was actually about 7.5 cc, and the pressure ratio was far below design. A redesign of the crankcase and motor area reduced the crankcase volume to approximately 2.75 cc, or 0.55 cc at 80°K . This makes the total reduced volume 0.93 cc, or $1.75 \times V_c$.

The reduction of dead volume in the redesign was accomplished in three major areas. (1) The large cross section connecting rods and oscillating hot piston extension were replaced by smaller rods operating in a stationary filler section. This is shown in Figure 101 which is a photograph contrasting initial and final designs in this area. (2) The large Barden main bearing was

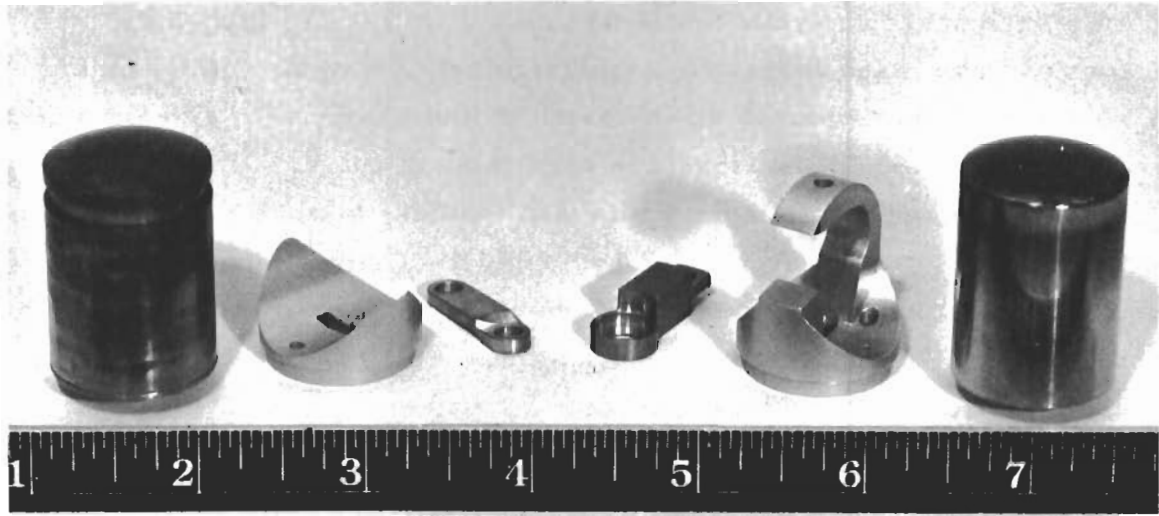


Figure 101. Hot displacer mechanism parts in unit X447525-100 (HAC photo 4R02725)

replaced by a much smaller split ballbearing type. (3) All clearances between parts were held to tightest practical tolerances, usually 0.001-0.002 inch. This required shimming in some areas, but no problems have been encountered in operation.

The present machine is unbalanced, for three reasons. (1) No real attempt has yet been made to equalize the weights of the hot and cold piston assemblies, necessary to achieve balance. (2) The use of a counterweight on one side of the connecting rods only creates an unbalanced couple. Areas on the crankshaft near the motor rotor that are presently used only as flywheels will be counterweighted to eliminate this. (3) A natural secondary unbalance will always exist in this crank-piston arrangement. However all of these loads are of a very low magnitude and will not appreciably affect machine performance.

HOT CYLINDER ASSEMBLY

The hot cylinder assembly consists of the hot cylinder, input heater and hot displacer as shown in Figure 102. The hot cylinder is required to hold 950 psi internal pressure, transfer heater input to the hot working volume, minimize heat loss by conduction, and act as part of the hot regenerator.

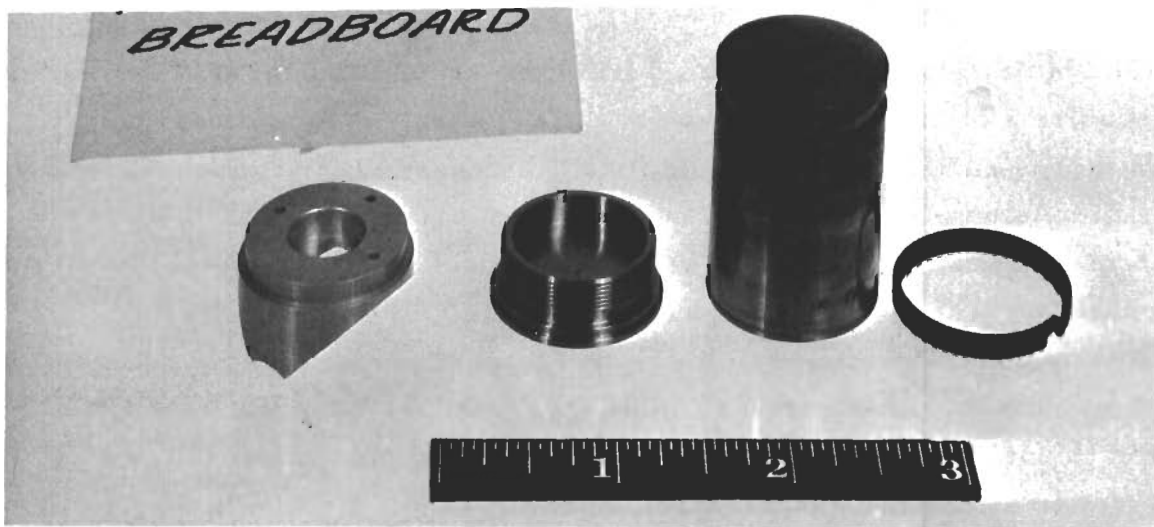


Figure 102. Hot displacer parts in unit X447525-100 (HAC photo 4R02914)

The basic cylinder is manufactured of Inconel 718, a material that maintains a high percentage of its strength at elevated temperatures and has a relatively low thermal conductivity. The side wall thickness is constant at 0.015 inches. The maximum design stress is 36,535 psi, and the stress allowable at 1200°F is 128,000 psi. The heat loss down the wall is presently about 14.4 watts. The dome, shaped on a 1.06 inch radius, is 0.030 inch thick to facilitate heat transfer from the heater to the center of the dome. The measured temperature differential is 50°F. The cylinder screws into the crankcase, and has an O-ring groove at the base of the threads to hold the internal pressure. A flange extends at the base to carry the insulation cover.

The heater, described in later discussion, is coiled around the top of the cylinder and brazed on with Ni Oro (AgNi), melting point 1750°F. This assembly is heat treated at 1350°F and aged at 1150°F.

The insulation consists of Refrasil A100 material wrapped around the cylinder to a thickness of 0.6 inch and covered with an aluminum can. A sheet of aluminum foil is inserted in the Refrasil 0.3 inch from the cylinder as a radiation shield. Loss is estimated at 8.4 watts.

The hot displacer is fabricated from the same material as the cylinder and conforms to the internal shape of the cylinder. It is operated with 0.006 inches radial clearance. The wall thickness is 0.016 inches, which since the piston is sealed, must be sufficient to prevent buckling at an external pressure of 950 psi. The critical buckling stress is 43,100 psi and the operating stress is 29,600 psi.

The top of the displacer is thickened to permit machining a groove 0.045 x 0.125 inch that carries the upper rider, a four-piece ring of DS13 carbon to position the displacer. The ring is scalloped on its outside diameter to allow free gas passage.

The bottom of the displacer is threaded on the inside, and a stainless steel disc screwed in to form the base. An O-ring between the base and displacer wall seals off the assembly. This internal volume of the displacer is filled with insulation material to prevent losses due to convection. The total conduction losses are 13.2 watts. A carbon ring, identical to the top rider but unscalped and two-piece, is held between the displacer base and the extension. This ring centers the displacer and forces the gas to travel thru the crankcase heat exchanger.

No failures have been encountered in any of the above components during operation. One hot cylinder cracked during brazing for an as yet undetermined reason. The original displacer design contained valves in the base to allow pressurization of the interior, but these were troublesome and were eliminated. The initial top rider showed signs of excess wear, and was replaced with grade 3310 carbon which is better suited to the high temperatures.

INPUT HEATER

The thermal input to the machine is provided from an electric heater that must maintain a temperature of approximately 1200°F in the hot working volume. The heater operates on 28 vdc. The initial calculation showed that a total of 90 watts input would be required at the hot cylinder to provide for the work and the losses. The heater is shaped and brazed to the top of the hot cylinder as shown in Figure 103.



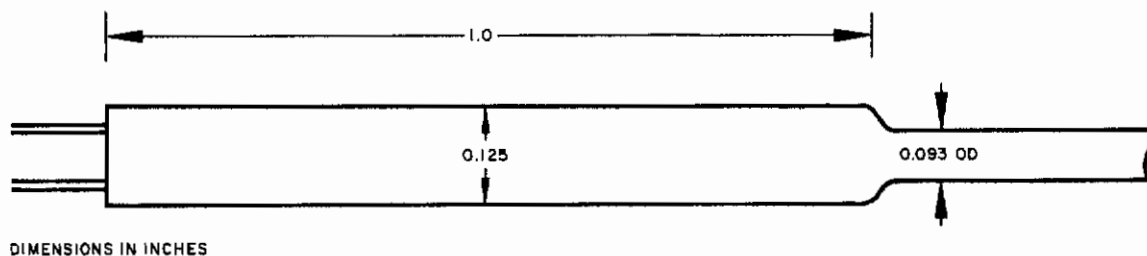
Figure 103. Input heater brazed to hot cylinder of unit 447525-100 (HAC photo 4R02722)

Several manufacturers of small heater elements were contacted, and a two-wire element from American Standard Company was selected. These consist of a nichrome hairpin shaped wire loop housed in a magnesium oxide filled inconel sheath, one end is closed. This configuration was selected in order that both lead wires would terminate at the same point thus simplify the input wiring. At this time it was also decided to size the heater for approximately 150 watts to allow for higher input power levels that were anticipated during early development. To obtain this output with 28 vdc input requires a heater with approximately 5 ohms resistance. Accordingly a heater was selected with 0.093-inch inconel sheath which is 10 inches in length. Extreme caution must be exercised during forming and brazing the heater in place to avoid damage to the sheath and leads.

The heater lead wires were exposed for about 1/2 inch at the termination for connection to the input leads. The initial connection was accomplished by spot welding the nichrome heater wire to copper lead wires.

After several hours of testing the original heater failed at or near the lead termination. Repetition of the failure occurred several times before the cause was determined for successful corrective action. It was determined that the failure was caused by a high resistance at the splices which in turn increased the heat energy at this point. Because there was no sheath at the splice point to dissipate the energy and in addition the whole area was insulated, the temperature climbed above the critical point and the nichrome wire parted.

To remedy this problem a new heater was obtained with nickel lead wires spliced to the nichrome at the input termination. The lower resistance of the nickel wire decreases the heat generated at the junction.



This configuration affords sufficient conduction path to dissipate the energy output at the junction and no heater failures have been experienced since the change.

Currently connections are made to the input leads by silver soldering. Thermocouples attached to the top of the hot cylinder monitor temperature and input control is achieved using a Variac during the test runs.

DRIVE MOTOR AND INVERTER

The mechanical power required to overcome gas friction, bearing losses, and mechanical rubbing interference of the reciprocating and rotating parts is supplied by a small induction motor. A canned design, one in which the field windings are hermetically sealed from the rotor, was used to prevent

contamination of the working gas and to keep the crankcase volume small without the use of seals.

The power available for the refrigerator was 28 vdc. Thus it was necessary to use either a dc motor or include a device to convert the dc to ac power. Numerous dc motors are available that could supply the required power in an acceptable sized package, but for the most part they employ brushes for commutation. These brushes would be used in a dry, unlubricated, helium atmosphere for which there was little past history of successful application. Since it was a design goal to develop a machine with a 3000 hour life it was decided not to use a brush type motor for which there was little history of successful application in this type of environment.

A review of brushless types of dc motors using commutation by optical or magnetic switching showed that in general these motors were not readily available, they were costly, and there was no data to show that they could withstand the probable environmental conditions imposed by vibration and temperature.

An induction motor was therefore considered. Hughes Aircraft Company has had considerable experience with the use of induction motors in development of other cryogenic refrigerators which indicated that there were no basic problems operating in the dry helium atmosphere. However the experience did show that the field winding was a major source of contamination of the working helium gas and could cause the refrigerator to lose capacity over an extended time period. To prevent any possibility of contamination the sealed induction motor was selected since it offered the following advantages:

1. The field winding could not contaminate the working gas and did not have to be specially treated or cleaned.
2. The dead volume of the machine was minimized in the crankcase-motor region without the use of seals. This allowed use of a simple mechanical design of the drive-crankshaft subassembly.

The investigation of induction motors presumed an acceptable means of converting from dc to ac power. Many of the manufacturers of special purpose motors also supply inverters so that their motors can be used with either ac or dc power. The inverter is usually composed of highly reliable electronic components, is small, lightweight and can be adjusted to deliver a wide range of frequency outputs which can be used to vary motor speed. It was only necessary to specify that the inverter not use saturating magnetic components that might later cause systems problems in the event that the refrigerator should be used as a part of some electronics system.

As a result of the decision to use a canned induction motor the mechanical design of the drive-crankshaft and the crankcase was simplified. There have been no problems associated with the motor or inverter after the initial debugging of the assembly in which interference problems were corrected. Frictional losses however were higher than predicted. To provide the additional torque requirement at 28 vdc input required that the initial motor design be rewound. This has required that the motor be operated at a higher voltage (34 vdc) to furnish the required torque. Operational experience is continually being applied toward reducing points of excessive friction and the motor can now be operated at design voltage. However to improve the reliability of the drive, it was decided to have the motor rewound to produce torque equivalent of 35 vdc operation at the 28 vdc input. Present power requirement is approximately thirty watts.

The inverter supplied with the unit is designed according to military specifications. It is equipped with speed control to permit continuous variation of output frequency from 50 Hz to 100 Hz. This varies the speed of the motor from 450 to 900 rpm.

COLD CYLINDER ASSEMBLY

The cold cylinder assembly consists of the vacuum dewar, cold cylinder and cold displacer. This assembly is of critical importance since it develops the refrigeration for productive use.

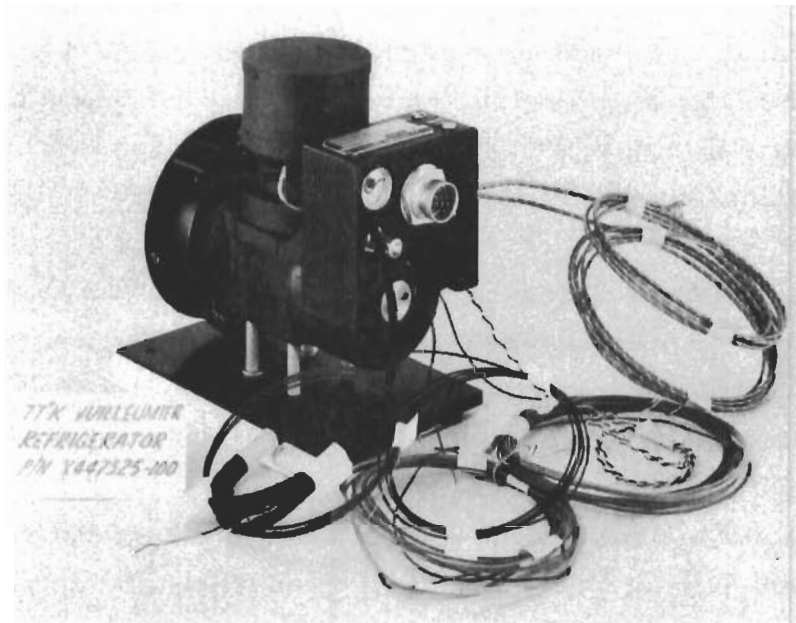


Figure 104. 77°K VM refrigerator breadboard with instrumentation (HAC photo 4R04049)

It is the function of the dewar to minimize the ambient heat load, in the form of radiation and convection, to the cold cylinder where the refrigeration is being produced. Normal practice is to use vacuum insulation combined with very low emissivity surfaces to accomplish this, or carefully sealed closed cell foams. In the case of miniature machines the vacuum technique is used almost exclusively due to its greater effectiveness. The most straight forward way of providing a vacuum dewar is to enclose the cold cylinder with a gold plated (for low emissivity) container and then evacuate the space between the container and the cold cylinder. This approach is satisfactory for laboratory conditions, but in general is not acceptable for use in the field. The reasons being that usually the device being cooled, say an infrared detector, is dirty from a vacuum viewpoint, tends to out gas and cannot endure the processes required to adequately clean it. Hence if the device is within the vacuum insulation region the vacuum must be periodically or even constantly renewed. This increases the complexity of the entire system and adds size at a very inconvenient region. To circumvent this problem a glass

dewar with silvered walls was selected. This allowed the device being cooled to be mounted directly to the refrigerator, but does not place the cooled device in the vacuum. In this way the dewar can be properly cleaned and processed to maintain a permanent vacuum and the device being cooled is not compromised.

For the actual dewar used in this application the calculation heat load was 0.55 watt for temperature limits of 350°K and 77°K and the measured heat load was 0.48 watt. Installation of the dewar is accomplished with an R. T. V. seal at the ambient end that provides a convenient feed-thru for the thermocouple and heater leads.

The purpose of the cold cylinder is to contain the working gas while minimizing conduction heat leak into the region where the refrigeration is being produced. Also the cylinder must provide a sealing area where the cold displacer can be sealed to it such that the working gas (helium) must traverse the cold regenerator. The cold cylinder must be fabricated from a material that has the following properties:

1. High strength so that this section can be used to contain the high pressure working gas.
2. Low thermal conductivity to keep the conduction heat leak to a minimum.
3. Good machinability.
4. The material should be capable of welding and brazing operations without becoming brittle at cryogenic temperatures.

To meet these requirements stainless steel alloys 321, 347 and 304 were found to be equally acceptable. Alloy 304 was used because of its ready availability.

The cold displacer consists of three basic parts. The displacer body, the cold regenerator which is contained within the body, and the seal. For this type of design the seal is located at the warm end of the displacer and seals the gas between the displacer and cold cylinder. This constrains the working gas to flow through the cold regenerator.

Design of the body is based upon several material requirements. The material used must not be porous to the working gas or the gas will not flow properly through the regenerator, thermal conductivity must be low to prevent excessive heat leak, thermal expansion must be matched to the mating parts (cold cylinder and regenerator) and the material must be able to withstand extreme temperature shock. Glass cloth laminated with epoxy, formed on a mandrel concentric with the centerline of the body, was used to fulfill these requirements. The importance of using a material that matches the thermal expansion rate of the cold cylinder and regenerator is worthy of further comment. Besides the obvious advantages of preventing thermal stresses from developing and allowing simplified fabrication methods there are several thermodynamic reasons. First, the gap between the cold cylinder and the displacer remains constant as the refrigerator goes from room temperature to cryogenic temperature. There is an optimum gap for best performance. If the gap is too small heat will be transferred from the warm end of the displacer by a process that is basically gaseous conduction. Conversely if the gap is too large energy will be transferred from the warm end to the cold end of the cylinder by the mass and thermal transfer of the gas in the volume defined by the gap. Hence there is an optimum gap for least losses and, there is much to be gained by maintaining the gap accurately. A second reason concerns the regenerator. By using a material matched to the regenerator material throughout the operating temperatures range it is possible to prevent distortion of the regenerator by squeezing or gas by-passing due to loose fit.

Regenerator design is one of the most important aspects of this type of cryogenic refrigerator. Basically the regenerator is a thermal energy storage device that must be able to take in and release the energy very rapidly and with very high efficiency. To accomplish this cryogenic regenerators are usually made up of finely divided material such as steel wool, fine mesh screens, small spheres and etc. The purpose is to give a flow path that will offer a minimum of fluid friction and expose a maximum of surface area to the fluid. For closed cycle, heat powered, cryogenic refrigerator the successful cold regenerator design is a balance of conflicting aims. The main goals are:

1. High heat transfer efficiency.
2. Low pressure drop.
3. Minimum void volume.

There is a great deal of both theoretical and experimental data available that correlates the relationship between pressure drop and heat transfer for packed beds - regenerators being a form of packed bed. From this information it is apparent that heat transfer values can be increased for a fixed volume bed by increasing the pressure drop of the bed, but there is usually no indication as to how this information can be used to design a practical regenerator. Of course, a cut and try approach can be used, but with the large number of variables involved this can be a lengthy procedure. The approach used in this development was to choose a desired heat transfer efficiency and allowable pressure drop. From this choice and the experimental data relating pressure drop and heat transfer efficiency a unique characteristic of the regenerator is fixed. That characteristic is the mass flow rate per unit area. With the mass flow rate per unit area known it is possible to select the particle size and length of the bed. The two are related - the smaller the particle, the shorter the bed length required to give the selected values of pressure drop and heat transfer efficiency. This procedure is simple and effective. In practice it is complicated due to the large temperature range involved, the unsteady state heat and mass transfer, and drastic changes of some properties of materials at cryogenic temperature. But by dividing the regenerator into small sections, each covering a limited temperature range, this procedure is applied to each section for a series of small time periods that sum up to a complete cycle.

The seal used with the cold displacer is located at the warm end of the displacer (see Figure 105). Its function is to prevent the working gas from bypassing the cold regenerator as the gas is displaced from the ambient end to the cold end and back. The operating conditions are severe in that no lubricants can be used and the wear must be limited. However, the pressure against which the seal must act is only that which is developed across the regenerator due to pressure drop. To meet the conditions of

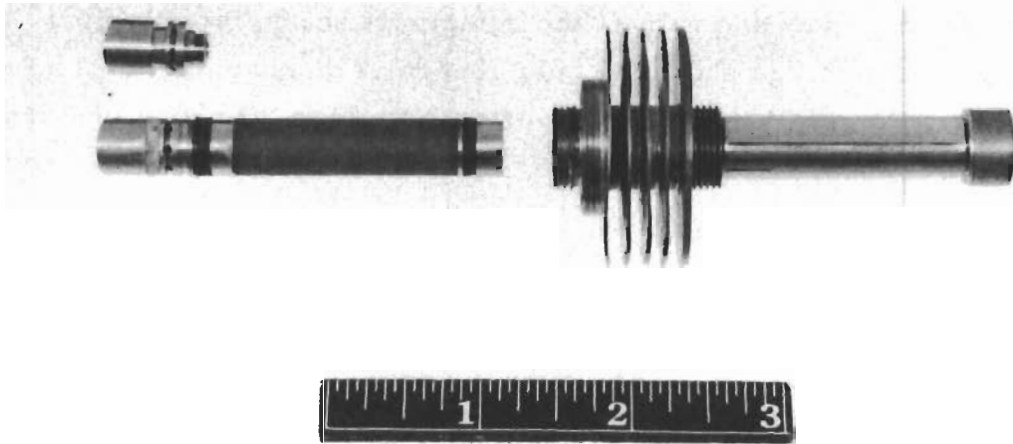


Figure 105. Cold displacer - cold cylinder assemblies (HAC photo 4R02916)

wear and non-lubrication the seal is made from glass filled teflon and is pushed into a sealing position by a O-ring. The teflon material has good wear characteristic and is flexible enough to compensate for small imperfections on both the displacer and cylinder sealing surfaces.

Tests to date indicate that the seal is adequate from a sealing and wear viewpoint, but that it is consuming too much motor power. To improve this situation several changes are being investigated. One is to provide a special cast iron surface for the seal to slide on, and the second is to replace the O-ring with a special garter spring that puts an almost constant load on the seal and is not affected by temperature changes.

TEST STATION

During testing, the machine is evaluated on the basis of refrigeration power at temperature, and input power. Pressure, hot cylinder temperature, and speed can be varied, but are generally left constant in a given series of tests. The instantaneous internal pressure versus crank position readings allow evaluation of the gross refrigeration power.

Figure 106 is a flow diagram of the equipment set up for a typical development test. Instrumentation could generally be characterized as conventional off-the-shelf hardware. During a test the following performance parameters were monitored:

- a. Cold spot temperature.
- b. Cold spot load.
- c. Hot cylinder temperature.
- d. Hot cylinder power input.
- e. Speed.
- f. Motor power input.
- g. Internal pressure.
- h. Crankshaft position.
- i. Crankcase temperature.

All temperatures are measured by means of thermocouples. Two copper-constantan thermocouples are mounted on the cold spot. These are redundant, and allow a quick check in case of suspected failure. The readout is on a Leeds & Northrup K3 potentiometer using liquid nitrogen as a reference junction temperature.

Two chromel-constantan thermocouples are mounted on the hot cylinder. They are in different positions, and indicate the temperature gradient across the top of the cylinder. Input power is controlled to maintain the hot cylinder at 1300°F. Readout is via a Honeywell Recorder. Several copper-constantan thermocouples are mounted at various points on the crankcase as a means of approximating the internal case temperature and ambient cooling effectiveness. They are also recorded on the Honeywell Recorder.

To simulate the 2 watt thermal load, 0.005 in. dia. nichrome wire is wrapped around the end 1/4 inch of the cold cylinder and connected to a dc power supply. Input voltage and amperage are monitored to control the load value. The heater resistance is about 60 ohms.

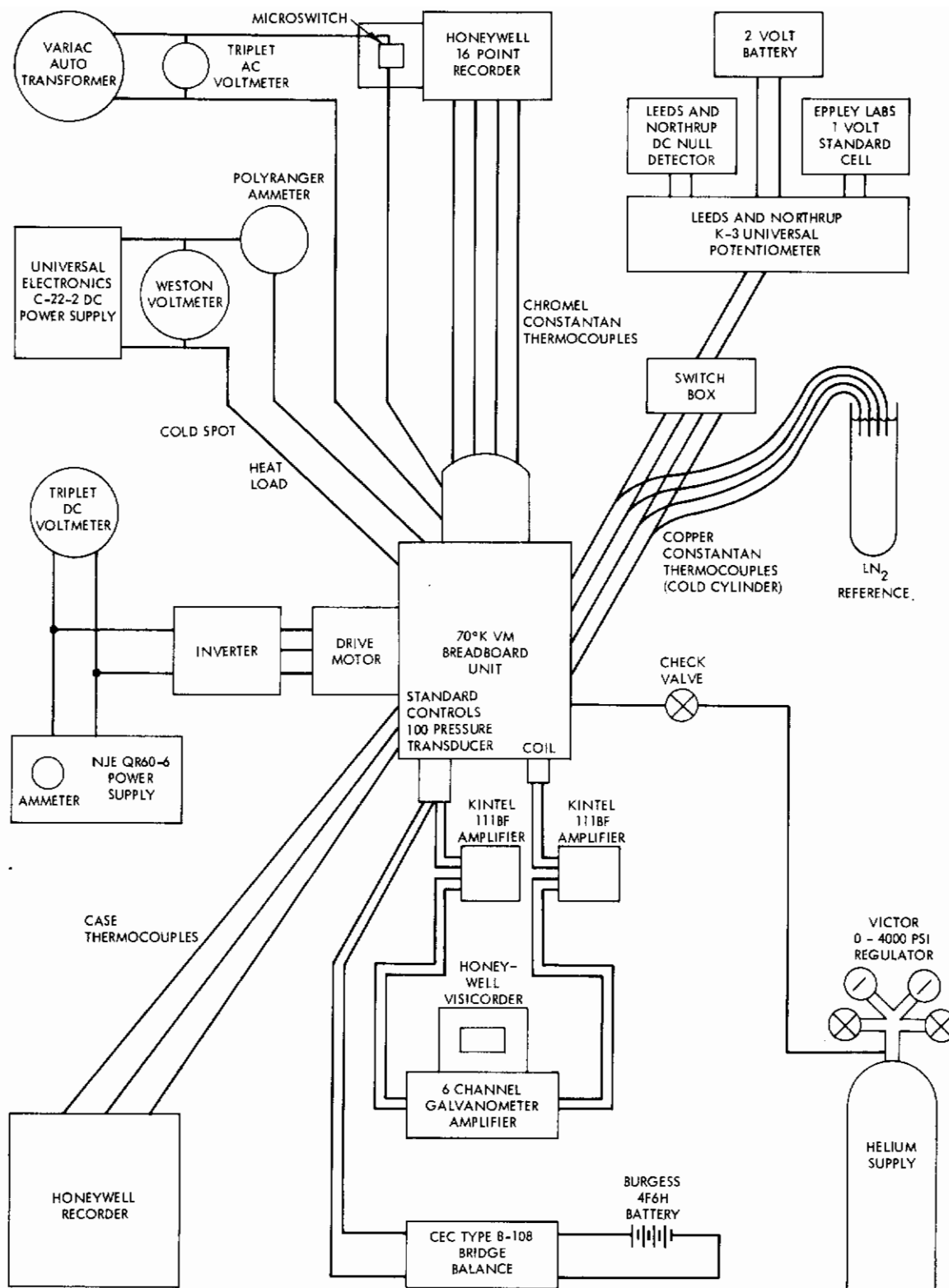


Figure 106. Flow diagram of test equipment for 77°K VM refrigerator

Hot cylinder heater input power is controlled by a Variac. The input voltage is measured, and power is calculated using the known resistance.

Motor input is from a dc power supply through a laboratory breadboard 2 phase variable frequency inverter. Voltage and current are measured. Speed can be controlled by varying frequency or voltage.

The basic speed measurement comes from an emf generated in a coil outside the machine by a magnet mounted in the rotating counterweight. This signal is amplified by a Kintel and sent to a Viscorder and a digital counter. The counter gives speed in cps directly, while the Viscorder trace, consisting of a small pip, gives the piston position in relation to the pressure.

Internal pressure is measured by a Standard Controls Inc. Model 100 0-1000 psi transducer screwed into a small port in the crankcase. Input to the transducer is 9 volts dc from a dry cell battery through a bridge balance. Output is amplified by another Kintel and read on the Viscorder. The combination of simultaneous pressure and crankshaft position traces allows plotting of a pressure versus volume diagram.

Helium is supplied to the machine through a Victor regulator, and the bottle is generally left attached. A check valve is used at the crankcase end of the line to prevent the hose volume acting as dead volume.

The principal danger in operation of the machine is overheating due to sudden slow down or stoppage of the motor. To prevent this, a microswitch is installed in the heater input line and attached to the hot temperature recorder. It is tripped by the recorder mechanism if the temperature exceeds 1300°F, shutting off the heater.

CONCLUSIONS

The design and development of the present VM refrigerators has resulted in operational machines that perform close to design parameters. The experience gained during the development indicates the following areas should be studied further.

1. Increased motor power in the order of two to three times that predicted has been required. Some of this is in the motor-crank mechanism, but it appears that the seal on the cold displacer is using a great portion of the extra power. This statement is supported

by the observation that the machine speeds up whenever the cold cylinder was cooled with a Freon spray in the area of the seal. The importance of reducing the power consumed by the seal is related to the life of the refrigerator in two ways. The first is the effect on seal life - large drag force will result in greater wear, and the second is bearing life since the main bearings and the bearings on the connecting rod of the cold displacer will see the reaction of the larger drag force and will therefore have a shorter life.

2. Motor and crank speed. In the present machines the motor is directly coupled to the crank which results in a simple, highly reliable drive system. However, due to the relatively slow rotational speed of the machine the efficiency of the motor is low and it is difficult to wind the required number of electrical poles on the motor. To circumvent these problems a higher speed motor coupled with a simple gear reduction system should be explored. The motor would be smaller in size and more efficient so that less motor power would be required. The gear reduction system could consist of a single stage of spur gears. Material selection for use in the dry helium, unlubricated environment would be the biggest problem. Due to a lack of test data the most probable choice for the gear materials would be Meehanite (cast iron) and loaded Teflon for the reason that these materials have performed well together in this type of environment under conditions of rubbing. Test stations for evaluation of various material combinations should be set up.
3. Hot displacer regenerator. The major portion of the power consumed by the Vuilleumier refrigerator is supplied as thermal energy to the hot cylinder. Aside from the conventional losses due to conduction down the cylinder and displacer, and through the insulation, there can be a considerable loss due to the regenerator if it does not perform effectively. The concept of using the walls of the cylinder and the displacer for the regenerator contributed to a simple, reliable machine by not requiring a seal, but it requires that

the gap between the two cylinders be accurately maintained. If the gap is allowed to be greater in one area than in another the gas will not flow uniformly over the regenerator area and the efficiency of the regenerator will fall off rapidly. On the present machines guides are used on both ends of the hot displacer to maintain the alignment of the two surfaces with fair results in that there is agreement between calculated and measured values. The problem is that larger and/or more efficient machines will require very long hot displacers in order to obtain enough regenerator area. Several solutions involving extended surface area are feasible and should be investigated.

Figures 107 and 108 illustrate the mean final performance capability of the delivered hardware.

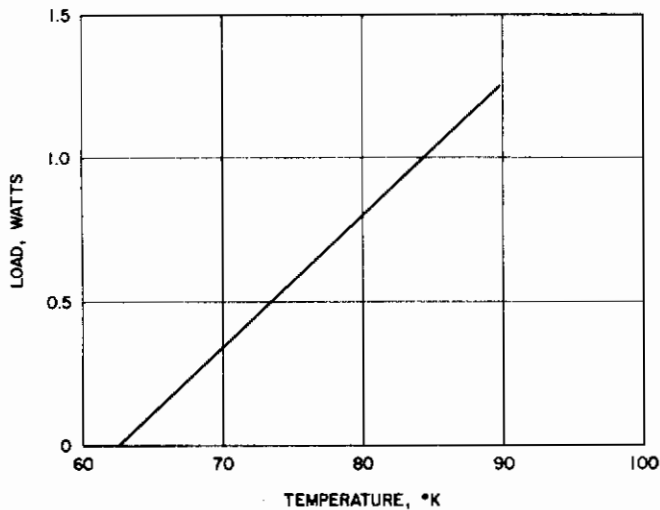
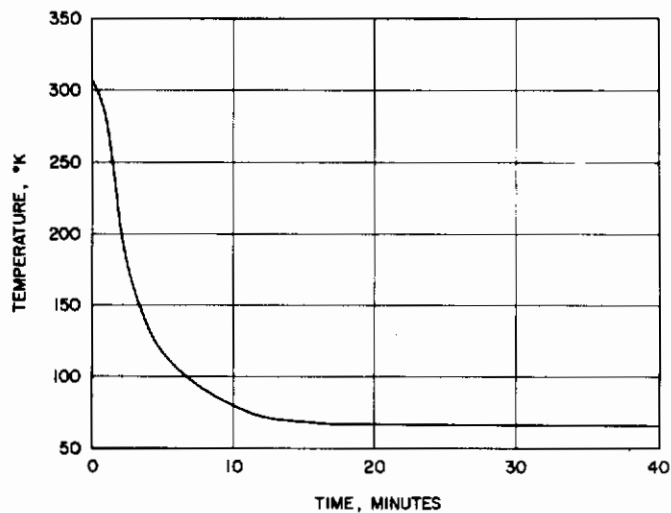


Figure 107. Load capacity curve (VM refrigerator unit X447525-100)

(Does not include dewar load of 0.70 watt)

Figure 108. Cool down time (VM refrigerator unit X447525-100)



REFERENCES

1. F. F. Chellis and W. H. Hogan, A Liquid Nitrogen-Operated Refrigerator for Temperatures Below 77°K, Ado Cryo-Eng 9 Plenum Press (1964).
2. R. White, Communication to R. Doering, Hughes Aircraft Company.
3. K. W. Cowans, "Design of Stirling-Cycle Machinery," Hughes Aircraft Company Document (26 July 1963).
4. M. Jakob, Heat Transfer, Vol. II, John Wiley and Sons, Inc., New York (1957).
5. G. Walker, "Operations Cycle of the Stirling Engine with Particular Reference to the Function of the Regenerator," Journal of Mech. Eng. Sci., Vol. 3, No. 4 (1961).
6. G. Walker, "Regeneration in Stirling Engines," The Engineer (December 1962).
7. J. L. Smith, Jr., "Some Aspects of the Selection of Regenerators," Cryogenics (December 1965).
8. J. W. Kohler and C. O. Jonkers, "Construction of a Gas Refrigerating Machine," Philips Technical Review (October 1954) p. 107.
9. N. A. Hall, Thermodynamics of Fluid Flow, p. 26, Prentice-Hall, Inc., New York (1951)
10. T. Finkelstein, "Optimization of Phase Angle and Volume Ratio for Stirling Engines," Engineering Experiment Station, University of Wisconsin, Madison, Wisconsin (1960).
11. T. Finkelstein, "Analysis of Practical Reversible Thermodynamic Cycles," ASME Paper 64-HT-37 (1964).
12. T. Finkelstein, "Thermodynamics of Regenerative Energy Conversion," AIAA Paper No. 67-216, AIAA 5th Aerospace Science Meeting, New York City (23-26 January 1967).
13. T. Finkelstein, "Generalized Thermodynamic Analysis of Stirling Engines," Society of Automotive Engineers Annual Meeting, Paper 118B (February 1960).

Contrails

14. T. Finkelstein, "Cyclic Processes in Closed Regenerative Gas Machines Analyzed by a Digital Computer Simulating a Differential Analyzer," ASME Paper 61-SA-21, Los Angeles, California (11-14 June 1961).
15. Gifford, W.E., "Basic Investigation of Cryogenic Refrigeration Methods," Technical Report AFFDL-TR-66-26, Wright-Patterson Air Force Base, Ohio, (May 1966)
16. R. Wolfe and G.E. Smith, "Effects of a Magnetic Field on the Thermo-electric Properties of a Bismuth-Antimony Alloy," Applied Physics Letters, Vol. 1, No. 1 (September 1963).
17. B.J. O'Brien and D.S. Wallace, "Ettingshausen Effect and Thermomagnetic Cooling," J. Appl. Physics 29, 1010 (1958).
18. C. F. Kooi, et al., "Solid State Cryogenics, Final Report," Technical Documentary Report No. ASD-TDR-62-1100.
19. C.A. Stochl and E.R. Nolan, "Current Status and Future Trends of Cryogenic Coolers for Electronic Applications, Engineering Design Division, Engineering Sciences Department, Technical Report ECOM-2524, DA Task Nr. 1E6-41209-D-536-07, U.S. Army Electronics Laboratories, U.S. Army Electronics Command, Fort Monmouth, New Jersey (July 1964).

BIBLIOGRAPHY

- "Aerorod Miniature Electric Heating Element," ATL Catalog 53-01, American Radiator and Standard Sanitary Corporation, Advanced Technology Laboratories Division, Aero Research Instrument Department, Sept. 1963.
- "Aircraft Bearing Catalog," The Fafnir Bearing Company, Form No. 522, 1966.
- "Bal-Seals," Bal-Seal Engineering Co., 1966.
- Barden Corporation, Dan Bury, Conn., Barden Engineering Data Pkg. 3-2, Feb. 1964.
- Barden Corporation, Dan Bury Conn., Barden Engineering Catalogue G-3, 1964.
- Chironis, Nicholas P., "Designing for Zero Wear — or a Predictable Minimum," Product Engineering, August 1966, pp. 41-50.
- Gifford, W. E., "Basic Investigation of Cryogenic Refrigeration Methods," Technical Report AFFDL-TR-66-26, May 1966. Wright-Patterson Air Force Base, Ohio, 45433.
- Hall, R. C., "The Metallurgy of Alloy 718," American Society of Mechanical Engineers, Paper No. 67-Met-5, April, 1967.
- Heikes, R.R. and Ure, R.W., "Thermoelectricity," Science and Engineering Interscience Publishers, London, 1961.
- Kooi, C.F. et al., "Solid State Cryogenics, Final Report," Technical Documentary Report No. ASD-TDR-62-1100.
- O'Rourke, J. Tracy, "Design Properties of Filled-TFE Plastics," Machine Design, Sept. 1962.
- "Parker O-Ring Handbook," Catalog OR5700, Parker Seal Company, April 1967.
- "Pressure Instruments and Components," Glassco Instrument Company.
- Products Bulletin PB 1-2A, H.I. Thompson Fiber Glass Co., Apr. 19, 1961.
- "Purebon," Pure Carbon Co., Inc., Catalog PC-4-5753.
- "Star Industrial Wire Cloth and Screens," Catalog 62, Star Wire Screen and Iron Works, Inc.
- "Thermon Heat Transfer Products," Engineering Data Book T-10, Thermon Manufacturing Company, 1966.

Contrails

APPENDIX

OTHER PRACTICAL CRYOGENIC CYCLES AND REFRIGERATORS

The discussion in this appendix centers around other dynamic and closed-cycle refrigeration systems that have been improved or developed into practical cryogenic refrigerators. These systems and their features or performances are discussed in sequence below. A short discussion of thermoelectric and thermomagnetic refrigerators is also presented.

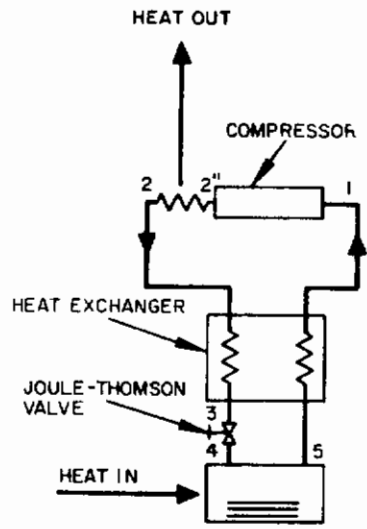
DYNAMIC REFRIGERATION SYSTEMS

1. Joule-Thomson System

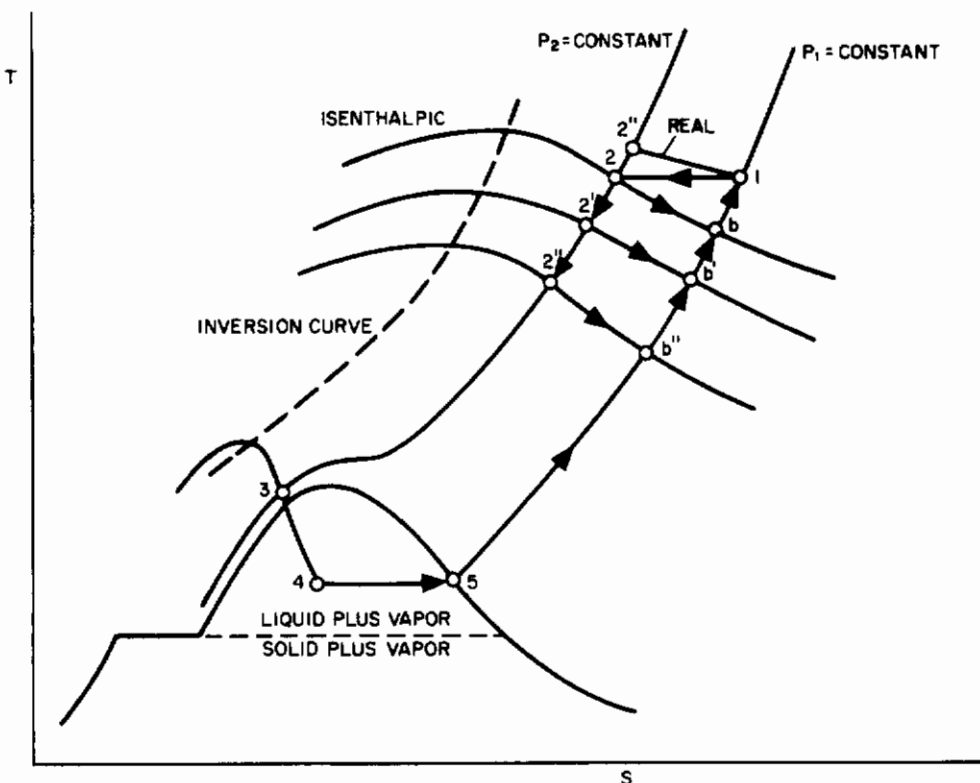
The Joule-Thomson system and its thermodynamic cycle are shown schematically in Figure 109a; the thermodynamic behavior of a unit mass of fluid, after equilibrium has been established in the system, is shown in the temperature-entropy diagram in Figure 109b. This figure also shows the ideal cool-down process of the system before equilibrium is reached.

Under ideal conditions of operation and when the system has reached equilibrium conditions, the working fluid is compressed isothermally from P_1 to P_2 ; see Figure 109b. It is then cooled in the heat exchanger from temperature T_2 to temperature T_3 and throttled through the Joule-Thomson valve from State 3 to State 4. After the throttling process, the fluid is in the two-phase state and as it absorbs heat from the object that is cooled, it passes from State 4 to State 5. Finally, the fluid is heated from State 5 to State 1 in the heat exchanger.

Before equilibrium is established in the system, the temperature of each unit of mass varies at the inlet to the throttling valve. The whole system is at ambient temperature before any processes take place. At the beginning, under ideal conditions, the first unit mass is compressed isothermally from State 1 to State 2 (see Figure 109b), throttled from State 2 to State b, and then heated in the heat exchanger from State b to State 1. The second unit of mass is cooled in the heat exchanger by the first unit of mass and is then throttled from State 2' to State b'; it is then heated



(a) Closed Joule-Thomson system



(b) Ideal cooldown process for Joule-Thomson system, which cools in two-phase region of refrigerant

Figure 109. Joule-Thomson refrigeration system and thermodynamic cycle

in the heat exchanger from State b' to State 1 in cooling the third unit of mass from State 2 to State $2'$. Hence, each unit of mass is throttled from a lower temperature until the system reaches equilibrium and the temperature of the refrigerant becomes stable just before the throttling valve. In other words, the system works gradually down to lower temperatures. After a period of time, States 3 and 4 are observed before and after the throttling valve as shown in Figure 109. Since the State 4 point lies in the two-phase region, the heat of vaporization of the refrigerant is used for cooling.

2. Claude System

Applying the Joule-Thomson effect in a closed cycle results in a very reliable system when large refrigeration power is needed. However, the coefficient of performance of this system is low with respect to that of a Carnot system operating between the same temperature limits. Efforts have therefore been made to replace the irreversible Joule-Thomson valve with a reversible device. The best improvement was made by Claude, who substituted an expansion engine for this valve. This modification, which made the system partially thermodynamically reversible and decreased the higher pressure of the system, was not completely successful because the expansion engine could not produce liquid air directly. Although Claude replaced the Joule-Thomson throttling as a main source of refrigeration, he still had to use it to achieve liquefaction outside the engine. Hence, the ideal Claude cycle is based on a reversible adiabatic expansion of a portion of the working fluid to precool a second portion, which is then liquefied by a low-temperature Joule-Thomson throttling process. The Claude refrigeration system and thermodynamic cycle are shown schematically in Figure 110. In the ideal Claude cycle and under conditions of equilibrium, a unit mass of refrigerant is compressed isothermally from 1 to 2 and then cooled in a heat exchanger by the refrigerant returning from 8 to 7. At 3, a certain amount of the unit mass is bled off and expanded through the engine, where it produces work and cools. The rest of this unit mass continues through the heat exchangers and is throttled from 6 into the two-phase region 7; it then absorbs heat from 7 to 4, joins the bled-off mass at 4, and flows back to the compressor. In

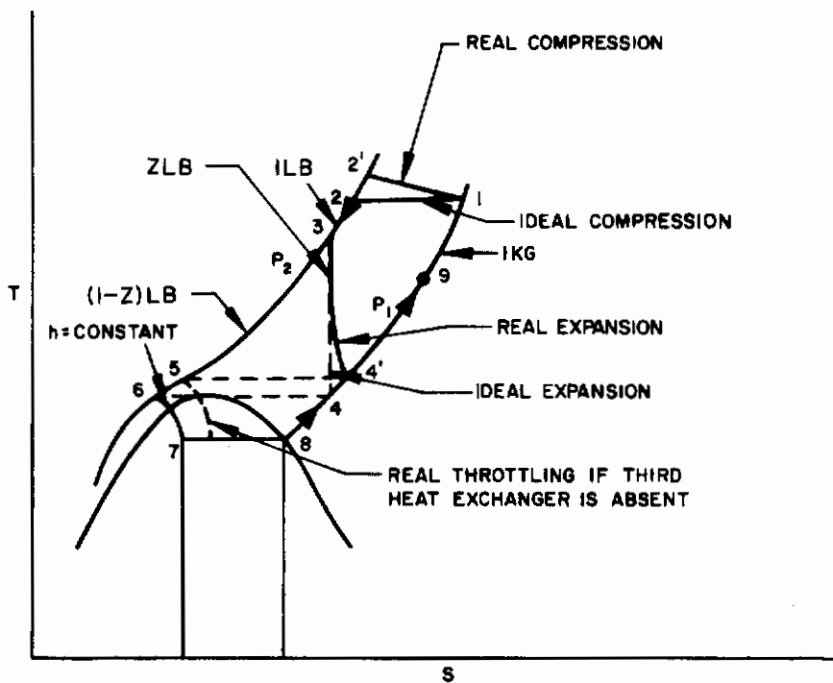
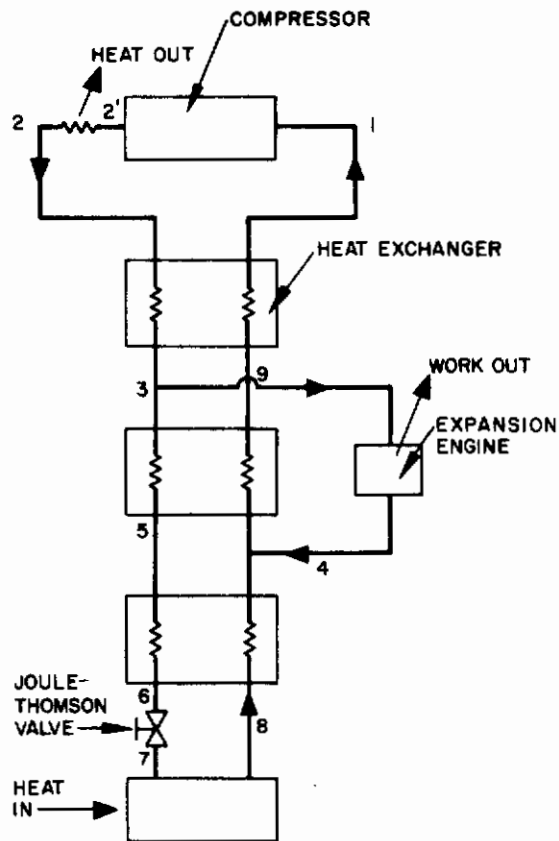


Figure 110. Claude liquid cycle

the Claude system, the cool-down process is similar to that in the Joule-Thomson system.

The Claude system can also be so designed that the working fluid always remains in one phase during the cycle. Such a system is shown schematically in Figure 111. Here, refrigerant is ideally compressed isothermally from State 1 to State 2, then cooled in the first heat exchanger and expanded in the engine in order to cool it further. The refrigerant is thereafter heated in the second and first heat exchangers by absorbing heat from the object that is to be cooled and from the high-pressure fluid from the compressor. The refrigerant then returns to the low-pressure side of the compressor. This process is called the Claude gas cycle.

3. Stirling System

The Stirling system differs from the two previous systems in that it employs a regenerator or periodic heat exchanger instead of a direct-transfer heat exchanger. Two modern versions of the Stirling system are shown in Figure 112, together with the ideal Stirling cycle, which is represented in the pressure-volume and the temperature-entropy diagrams. The Stirling system contains no valves; in a two-piston type of system, compression and the rejection of heat take place in one cylinder with a heat exchanger, and expansion and the absorption of heat are carried out in another cylinder with a heat exchanger. In a displacer type of system, compression and heat rejection as well as expansion and heat absorption take place in one cylinder, and two heat exchangers are used (see Figure 112).

4. Gifford McMahon or Modified Ericsson System

In this modified system, the open expansion and the regenerator that are used make it resemble the Ericsson cycle. The real Ericsson cycle consists of two isothermal processes and two constant-pressure processes. It differs from the Stirling cycle in the method in which heat is rejected and absorbed in the regenerator. The Ericsson cycle applies the constant-pressure process instead of the constant-volume process and, like the Stirling cycle, it is thermodynamically reversible.

Contrails

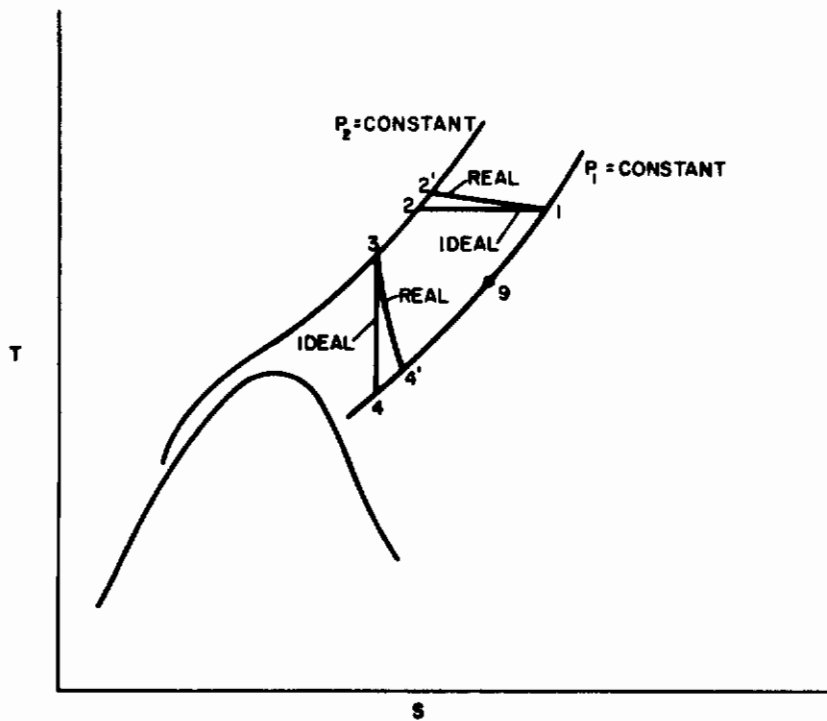
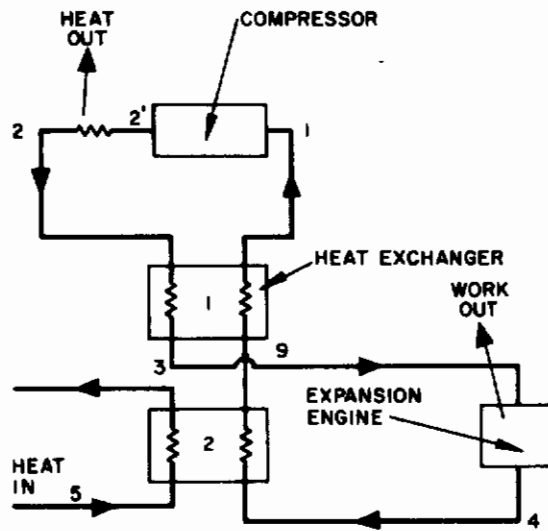
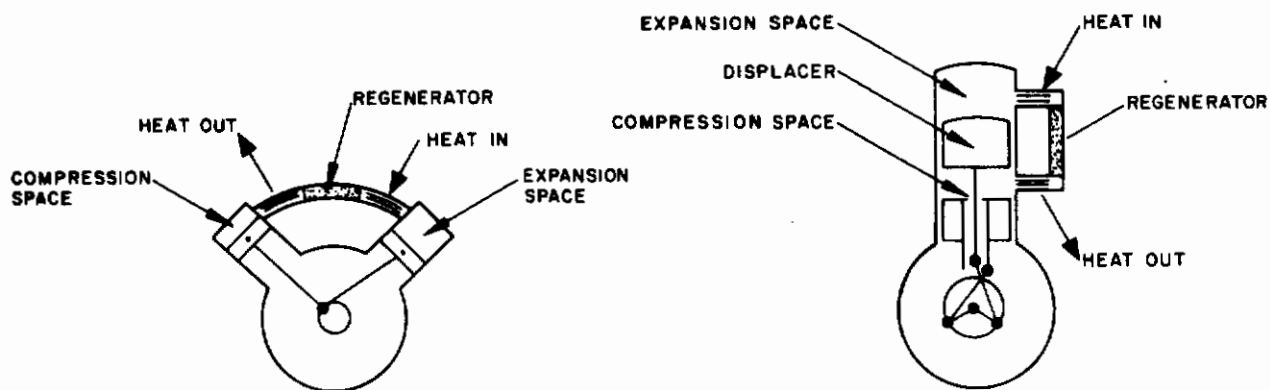


Figure 111. Claude gas cycle



(a) Two-piston type of system

(b) Displacer type of system

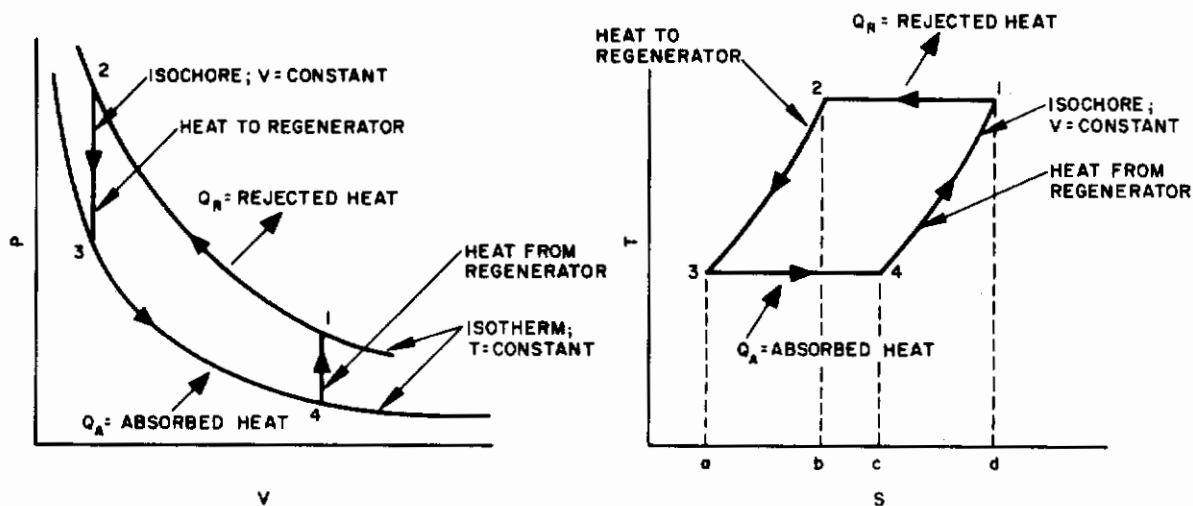


Figure 112. Stirling-cycle refrigeration systems with ideal pressure-volume and temperature-entropy diagrams

The modified Ericsson system employs a separate compressor, and inlet and exhaust valves are needed for proper phasing of the flow of gas between the compressor and the expansion space displacer; this cycle is shown in Figure 113. In discussing this cycle, it is assumed that the refrigerator has been in operation sufficiently long that the cold and warm regions have reached steady-state temperature.

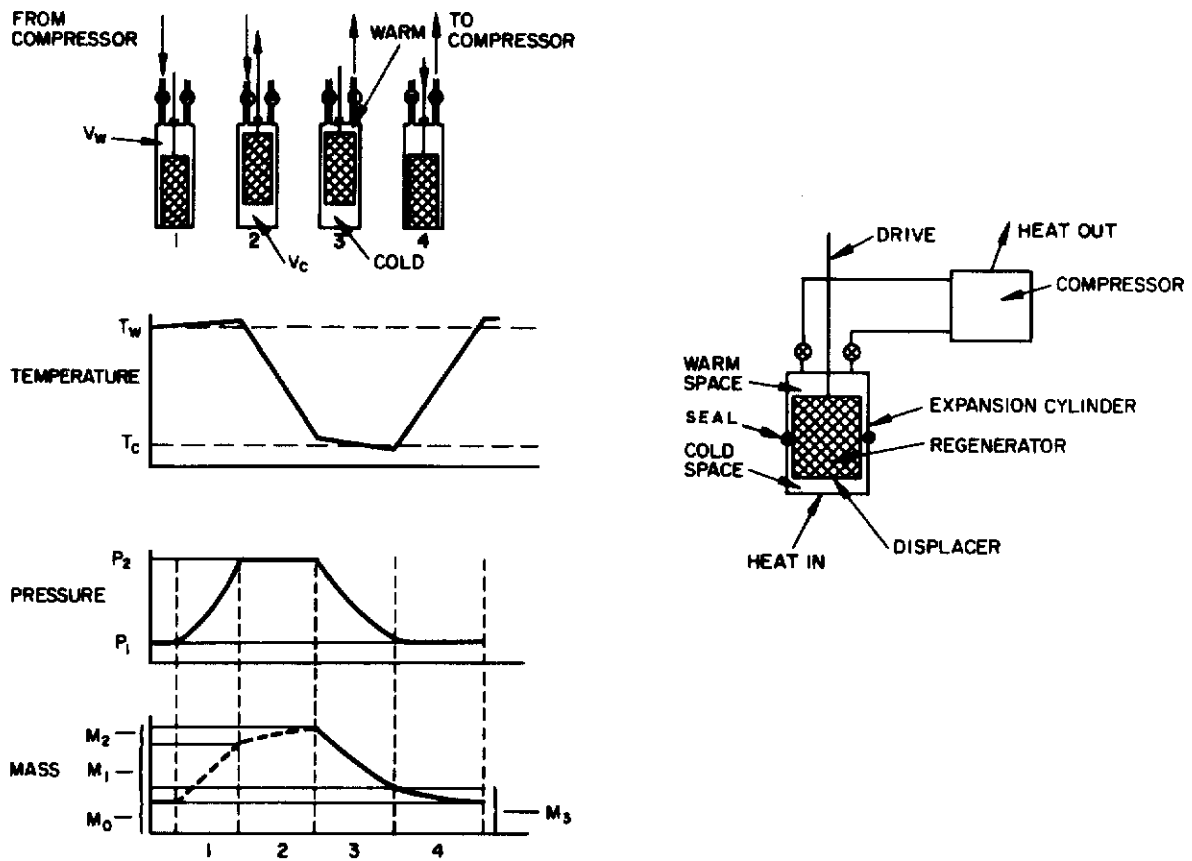


Figure 113. Modified Ericsson system

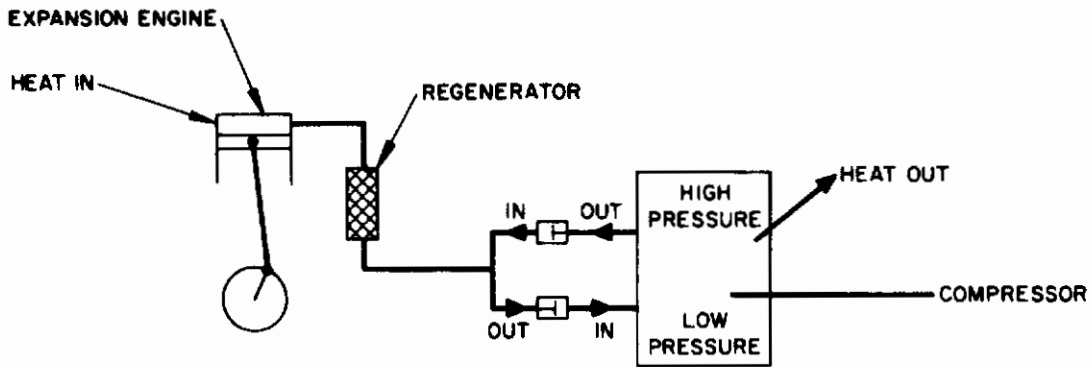
The process begins when the displacer in the inlet position produces an inlet volume V_w that is filled with gas at the exhaust pressure P_1 . The following operations then take place:

1. The inlet valve opens and admist gas at a pressure P_2 to the volume V_w and to the residual volumes in the regenerator and cold end.
2. With the inlet valve open, the displacer is moved to produce volume V_C in the cold section, and gas at a pressure P_2 flows from volume V_w and from the compressor to fill the volume V_C , the regenerator, and residual volume in the warm end.

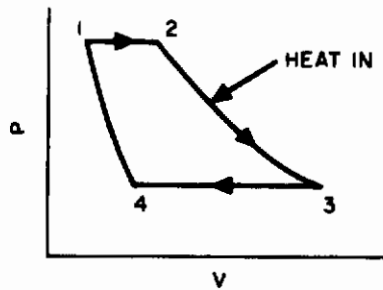
3. The inlet valve then closes, and the exhaust valve opens to allow the entire mass of gas to expand to the exhaust pressure P_1 and leave the system with the volume at the warm end with gas at a temperature near T_w , and the volume in the regenerator with gas at temperatures between T_C and T_w . Refrigeration is produced during this process.
4. Finally, while the exhaust valve is still open, the displacer moves to transfer the cold gas under constant pressure past the heat surface in the regenerator to the compressor inlet. The gas throughout the system is then at pressure P_1 and has a temperature T_C in the cold end. The temperature of the gas in the warm-end volume V_w is T_w . The temperature of the regenerator varies between T_w and T_C .

5. Solvay System

The modern version of the Solvay system (see Figure 114) consists of a compressor, a regenerator, inlet and outlet valves, and a piston expansion engine. This engine and the compressor operate as steady-flow devices in the over-all system. During the cycle, warm gas under high pressure enters the regenerator through the outlet poppet valve in the compressor, is cooled as it flows through the regenerator, and then enters the expansion engine in the process designated 1-2 in the pressure-volume diagram. The gas then expands in the engine and absorbs heat from the object being cooled through the cylinder walls; this is process 2-3. Thereafter, it is expelled from the engine (process 3-4), and the residual gas in the clearance volume of the engine is compressed from 4-1. The expelled gas now flows toward the compressor and through the regenerator where it absorbs heat. It then enters the low-pressure side of the compressor through the inlet poppet valve and is again compressed. The ideal cycle for a unit mass of gas as it flows through the Solvay system is shown in the temperature-entropy diagram in Figure 114. As can be seen, a unit mass of gas goes through two isothermal processes and two constant-pressure processes. Hence, the



(a) Solvay system



(b) P-V diagram for expansion engine

(c) T-S diagram for Solvay system (1'-2' isothermal compression in compressor; 2'-3' heat rejected to regenerator; 3'-4' isothermal expansion in expansion engine; 4'-1' heat absorbed in regenerator)

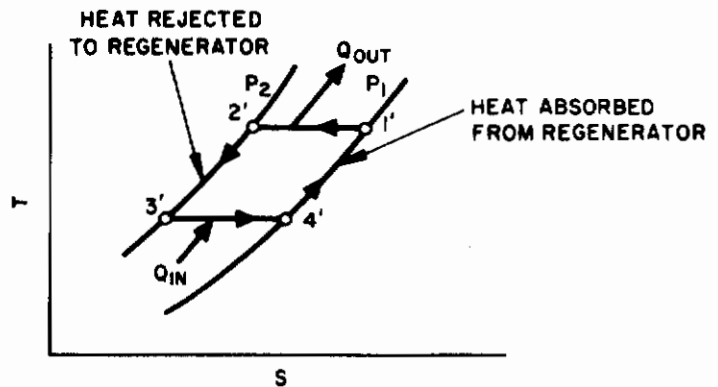


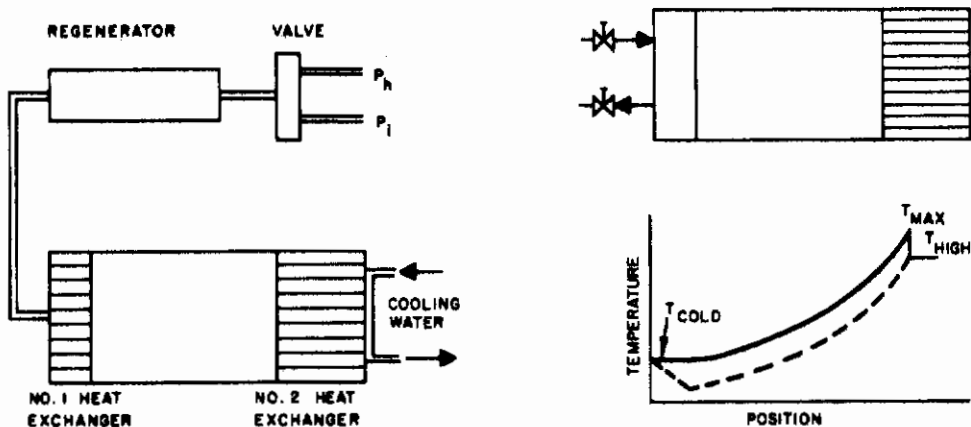
Figure 114. Solvay cryogenic refrigerator

Ericsson cycle can also be accomplished by means of the Solvay system. The difference between Ericsson's original system and the modified Ericsson and Solvay systems lies in the heat exchanger and assembly. Ericsson used a direct type of heat exchanger with a compact compression and expansion

system while the other two systems employ a periodic type of heat exchanger or regenerator with separate compression and expansion devices.

6. Pulse Tube System (See Reference 15)

This new system is shown schematically in Figure 115. It consists of a compressor, a regenerator, two heat exchangers, and a tube which is cooled at one end. Under equilibrium conditions, a mass of working fluid is cooled as it flows from the compressor through the regenerator and to the tube inlet. It is then compressed as the tube is being filled and the temperature of the mass of fluid increases. The mass of fluid rejects heat to the heat exchanger at the closed end of the tube when it reaches this position since this heat exchanger 2 is being cooled. As the tube begins to empty, the mass of fluid expands as it flows out of the tube since it is producing work in pushing out the gas that is ahead of it. The temperature of the mass of fluid now decreases below that of the coolant and the mass therefore absorbs heat or produces refrigeration in heat exchanger 1. The mass of fluid then flows through the regenerator where it absorbs heat from the regenerator before



(a) Schematic diagram of single stage pulse tube temperature

(b) Temperature patterns of gas filling and exhausting from pulse tube refrigerator

Figure 115. Pulse tube system

it enters the suction side of the compressor. The temperature pattern of the mass of working fluid is shown in Figure 115b as the mass flows in and out of the tube.

SOLID-STATE DEVICES

Within the past ten years, solid-state devices have been developed to the extent that they can compete effectively with other refrigerating systems in certain applications and within certain temperature limits. Such devices contain no moving parts and their construction is therefore simple.

1. Thermoelectric System

Figure 116 is a schematic of a simple semiconductor thermoelectric refrigerating system; the element shown provides refrigeration by means of the Peltier effect.

Electricity fed to the system cools the junction of the two dissimilar semiconductors and makes it absorb heat from the object that is cooled. Heat is rejected at the junction between the power input and the system.

The Seebeck coefficient is used to express the performance of the thermoelectric refrigerator despite the presence of the Peltier effect. The

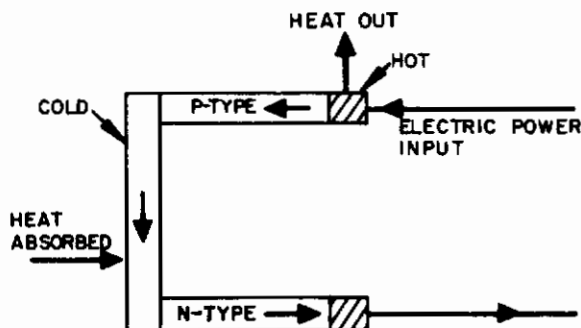


Figure 116. Thermoelectric refrigeration system

maximum temperature difference between the hot and cold ends of a thermoelectric refrigerator is expressed in Reference 19 as

$$\Delta T_{\text{Max}} = \frac{Z T_{\text{cj}}^2}{2} \quad (58)$$

where T_{cj} is the absolute temperature of the cold junction and Z is the thermoelectric figure of merit or

$$Z = \frac{(\alpha_p - \alpha_n)^2}{\left[(k_p \rho_p)^{1/2} + (k_n \rho_n)^{1/2} \right]^2} \quad (59)$$

The Seebeck coefficients (α_p) and (α_n) are coefficients with respect to a specific standard material and are defined as the ratio of the open-circuit voltage to the temperature difference between the hot and cold junctions of a thermoelectric material and the reference or standard material. Thus,

$$\alpha_p = \frac{V_{p-s}}{\Delta T} \quad (60)$$

and

$$\alpha_n = \frac{V_{n-s}}{\Delta T} \quad (61)$$

The expression for the heat absorbed at the cold junction for a maximum value of performance is

$$Q_{\text{max COP}} = \phi_{\text{max}} P' \quad (62)$$

or

$$Q_{\max \text{ COP}} = \frac{(T_{cj}/\Delta T) \left[(1 + Z\bar{T})^{1/2} - (T_{hj}/T_{cj}) \right]}{(1 + Z\bar{T})^{1/2} + 1} V_{\text{app}} I_{\text{app}} \quad (63)$$

The maximum heat absorbed by a thermoelectric refrigerator is

$$Q_{\max} = \frac{(1/L) (\alpha_p - \alpha_n)^2 T_{cj}^2}{2 \left[(\rho_n/A_n) + (\rho_p/A_{p'}) \right]} - \Delta T \left[(A_n k_n) + (A_{p'} k_{p'}) \right] \quad (64)$$

2. Thermomagnetic System

A thermomagnetic system is a solid-state system that produces refrigeration by means of the Ettingshausen effect. In 1887, Ettingshausen found that the temperature of one side of a current-carrying conductor like copper is lower than that of the opposite side if the conductor is placed in a magnetic field that is perpendicular to the current. This difference in temperature is due to the Lorentz force that acts on the electron flow. The faster or "hotter" electrons experience a greater force than the slower or "colder" electrons and therefore concentrate at one side of the conductor. The temperature of this side of the conductor will therefore be equal to the ambient temperature while that of the other side will be less. Figure 117 shows simple thermomagnetic or Ettingshausen refrigerator. Figure 118 shows an infinitely staged thermomagnetic refrigerator (Reference 16) with respect to a two-stage thermoelectric refrigerator.

The maximum temperature difference between the warm and cold sides of an Ettingshausen refrigerator is expressed in Reference 17 as

$$(T_H - T_C)_{\max} = \frac{Z_{yx} T_H^2}{2} \quad (65)$$

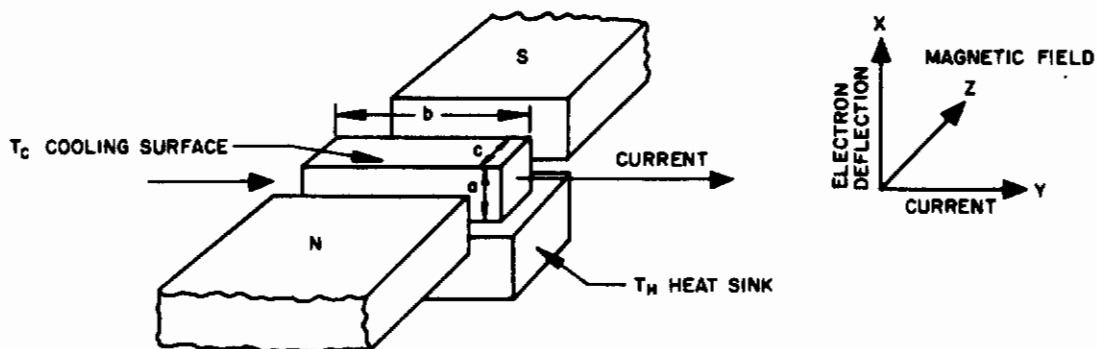


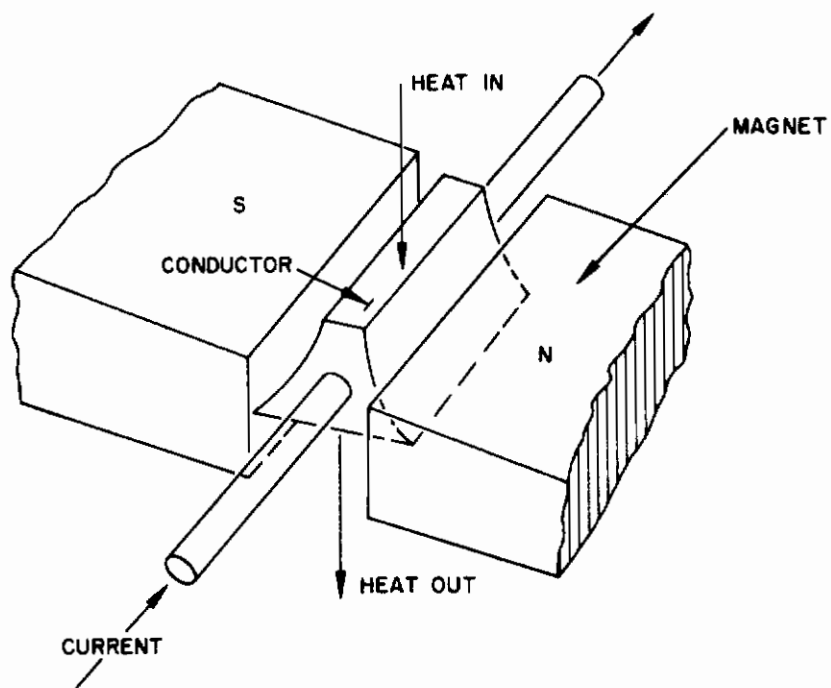
Figure 117. Schematic of Etingshausen cooler

and the heat absorbed at the cold side is

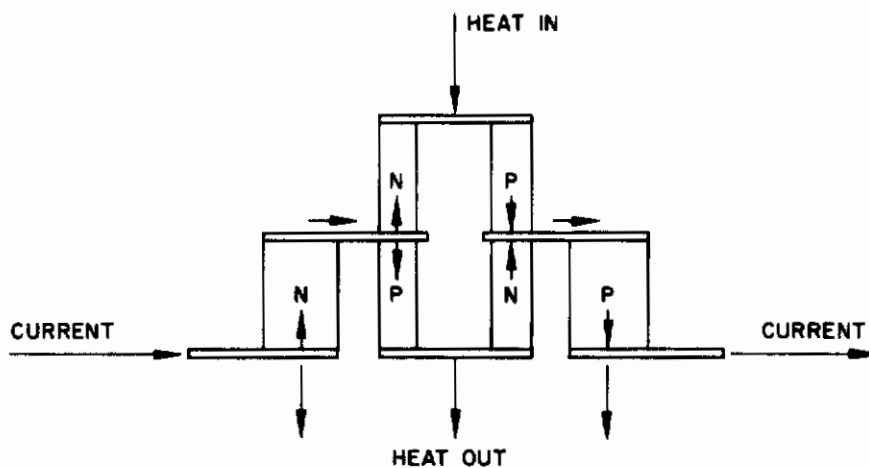
$$Q_{in} = \left(\frac{E_y}{\rho_{yy}} \right) \alpha_{yx} T_C - 1/2 \left(\frac{E_y^2 a}{\rho_{yy}} \right) - \frac{(1 - Z_{yx} \bar{T}) k_{xx} (T_H - T_C)}{a} \quad (66)$$

The electrical power needed for a given difference in temperature is

$$P_{in} = \left(\frac{E_y^2}{\rho_{yy}} \right) abc + \left(\frac{E_y}{\rho_{yy}} \right) \alpha_{yx} (T_H - T_C) bc \quad (67)$$



(a) Infinitely staged thermomagnetic refrigerator



(b) Two-stage thermoelectric refrigerator

Figure 118. Thermomagnetic and thermoelectric refrigerators

Unclassified

Security Classification

| DOCUMENT CONTROL DATA - R & D | | |
|---|--|-----------------|
| (Security classification of title, body of abstract and indexing annotation must be entered when the overall report is classified) | | |
| 1. ORIGINATING ACTIVITY (Corporate author) Hughes Aircraft Company Research and Development Division Culver City, California | 2a. REPORT SECURITY CLASSIFICATION Unclassified | |
| 3. REPORT TITLE Vuilleumier Cycle Cryogenic Refrigerator Development | | |
| 4. DESCRIPTIVE NOTES (Type of report and inclusive dates) Final Technical Report | | |
| 5. AUTHOR(S) (First name, middle initial, last name) Robert D. Doering Fred N. Magee | | |
| 6. REPORT DATE September 1968 | 7a. TOTAL NO. OF PAGES | 7b. NO. OF REFS |
| 8a. CONTRACT OR GRANT NO. AF33615-67-C-1532 | 9a. ORIGINATOR'S REPORT NUMBER(S) P68-155 | |
| b. PROJECT NO. 1470 | 9b. OTHER REPORT NO(S) (Any other numbers that may be assigned this report) AFFDL-TR-68-67 | |
| c. Task 147001 | | |
| d. BPS No. 7(680100-61430014) BPS No. 7(611470-62405334) | | |
| 10. DISTRIBUTION STATEMENT Released to DDC. This document is subject to special export control and each transmittal to foreign governments or foreign nationals may be made only with prior approval of AFFDL, (FDFE) WPAFB, Ohio 45433. | | |
| 11. SUPPLEMENTARY NOTES | 12. SPONSORING MILITARY ACTIVITY Air Force Flight Dynamics Laboratory Wright Patterson AFB, Ohio 45433 | |
| 13. ABSTRACT <p>This report covers Phase I effort in an exploratory development program to evaluate the Vuilleumier heat driven refrigeration cycle for aircraft and spacecraft cryogenic applications. The effort includes a study of the theoretical aspects of the cycle and development of three miniature breadboard cryogenic refrigerators based on the cycle and operated by electric powered heating capsules. Two of the breadboard units are of identical design; these deliver 2 watts cooling capacity at 77°K. The remaining breadboard is a two-stage unit designed to deliver 0.5 watt at 30°K and 5 watts at 75°K. Performance data from these units were incorporated in the theoretical study. All units met their design requirements and confirmed the feasibility and inherent advantages of the Vuilleumier cycle for miniature long-life cryogenic refrigerators for both aircraft and spacecraft applications.</p> <p>This abstract is subject to special export controls and each transmittal to foreign governments or foreign nationals may be made only with prior approval of AFFDL (FDFE), WPAFB, Ohio 45433.</p> | | |

DD FORM 1 NOV 65 1473

Unclassified

Security Classification

Unclassified
Security Classification

| 14. KEY WORDS | LINK A | | LINK B | | LINK C | |
|--|--------|----|--------|----|--------|----|
| | ROLE | WT | ROLE | WT | ROLE | WT |
| closed cycle cryogenic refrigerator Vuilleumier refrigeration cycle | | | | | | |

Unclassified
Security Classification